

Synthesis of In-Derived Metal-Organic Frameworks

by

Joseph John Mihaly

Submitted in Partial Fulfillment of the Requirements

for the Degree of

Masters of Science

in the

Chemistry

Program

YOUNGSTOWN STATE UNIVERSITY

July, 2016

Synthesis of In-Derived Metal-Organic Frameworks

Joseph John Mihaly

I hereby release this thesis to the public. I understand that this thesis will be made available from the OhioLINK ETD Center and the Maag Library Circulation Desk for public access. I also authorize the University or other individuals to make copies of this thesis as needed for scholarly research.

Signature:

Joseph John Mihaly, Student

Date

Approvals:

Douglas T Genna, Thesis Advisor

Date

John A. Jackson, Committee Member

Date

Sherri Lovelace-Cameron, Committee Member

Date

Dr. Salvatore A. Sanders, Dean of Graduate Studies

Date

Acknowledgements

I would like to thank the chemistry department at Youngstown State University for everything they have done regarding the last six years of my academic career. All faculty, as well as administrative personnel have always gone out of their way to help me in any way possible. I would also like to thank the fellow graduate students in my graduating class (Chris, Kate, Davena, and Jordan), it has been a fun ride, and I wish all of you the best of luck.

To put into words all that Dr. Genna has done for me over the past two years is quite a feat, but I would like to express my utmost gratitude to him as a mentor. When I joined the Genna lab I was the first person to accept a position in his group. He gave me every opportunity available to help construct the lab, recruit students, as well as to see the inner workings of how to properly run a research group. This experience was invaluable, and I thank him for taking the time to show me these things since many masters and even Ph.D students never obtain this type of knowledge.

Second, I would like to thank Dr. Genna for reinvigorating my love for chemistry. When I first started this program, I thought my desire for chemistry had been lost. His passion for this wonderful subject is so noticeable and contagious that it is almost impossible to not be excited about running new experiments or being able to publish data. He also taught me the value of reading recent literature, how to properly present your data in front of colleagues, and how great it feels to publish data that you have worked so hard to obtain. After being able to publish two papers here, I feel that I am leaving YSU with an advantage that few to none achieve, but more importantly Dr. Genna has made sure that I am leaving YSU with the most opportunities available both in doctorate school, and in my career after, I cannot thank him enough for that.

Lastly, I would like to thank him for providing me with a person that I can strive to be like in the future. Dr. Genna's knowledge of chemistry, instrumentation, and South Park is beyond reproach. He is held in the highest regard by everyone that knows him in the chemistry community. His work ethic is second to none, and I would like to think that he has instilled the same work ethic in me. I can only hope one day that my students and colleagues hold me in such high regards. Dr. Genna thank you for everything.

I would also like to thank Dr. John Jackson. I have learned so much about not only chemistry from him, but also teaching as well. His input on how to properly instruct students as well as just being the best teaching assistant you can be was irreplaceable. I hope that I can continue to make him proud while being a teaching assistant at Case Western Reserve University. Also, the ACS conference was a blast and something that I will always remember. Thanks for everything Dr. Jackson.

I would also like to quickly thank Dr. Peter Norris, he was my undergraduate research advisor and was the first person who allowed me to do “real” chemistry. Thank you Dr. Norris.

I would also like to thank everyone in the Genna lab group, but specifically Mike, Tyler, and Mariah. The four of us have been here since the beginning, and it has been a privilege getting to know you three. I can honestly say I feel lucky to call you colleagues and friends, which as any chemist can tell you doesn't always happen in a lab group. I wish everyone in group the best of luck in the future.

Lastly, I would like to thank my parents, grandparents, and my twin sister for all of their support through both my undergraduate and graduate work. Without your support I would not have made it through all of the trying times, thank you.

ABSTRACT

This thesis consists of two different sections: The first is template directed synthesis of metal-organic frameworks (MOFs). Where nine new structures that have previously never been synthesized are reported. The new frameworks are officially: two dimensional, anionic (4) YCM-21-Z (Youngstown Crystalline Material) (Z= template molecule), and 3-D, neutral YCM-23. YCM-22 contains an unprecedented dianionic $[\text{InCl}_3(\kappa^2\text{-O}_2\text{CAr})_2]^{2-}$ node and is 1-D in dimensionality. Another grouping of related MOFs synthesized using templating is YCM-31, YCM-32, and YCM-41 where each structure is observed with chemically related nodes ($\{\text{In}(\text{CO}_2\text{R})_3\text{X}\}$). Lastly, transformation studies were completed, where it was observed that ATF-1 can be transformed into certain YCM-21-Z structures through anion-cation mediated deinterpenetration.

Table of Contents

Title Page	i
Signature Page	ii
Acknowledgements	iii
Abstract	v
Table of Contents	vi
List of Figures	viii
List of Tables	x
List of Schemes	x
Introduction	
Metal-Organic Frameworks.....	1
MOF Applications.....	1
MOF Supramolecular Structure.....	4
Effects of Synthesis Parameters on Dimensionality and Topology.....	7
Template-directed MOF Synthesis.....	9
Indium-derived MOFs.....	11
Solid-state to solid-state MOF Conversion	15
Results and Discussion	
YCM-21 Series.....	20
ATF-1.....	21

YCM-21-TEBA.....	22
YCM-21-TEA.....	24
YCM-21-spPP.....	25
YCM-21-spMP.....	27
Framework-cation interaction.....	28
YCM-22.....	29
YCM-23.....	31
Comparison of YCM-20 series nodes.....	32
Experimental for YCM-20 series.....	33
Crystal-to-Crystal Transformation Studies.....	35
Transformation of ATF-1 to YCM-21-TEA.....	36
Transformation of ATF-1 to YCM-21-spMP.....	37
Transformation of ATF-1 to YCM-21-spPP.....	38
Transformation of ATF-1 to YCM-21-TEBA.....	39
Proposed Mechanism.....	40
MOF Structural Rearrangements Experimental.....	41
Continuation of Template-Directed MOF Synthesis.....	42
YCM-31.....	42
YCM-32.....	43
YCM-41.....	44
Conclusion.....	45
YCM-31, YCM-32, YCM-41 Experimental.....	46
References.....	48
Synthesis of In-Derived MOFs Experimental	
Materials and Methods.....	52
Cation Exchange Experiments.....	52
Synthesis.....	53
NMR Spectra of MOFs After Attempted Ammonium Cation	
Exchange.....	64
Supplemental Figures.....	66
X-Ray Crystallography.....	72

List of Figures

Figure 1 MOF 5.....	1
Figure 2 Means in which catalysts are incorporated into MOFs.....	2
Figure 3 Scheme of NU-601 catalyzed Friedal-Crafts reaction.....	3
Figure 4 HKUST-1.....	5
Figure 5 UIO-66.....	6
Figure 6 PCN-5.....	7
Figure 7 Dimensionality of MOFs.....	7
Figure 8 (Natarajan).....	9
Figure 9	10
Figure 10 FJI-C1.....	11
Figure 11 Common indium coordination modes (MOFs).....	12
Figure 12 Feng MOFs.....	12
Figure 13 Possible Crystal-to-Crystal Transformation Motifs.....	16
Figure 14 SBU comparison of MIL-68 and QMOF-2.....	17
Figure 15 Possible framework-template interactions that can occur in newly synthesized MOFs.....	20
Figure 16 YCM-21-TEBA stability studies (1 week).....	23
Figure 17 YCM-21-TEA stability studies (1 week).....	24
Figure 18 YCM-21-spPP stability studies (1 week).....	26
Figure 19 YCM-21-spPP stability studies (1 week).....	27
Figure 20 View of cation- π interactions between templating cations and the thiophene linker for each YCM-21 structure.....	28
Figure 21 YCM-22 stability studies (1 week) (calculated pattern was derived with $0.5^\circ 2\theta$ FWHM instrumental broadening).	30
Figure 22 YCM-23 stability studies (1 week).....	31
Figure 23 Comparison of the SBU for YCM-23, YCM-21-Z, and YCM-23.....	32

Figure 24 ATF-1 Suspended in TEBABr for 1 week.....	35
Figure 25 Scheme of ATF-1 transformed into YCM-21-TEA with overlaid powdered patterns.....	36
Figure 26 Scheme of ATF-1 transformed into YCM-21-spMP with overlaid powdered patterns.	37
Figure 27 : Scheme of ATF-1 transformed into YCM-21-spPP with overlaid powdered patterns.(Impurity pointed out by arrow).....	38
Figure 28 Scheme of ATF-1 partially transformed into YCM-21-TEBA with overlaid powdered patterns.(Impurity pointed out by arrow).....	39
Figure 29 Proposed Mechanism for the Transformation of ATF-1 to YCM-21.....	40
Figure 30 PXRD Patterns of ATF-1, YCM-21 series, and YCM-23 after being soaked in 1M HCl for one week.....	66
Figure 31 PXRD Patterns of YCM-21-spMP after Li ⁺ uptake.....	66
Figure 32 PXRD Patterns of YCM-21-spPP after Li ⁺ uptake.....	67
Figure 33 PXRD Patterns of YCM-21-TEA after Li ⁺ uptake.....	67
Figure 34 PXRD Patterns of YCM-21-TEBA after Li ⁺ uptake.....	68
Figure 35 PXRD Patterns of YCM-21-TEBA after being soaked in DMF solution of spPPBr.....	68
Figure 36 PXRD Patterns of YCM-21-spPP after being soaked in DMF solution of TEBABr.....	69
Figure 37 TGA for YCM-21-TEA.....	69
Figure 38 TGA for YCM-21 TEBA.....	70
Figure 39 TGA for YCM-21-spMP.....	70
Figure 40 TGA for YCM-21-spPP.....	71
Figure 41 TGA for YCM-22.....	71
Figure 42 TGA for YCM-23.....	72

List of Tables

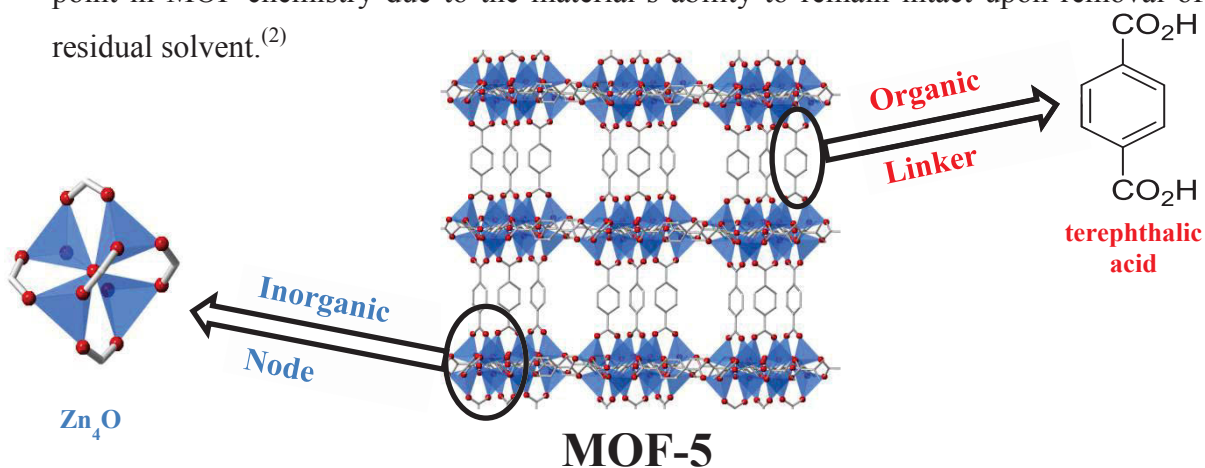
Table 1 Scheme of ATF-1 transformed into YCM-21-TEA with overlaid powdered patterns.....	37
Table 2 Tabular Data for Crystal Structures of the YCM-20 Series.....	74
Table 3 YCM-31 Crystal Data.....	80
Table 4 YCM-32 Crystal Data.....	96
Table 5 YCM-41 Crystal Data.....	113

List of Schemes

Scheme 1 Synthesis of ZJU-28.....	13
Scheme 2 Synthesis of QMOF-2.....	14
Scheme 3 Synthesis of ATF-1.....	15
Scheme 4 Transformation of bio-MOF-101 to bio-MOF-100 and bio-MOF-100 to bio-MOF-102.....	16
Scheme 5 Transformation of MIL-68 to QMOF-2.....	17
Scheme 6 Transformation of SUMOF-1-Zn to SUMOF-1-Cu.....	18
Scheme 7 Transformation of NU-505-Zn to NU-505-Ni.....	18
Scheme 8 Transformation of P11 to P11-Cu.....	19
Scheme 9 Synthesis of ATF-1.....	21
Scheme 10 Synthesis of YCM-21-TEBA.....	22
Scheme 11 Synthesis of YCM-21-TEA.....	24
Scheme 12 Synthesis of YCM-21-spPP.....	25
Scheme 13 Synthesis of YCM-21-spMP.....	27
Scheme 14 Synthesis of YCM-22.....	29
Scheme 15 Synthesis of YCM-23.....	31
Scheme 16 Synthesis of YCM-31.....	42
Scheme 17 Synthesis of YCM-32.....	43
Scheme 18 Synthesis of YCM-41.....	45

Chapter 1: Introduction

‘Metal-organic frameworks (MOFs) are a group of materials that are defined as crystalline inorganic-organic hybrid network structures assembled and sustained by coordination bonds between metal ions or metal-clusters and polydentate organic linking groups.’⁽¹⁾ **Figure 1** displays MOF-5, a three dimensional MOF that is formed by the coordination of terephthalic acid (organic linker) and a zinc oxide cluster (inorganic node). MOF-5, solvothermally synthesized by the Yaghi group in 1999 was a turning point in MOF chemistry due to the material’s ability to remain intact upon removal of residual solvent.⁽²⁾



MOF-5

Figure 1: MOF-5

However, before an in-depth analysis of MOF structure, synthesis, and transformation is given, it is necessary to comment on why MOFs are considered such important materials. The demonstration of permanent porosity by Yaghi’s MOF-5 was groundbreaking since one could now imagine using these materials to house or trap a wide array of molecules that could range from liquids to gases.

MOF Applications

MOFs have since been used in applications such as: gas storage, catalysis, separations, etc.⁽³⁾ A viable application that was quickly realized for MOFs was the possible storage of gases, such as hydrogen gas. Hydrogen fuel cells are thought to be able to compete with gasoline as possible new fuel sources because of their ability to create large amounts of energy while only creating water as a by-product; however, current methods of storing hydrogen gas are extremely unsafe and inefficient.⁽⁴⁾ Overtime, MOFs have come to be thought of as a viable solution to this problem.

In 2003, Yaghi published the hydrogen adsorption properties of MOF-5, IRMOF-6, and IRMOF-8.⁽⁵⁾ This study demonstrated that MOFs have the potential to be very good hydrogen storing materials. Since then, many studies have been conducted on hydrogen adsorption in MOFs, and this experiment has become a benchmark characterization technique in the field. One study that established MOFs as good materials for hydrogen storage was conducted on MOF-177 by the Yaghi group in 2007. This study showed that MOF-177, which is composed of a zinc oxide node coordinated to 1,3,5-benzenetribenzoate (BTB) could adsorb 7.5 wt% H₂ gas at 70 bar.⁽⁶⁾ Since 2007, only two MOFs NU-100 (7.9 wt%, 56 bar) and MOF-210 (9.0 wt%, 56 bar) have reported higher wt% values than MOF-177.^(7,8) It is worthy to note that MOFs have been explored as storage materials for a variety of other gases, but that topic is beyond the scope of this introduction.

MOFs are also widely used in the field of catalysis, and there are currently three ways in which catalytically active sites are incorporated into MOFs: (1) the metal catalyst is used in the construction of the framework as the structural building unit (SBU), (2) incorporating the catalyst into the linker, or (3) post-synthetically loading the MOF with a preferred catalyst (**Figure 2**).⁽⁹⁾

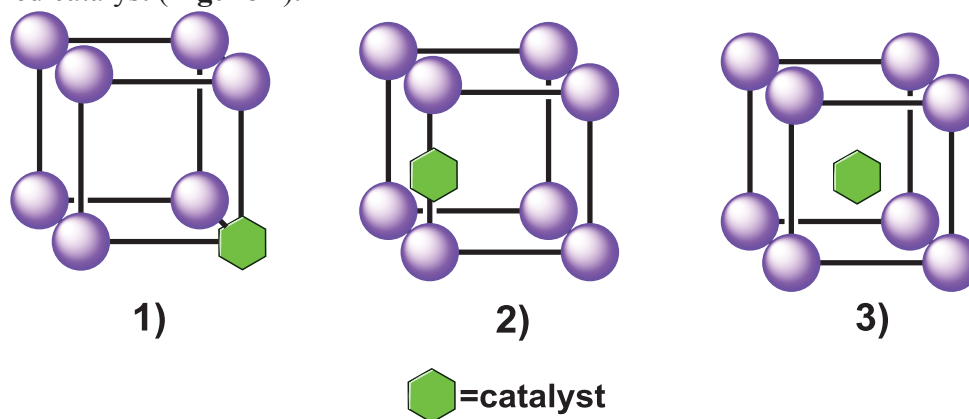


Figure 2: Means in which catalysts are incorporated into MOFs: 1) catalyst incorporated into node or SBU 2) catalyst incorporated into linker. 3) catalyst is post-synthetically loaded into MOF

The earliest reports concerning MOFs as catalysts dealt with the metal center of the SBU becoming unsaturated and participating in catalysis. However, one of the first distinguished MOFs used in Lewis acid catalysis was reported by Kaskel using HKUST-

1 $[\text{Cu}_3(\text{btc})_2(\text{H}_2\text{O})_3]$ to catalyze the cyanosilylation of an aldehyde by the unsaturated Cu(II) metal center.^(10,11,12) Another widely known MOF Cr-MIL-101 has been shown to catalyze a wide range of organic reactions that include allylic oxidations of alkenes to enones, cyanosilylations, as well as others.^(13,14,15)

A second manner in which MOFs participate in catalysis is through substrate-linker interactions. One of the first reports of this type of catalysis was from Lin whom demonstrated that a MOF with a BINOL derived linker can selectively catalyze aromatic aldehydes to secondary alcohols.⁽¹⁶⁾ More recently, Scheidt, Hupp, and Farha have synthesized a MOF with an NHC-derived linker that catalyzes the conjugate addition of alcohols to enones, as well as a MOF with a urea-derived linker (NU-601) that catalyzes a Friedal-Crafts reaction between pyrroles and nitroalkenes (**Figure 3**).^(17,18)

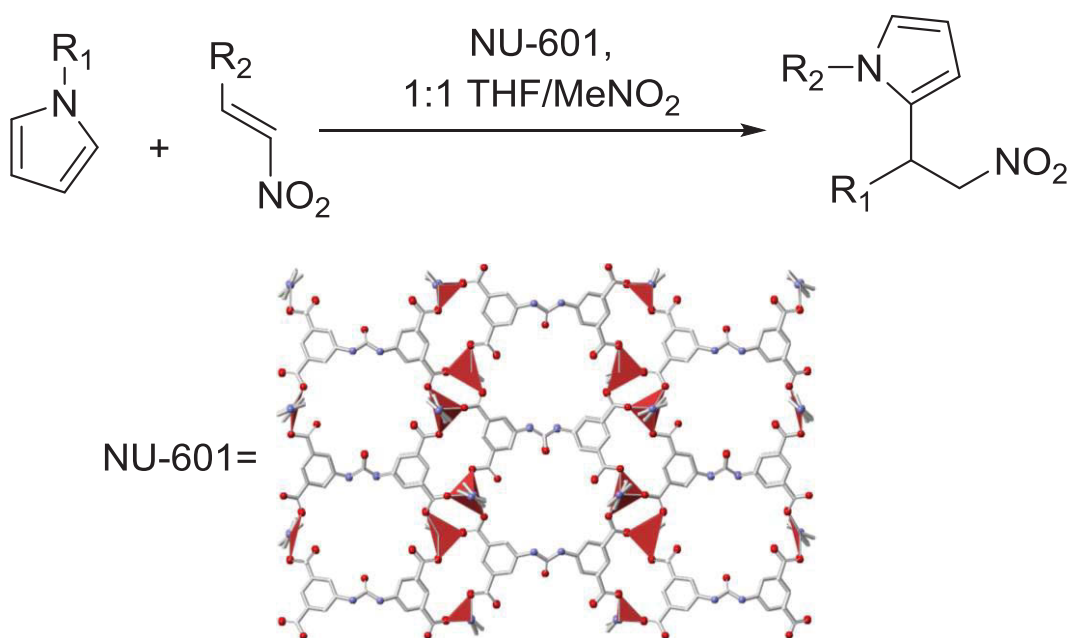


Figure 3: Scheme of NU-601 catalyzed Friedal-Crafts reaction

Thirdly, catalysts can be placed inside the pores of MOFs themselves allowing for a catalyst-substrate interaction. Most of the work completed on this topic has to do with

the loading of nanoparticles or transition metal complexes into the pores of MOFs and then preferentially performing catalysis.^(19, 9) Ferey has demonstrated that MIL-101 housing palladium nanoparticles can catalyze the Heck reaction and Sanford and co-workers have concluded that rhodium transition metal complexes housed in ZJU-28 and MIL-101-SO₃ can catalyze the hydrogenation of alkenes.^(20,21)

Lastly, MOFs have been used in separations, biomedical and sensor applications, as well as conductors.^(3,22) Yan and co-workers have demonstrated that MOF-1 can selectively separate xylene isomers, while Ferey and co-workers have shown that MIL-53 can up-take 20 wt% ibuprofen and systematically deliver the drug over a 3 week period.^(23,24) Also, Chen twice reported MOFs that have luminescent sensor capabilities along with Natarajan and Kim, showing that MOFs can be applicable as conductors in fuel cells.^(25, 26, 27)

MOF Supramolecular Structure

Describing applications in MOF chemistry is of the utmost importance since they are the driving force behind the field. However, my work focuses on MOF synthesis and transformation, more specifically of In-derived MOFs, which will be the topics discussed going forward. There are a variety of characteristics in which MOFs vary: 1) supramolecular structure and dimensionality, 2) linker system (i.e. single or mixed), and 3) structural building unit (SBU) (it is worth noting that all of these factors are interrelated). Due to a wide array of changeable parameters, MOFs can be synthesized to produce a variety of complex and interesting structures. The supramolecular structure of a MOF can be influenced by many factors, but since the linker and node parameters will be focused on later, catenation and important MOFs in the literature will be discussed. There have been many important MOFs synthesized since the field exploded in 1999, but there are a handful that were benchmarks in the field: HKUST-1, UiO-66, and PCN-5 are three of the most recognized MOFs and will be briefly discussed based on their supramolecular differences.

HKUST-1 is a 3-dimensional, non-interpenetrated MOF; the framework is composed of trimesic acid linkers coordinately bound to copper dimers.⁽²⁸⁾ **Figure 4**

shows the crystal structure of HKUST-1 from two different perspectives: **a)** shows how HKUST-1 is 3-dimensionally connected by the two different copper centers, the “center” of the paddle-wheel being of octahedral geometry (**red**), while the other metal center is pseudo-octahedral (**black**), this accounts for the overall supramolecular structure being 3-D.

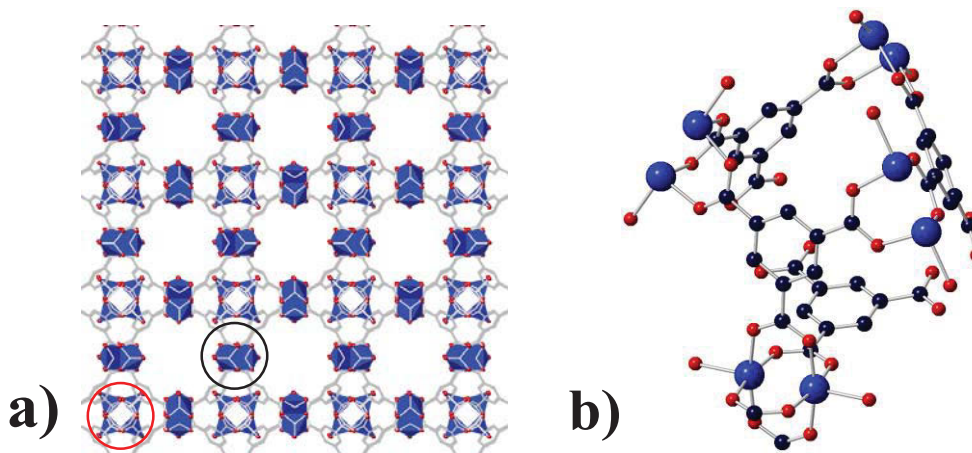


Figure 4: **a)** HKUST-1 with a view of 3-D paddle-wheel supramolecular structure $\{C_{18}H_6Cu_3O_{12}\}$ **b)** HKUST-1 representation showing copper dimers

b) shows a close up view of the dimeric centers of HKUST-1; both copper dimers are chemically identical (geometrically different) with the six oxygens of each linker coordinating to six chemically identical copper atoms, this allows for each dimer to accept eight carboxylate coordinations along with two water ligands, rendering the overall charge neutral. According to the authors, the overall supramolecular structure affords pores of almost one nanometer and a BET surface area of $692.2 \text{ m}^2/\text{g}$ making this material both structurally interesting and important from an applications perspective.⁽²⁸⁾

A second MOF with both an interesting structure and yet a vast supramolecular alteration from HKUST-1 is UiO-66.⁽²⁹⁾ UiO-66 is a 3-D MOF that implements terephthalic acid as the organic linker. UiO-66 forms an SBU with six zirconium atoms, a feat that at the time was unaccomplished in MOF chemistry according to Lillerud (**Figure 5**).

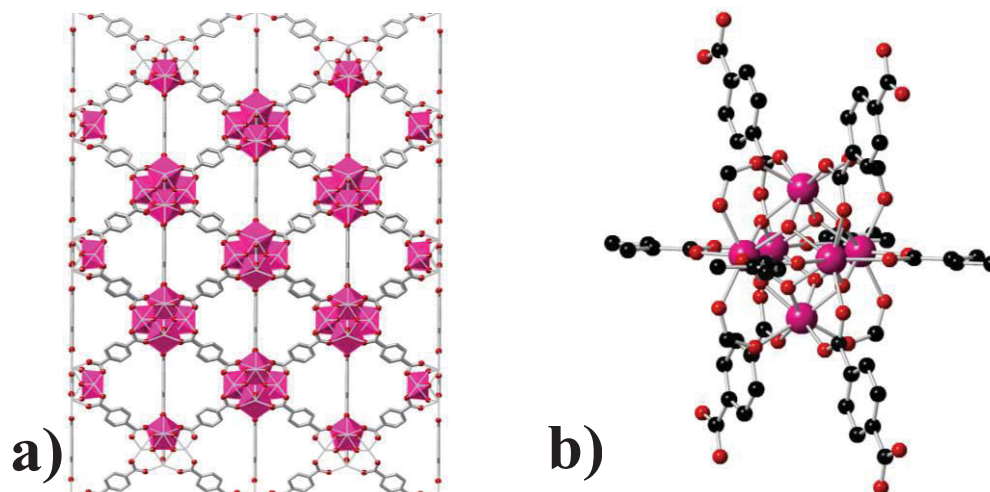


Figure 5: a) 3-dimensional depiction of UiO-66 b) View of UiO-66 SBU

UiO-66 has an $Zr_6O_4(OH)_4$ based SBU where each of the four oxygens from BDC coordinates to four distinct zirconium atoms (12 linkers total); each individual zirconium atom is then coordinated to either four oxygen atoms or hydroxyl molecules allowing each zirconium atom to participate in eight total coordinations.⁽²⁹⁾ UiO-66 forms pores that are ~ 6 Å and produces a BET surface area of 1187 m²/g.⁽²⁹⁾ UiO-66 in comparison to previously mentioned HKUST-1 is both structurally and chemically different. This demonstrates how an almost endless amount of variation can be implemented into MOF synthesis strategy to produce an array of interesting and useful structures.

Lastly, PCN-5 is a 3-dimensional MOF that again exhibits unique properties, but more particularly when in regards to the two previously mentioned MOFs.⁽³⁰⁾ PCN-5 is an interpenetrated MOF, meaning that the two independent frameworks (**Figure 6**) are interwoven and cannot be unlinked unless one of the frameworks is removed. This is a characteristic that neither HKUST-1 or UiO-66 exhibit, but is still fairly common in MOF literature. PCN-5 forms a trimeric nickel SBU where the three nickel atoms are coordinated to 6 triazine tribenzoate ligands and are also coordinately bound to 6 oxygen atoms. The largest pore apertures are ~ 15 Å wide and PCN-5 exhibits a Langmuir surface area of 225 m²/g.⁽³⁰⁾

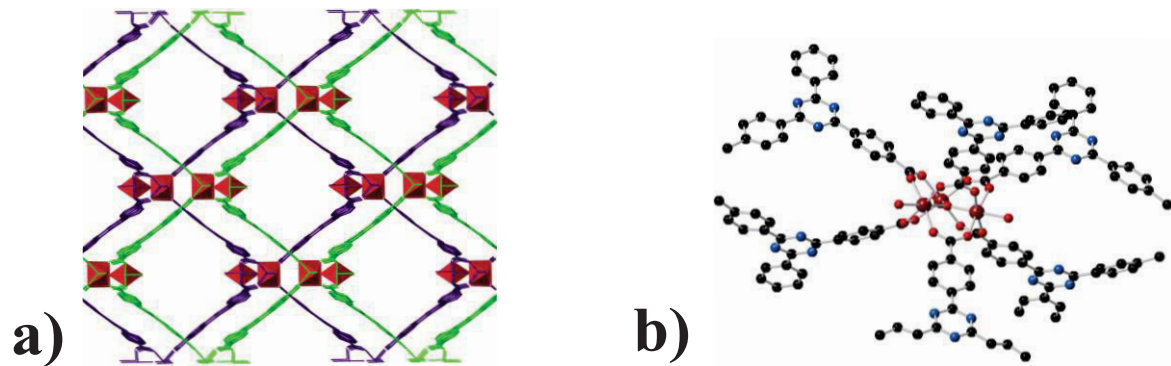


Figure 6: a) View of PCN-5 and its interpenetrated structure b) View of the trimeric, nickel PCN-5 SBU

Effects of Synthesis Parameters on Dimensionality and Topology

Now that demonstration of structure and application diversity of MOFs has been established, a discussion of how a change in synthesis parameters can affect dimensionality and topology will be discussed. MOFs can be synthesized to in three different dimensionalities: three-dimensional (3-D), two-dimensional (2-D), and one-dimensional (1-D).

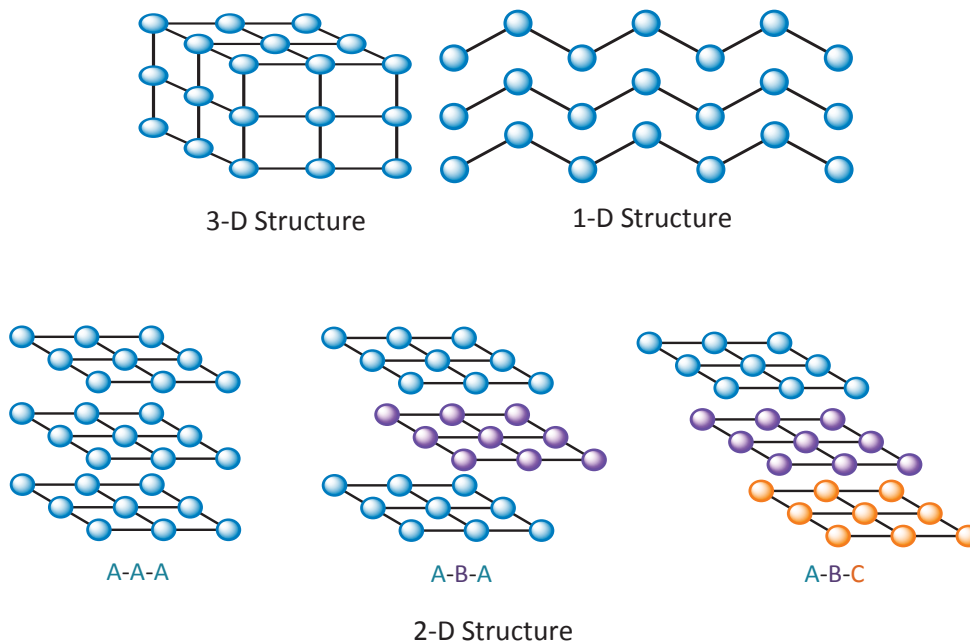


Figure 7: Dimensionality of MOFs

Figure 7 shows a depiction of what 3-D, 2-D, and 1-D MOFs look like in space. A 3-D framework's linker extends from the node in all three Cartesian coordinates (x, y, and z),

a 2-D framework has the linker extending from the node in two Cartesian coordinates, and a 1-D framework has the linker extending from the node in just one Cartesian coordinate, making the linker only coordinately bound to the node through two X type ligand bonds. 2-D frameworks can also vary in the pattern of their individual sheets. One can imagine that a MOF can produce sheets that stack directly on top of one another in a (A-A-A) like fashion; the sheets can stack in such a way that the first two sheets are offset, while the first and third are directly stacked (A-B-A); and lastly the sheets can form in a “stair-like” fashion where all sheets are offset from one another (A-B-C). Dimensionality and topology are such fundamental characteristics in MOF chemistry, and yet so many parameters can affect them. It is well documented that the organic linker and the metal node have perhaps the most significant impact on the dimensionality and topology of the framework; however, it has also been demonstrated that temperature, solvent, and pH can affect those MOF characteristics as well.⁽³¹⁾

It has been shown that the pH of the growth solution can have a significant influence on the produced structure: Cai and Gascon have shown that a change of half a pH unit can drastically change the topology of a framework, while Stock and Bein have shown that pH changes in the synthesis of MOF-5 can produce structures with different topologies and dimensionalities.^(32,33,34) The temperature the MOF is synthesized at can also affect growth: Cepeda and Castillo demonstrated in 2015 that both temperature and pH have a drastic effect on the dimensionality and topology of scandium (III) MOFs, while Natarajan demonstrated that temperature alone affects the dimensionality of manganese MOFs (**Figure 8**).^(35,36) Lastly, Zaworotko has shown that varying temperature and concentration can produce two distinct Cadmium (II) MOFs.⁽³⁷⁾ Choice of solvent in a synthesis is also extremely important; Many MOF chemists have shown that choice of solvent can control whether catenation is observed or not, while Mazaj demonstrated that different ratios of ethanol to water directly controls dimensionality in magnesium (II) MOFs.^(38,39,40,41)

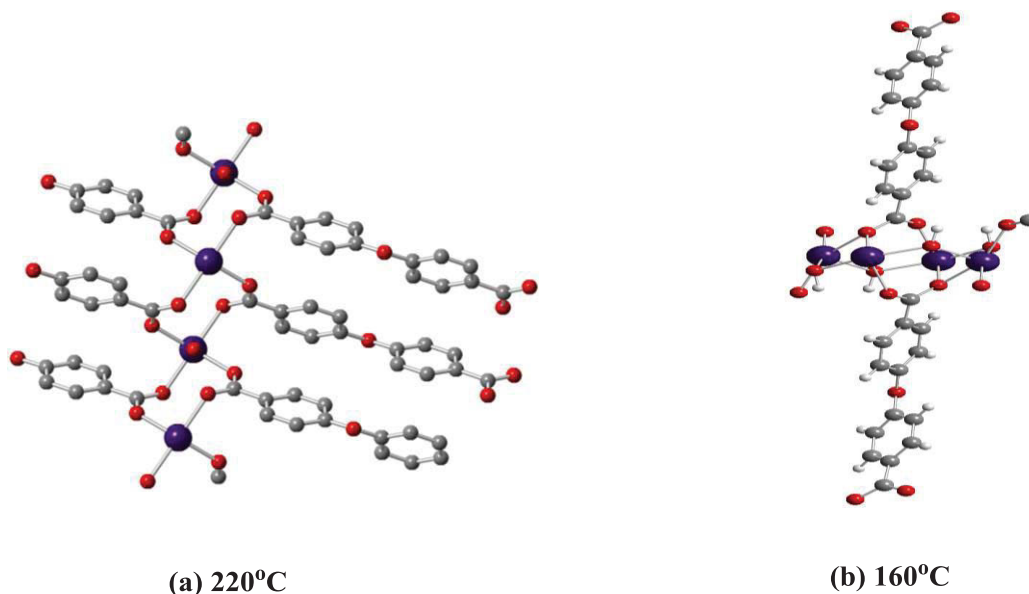


Figure 8 (Natarajan): (a) 2-D MOF: $[\text{Mn}(\text{H}_2\text{O})\{\text{C}_{12}\text{H}_8\text{O}(\text{COO})_2\}]$, (b) 3-D MOF: $[(\text{Mn}(\text{OH})_2)\{\text{C}_{12}\text{H}_8\text{O}(\text{COO})_2\}]$,

All of the parameters previously mentioned can affect the outcome of a MOF growth, but the use of additives or template directed synthesis is another useful facet of MOF synthesis that can affect topology and dimensionality. It is also worth mentioning that template directed synthesis has been known to produce structures that were previously thought to be inaccessible.

Template-directed MOF Synthesis

There are several examples in the literature that demonstrate the usefulness of template directed synthesis. In 2012 Kwon and Cunha-Silva reported that imidazolium salts with variation in functional group produced two structurally different manganese MOFs.⁽⁴³⁾ When an ethyl functionalized imidazolium salt was implemented a 3-D framework was produced. The SBU of this MOF's coordination environment has two bound carboxylates to two different metals while the other two are singly bound by one oxygen (monodentate).

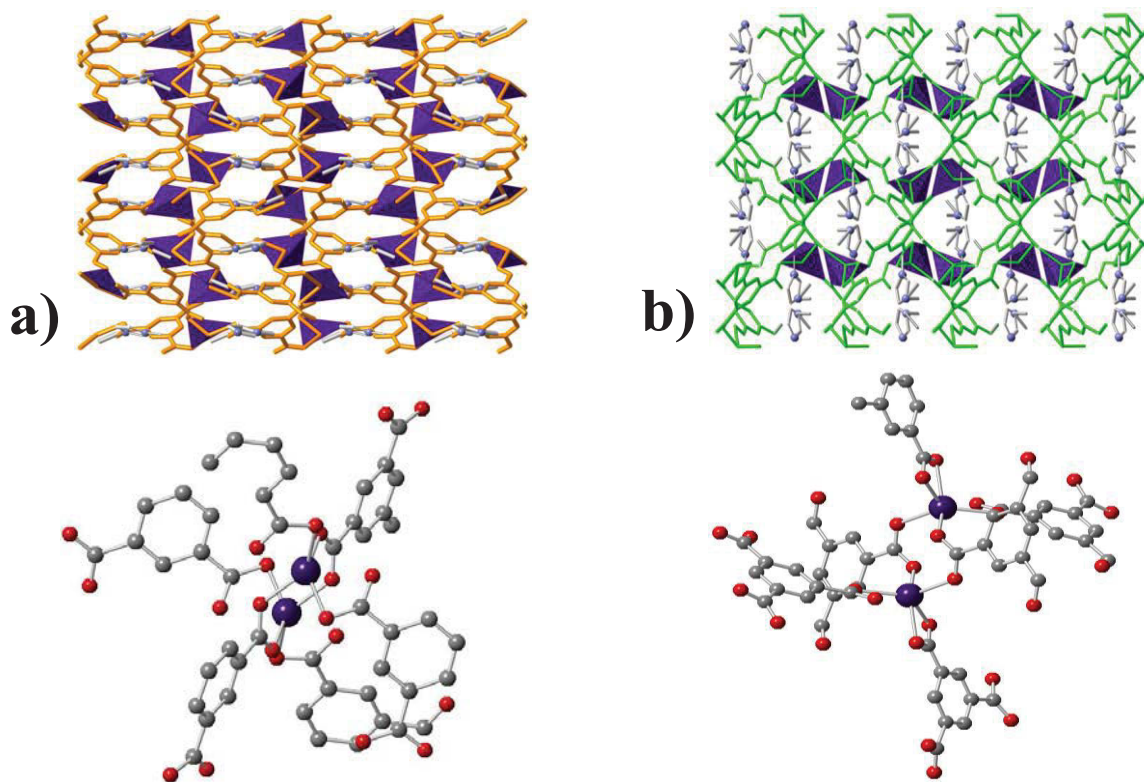


Figure 9: a) View of MOF synthesized from ethyl imidazolium salt with its corresponding node underneath b) View of MOF synthesized from propyl imidazolium salt with its corresponding node underneath

When the additive is then switched to a propyl functionalized imidazolium salt, the SBU changes. The coordination environment (Mn) now has one κ^2 -coordination to a linker, one singly bound oxygen from another linker (monodentate), and two carboxylates where each oxygen is bound to a different metal (**Figure 9**). In both cases the cation is observed crystallographically inside the pores; this is an important aspect of these two structures since the additive is the only chemical difference. This leads one to assume the cation is acting as a directing agent for overall structure.

Secondly, in 2014 Cao reported an indium-derived MOF (FJI-C1) with the use of a tetraethyl ammonium salt. FJI-C1 is a 3-D interpenetrated MOF with an indium (III) metal center; The indium is coordinately bound to four carboxylates (κ^2 -coordination) rendering the entire framework negatively charged with the cation resting inside the pores of said framework (**Figure 10**).⁽⁴⁴⁾

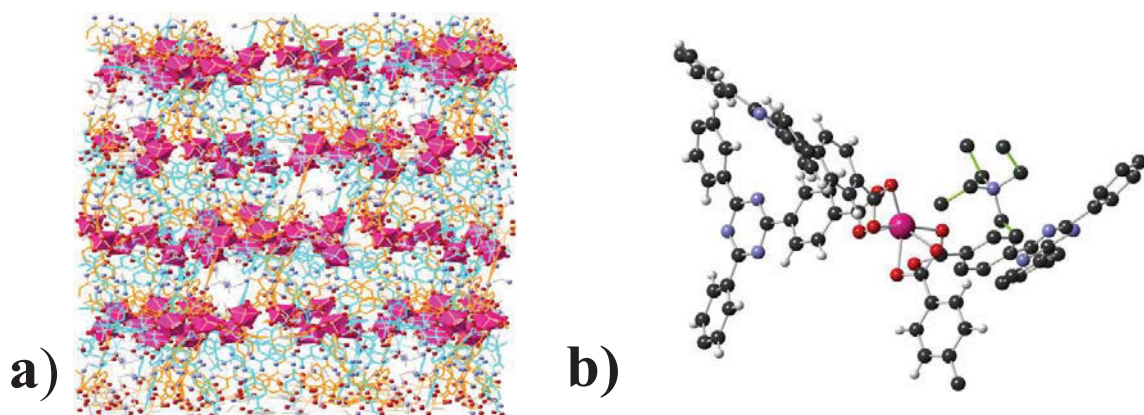


Figure 10: a) 3-D view of FJI-C1 b) View of FJI-C1 SBU

The SBU of this MOF produces a tetrahedral geometry which accounts for the dimensionality of the framework. FJI-C1 was also subjected to a series of application driven experiments and it was found that this MOF can selectively separate C_2 hydrocarbons, an astonishing feat due to a cation already resting inside of the framework itself.

Indium-derived MOFs

Now that template directed synthesis has been discussed, it is now fitting to present a summary of important indium based MOFs due to their relativeness to my own project. Indium MOFs like all others can vary in linker, but it is more common practice to categorize indium MOFs based on SBU or the coordination environment of indium itself. Indium is very versatile in its coordination chemistry and is known to be able to bind up to seven X-type ligands producing an overall formal charge of negative four.^(45,46) Although indium is very adaptable in regards to number of ligands it accepts, in MOF chemistry it is customarily found as either monomeric $[In(O_2CR)_4]^-$, trimeric $\{In_3O(O_2CR)_6(H_2O)_3\}^+$, or infinite chain $[In(\mu-O_2CR)_2(\mu-OH)]_\infty$ (**Figure 11**).⁽⁴⁷⁻⁵⁹⁾ Furthermore, each coordination mode varies in formal charge which allows for vast combinations in structure.

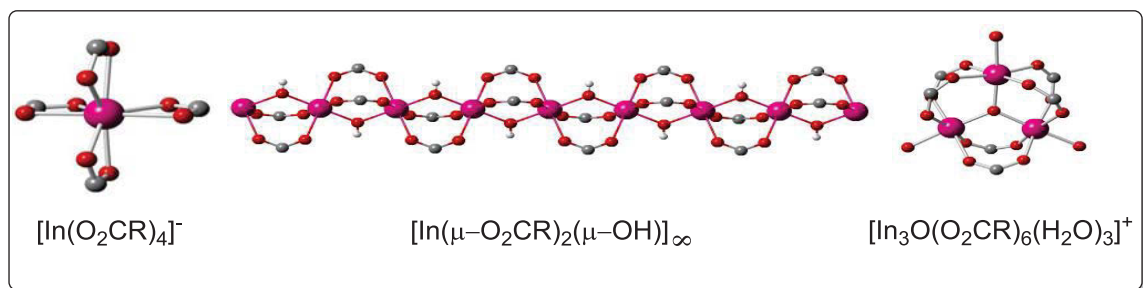


Figure 11: Common indium coordination modes (MOFs)

There are numerous examples of these three coordination modes in the literature with respect to MOF chemistry, but recently Feng demonstrated that three coordination modes were accessible through minuscule changes in synthetic condition.⁽⁶⁰⁾

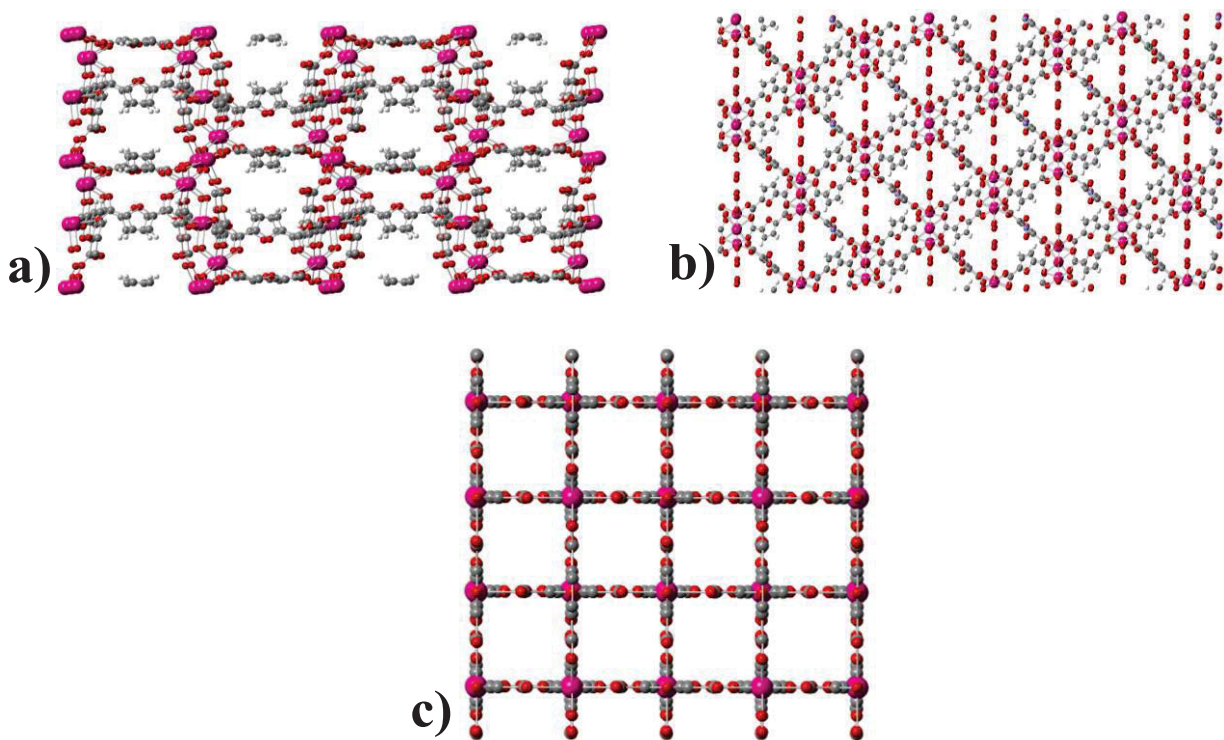
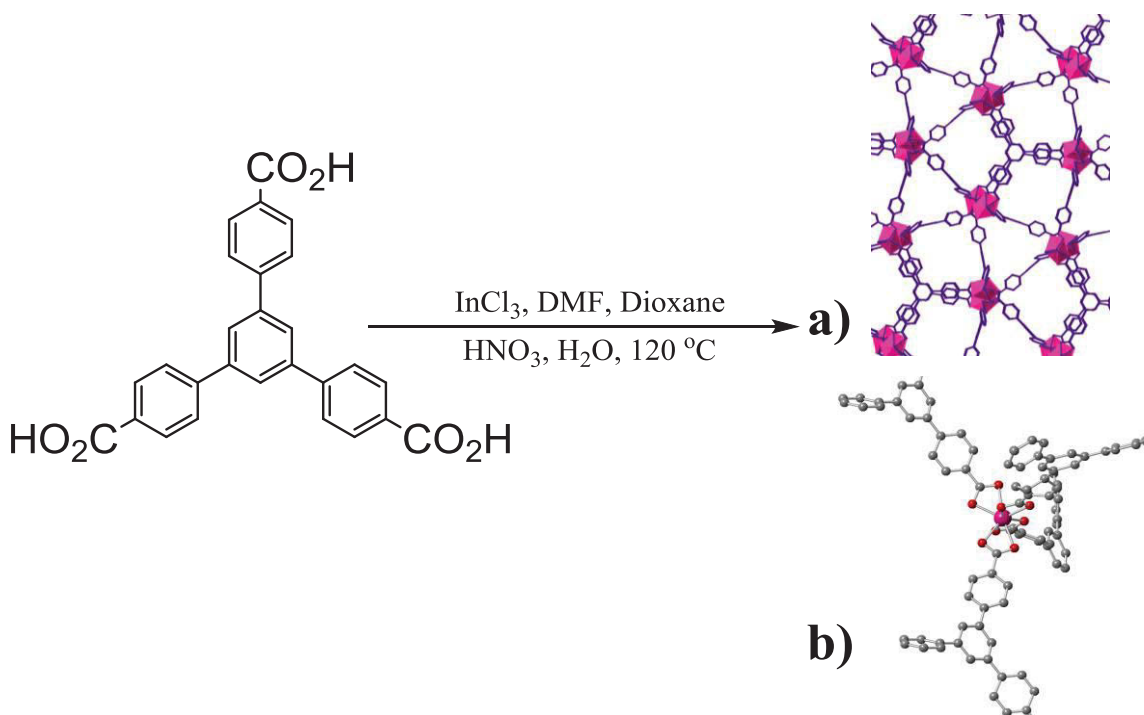


Figure 12: a) 3-D MOF with indium infinite chain b) 3-D MOF with indium oxide SBU (trimer) c) 2-D MOF with indium tetracarboxylate SBU (monomer)

When a 1:1 mixture of linker (2, 5-furandicarboxylic acid (FDA)) and metal ($\text{In}(\text{NO}_3)_3 \cdot \text{XH}_2\text{O}$) is applied, a 3-D framework with an indium oxide (trimer) SBU is produced. In contrast, when the amount of metal is decreased by half, a 2-D MOF is observed with a negatively charged monomeric SBU. Lastly, with a 1:1 mixture of linker

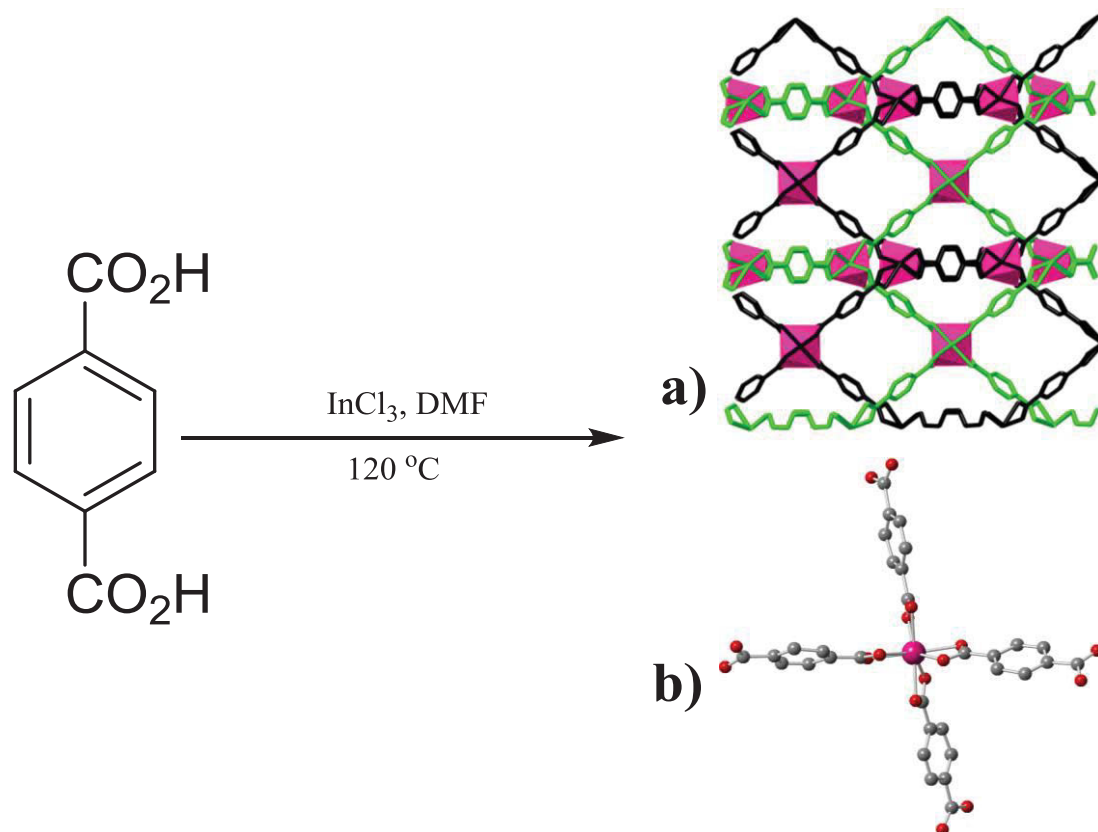
to metal and with the addition of tetramethylurea as a template, a 3-D MOF with the infinite chain SBU is witnessed (**Figure 12**).

In MOF literature, there are several examples of anionic indium MOFs; however, a few that I have dealt with specifically are ZJU-28, QMOF-2, and ATF-1. ZJU-28 is a 3-D, interpenetrated, anionic MOF that utilizes BTB or (1, 3, 5-benzenetricarboxylic acid) as the organic linker and indium chloride as the metal source.⁽⁶¹⁾ The framework's largest pore aperture is ~ 9 Å and the SBU of ZJU-28 is pseudo-tetrahedral with the indium metal κ^2 -coordinated to four BTB linkers producing the 3-D MOF (**Scheme 1**).



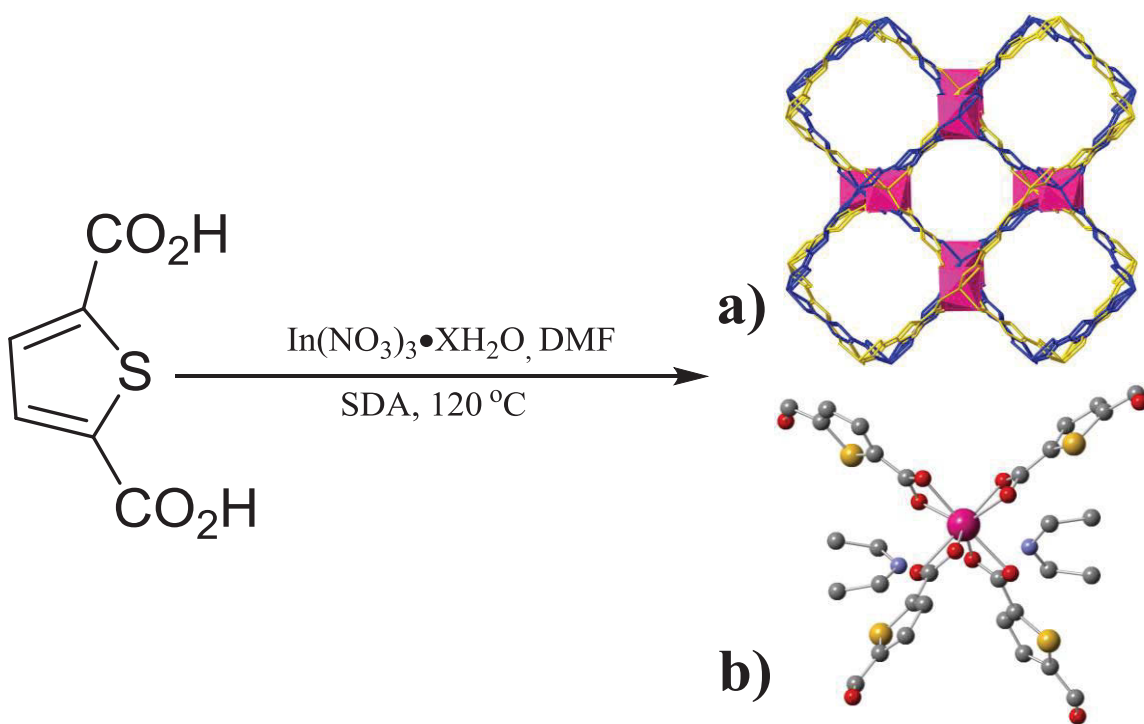
Scheme 1: Synthesis of ZJU-28 **a)** 3-D view of ZJU-28 **b)** SBU of ZJU-28

QMOF-2 is a 3-D, anionic MOF that employs terephthalic acid as the organic linker and indium chloride as the metal source.⁽⁶²⁾ QMOF-2 exhibits 2-fold interpenetration with a “quartz-like” topology. The SBU of QMOF-2 includes four terephthalic acid linkers coordinated to a single indium atom (κ^2 -coordination). The overall geometry of the SBU itself is pseudo-tetrahedral accounting for the overall 3-D geometry of the MOF, and the largest aperture size being ~ 10 Å (**Scheme 2**).



Scheme 2: Synthesis of QMOF-2 **a)** 3-D view of 2-fold interpenetrated QMOF-2 **b)** SBU of QMOF-2

Lastly, and most pertinent to my own research is ATF-1. ATF-1 is a homochiral, 3-D, interpenetrated framework that like the two formerly mentioned MOFs is anionic; the material is synthesized from 2,5-thiophenedicarboxylic acid (TDC) and indium nitrate hydrate.⁽⁶³⁾ Interestingly, when either (-)-cinchonidine or (+)-cinchonine is added to the synthesis, the MOF is grown enantiopure. The largest pores of ATF-1 are around $\sim 14\text{ \AA}$ in diameter, while the SBU of ATF-1 contains one indium metal κ^2 -coordinated to four carboxylates and is observed in a pseudo-tetrahedral geometry (**Scheme 3**). Lastly, ATF-1, ZJU-28, and QMOF-2 all exhibit the monomeric SBU $[\text{In}(\text{O}_2\text{CR})_4]^-$, which is what allows these MOFs to be geometrically and electronically related.



Scheme 3: Synthesis of ATF-1 **a)** 3-D view of 2-fold interpenetrated ATF-1 **b)** SBU of ATF-1

Solid-state to solid-state MOF Conversion

Solid-state to solid-state conversion of MOFs, a form of post-synthetic modification (PSM) will be discussed. In its simplest form, solid-state to solid-state MOF reactions involve subjecting a pre-synthesized MOF to a exogenous chemical species that allows for a new material to be formed.⁽⁶⁴⁾ Currently, two different approaches exist in regards to transforming a pre-existing MOF. The first consists of subjecting the parent MOF to a chemically different linker; this permits a linker exchange that yields either an isorecticular structure or a MOF that is structurally different from the parent.^(65, 66) A similar alteration can occur with the addition of exogenous metal; this allows for either a transmetalation that produces an isorecticular structure or a metal exchange that allows for structural rearrangement leading to an architecturally distinct supramolecular material (**Figure 13**).^(67, 68)

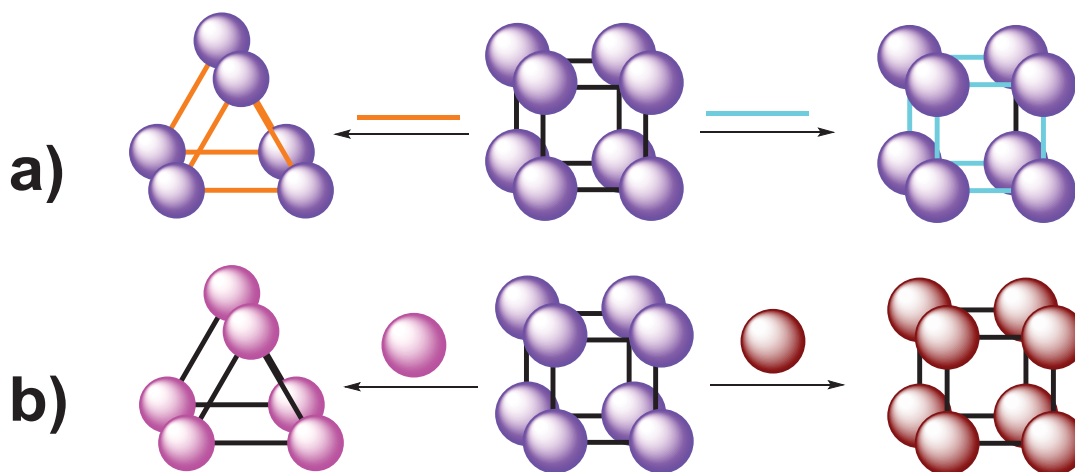
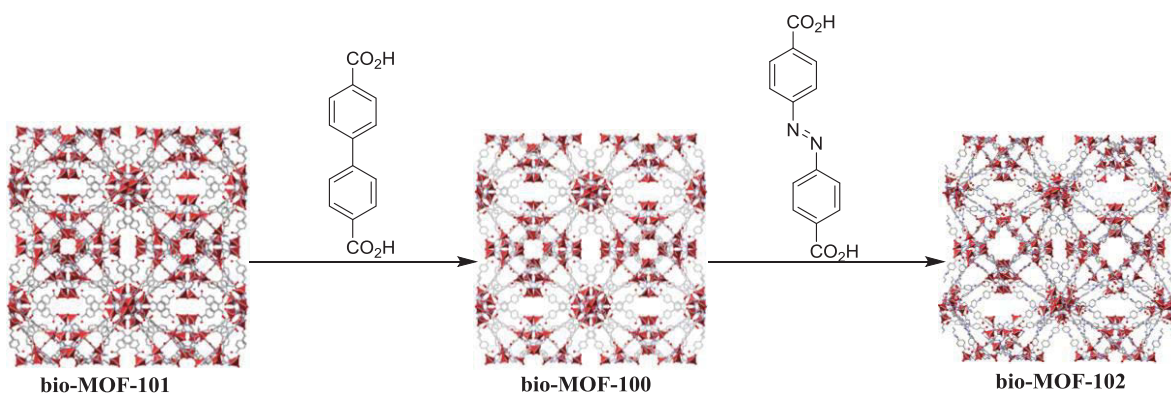


Figure 13: a) linker exchange with supramolecular amendment (blue) and without (orange) b) metal exchange with supramolecular amendment (blue) and without (orange)

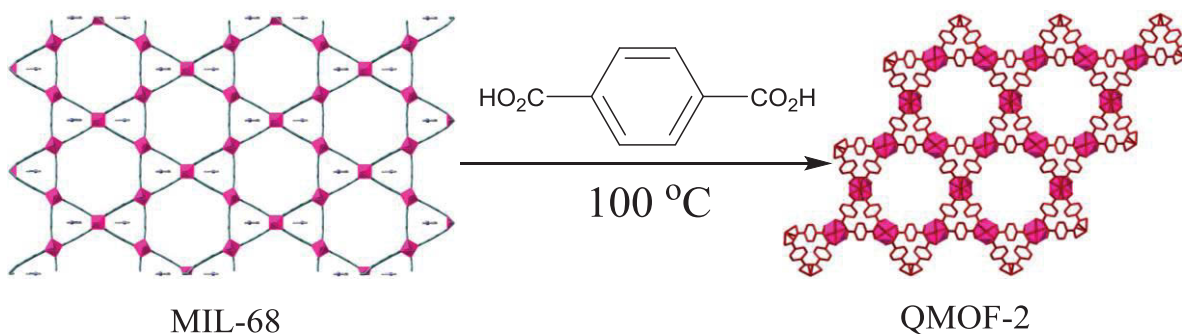
Linker exchange that produces isorecticular structures has been extensively studied. Rosi reported in 2013 two separate transformations: The first involved subjecting pre-synthesized bio-MOF-101 ($\text{Zn}(\text{OAc})_2 \cdot 6\text{H}_2\text{O}$, adenine, and 2,6-naphthalene dicarboxylic acid) to a solution of 4,4-biphenyldicarboxylate; after 24 h it was observed that bio-MOF-101 had fully transformed into bio-MOF-100, an isorecticular structure to its parent MOF. Sequentially, pre-synthesized bio-MOF-100 ($\text{Zn}(\text{OAc})_2 \cdot 6\text{H}_2\text{O}$, adenine, and 4,4-biphenyldicarboxylate) was then subjected to azobenzene-4,4'-dicarboxylate, and a structure was observed that was isorecticular to both bio-MOF-101 and bio-MOF-100 (Scheme 4).⁽⁶⁵⁾



Scheme 4: Transformation of bio-MOF-101 to bio-MOF-100 and bio-MOF-100 to bio-MOF-102

Seth Cohen has also contributed substantially to this particular type of research. Cohen has demonstrated that if two different MIL-53/MIL-68 derivatives are suspended in solution, a new MOF that incorporates components of both structures is produced (solid-solid), as well as the more common exchange of either linker or metal through the addition of a said solution to a suspended MOF (solid-liquid).⁽⁶⁶⁾

The other possible outcome when a pre-synthesized MOF is subjected to a new linker, is a rearrangement of the supramolecular structure. Though there are fewer examples of this type of transformation in the literature; Oh demonstrated in 2014 that when MIL-68 was subjected to an excess of linker at 100 °C, a transformation from MIL-68 to QMOF-2 occurs (**Scheme 5**).⁽⁶⁷⁾



Scheme 5: Transformation of MIL-68 to QMOF-2

MIL-68 is a 3-D, neutral, non-interpenetrated MOF connected by either hexagons or triangles, with indium at the vertices. In contrast, QMOF-2 is a 3-D, anionic, interpenetrated MOF that forms with a “quartz-like” topology (**Scheme 5**).

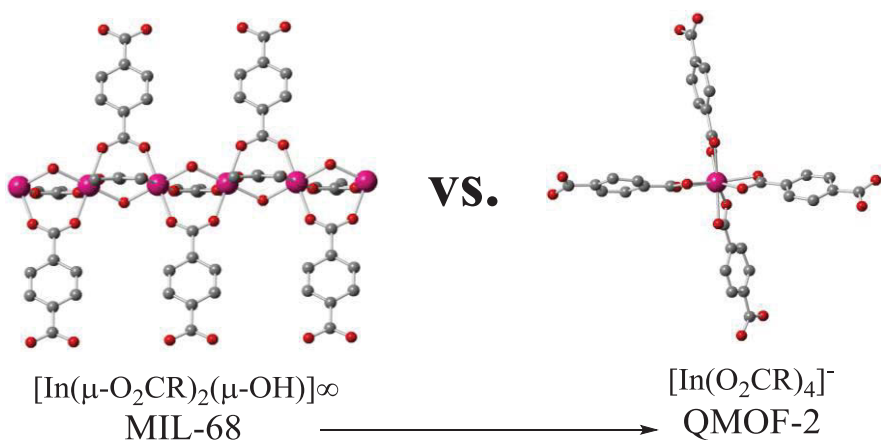
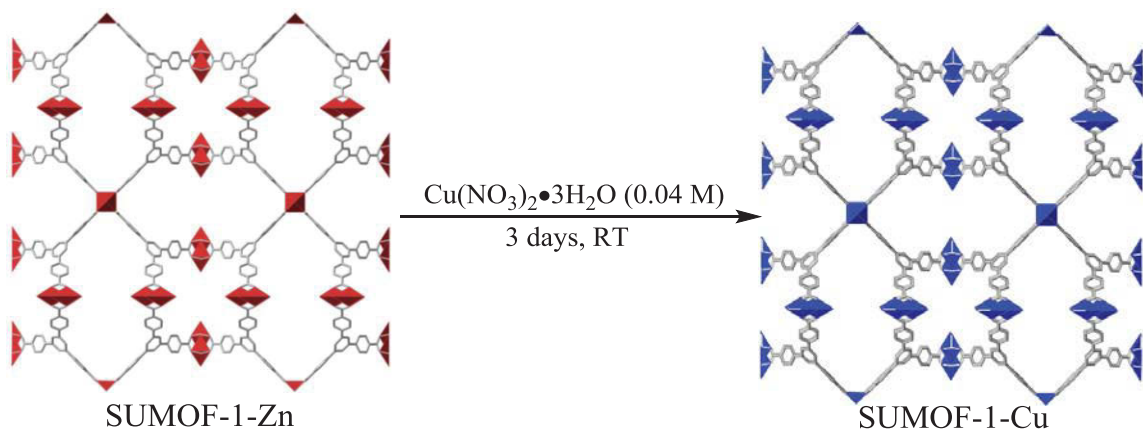


Figure 14: SBU comparison of MIL-68 and QMOF-2

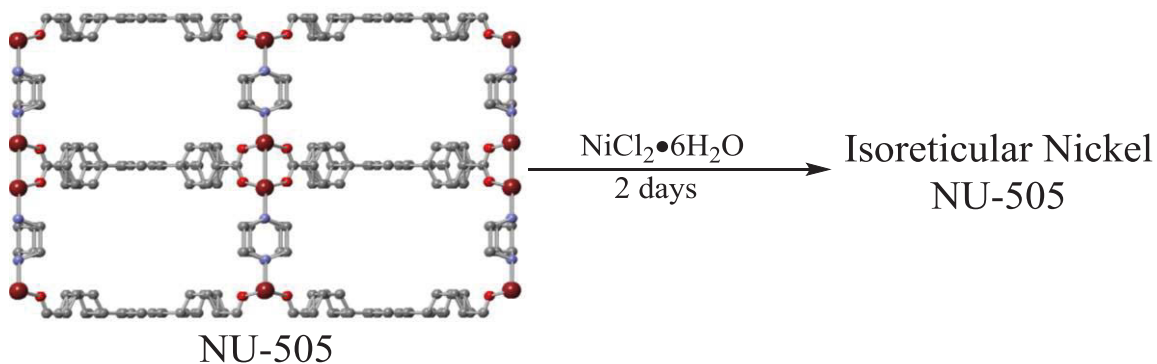
Though the supramolecular differences between MIL-68 and QMOF-2 are apparent, the difference in SBU is not. With further investigation into the two structures, realization that MIL-68 forms the infinite chain SBU, while QMOF-2 forms the monomeric SBU sheds light in regards to why these two structures appear so three-dimensionally different (**Figure 14**).

Switching focus to solid-state to solid-state conversion of MOFs with the metal as the additive, much has been done in the field of transmetalation. Zou and co-workers revealed in 2012 that subjecting pre-synthesized SUMOF-1



Scheme 6: Transformation of SUMOF-1-Zn to SUMOF-1-Cu

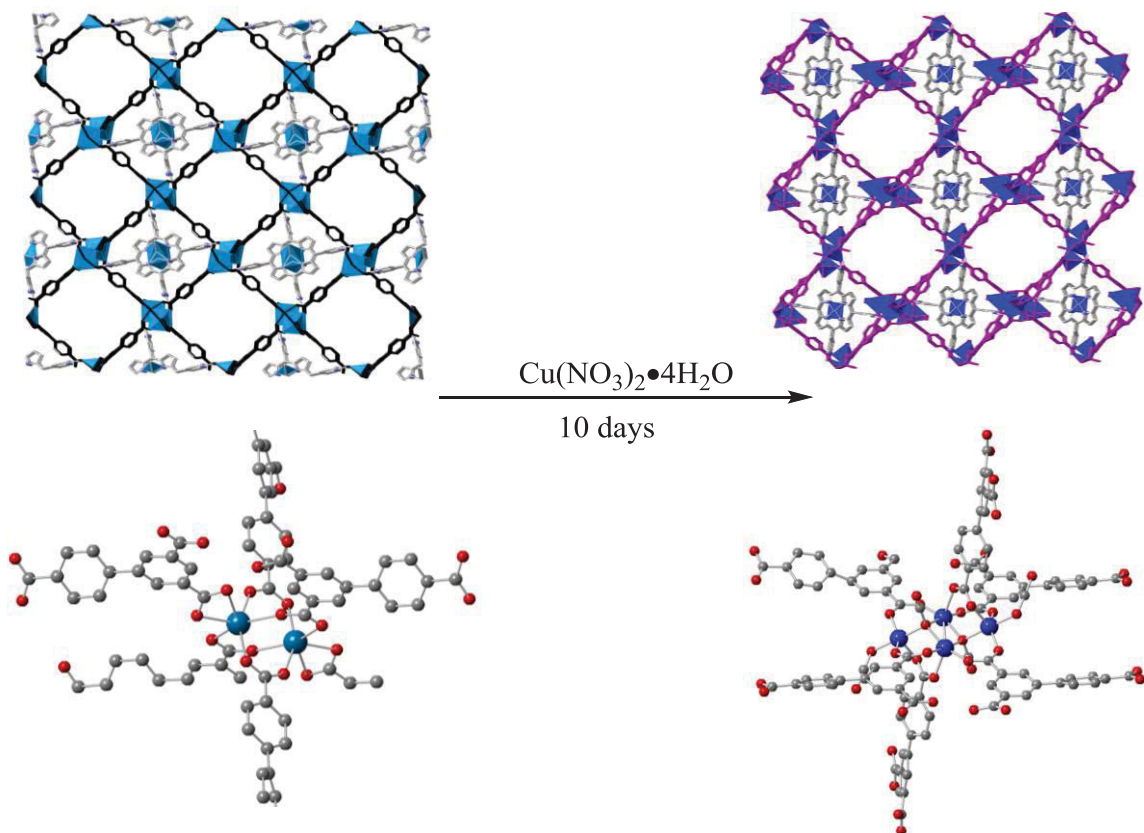
(H₃BTB, bipyridine, Zn(NO₃)₂·6H₂O) to copper nitrate hydrate for three days afforded isorecticular SUMOF-1-Cu, where a complete transmetalation of zinc to copper was observed (**Scheme 6**).⁽⁶⁸⁾ Similarly, Hupp and co-workers established that subjecting NU-505 (H₄TBAPy, Zn(NO₃)₂·6H₂O) to a solution of nickel chloride hydrate for 2 days yielded completely transmetalated NU-505-Ni (**Scheme 7**).⁽⁶⁹⁾



Scheme 7: Transformation of NU-505-Zn to NU-505-Ni

(More extensive reviews on this subject can be found in the references).^(70, 71)

Lastly, a second mode of action that can occur when a pre-synthesized MOF is subjected to a metal additive is a rearrangement of structure. Literature on this topic is extremely limited, however; Zaworotko reported that porphyrin encapsulated MOFs could participate in complete metal exchange with both the SBU and the porphyrin molecule, interestingly with complete rearrangement of the SBU itself (**Scheme 8**).⁽⁷²⁾



Scheme 8: Transformation of P11 to P11-Cu

porph@MOM-11 or P11 ($\text{Cd}(\text{NO}_3)_2 \cdot 4\text{H}_2\text{O}$), biphenyl-3,4,5-tricarboxylate (H_3BPT), and meso-tetra(*N*-methyl-4-pyridyl) porphinetetratosylate (TMPyP)) is a 3-D MOF with a dinuclear cadmium SBU and porphyrin molecules encapsulated in the structure. Each cadmium is coordinated to four organic linkers and κ^2 -coordinated to one. Remarkably, when P11 is introduced to a copper nitrate hydrate solution for ten days, complete cadmium to copper metal exchange occurs. Furthermore, P11-Cu is a tetranuclear SBU with two different geometrical copper sites, however; both sites are chemically equivalent with each copper bound to three organic linkers and coordinated to two oxygen atoms. It is important to note that although the SBU of P11-Cu is geometrically and chemically

different than P11, only changes in pore size and torsion angle of the linker are observed. The “core” supramolecular structure of P11 seems to remain intact.

Results and Discussion

Chapter 2: YCM-20 Series

The original goal of our research was to synthesize new and interesting MOF structures through a directly correlatable template effect. The organic linker and metal source were then chosen based on a number of possible interactions we believed could occur between the exogenous cation and the new framework. 2,5-thiophenedicarboxylic acid (TDC) was chosen as the organic linker due to the hypothesis that the thiophene ring could participate in: π interactions (purple); as well as the sulfur atom being able to participate in Lewis base interactions (orange) or hydrogen bonding interactions (pink). Lastly, it was thought the carboxylate could participate in hydrogen bonding (red). Indium chloride was also chosen purposefully due to **1**) indium’s versatile coordination chemistry, **2**) its ability to form anionic frameworks, and **3**) it could participate in hydrogen bonding (blue) (**Figure 15**).

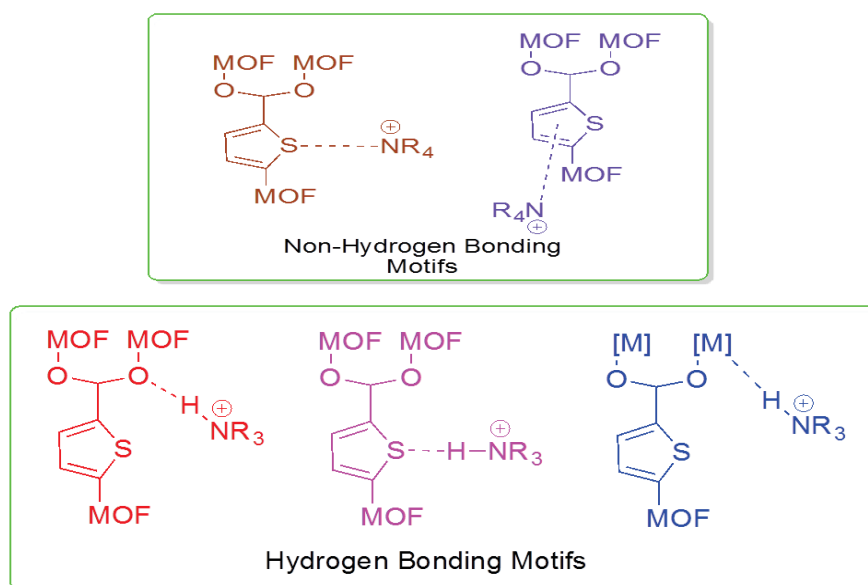
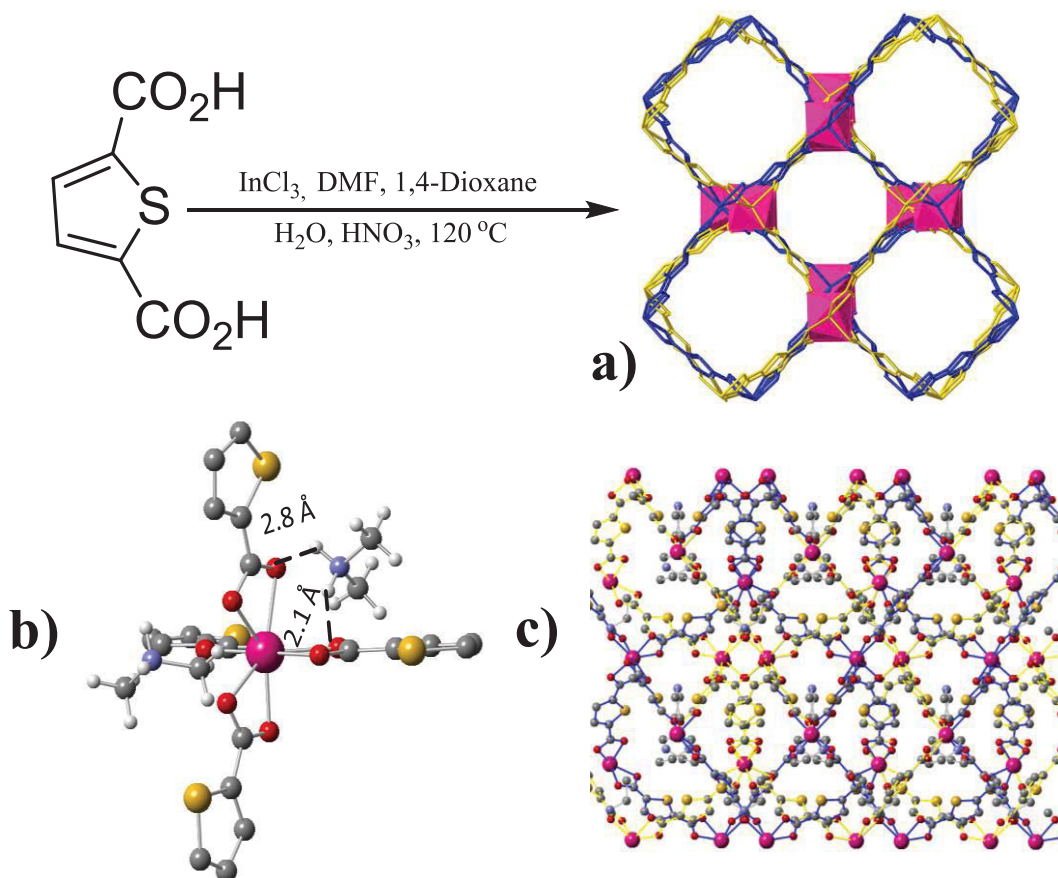


Figure 15: Possible framework-template interactions that can occur in newly synthesized MOFs

With Bu's research in mind, research commenced by addition of InCl_3 (2.13 equiv) and TDC (1.00 equiv) to a mixture of DMF, 1,4-dioxane, and water. To that solution, conc. HNO_3 was added and solvothermal synthesis at 120°C yielded previously reported homochiral ATF-1 (**Scheme 9**).⁽⁷³⁾

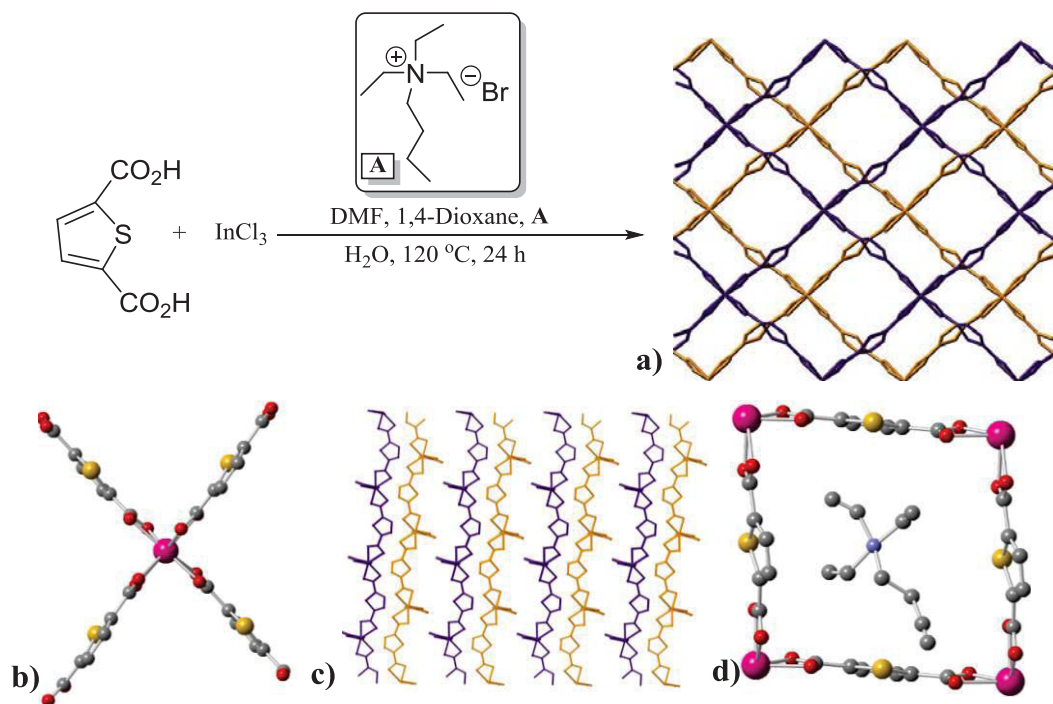


Scheme 9: Synthesis of ATF-1 **a)** ATF-1 showing interpenetrated frameworks **b)** ATF-1 node with O-N bond distances **c)** Single sheet of ATF-1 showing 2-fold interpenetration

ATF-1 is a three-dimensional, anionic, interpenetrated MOF. Dimethylammonium (DMA) cation, from the thermal decomposition of DMF, sits in the apertures of ATF-1 as a charge balancing cation. ATF-1 exhibits *cis* In-In-In bond angles of 83.7° , 97.7° , 98.7° and 113.3° and *trans* In-In-In bond angles of 131.0° and 133.8° making the geometry of the SBU pseudo-tetrahedral. The hydrogen-oxygen distances are 2.1 Å and 2.8 Å demonstrating a hydrogen bonding interaction with the DMA cation. Research efforts

were then shifted to replacing the nitric acid in the ATF-1 synthesis with quaternary ammonium cations in the hopes that a template effect would be achieved, leading to new and architecturally different MOFs. This allowed the solvothermal synthesis of four new two-dimensional, anionic MOFs YCM-21-Z (Youngstown Crystalline Material) with Z indicating templating cation.

The first MOF of the YCM-21 series was synthesized using ATF-1 conditions, with nitric acid being replaced with triethylbutylammonium bromide (TEBA) (**A**) (1.77 equiv) (**Scheme 10**). YCM-21-TEBA is a 2-D, anionic MOF with an **A-B-A-B** (isomorph is **A-B-A'-B'**) sheet pattern. The node of YCM-21-TEBA adopts a pseudo-square planar geometry with trans In-In-In bond angles of 180.0° and cis In-In-In bond angles of 96.5° and 83.5° . The carbon-carbon distances between sheets **B-A** and **A-B** are 9.0 \AA and 5.0 \AA respectively. Each pore is $10.2 \times 10.2 \text{ \AA}$ with the nitrogen of the cation sitting approximately in the “center” of the pore (S-N distances of 5.1 \AA and 5.2 \AA).



Scheme 10: Synthesis of YCM-21-TEBA a) 3-D view of YCM-21 TEBA b) YCM-21-TEBA node c) View of repeating **A-B-A-B** sheet pattern d) YCM-21-TEBA pore with cation

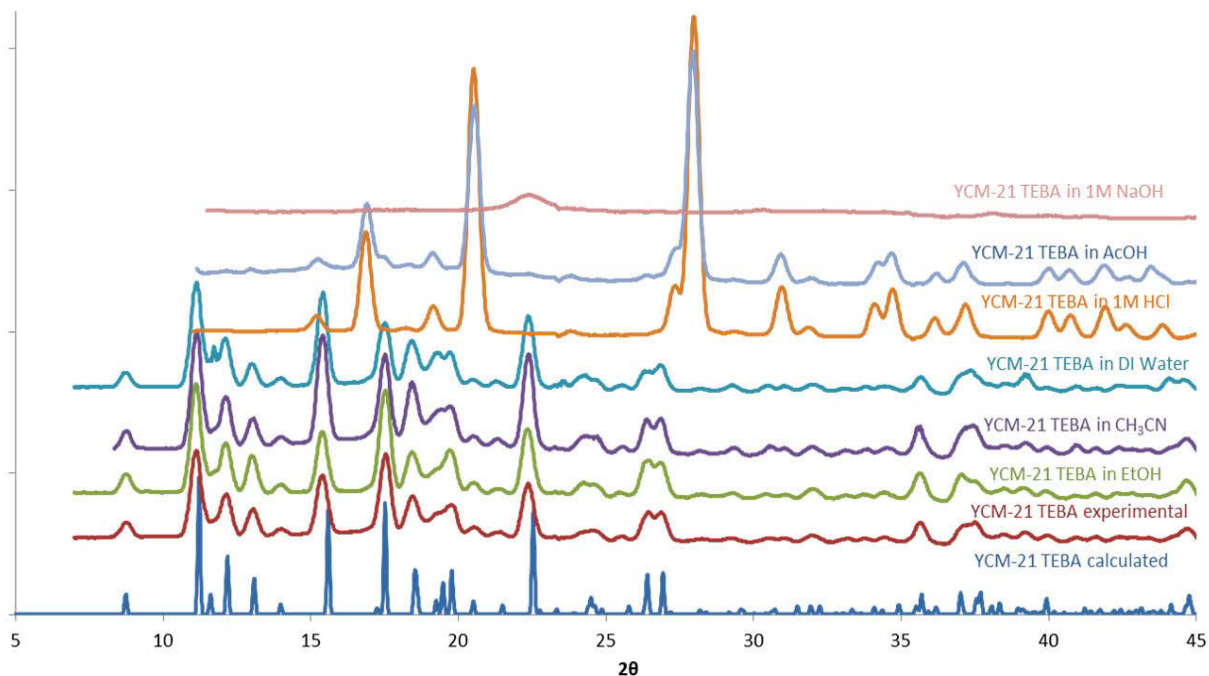
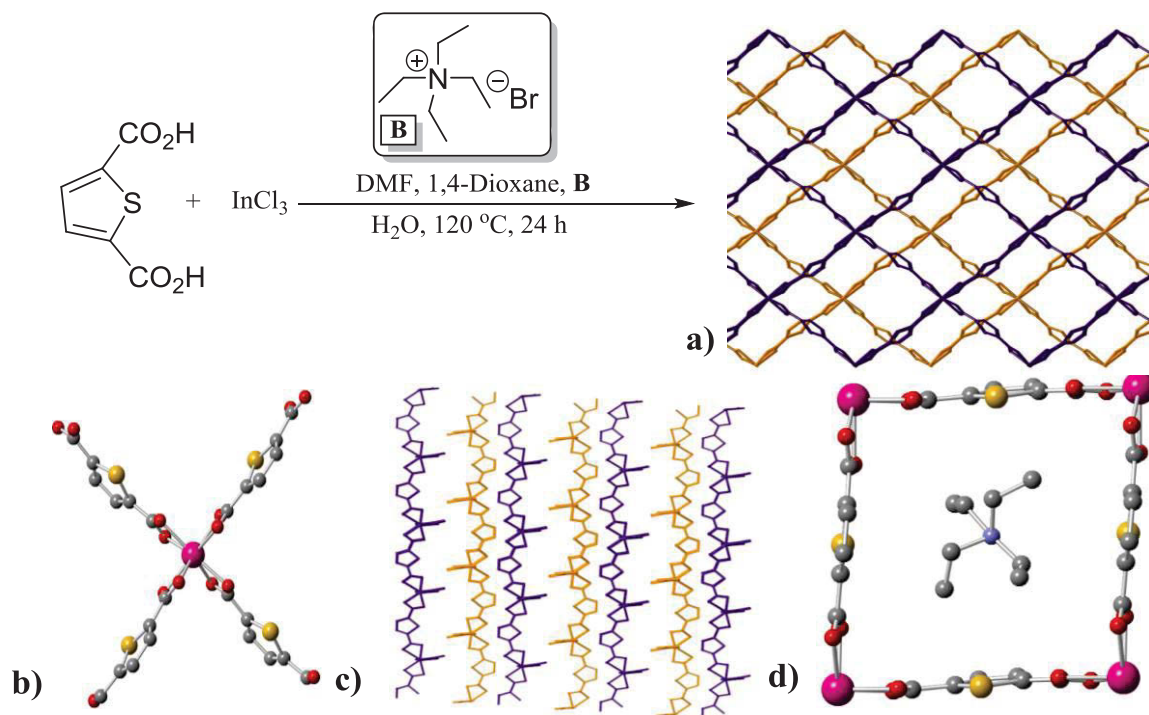


Figure 16: YCM-21-TEBA stability studies (1 week)

Figure 16 shows overlaid PXRD patterns of YCM-21-TEBA suspended in listed solvent for 1 week. YCM-21-TEBA's structure remains intact after one week suspended in EtOH, CH₃CN, and DI water, though the structure begins to decompose in 1M HCl, 1M NaOH, and conc.

The second structure that was achieved in the YCM-21 series was YCM-21-TEA (**Scheme 11**). This structure is synthesized using tetraethylammonium bromide (**B**) as a templating additive. The YCM-21-TEA structure is a 2-D, anionic MOF with an A-B-A-B sheet pattern and is isomorphous to previously mentioned YCM-21-TEBA. The node of YCM-21-TEA adopts a pseudo-square planar geometry with *trans* In-In-In bond angles of 180.0° and *cis* In-In-In bond angles of 93.6° and 86.4°. The carbon-carbon distances between sheets B-A and A-B are 8.9 Å and 5.1 Å respectively. Each pore is 10.2 x 10.2 Å with the nitrogen of the cation sitting approximately in the “center” of the pore (S-N distances of 5.3 Å and 4.9 Å).



Scheme 11: Synthesis of YCM-21-TEA **a)** 3-D view of YCM-21-TEA **b)** YCM-21-TEA node **c)** View of repeating A-B-A-B sheet pattern **d)** YCM-21-TEA pore with cation

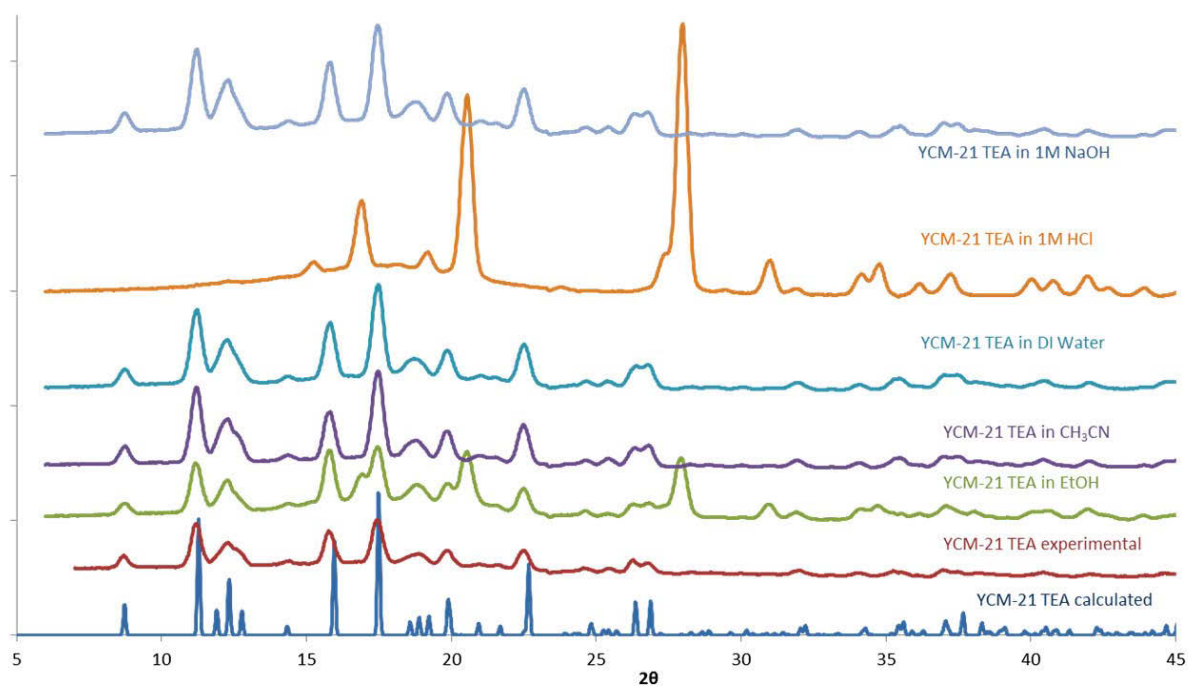
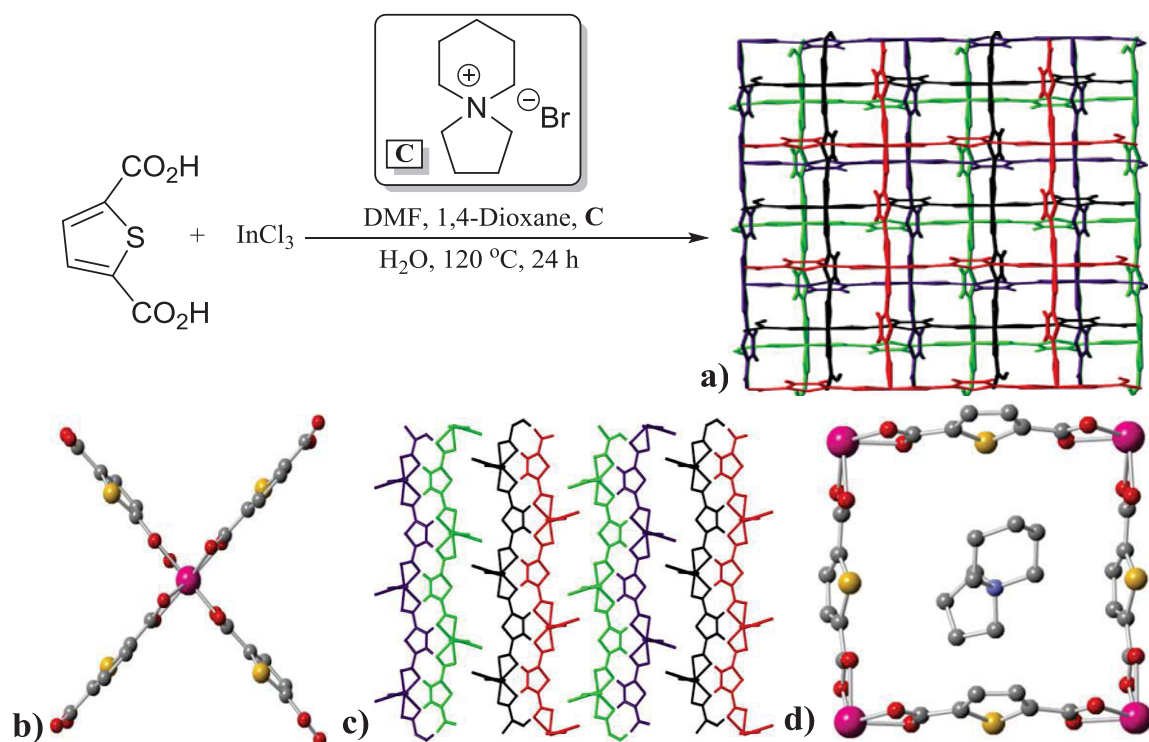


Figure 17: YCM-21-TEA stability studies (1 week)

Figure 17 shows overlaid PXRD patterns of YCM-21-TEA suspended in listed solvent for 1 week. YCM-21-TEA's structure remains intact after one week suspended in EtOH, CH₃CN, and DI water; however, it begins to decompose in 1M HCl, 1M NaOH, while completely decomposing in conc. AcOH.

Thirdly, YCM-21-spPP is synthesized using *N*-spirocyclicpiperidiniumpyrole bromide (**C**) as a templating additive (**Scheme 12**). YCM-21-spPP structure is a 2-D, anionic MOF with an **A-B-A'-B'** sheet pattern. The node of YCM-21-spPP adopts a *pseudo*-square planar geometry with *trans* In-In-In bond angles of 180.0° and *cis* In-In-In bond angles of 90.0°. The carbon-carbon distances between sheets: **A-B** is 5.0 Å, **B-A'** is 9.2 Å, **A'-B'** is 5.0 Å, and **B'-A** is 9.3 Å respectively. Each pore is 10.2 x 10.2 Å with the nitrogen of the cation sitting approximately in the “center” of the pore (S-N distances of 5.2 Å, 5.0 Å, 5.2 Å, 5.1 Å)



Scheme 12: Synthesis of YCM-21-spPP **a)** 3-D view of YCM-21-spPP **b)** YCM-21-spPP node **c)** View of repeating **A-B-A'-B'** sheet pattern **d)** YCM-21-spPP pore with cation

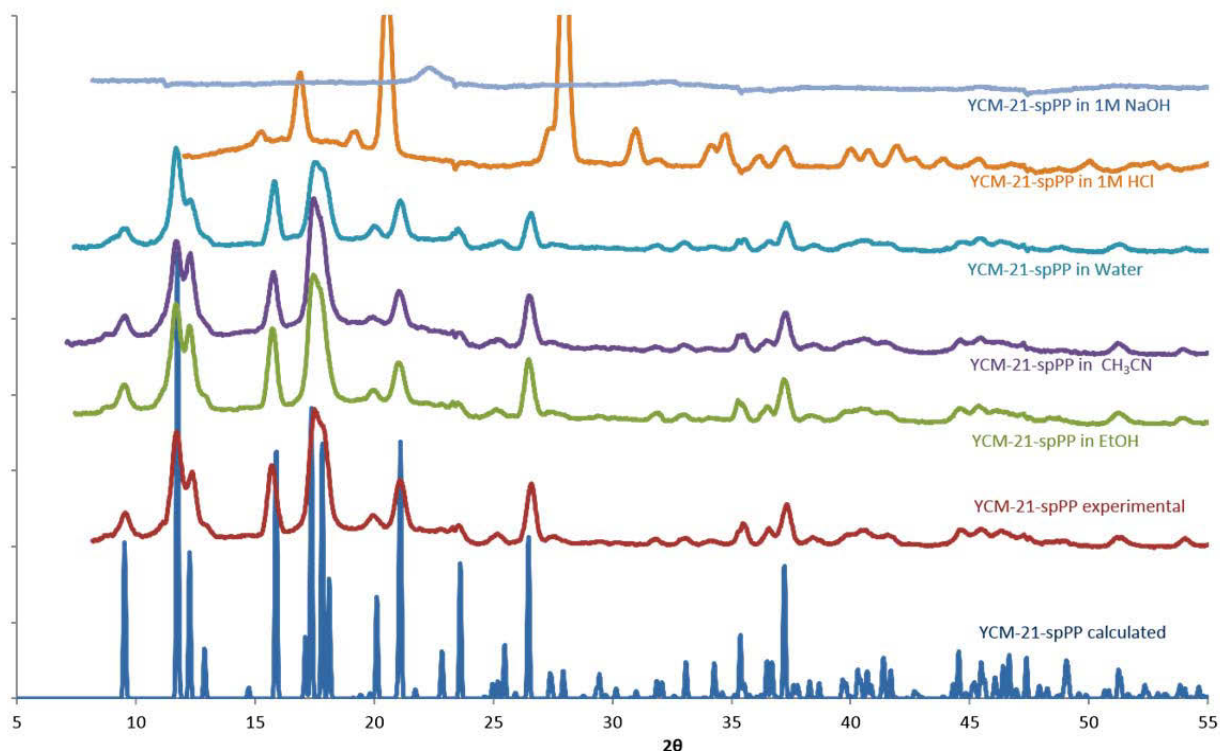
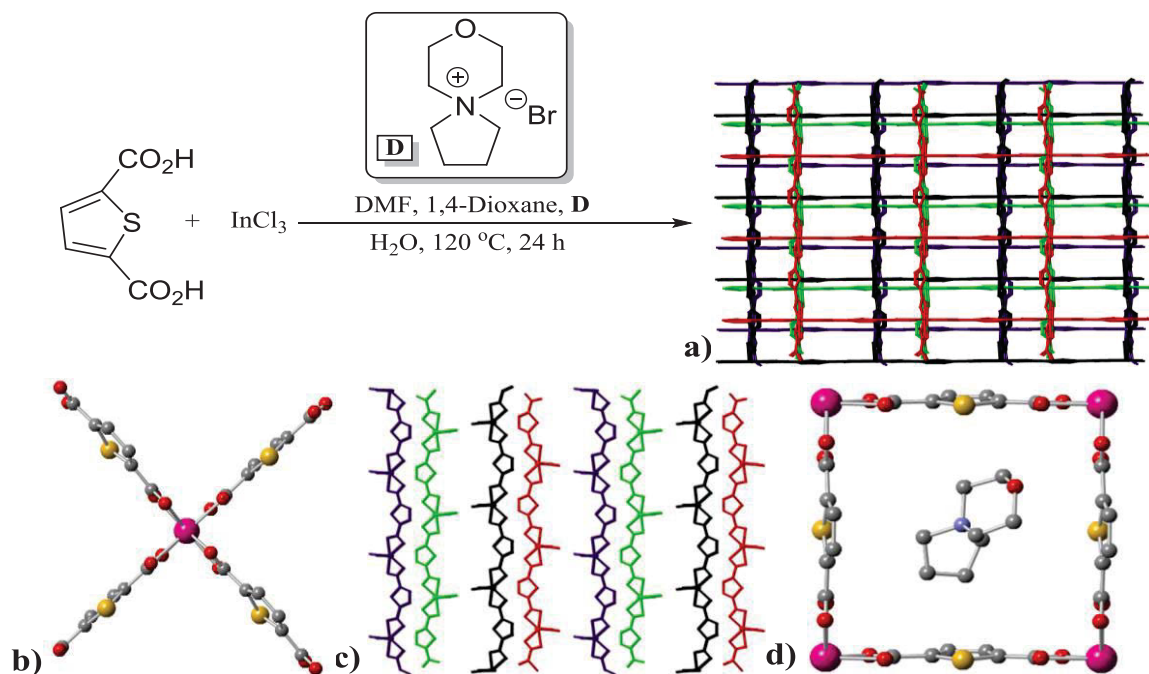


Figure 18: YCM-21-spPP stability studies (1 week)

Figure 18 shows overlaid PXRD patterns of YCM-21-spPP suspended in listed solvent for 1 week. YCM-21-spPP structure remains intact after one week suspended in EtOH, CH₃CN, and DI water; however, it begins to decompose in 1M HCl, and completely decomposes in 1M NaOH and conc. AcOH.

Lastly, YCM-21-spMP is synthesized using *N*-spirocyclicmorpholiniumpyrole bromide (**D**) as the templating additive (**Scheme 13**). YCM-21-spMP structure is again a 2-D, anionic MOF with an A-B-A'-B' sheet pattern. The node of YCM-21-spPP adopts a pseudo-square planar geometry with *trans* In-In-In bond angles of 180.0° and *cis* In-In-In bond angles of 90.0°. The carbon-carbon distances between sheets: (A-B/A'-B') is 5.3 Å, while (B-A'/B'-A) is 10.6 Å respectively. Each pore is 10.2 x 10.2 Å with the nitrogen of the cation sitting approximately in the “center” of the pore (S-N distances of 5.0 Å, 5.1 Å, 5.3 Å, and 5.6 Å).



Scheme 13: Synthesis of YCM-21-spMP **a)** 3-D view of YCM-21-spMP **b)** YCM-21-spMP node **c)** View of repeating A-B-A'-B' sheet pattern **d)** YCM-21-spMP pore with cation

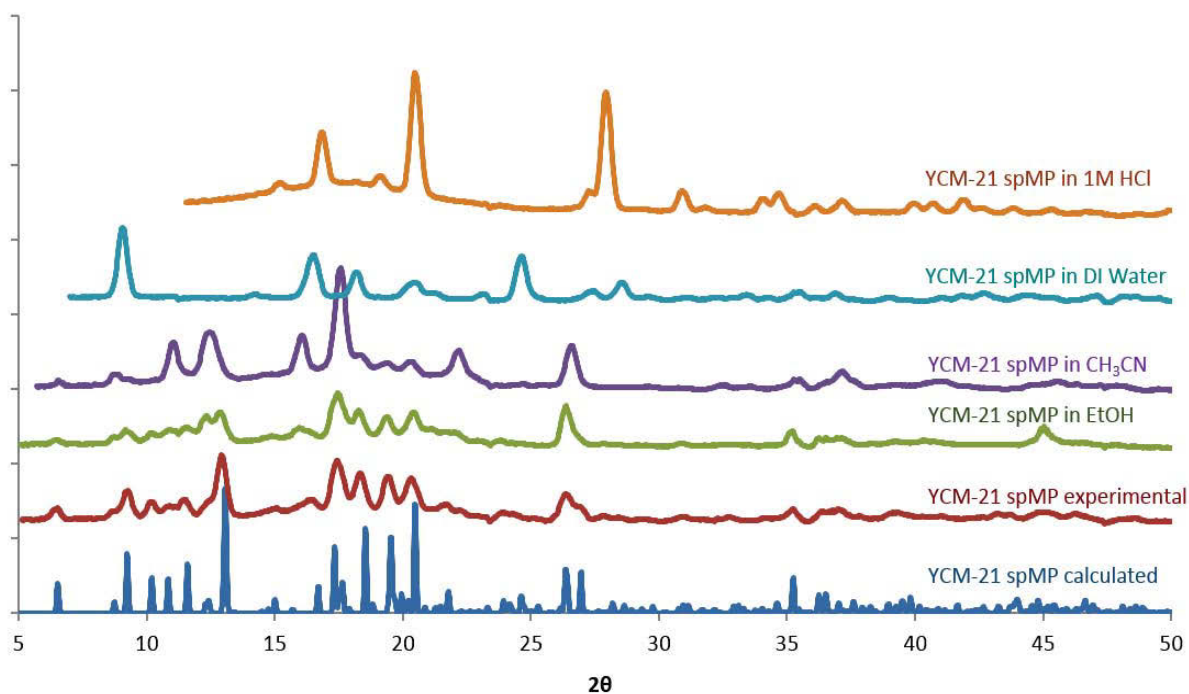


Figure 19: YCM-21-spPP stability studies (1 week)

Figure 19 shows overlaid PXRD patterns of YCM-21-spMP suspended in listed solvent for 1 week. YCM-21-spMP structure remains intact after one week suspended in EtOH. YCM-21-spMP begins to decompose in CH₃CN, DI water, and 1M HCl; while the MOF completely decomposes in 1M NaOH and conc. AcOH.

Analysis of the ammonium cations in the YCM-21 series indicates the interaction between the framework and template cation is cation- π . The arrival to this conclusion came from the following reasons: 1) the cation- π distance is within 3.5 Å for all *N*-centered cations 2) The cation is coplanar with the pi system of the thiophene linker and is not coplanar with the sulfur atom of the thiophene, this essentially eliminates the possibility of the interaction being Lewis base-cation (**Figure 20**).

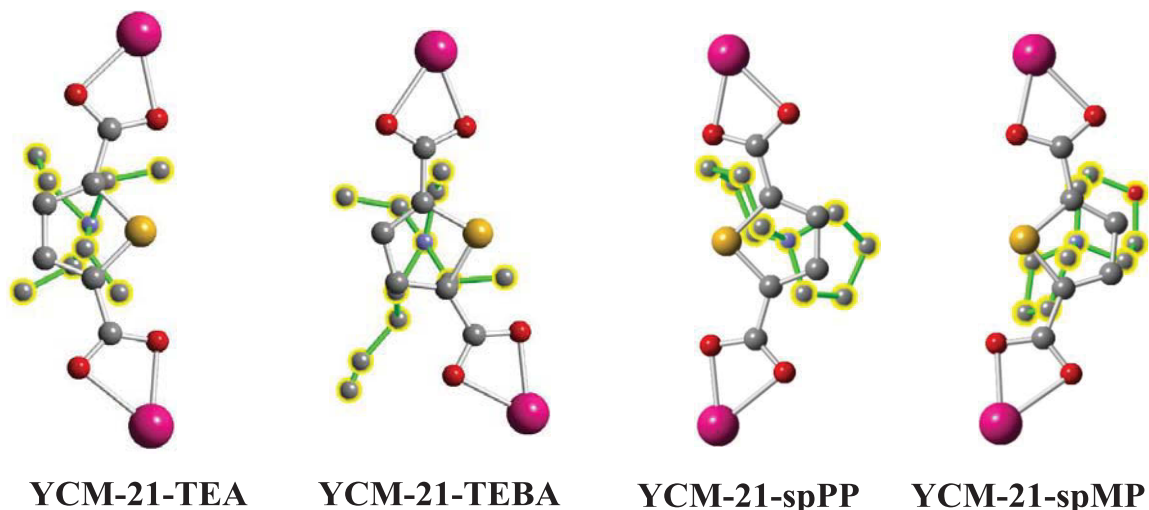
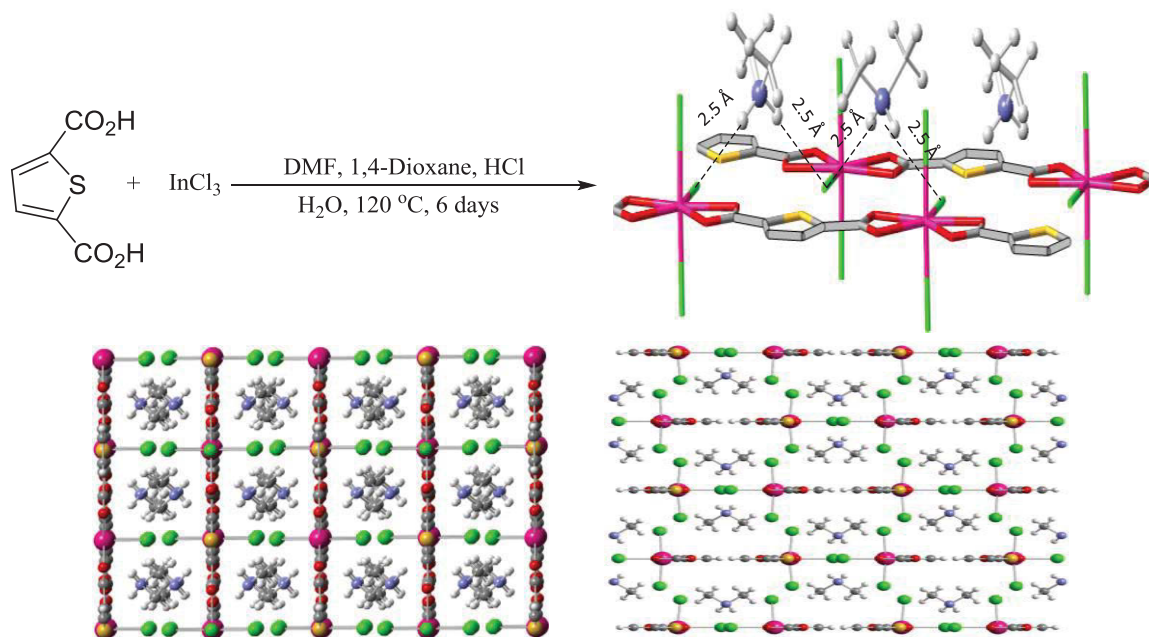


Figure 20: View of cation- π interactions between templating cations and the thiophene linker for each YCM-21 structure

In our quest to employ a wide range of *N*-centered templating cations; two new MOFs with structurally different SBUs from ATF-1 or the YCM-21 series were synthesized, and under very similar synthetic conditions. Highly chlorinated YCM-22 was originally synthesized using pyridinium chloride as an additive (the effect of templating cations with only one HBD was being studied). These conditions yielded a mixture of ATF-1 and YCM-22. It was then hypothesized that pyridinium chloride was acting as an HCl surrogate, so a decision to add conc. HCl in place of the previously

mentioned additive was employed. Fortuitously, the formerly mentioned hypothesis was correct and after 6 days pure YCM-22 was observed (**Scheme 14**). YCM-22 is a one-dimensional MOF that is dianionic at indium. The SBU of YCM-22 $[\text{InCl}_3(\kappa^2\text{-O}_2\text{CAr})_2]^{2-}$ to my knowledge had not been reported previously in the literature and appears to be pseudo-trigonal bipyramidal. Each equatorial chloride (from spatially offset strands) partakes in hydrogen bonding with a single hydrogen from two different DMA cations.

This is reasonable due to the fact that the framework exhibits an overall negative two charge. It is believed that the excess chloride from HCl allows for three chlorides to remain intact through a blocking of dissociation; which is why only two carboxylates can participate in coordination with the indium center. **Figure 21** shows overlaid PXRD patterns of YCM-22 suspended in listed solvent for 1 week. YCM-22 structure remains intact after one week suspended in EtOH and CH_3CN . All other solvents either fully or partially decompose YCM-22 after 1 week (DI water, 1M HCl, 1M NaOH and conc. AcOH).



Scheme 14: Synthesis of YCM-22 a) View of YCM-22 offset strands with H-bonding distances b) View of YCM-22 apertures c) View of the one-dimensionality of YCM-22

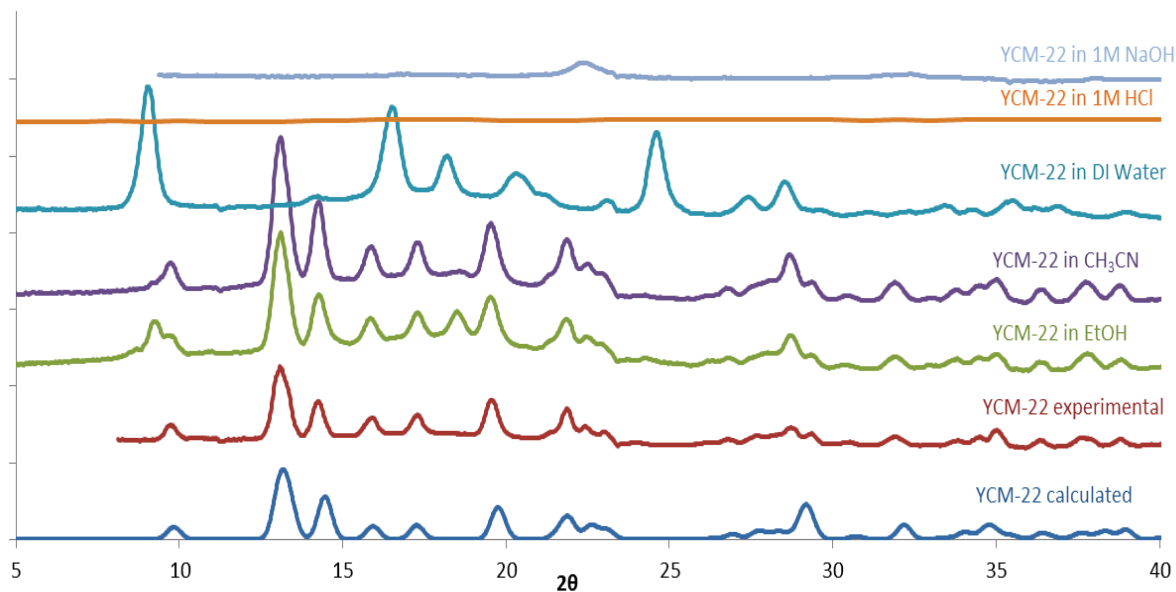
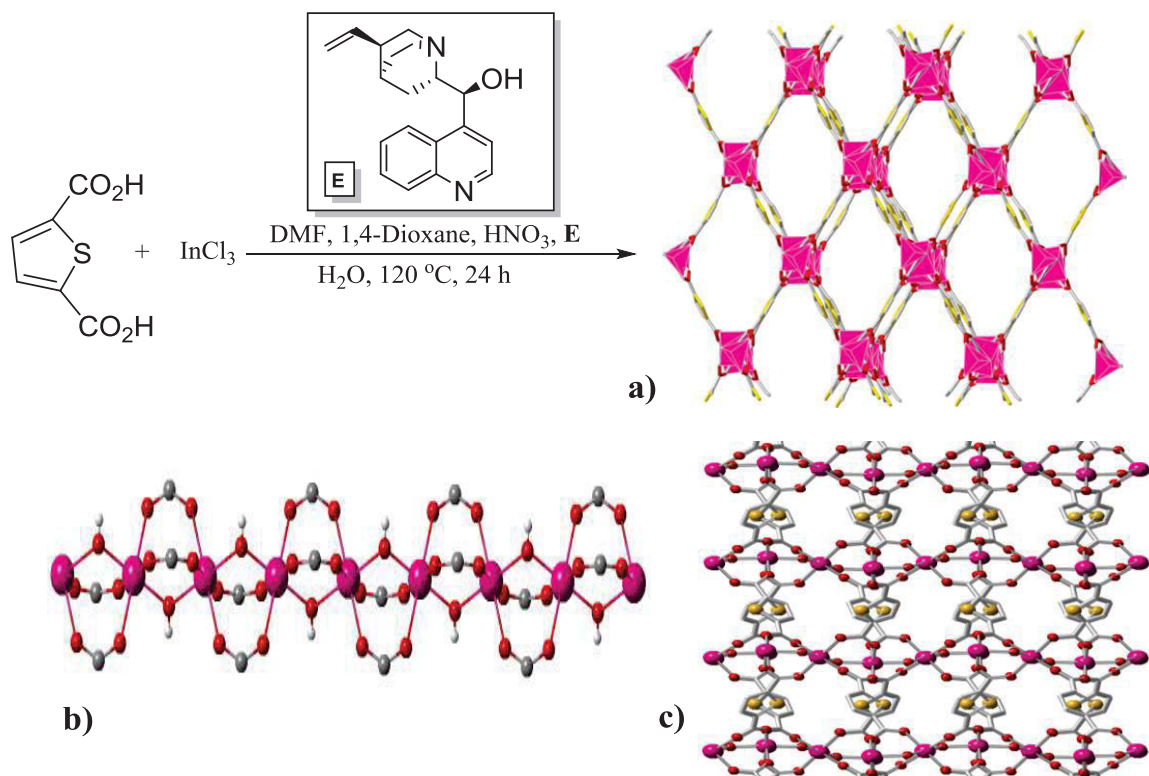


Figure 21: YCM-22 stability studies (1 week) (calculated pattern was derived with 0.5° 2θ FWHM instrumental broadening).

YCM-23 a 3-D, neutral framework is synthesized with cinchonium nitrate as a template molecule. YCM-23 is structurally significant for two reasons: 1) Bu's synthesis that produces enantiopure ATF-1 uses chiral cinchonine as an additive. An important conclusion from Bu's work is that the chiral cinchonine does in fact act as a template, and ATF-1 is produced with the monomeric (anionic) SBU. However, when cinchonium nitrate was added under similar conditions, a chemically and structurally different MOF, YCM-23 is observed (cation not observed crystallographically) (**Scheme 15**). 2) To my knowledge, literature precedent states that to either convert to or produce the infinite chain SBU, a change in stoichiometry between metal source and linker is necessary.^(60, 66) In this case the only parameter that changes between our ATF-1 and YCM-23 syntheses is the introduction of the cinchonium nitrate additive.



Scheme 15: Synthesis of YCM-23 a) 3-D view of YCM-23 b) View of YCM-23 infinite chain SBU c) YCM-23 ball and stick

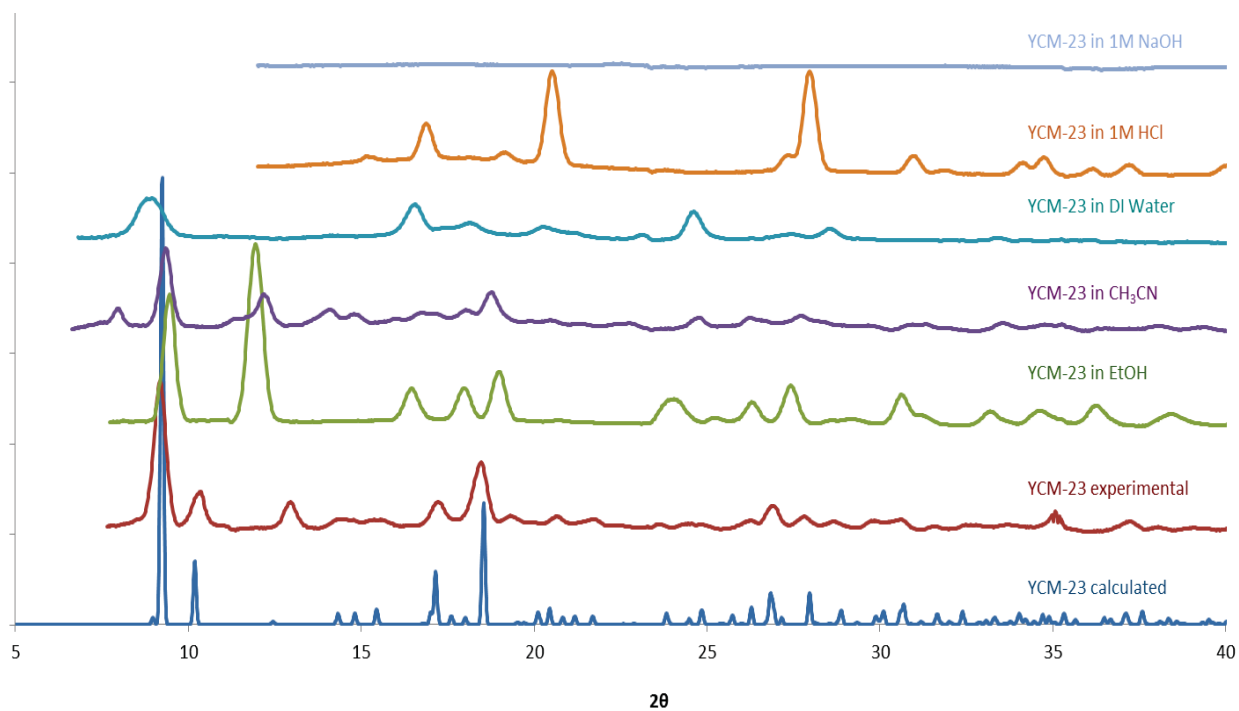


Figure 22: YCM-23 stability studies (1 week)

Figure 22 shows overlaid PXRD patterns of YCM-23 suspended in listed solvent for 1 week. The YCM-23 structure is not stable in any of the solvents listed above, and the material needed to be taken straight out of the oven to obtain an accurate experimental PXRD pattern. If the material was even left in fresh DMF overnight the material began to decompose.

As a last note about these six new structures (YCM-21-Z, YCM-22, YCM-23); three different indium MOF SBU's were synthesized by simply changing the type of additive that was employed (producing six new MOFs). These SBU's do not only differ chemically; they also differ in geometry and electronics which has played a significant role in the structural diversity of these MOFs; particularly between YCM-23, YCM-22, and the four YCM-21 structures (**Figure 23**).

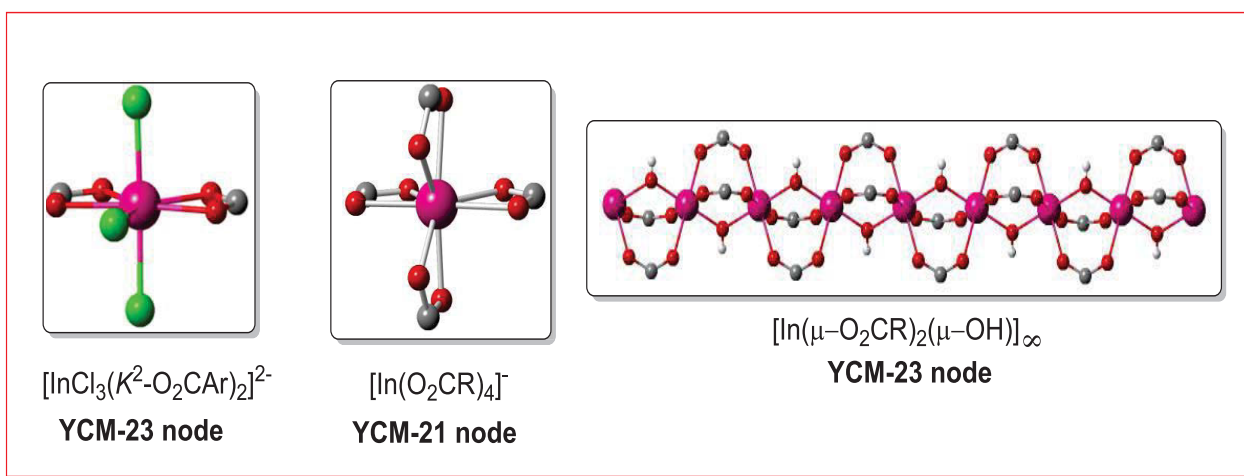
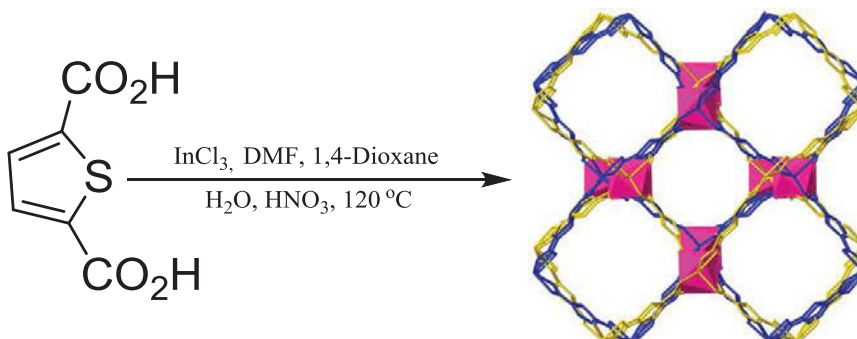


Figure 23: Comparison of the SBU for YCM-23, YCM-21-Z, and YCM-23

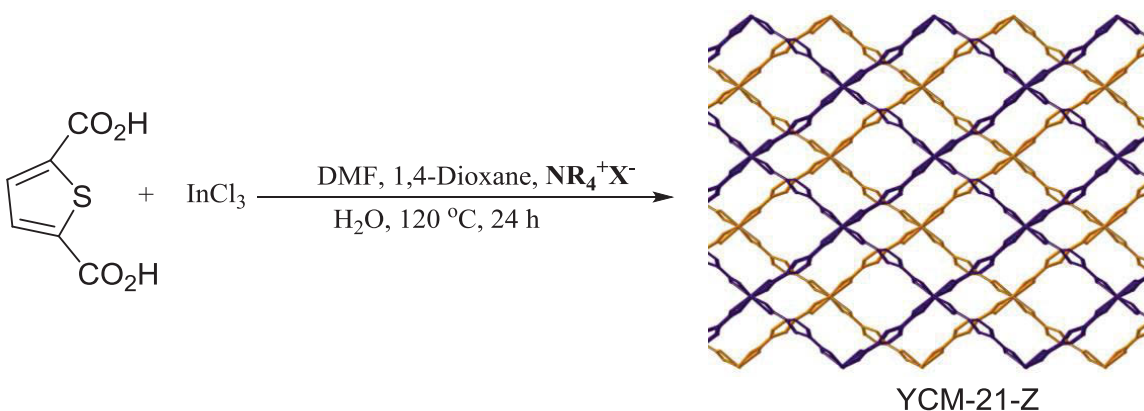
Experimental for YCM-20 series

Synthesis of ATF-1



To a premixed solution of DMF (18 mL) and dioxane (12 mL) was added 2,5-thiophenedicarboxylic acid (107 mg, 0.620 mmol, 1.00 equiv) and InCl_3 (291 mg, 1.32 mmol, 2.13 equiv), followed by a premixed solution of concentrated nitric acid (0.025 mL) in 2 mL of deionized water. The resulting mixture was sonicated for 10 minutes until a homogeneous solution was obtained. The resulting solution was then filtered through a GE 25 mm PVDF syringe filter (0.45 μm) in 6 mL portions, into 6 individual 20 mL scintillation vials. The vials were sealed with Teflon-lined caps and heated in a 120 °C oven for 24 h. The vials were then removed from the oven and were set aside to cool to room temperature. The contents of each individual vial were combined and washed with 3 x 10 mL portions of fresh DMF. The DMF was decanted and the crystals were activated by drying overnight under vacuum at 100 °C.

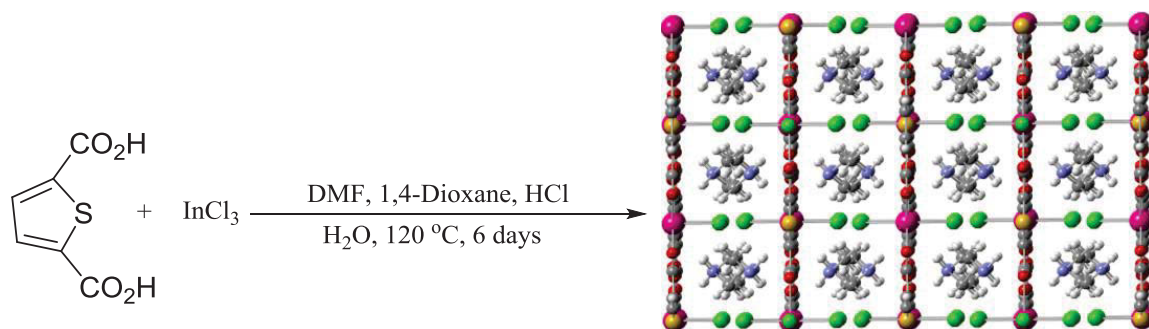
General Synthesis for the YCM-21 Series.



To a premixed solution of DMF (18 mL) and dioxane (12 mL) was added 2,5-thiophenedicarboxylic acid (107 mg, 0.620 mmol, 1.00 equiv) and InCl_3 (291 mg, 1.32 mmol, 2.13 equiv), followed by ammonium cation (1.10 mmol, 1.77 equiv) and 2 mL of deionized water. The resulting mixture was sonicated for 10 min until a homogeneous solution was obtained. The resulting solution was then filtered through a GE 25 mm PVDF syringe filter (0.45 μm) in 6 mL portions, into 6 individual 20 mL scintillation

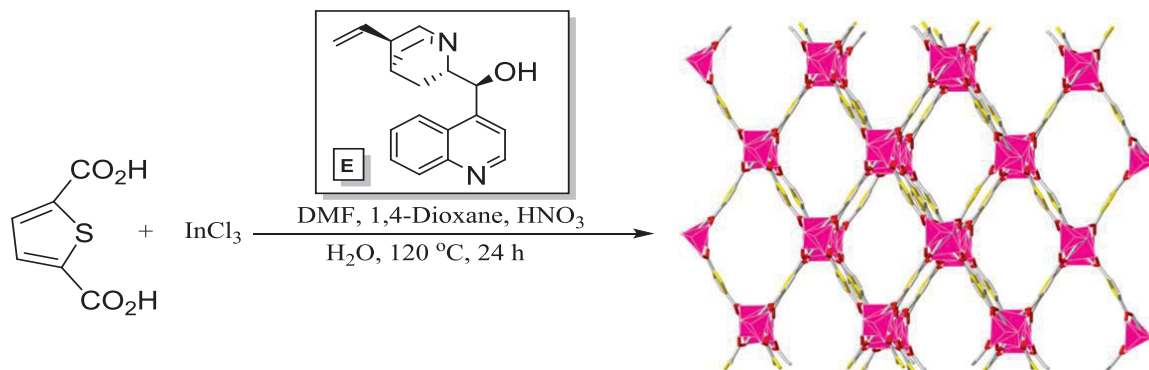
vials. The vials were sealed with Teflon-lined caps and heated in a 120 °C oven for 24 h. The vials were then removed from the oven and were set aside to cool to room temperature. The contents of each individual vial were combined and washed with 3 × 10 mL portions of fresh DMF. The DMF was decanted, and the crystals were activated by drying overnight under vacuum at 100 °C.

Synthesis of YCM-22.



To a premixed solution of DMF (18 mL) and dioxane (12 mL) was added 2,5-thiophenedicarboxylic acid (107 mg, 0.62 mmol, 1.00 equiv) and InCl₃ (291 mg, 1.32 mmol, 2.13 equiv), followed by concentrated HCl (0.034 mL) and 2 mL of deionized water. The resulting mixture was sonicated for 10 min until a homogeneous solution was obtained. The resulting solution was then filtered through a GE 25 mm PVDF syringe filter (0.45 μm) in 6 mL portions into five individual 20 mL scintillation vials. The vials were sealed with Teflon-lined caps and heated in a 120 °C oven for 6 days. The vials were then removed from the oven and were set aside to cool to room temperature. The contents of each individual vial were combined and washed with 3 × 10 mL portions of fresh DMF. The DMF was then decanted, and the crystals were activated by drying overnight under vacuum at 100 °C.

Synthesis of YCM-23.



To a premixed solution of DMF (18 mL) and dioxane (12 mL) was added 2,5-thiophenedicarboxylic acid (107 mg, 0.620 mmol, 1.00 equiv) and InCl₃ (291 mg, 1.32 mmol, 2.13 equiv). In a separate vial, cinchonine (324 mg, 1.10 mmol, 1.77 equiv), 3 mL of deionized water, and 0.050 mL of concentrated HNO₃ were mixed, and the entire vial

was sonicated until all solids were dissolved. The contents of the vial was then added to the DMF mixture, and the entire solution was sonicated for 10 min. The resulting solution was then filtered through a GE 25 mm PVDF syringe filter (0.45 μm) in 6 mL portions into six individual 20 mL scintillation vials. The vials were sealed with Teflon-lined caps and heated in a 120 $^{\circ}\text{C}$ oven for 24 h. The vials were then removed from the oven and were set aside to cool to room temperature. The contents of each individual vial were combined and washed with 3×10 mL portions of fresh DMF. The DMF was decanted, and the crystals were activated by drying overnight under vacuum at 100 $^{\circ}\text{C}$.

Chapter 3: Crystal-to-Crystal Transformation Studies

After publication of the syntheses discussed above, a decision to pursue crystal-to-crystal transformations was made due to a surprising result obtained in a stability study of ATF-1. Shockingly, when ATF-1 was subjected to a 0.16 $M_{(\text{DCM}/\text{DMF})}$ solution of TEBABr for 7 days, partial conversion to YCM-21-TEBA was observed through powder X-ray diffraction (PXRD) (**Figure 24**). A choice to then switch to commercially available TEABr and simply double the concentration of salt was implemented, and after 7 days full conversion of ATF-1 to YCM-21-TEA was detected (**Figure 25**).

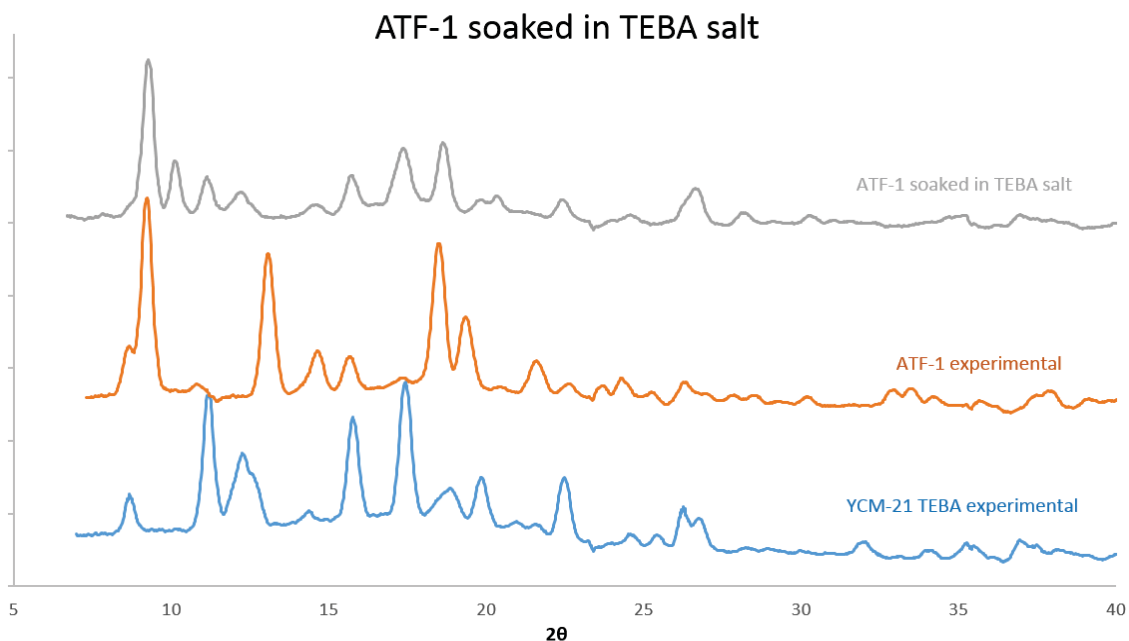


Figure 24: ATF-1 Suspended in TEBABr for 1 week

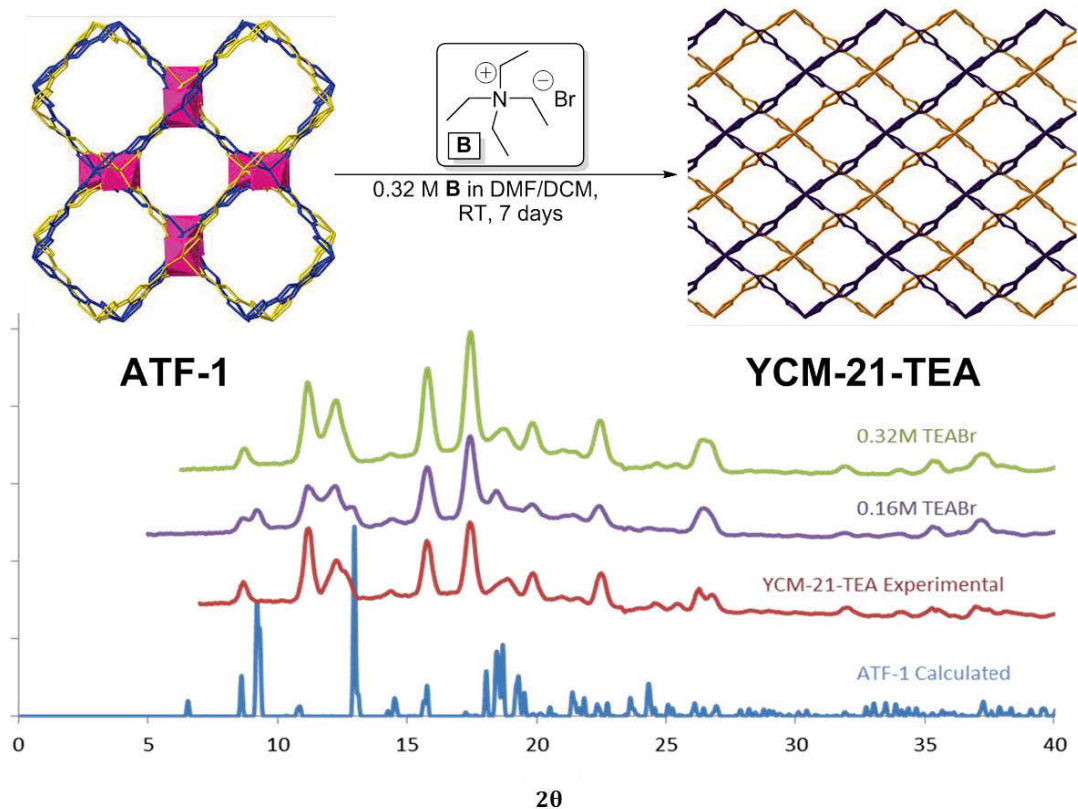


Figure 25: Scheme of ATF-1 transformed into YCM-21-TEA with overlaid powdered patterns.

After encountering solubility issues, a decision was made to cease the use of the DCM/DMF solvent mixture and continue the investigation using only DMF. ATF-1 was then subjected to a variety of TEA salts that varied in anion (these experiments were run to determine the effect anion has on not only result, but also to give insight into a possible mechanism). To our surprise, it was found that in salt solutions of DMF: TEACl and TEAF hydrate fully transformed ATF-1 into the corresponding 2-D YCM-21 structure, while a salt solution of TEABr left ATF-1 intact after 1 week. It is believed that a possible explanation for the TEABr salt working in the DCM/DMF mixture, and not in just DMF, is that the bromide anion of TEABr attacks DCM, displacing chloride anions. It is then postulated that this displaced chloride initiates the deintercalation (**Table 1**).

X	Outcome
F	Complete Conversion
Cl	Complete Conversion
Br	No Reaction
BF ₄	No Reaction
NO ₃	No Reaction
OTf	No Reaction

Table 1: Table of transformation outcomes for 0.32 M TEA(X) (DMF) for 7 days.

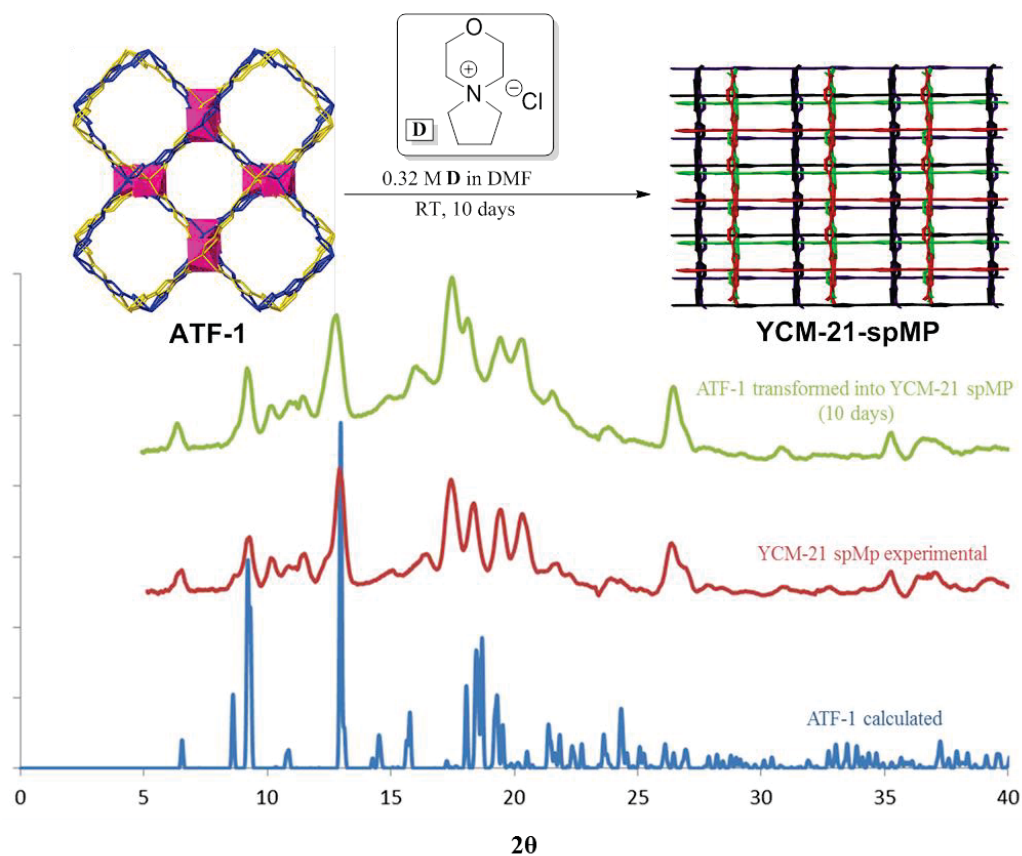


Figure 26: Scheme of ATF-1 transformed into YCM-21-spMP with overlaid powdered patterns.

The next focus was to accomplish full transformations for the remaining three YCM-21 structures (TEBA, spPP, spMP). After subjecting ATF-1 to a 0.32 M solution of spMP chloride for 10 days, full transformation of ATF-1 to YCM-21 spMP was observed (**Figure 26**). Transformation of ATF-1 to YCM-21-TEBA and YCM-21-spPP proved more troublesome. Originally, when ATF-1 was introduced to a 0.32 M solution of spPPBr in DCM/DMF full conversion was observed except for a small impurity that could not be identified. A switch to a solution of spPPCl was then implemented; after monitoring the reaction between 7-14 days it was determined that spPPCl did not transform ATF-1 into YCM-21-spPP (reason unknown). **Figure 27** shows the overlaid patterns with the pointed out unknown impurity.

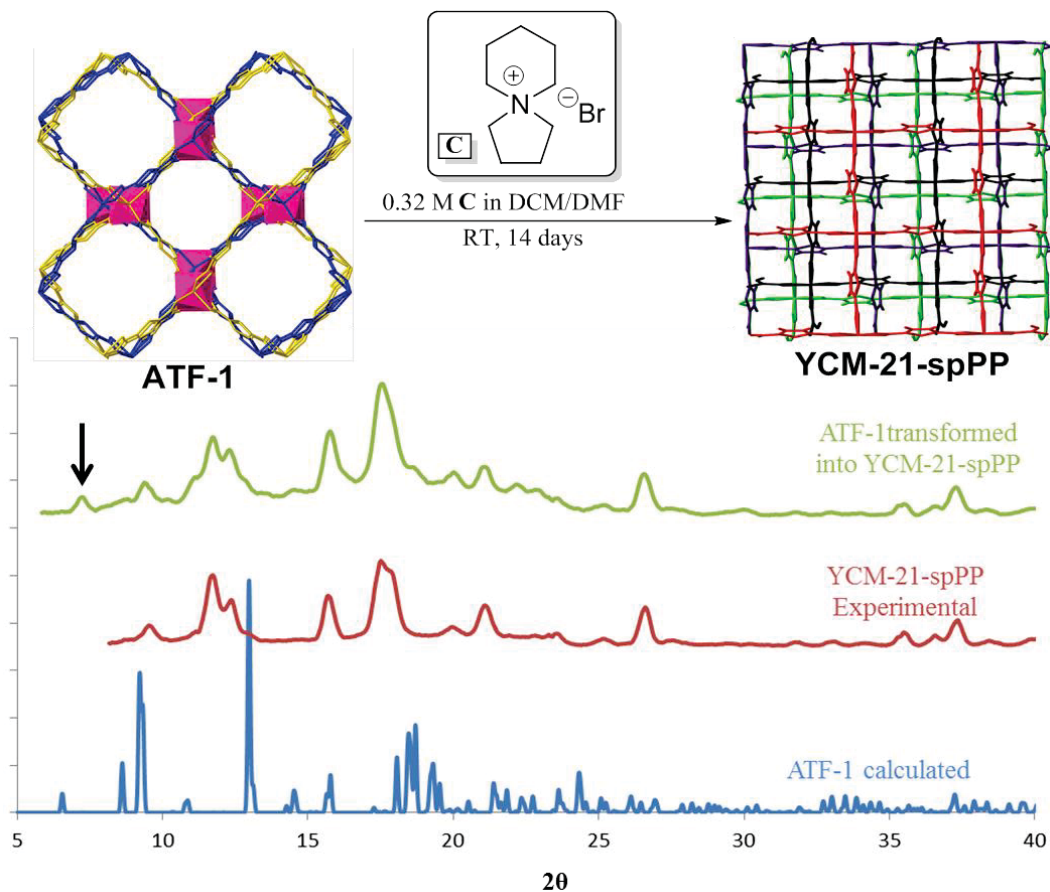


Figure 27: Scheme of ATF-1 transformed into YCM-21-spPP with overlaid powdered patterns. (Impurity pointed out by arrow).

Lastly, an attempt to transform ATF-1 into YCM-21-TEBA was conducted. The first effort towards this transformation applied TEBABr. This reaction was again monitored for 7-14 days and it was found that ATF-1 only partially transforms to YCM-21-TEBA after 7 days. When ATF-1 is subjected to these conditions for shorter amounts of time only unreacted ATF-1 is observed, and when the reaction is allowed to sit for longer time periods ATF-1 transforms into some unknown structure by PXRD. **Figure 28** shows the obtained pattern with impurity. An attempt to synthesize TEBACl under various conditions was attempted, but no useable synthesis was ever achieved (presumably because of the difference in electrophilicity between *n*-butyl bromide and its chloride counterpart).

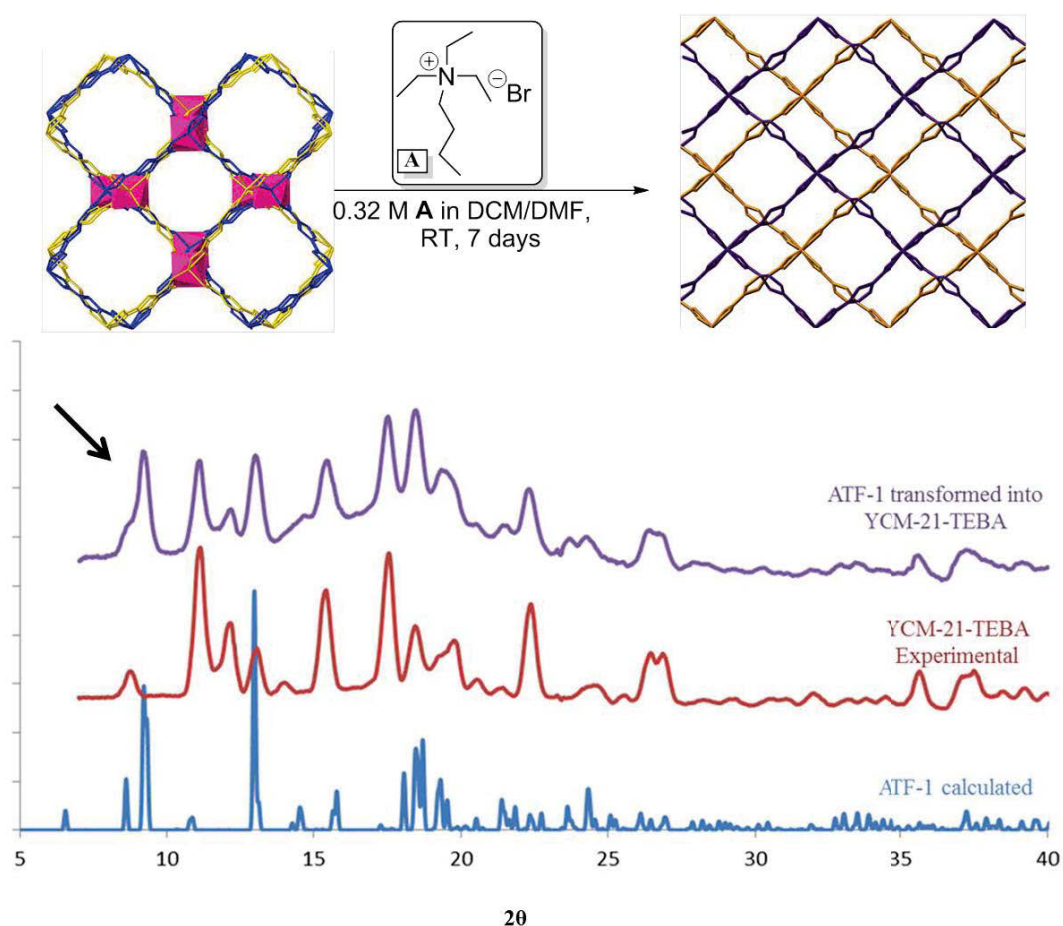


Figure 28: Scheme of ATF-1 partially transformed into YCM-21-TEBA with overlaid powdered patterns. (Impurity pointed out by arrow).

The last subject matter related to these transformations studies is to propose a possible mechanism. It is believed that X^- (Cl or F) attacks the tetrahedral indium SBU producing a negative charge that is stabilized by the dimethyl ammonium cation. Once this occurs, a cation exchange can take place between the weakly hydrogen bound dimethyl ammonium and the selected quaternary ammonium salt. From there, a deintercolation of individual frameworks transpires and the In-carboxylate coordination can reform by nucleophilic attack. Finally, the non-interpenetrated frameworks can flatten out and stack as observed in the YCM-21 series crystal structures (**Figure 29**).

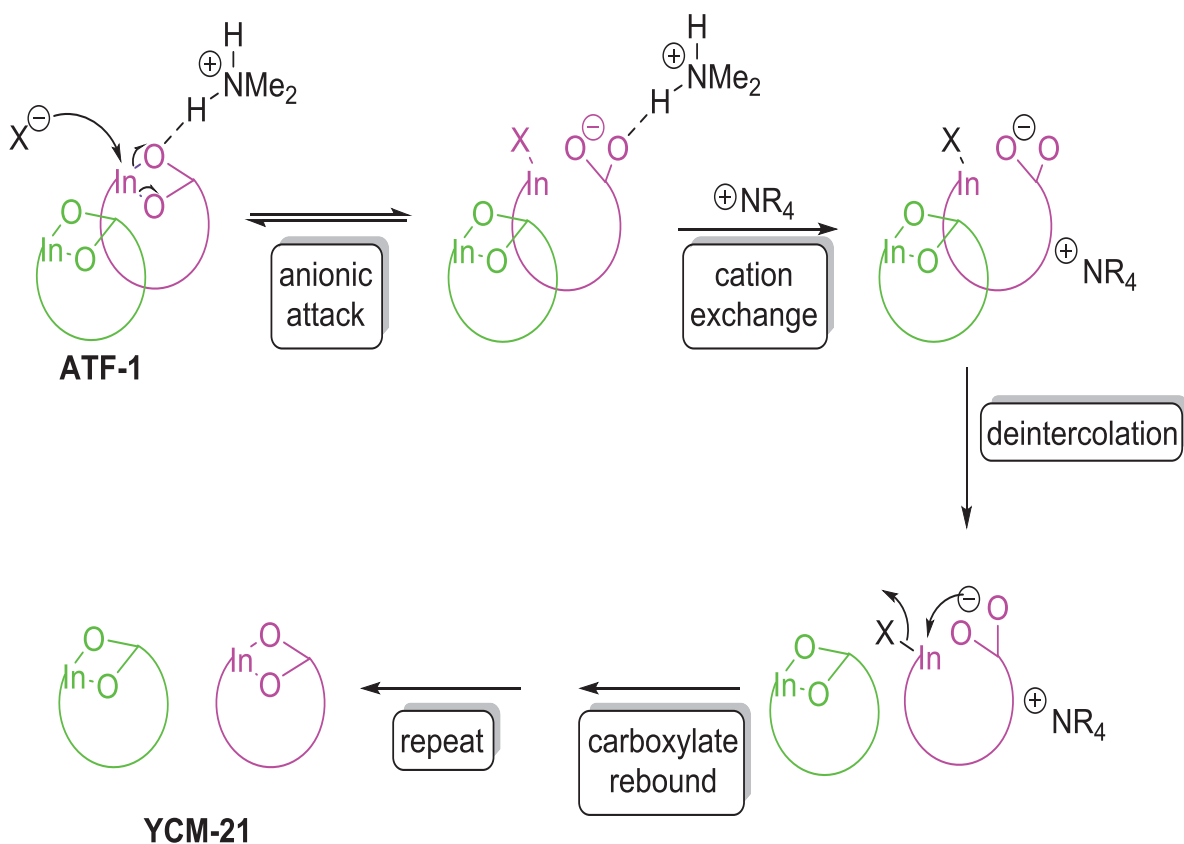
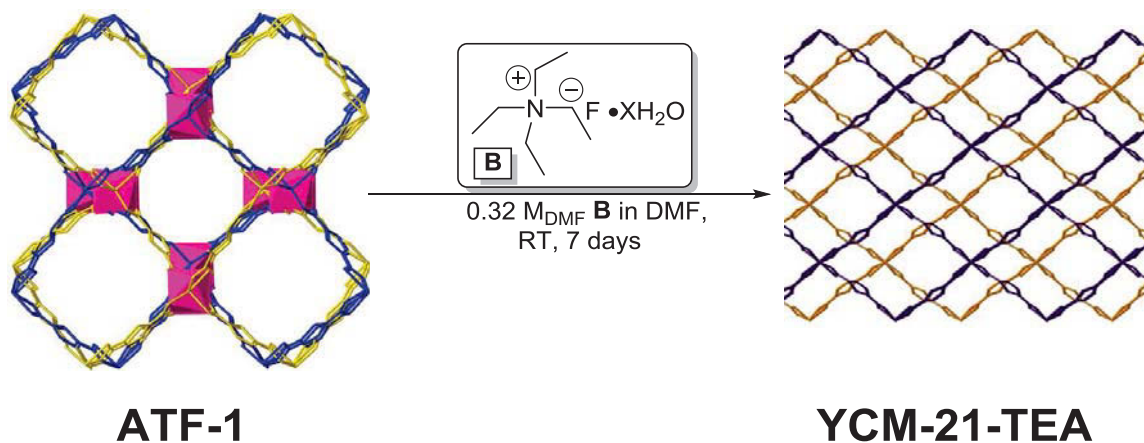


Figure 29: Proposed Mechanism for the Transformation of ATF-1 to YCM-21

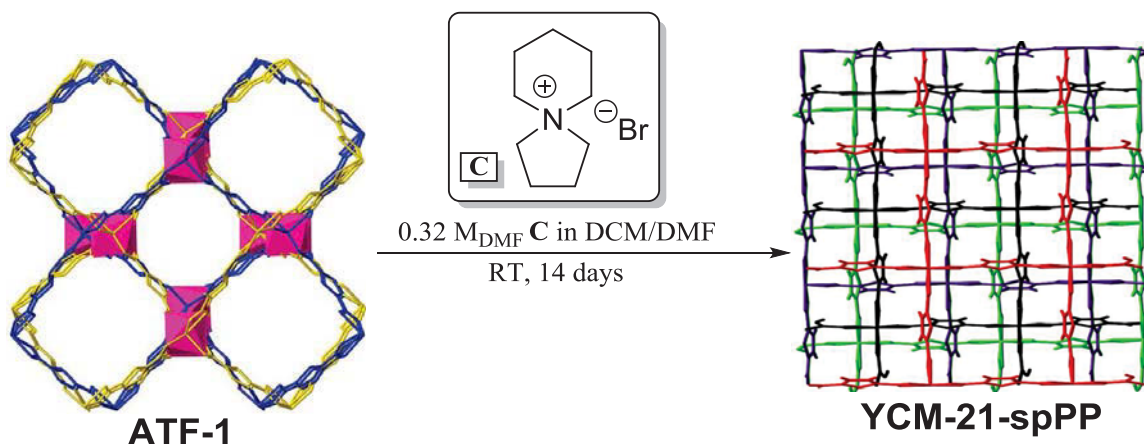
Chapter 3 Experimental: MOF Structural Rearrangements

General Procedure with ammonium chloride or fluoride



To a 4 mL vial with a Teflon cap was added 25 mg of activated ATF-1, 1.5 mL of DMF, and 1.5 mL of 0.32M solution of the appropriate ammonium salt (0.48 mmol) in DMF. The vial was then allowed to agitate on an orbital shaker at room temperature for 7 days (spMPCl 10 days). The vial was then removed from the shaker, and all liquids were decanted off. The remaining solid was then washed with fresh DMF (3 x 3 mL) and a PXRD pattern was then obtained immediately after.

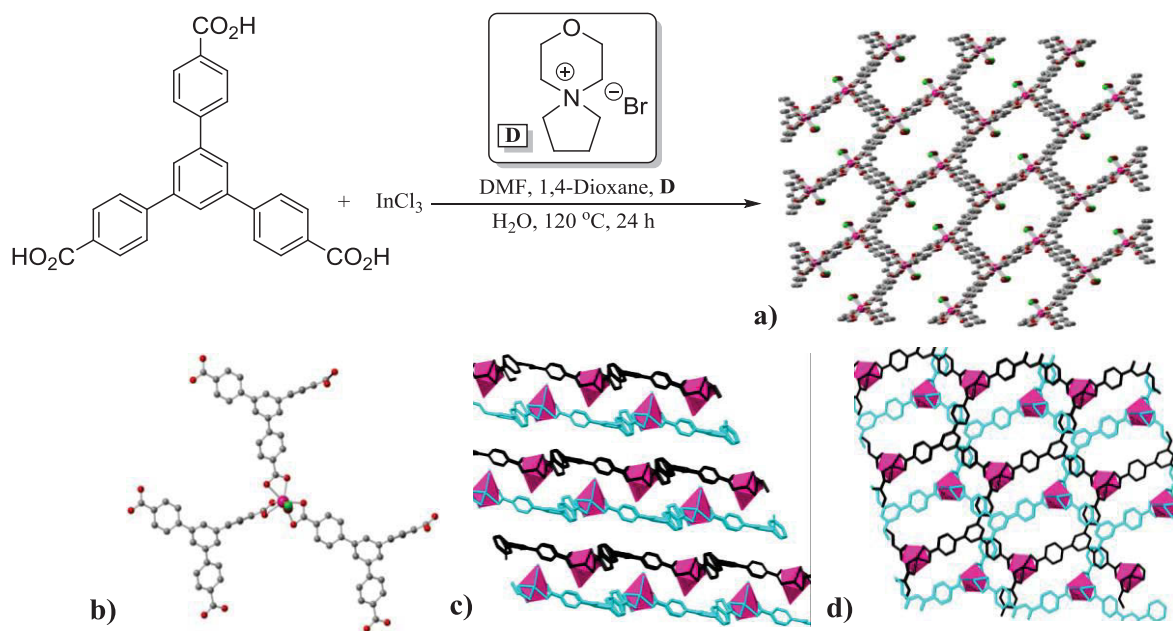
General Procedure with ammonium bromide



To a 4 mL vial with a Teflon cap was added 25 mg of activated ATF-1, 1.5 mL of DMF, and 1.5 mL of 0.32M solution of the appropriate ammonium bromide (0.48 mmol) in DCM. The vial was then allowed to agitate on an orbital shaker at room temperature for 14 days. The vial was then removed from the shaker, and all liquids were decanted off. The remaining solid was then washed with fresh DMF (3 x 3 mL) and a PXRD pattern was then obtained immediately after.

Chapter 4: Continuation of Template-Directed MOF Synthesis

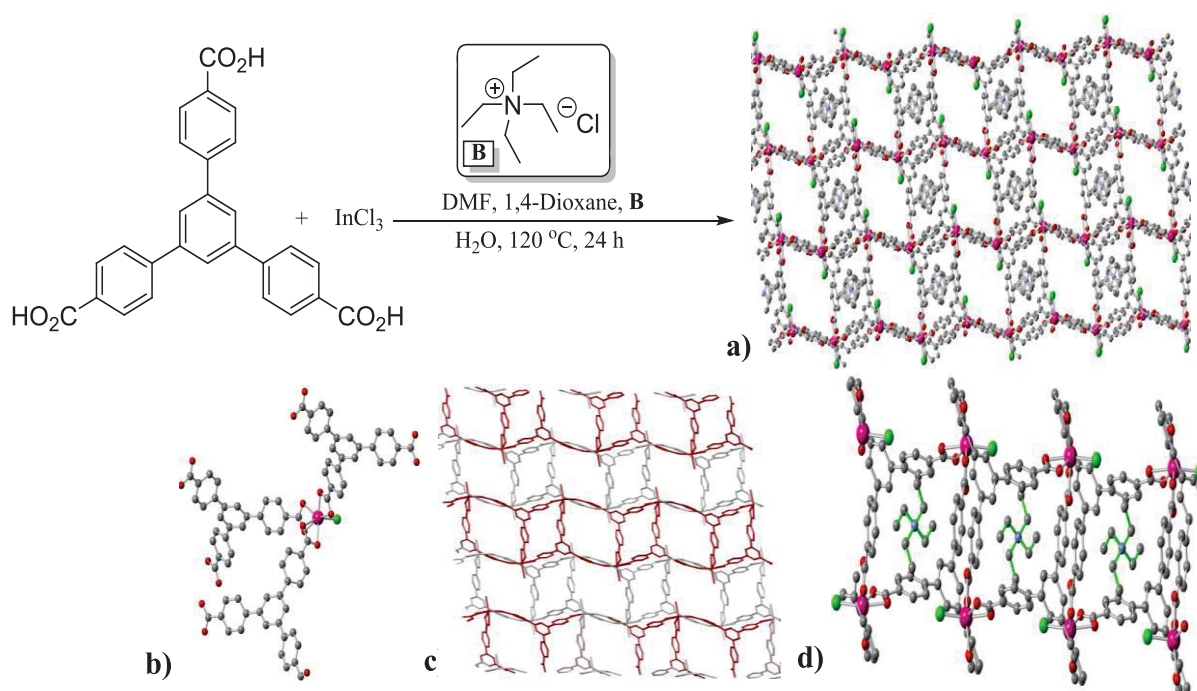
While in pursuit of template directed synthesis for the YCM-21 series, similar conditions were also applied to the linker BTB. Fortuitously, three new MOF structures with chemically related SBUs were synthesized (two structures with BTB and one with BPDC). Those structures will now be discussed in their entirety. YCM-31 is synthesized using general YCM-21-spMP conditions, but with BTB as the linker (**Scheme 16**). YCM-31 is a 2-D, anionic MOF with an A-B-A-B sheet pattern. The spirocyclic morpholinium cation rests inside the apertures of the MOF and appears crystallographically disordered. Each BTB linker partakes in κ^2 - coordination with its corresponding indium metal; with the last X type ligand being a mixture between a chlorine and a bromine. YCM-31 exhibits In-In-In *trans* bond angles of 180.00° and *cis* In-In-In bond angles of 74.45° and 105.55° making the SBU of YCM-31 pseudo-square planar.



Scheme 16: Synthesis of YCM-31 a) 3-D view of YCM-31 and its apertures b) YCM-31 node c) View of repeating A-B-A-B sheet pattern d) View of two sheets stacked on top of one another

Each pore of YCM-31 is $17.7 \text{ \AA} \times 8.8 \text{ \AA}$ with the distance between sheets A-B being 9.0 \AA and B-A being 11.3 \AA (In-In distances).

A second synthetically related structure to YCM-31, yet supramolecularly different is YCM-32. YCM-32 is synthesized under the exact conditions used for YCM-31, the only difference being the additive (TEACl); YCM-32 is a structure that is 2-D in overall geometry, but each individual sheet is 3-D with respect to the SBU. The MOF is anionic and utilizes TEACl as the template molecule with said molecules lying in every other pore of the MOF (**Scheme 17**). Each BTB linker partakes in κ^2 -coordination in regards to the indium metal; with the last X type ligand being a chlorine atom ($\{\text{In}(\text{CO}_2\text{R})_3\text{Cl}\}$). Each individual sheet sits in-between 2 others sheets (offset) allowing the structure to arrange in a “zipper-like” fashion (**Scheme 17 c**). The aperture size for YCM-32 is 9.3 Å by 9.0 Å.



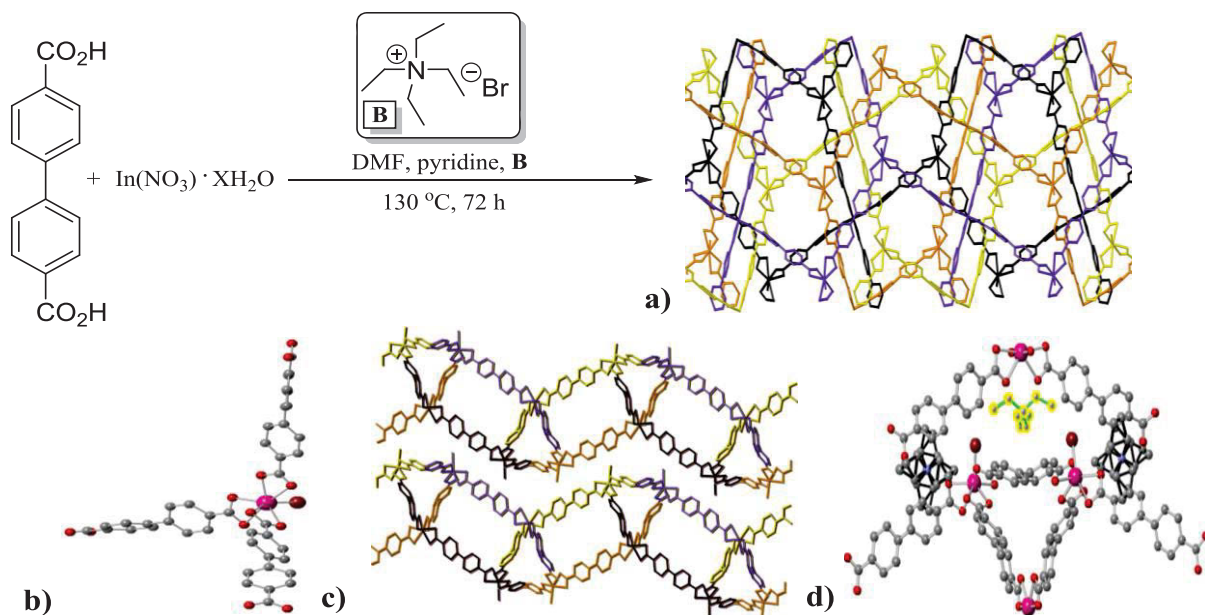
Scheme 17: Synthesis of YCM-32 **a)** 3-D view of YCM-32 and its apertures **b)** YCM-32 node **c)** View of repeating A-B-A-B sheet pattern **d)** Up close view of pore with TEA cation resting inside.

After exhausting synthetic efforts with BTB (in regards to nitrogenous salt screening) as the linker, it was decided that other linkers that were commercially

available would be implemented. The next linker implemented was BPDC; After screening, a new MOF related to YCM-31 and YCM-32 was synthesized with BPDC as the linker (YCM-41).

YCM-41 overall is a 2-D MOF with each two-dimensional “helix” comprised of four 3-D, interpenetrated frameworks (**Scheme 18**). YCM-41 consists of two chemically distinct nodes, the first has three biphenyl linkers partaking in κ^2 -coordination with the indium metal, while the fourth X-type ligand arises from a coordination bond between bromine and indium. The second has all four biphenyl linkers participating in κ^2 -coordination with the indium metal. The distance between each individual 2-D framework is 10.9 Å (In-In). Each individual “aperture” contains the template molecule (TEA cation), along with disordered pyridine. There are two key roles that pyridine seems to play in the synthesis of YCM-41: 1) it allows the linker to be soluble in the solvent mixture. 2) It is possibly involved in templating to some extent (disordered pyridine is found throughout the structure).

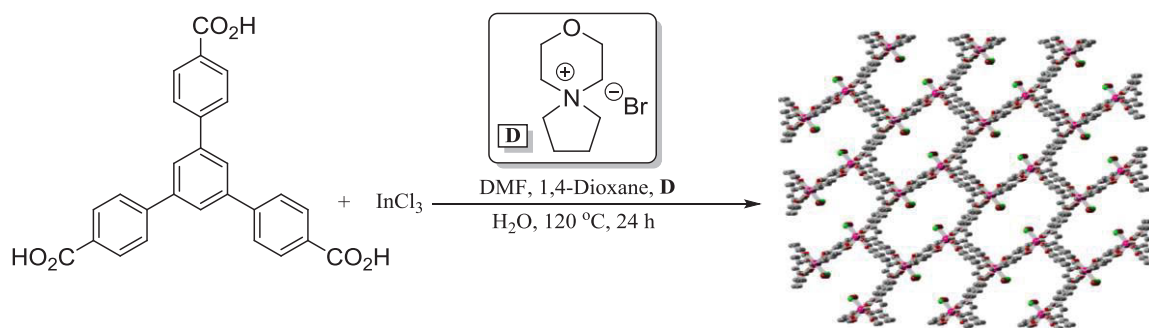
To conclude: For the last two years I have synthesized MOFs that can be characterized as both chemically related (YCM-21 series), and spatially related (YCM-31, 32, 41). YCM-22 is a structure that again to my knowledge produces an unprecedented $[\text{InCl}_3(\kappa^2\text{-O}_2\text{CAr})_2]^{2-}$ node in both MOF and indium coordination chemistry; while YCM-23 produces an infinite chain SBU over the monomeric SBU through the use of an additive rather than a change in stoichiometry. It is worth mentioning that studies like the ones just described along with many others, give optimism that MOF structure (i.e. topology, dimensionality, etc) might someday be able to be fully controlled which will allow many new doors to be opened in



the field of MOF chemistry. Lastly, with the ATF-1 to YCM-21 series transformation studies: we have demonstrated that a 3-D interpenetrated framework can be transformed into 2-D, non-catenated frameworks through salt mediated transformation (change in SBU geometry) which allowed for a mechanism of transformation to be proposed. To our knowledge this is one of the first, if not the first report of this type of MOF transformation chemistry.

Chapter 4 Experimental: YCM-31, YCM-32, YCM-41

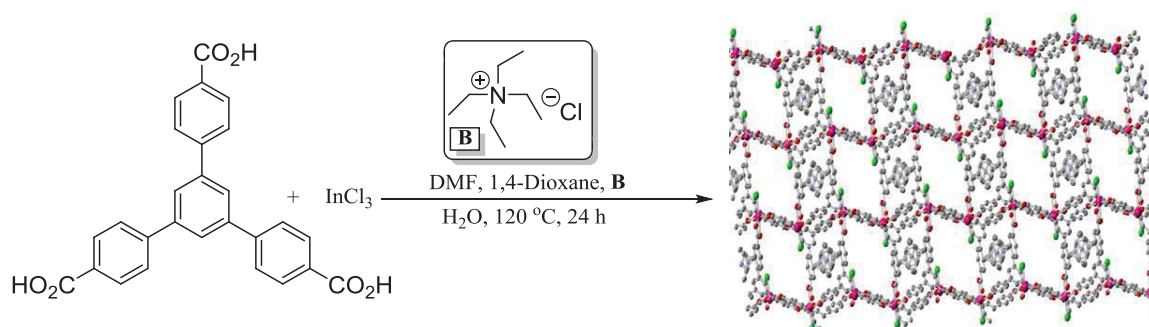
Synthesis of YCM-31



To a premixed solution of DMF (18 mL) and dioxane (12 mL) was added benzene tribenzoic acid (BTBH₃) (0.260 g, 0.60 mmol, 1.00 equiv) and InCl₃ (291 mg, 1.32 mmol, 2.13 equiv). In a separate vial, spMPBr (254 mg, 1.10 mmol, 1.77 equiv) was dissolved in 2 mL of deionized water. The entire vial was sonicated until all solids were dissolved. The contents of the vial was then added to the DMF mixture, and the entire solution was sonicated for 10 min. The resulting solution was then filtered through a GE 25 mm PVDF syringe filter (0.45 μm) in 6 mL portions into six individual 20 mL scintillation vials. The vials were sealed with Teflon-lined caps and heated in a 120 °C oven for 24 h. The vials were then removed from the oven and were set aside to cool to room temperature. The contents of each individual vial were combined and washed with 3 × 10 mL portions of fresh DMF. The DMF was decanted, and the crystals were activated by drying overnight under vacuum at 100 °C.

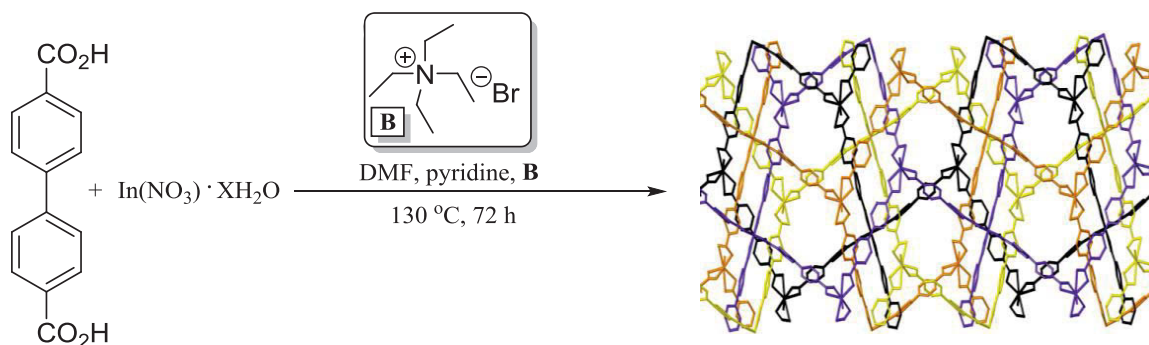
note, this procedure has not exhibited reproducibility

Synthesis of YCM-32



To a premixed solution of DMF (18 mL) and dioxane (12 mL) was added BTBH₃ (275 mg, 0.620 mmol, 1.00 equiv) and InCl₃ (291 mg, 1.32 mmol, 2.13 equiv), followed by tetraethylammonium chloride (182 mg, 1.10 mmol, 1.77 equiv) and 2 mL of deionized water. The resulting mixture was sonicated for 10 min until a homogeneous solution was obtained. The resulting solution was then filtered through a GE 25 mm PVDF syringe filter (0.45 μm) in 6 mL portions, into 6 individual 20 mL scintillation vials. The vials were sealed with Teflon-lined caps and heated in a 120 °C oven for 24 h. The vials were then removed from the oven and were set aside to cool to room temperature. The contents of each individual vial were combined and washed with 3 × 10 mL portions of fresh DMF. The DMF was decanted, and the crystals were activated by drying overnight under vacuum at 100 °C.

Synthesis of YCM-41



To a Teflon-lined stainless steel autoclave with 10 mL of DMF was added In(NO₃)₃ ·XH₂O (151 mg, 0.50 mmol, 1.00 equiv) and 4,4-biphenyldicarboxylic acid (0.289 g, 1.19 mmol, 2.38 equiv). Pyridine (0.19 μL, 2.38 mmol, 4.76 equiv) was then added to the autoclave along with tetraethylammonium bromide (231 mg, 1.10 mmol, 2.20 equiv). The autoclave was then sealed and heated in a 130 °C oven for 3 days. The autoclave was then removed from the oven and was set aside to cool to room temperature. The contents of the autoclave were washed with 3 × 10 mL portions of fresh DMF. The DMF was decanted, and the crystals were activated by drying overnight under vacuum at 100 °C.

References

1. Spagnolo, L. L.; El-Hankari, S.; Bradshaw, D. *Chem. Soc. Rev.* **2014**, *43*, 5431.
2. Li, H.; Eddaoudi, M.; O'Keeffe, M.; Yaghi, M. O. *Nature.* **1999**, *402*, 276.
3. Furukawa, H.; Cordova, E. K.; O'Keeffe, M.; Yaghi, O. *Science.* **2013**, *341*, 123044.
4. Schlapbach, L.; Züttel, A. *Nature.* **2001**, *414*, 353.
5. Rowsell, C. J.; Yaghi, M.O. *Angew. Chem. Int. Ed.* **2005**, *44*, 4670.
6. Furukawa, H.; Miller, A. M.; Yaghi, M. O. *J. Mater. Chem.* **2007**, *17*, 3197.
7. Furukawa, H et al. *Science.* **2010**, *329*, 424.
8. Farha, O. K et al. *J. Am. Chem. Soc.* **2010**, *2*, 944.
9. Liu, J.; Chen, L.; Cui, H.; Zhang, J.; Zhang, L.; Su, C. *Chem. Soc. Rev.* **2014**, *43*, 6011.
10. Chui, S, S.; Lo, M, S.; Charmant, P, J.; Orpen, G, A.; Williams, D, I. *Science*, **1999**, *283*, 1148.
11. Schlichte, K.; Kratzke, T.; Kaskel, S. *Microporous Mesoporous Mater.* **2004**, *73*, 81.
12. Lee, J.; Farha, K, O.; Roberts, J.; Scheidt, A, K.; Nguyen, T, S.; Hupp, T, J. *Chem. Soc. Rev.* **2009**, *38*, 1450.
13. Maksimchuk, V, N.; Zalomaeva, V, O.; Skobelev, Y, I.; Kovalenko, A, K.; Fedin, P, V.; Kholdeeva. *Proc. R. Soc. A.* **2012**, *468*, 2017.
14. Henshel, A.; Gedrich, K.; Kraehnert, R.; Kaskel, S. *Chem. Commun.* **2008**, 4192.
15. Hong, D.; Hwang, Y.; Serre, C.; Ferey, G.; Chang, J. *Adv. Funct. Mater.* **2009**, *19*, 1537.
16. Wu, C.; Hu, A.; Xhang, L.; Lin, W. *J. Am. Chem. Soc.* **2005**, *127*, 8940.
17. Lalonde, B, M.; Farha, K, O.; Sheidt, A, K.; Hupp, T, J. *ACS Catal.* **2012**, *2*, 1550.
18. Roberts, M, J.; Fini, M, B.; Sarjeant, A, A.; Fraha, K, O.; Hupp, T, J.; Sheidt, A, K. *J. Am. Chem. Soc.* **2012**, *134*, 3334.
19. Arshad, A.; Xu, Q. *J. Phys. Chem. Lett.* **2014**, *5*, 1400.
20. Hwang, Y, K.; Hong, D, Y.; Chang, J, S.; Jhang, S, H.; Seo, Y, K.; Kim, J.; Vimont, A.; Datuvi, M.; Serre, C.; Ferey, G. *Angew. Chem., Int. Ed.* **2008**, *47*, 4144.
21. Genna, T, D.; Pfund, Y, L.; Samblanet, C, D.; Wong-Foy, G, A.; Matzger, J, A.; Sanford, S, M. *ACS Catal.* **2016**, *6*, 3569.
22. Kuppler, J, R.; Timmons, J, D.; Fang, Q.; Li, J.; Makal, A, T.; Young, D, M.; Yuan, D.; Xhuang, W.; Zhou, H. *Coordination Chemistry Reviews.* **2009**, *253*, 3042.
23. Gu, Z.; Jiang, D.; Wang, H.; Cui, X.; Yan, X. *J. Phys. Chem. C* **2010**, *114*, 311.
24. Loiseau, T.; Bataille, T.; Henry, M.; Taulelle, F.; Fink, G.; Huguenaud, C.; Serre, C.; Ferey, G. *Chem.-Eur. J.* **2004**, *10*, 1373.

25. Chen, B.; Wang, L.; Zapata, F.; Qian, G.; Lobkovsky, B, E. *J. Am. Chem. Soc.* **2008**, *130*, 6718.
26. Chen, B.; Wang, L.; Xiao, Y.; Fronczek, F, R.; Xue, M.; Cui, Y.; Qian, G. *Angew. Chem. Int. Ed. Engl.* **2008**, *48*, 500.
27. Yoon, M.; Suh, K.; Natarajan, S.; Kim, K. *Angew. Chem. Int. Ed.* **2013**, *52*, 2688.
28. Chui, S, S.; Lo, M, S.; Charmant, P, J.; Orpen, G, A.; Williams, D, I. *Science.* **1999**, *283*, 1148.
29. Cavka, H, J.; Jakobsen, S.; Olsbye, U.; Guillou, N.; Lamberti, C.; Bordiga, S.; Lillerud, P, K. *J. Am. Chem. Soc.* **2008**, *130*, 13850.
30. Ma, S.; Wang, Xi.; Manis, S, E.; Collier, D, C.; Zhou, H. *Inorg. Chem.* **2007**, *46*, 3432.
31. Kuppler, J. R.; Timmons, J. D.; Fang, R. Q.; Li, R. J.; Makal, A. T.; Young, D. M.; Yuan, D.; Zhao, D.; Zhuang, W.; Zhou, C. H. *Coordination Chemistry Reviews.* **2009**, *253*, 3042.
32. Seoane, B.; Dikhtiarenko, A.; Mayoral, A.; Tellez, C.; Coronas, J.; Kapteijn, F.; Gascon, J. *CrystEngComm.* **2015**, *17*, 1693.
33. Chen, L.; Jia, Y. H.; Hong.; Chen, H. D.; Zheng, P. Z.; Jin, G.H.; Gu, G.Z.; Cai, P.Y. *Inorganic Chemistry Communications.* **2013**, *27*, 22.
34. Biemmi, E.; Christian, S.; Stock, N.; Bein, T. *Microporous and Mesoporous Materials.* **2009**, *117*, 111.
35. Cepeda, J.; Yáñez, P. S.; Beobide, G.; Castillo, O.; Luque, A.; Wright, A. P.; Sneddon, S; Ashbrook E. S. *Cryst. Growth and Des.* **2015**, *15*, 2352.
36. Mahata, P.; Sundaresan, A.; Natarajan, S. *Chem. Commun.* **2007**, 4471.
37. Zhang, J.; Wojitas, L.; Larsen, W. R.; Eddaoudi, M.; Zaworotko, J. M. *J. Am. Chem. Soc.* **2009**, *131*, 17040.
38. Ma, L.; Lin, W. *J. Am. Chem. Soc.* **2008**, *130*, 13843.
39. Gou, M.; Sun, M. Z. *J. Mater Chem.* **2012**, *22*, 15939.
40. Yang, Q.; Chen, X.; Chen, Z.; Hao, Y.; Li, Y.; Lu, Q.; Zheng, H. *Chem. Commun.* **2012**, *48*, 10016.
41. Mazaj, M.; Čelič, T.; Mali, G.; Rangus, M.; Kaučič, V.; Logar, Z. N. *Cryst. Growth and Des.* **2013**, *13*, 3825.
42. Zhang, L.; Tian, X.; Jiang, X.; Wu, Y.; Wang, W.; Li, Z.; Xu, T.; Qia, L. *Angew. Chem. Int. Ed.* **2008**, *47*, 9487.
43. Xu, L.; Kwon, Y.; de Castro, B.; Cunha-Silva, L. *Cryst. Growth Des.* **2013**, *13*, 1260.
44. Huang, Y.; Lin, Z.; Fu, H.; Wang, F.; Shen, M.; Wang, Z.; Cao, R. *ChemSusChem.* **2014**, *7*, 2647.
45. Tuck, D. G. C.; Gislason, J.; Lloyd, M. H. *Inorg. Chem.* **1971**, *10*, 1907.
46. Contreras, J. G.; Poland, J. S.; Tuck, D. G. *DaltonTrans.* **1973**, 922.

47. Sun, J.; Weng, L.; Zhou, Y.; Chen, J.; Chen, Z.; Liu, Z.; Zhao, D. *Angew. Chem., Int. Ed.* **2002**, *41*, 4471.
48. Yang, S.; Lin, X.; Blake, A. J.; Thomas, K. M.; Hubberstey, P.; Champness, N. R.; Schroder, M. *Chem. Commun.* **2008**, 6108.
49. Sava, D. F.; Kravstov, V. C.; Nouar, F.; Wojtas, L.; Eubank, J. F.; Eddaoudi, M. *J. Am. Chem. Soc.* **2008**, *130*, 3768.
50. Liu, Y.; Kravtsov, V. C.; Eddaoudi, M. *Angew. Chem. Int. Ed.* **2008**, *47*, 8446.
51. Huh, S.; Kwon, T.-H.; Park, N.; Kim, S.-J.; Kim, Y. *Chem. Commun.* **2009**, 4953.
52. Anokhina, E. C.; Vouga-Zanda, M.; Wang, X.; Jacobson, A. J. *J. Am. Chem. Soc.* **2005**, *127*, 15000.
53. Gandara, F.; Gomez-Lor, B.; Gutierrez-Puebla, E.; Iglesias, M.; Monge, M. A.; Proserpio, D. M.; Snejko, N. *Chem. Mater.* **2008**, *20*, 72–76.
54. Jin, Z.; Zhao, H.-Y.; Zhao, X.-J.; Fang, Q.-R.; Long, J. R.; Zhu, G.-S. *Chem. Commun.* **2010**, *46*, 8612.
55. Stylianou, K. C.; Heck, R.; Chong, S. Y.; Bacsá, J.; Jones, J. T. A.; Khimiyak, Y. Z.; Bradshaw, D.; Rosseinsky, M. J. *J. Am. Chem. Soc.* **2010**, *132*, 4119.
56. Liu, Y.; Eubank, J.; Cairns, A. J.; Eckert, J.; Kravtsov, V. C.; Luebke, R.; Eddaoudi, M. *Angew. Chem., Int. Ed.* **2007**, *46*, 3278.
57. Gu, X.; Lu, Z.-H.; Xu, Q. *Chem. Commun.* **2010**, *46*, 7400.
58. Zheng, S.-T.; Bu, J. T.; Li, Y.; Wu, T.; Zuo, F.; Feng, P.; Bu, X. *J. Am. Chem. Soc.* **2010**, *132*, 17062.
59. Zhao, X.; Bu, X.; Wu, T.; Zheng, S.-T.; Wang, L.; Feng, P. *Nat. Commun.* **2013**, *4*, 2344.
60. Bu, F.; Lin, Q.; Zhai, Q.-G.; Bu, X.; Feng, P. *Dalton Trans.* **2015**, *44*, 16671.
61. Yu, J.; Cui, Y.; Wu, C.; Yang, Y.; Wang, Z.; O’Keeffe, M.; Chen, B.; Qian, G. *Angew. Chem. Int. Ed.* **2012**, *51*, 10542.
62. Sub, J.; Weng, L.; Zhou, Y.; Chen, J.; Chen, Z.; Liu, Z.; Zhao, D. Y. *Angew. Chem. Int. Ed.* **2002**, *41*, 4471.
63. Zhang, J.; Chen, S.; Wu, T.; Feng, T.; Bu, X. *J. Am. Chem. Soc.* **2008**, *130*, 12882.
64. (a) Oh, M.; Rajput, L.; Kim, D.; Moon, D.; Lah, S. M. *Inorg. Chem.* **2013**, *52*, 3891. (b) Marshall, J. R.; Griffin, L. S.; Wilson, C.; Forgan, S. R. *J. Am. Chem. Soc.* **2015**, *137*, 9527. (c) Zhang, Z.; Zaworotko, J. *J. Am. Chem. Soc. Rev.* **2014**, *43*, 5444.
65. Li, Tao.; Kozlowski, T. M.; Doud, A. Evan.; Blakely, N. Maiké.; Rosi, L. N. *J. Am. Chem. Soc.* **2013**, *135*, 11688.
66. Kim, M.; Cahill, F. J.; Fei, H.; Prather, A. K.; Cohen, M. S. *J. Am. Chem. Soc.* **2012**, *134*, 18082.
67. Choi, S.; Lee, J. H.; Kim, T.; Oh, M. *Eur. J. Inorg. Chem.* **2014**, 6220.

68. Yao, Q.; Sun, J.; Li, K.; Su, J.; Peskov, V, M.; Zou, X. *Dalton Trans*, **2012**, *41*, 3953.
69. Farha, K, D.; Yazaydin, O, A.; Eryazici, I.; Malliakas, D, C.; Hauser, G, B.; Kanatzidis, G, M.; Nguyen, T, S.; Snurr, Q, R.; Hupp, T, J. *Nature*, **2010**, *2*, 944.
70. Lalonde, M.; Bury, W.; Karagiari, O.; Brown, Z.; Hupp, T, J.; Farha, K, O. *J. Mater. Chem. A*. **2013**, 5453.
71. Deria, P.; Mondloch, E, J.; Karagiari, O.; Bury, W.; Hupp, T, J.; Farha, K, O. *Chem. Soc. Rev.* **2014**, *43*, 5896.
72. Zhang, Z.; Wojtys, L.; Eddaoudi, M.; Zaworotko, J, M. *J. Am. Chem. Soc.* **2013**, *135*, 5982.
73. Mihaly, J, J.; Zeller, M.; Genna, T, D. *Cryst. Growth Des.* **2016**, *16*, 1550.

Synthesis of In-Derived MOFs

Materials and Methods

Reagents and Instrumentation

Triethyl amine, morpholine, piperidine, 1-bromobutane, 1,4-dichlorobutane, 1,4-dibromobutane, tetraethylammonium bromide and cinchonine were purchased from Sigma-Aldrich and used as received. 2,5-Thiophenedicarboxylic acid (TDC) was purchased from TCI-America, InCl_3 was purchased from Alfa Aesar, and all solvents were purchased from Acros. All purchased reagents were used as received. TGA data were collected on a TA Instruments TGA Q50 from 40 °C to 600 °C at a rate of 10 °C per minute. NMR data were collected on a 400 MHz Bruker Avance NMR Spectrometer. ICP-MS data were collected on a ThermoScientific iCAP Q. All PXRD data were collected on a Bruker X8 PROSPECTOR.

Stability Studies

To a 20 mL vial charged with activated (dried overnight @ 100 °C) MOF (50 mg) was added the solvent of study (4 mL). The vial was sealed with a Teflon-lined cap and shaken on a ThermoFisher MaxQ orbital shaker at 100 rpm for one week at room temperature. The solvent was decanted off and the MOF was then analyzed immediately via PXRD without further manipulation.

Cation Exchange Experiments

General procedure for lithium cation exchange experiment.

To a suspension of 50 mg of activated MOF in 3 mL of DMF, 3 mL of a 0.16M acetone solution of $\text{Li}(\text{BF}_4)$ was added. The vial was then agitated on a ThermoFisher MaxQ orbital shaker at 100 rpm for 3 days at room temperature. The contents were then washed several times with fresh DMF, decanted, and dried under vacuum at 100 °C. After drying 1-2 mg of MOF were digested in conc. HNO_3 (3 mL) and then diluted with H_2O such that the final volume was 10 mL. This solution was subjected to ICP-MS analysis. Additional undigested MOF was analyzed via PXRD.

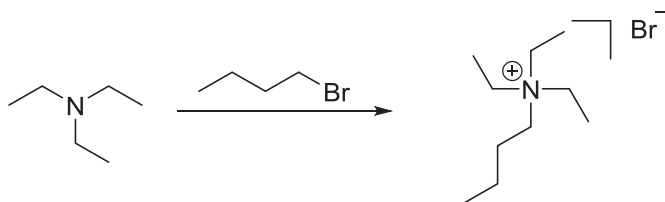
General procedure for ammonium cation exchange experiment.

To a suspension of 50 mg of activated MOF in 3 mL of DMF, 3 mL of a 0.16M dichloromethane solution of the appropriate ammonium salt was added. The vial was then agitated on a ThermoFisher MaxQ orbital shaker at 100 rpm for 7 days at room temperature. The contents were then washed several times with fresh DMF, decanted, and dried under vacuum at 100 °C. The MOF was then suspended in deuterated- $\text{AcOH}(\text{D}_4)$ and sonicated for 5 minutes until the MOF was completely dissolved. After

sonication, the homogeneous solution was transferred to an NMR tube for NMR analysis. Additional undigested MOF was analyzed via PXRD.

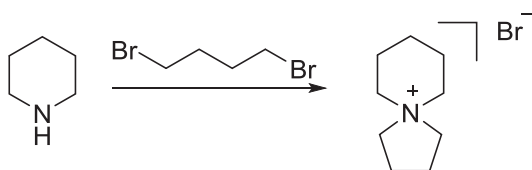
I. Synthesis

N-butyl triethyl ammonium bromide (TEBABr)



To a 20 mL scintillation vial equipped with a stir bar was added triethyl amine (5.02 mL, 36.0 mmol, 1.00 equiv) and *n*-butyl bromide (3.86 mL, 36.0 mmol, 1.00 equiv) via syringe. The resulting mixture was heated at 85 °C for 24 h and then allowed to cool to room temperature. The suspension was then concentrated *in vacuo* yielding a crude white solid. The solid was transferred to a 50 mL conical centrifuge tube and was suspended in diethyl ether (45 mL). The tube was subjected to centrifugation at 5000 rpm for 1 minute and the solvent was decanted. This procedure was repeated four additional times. The precipitate was then dried under reduced pressure to yield a white solid (1.53 g, 18 % yield). ¹H NMR (CDCl₃, 400 MHz) δ 1.01 (t, 3H, *J* = 7.3 Hz), 1.39 (t, 9H, *J* = 7.3 Hz), 1.46-1.51 (m, 2H), 1.70 (q, 2H, *J* = 8.0 Hz), 3.32 (t, 2H, *J* = 8.5 Hz), 3.52 (q, 6H, *J* = 7.3 Hz) ¹³C NMR (CDCl₃ 100 MHz) δ 8.17, 13.70, 19.84, 24.02, 53.64, 57.46.

Spirocyclic piperidinium bromide (spPPBr)

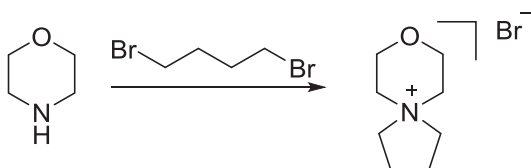


To a 20 mL scintillation vial equipped with a stir bar was added piperidine (1.78 mL, 18.0 mmol, 1.00 equiv) and 1,4-dibromobutane (2.15 mL, 18.0 mmol, 1.00 equiv) via syringe. The resulting mixture was stirred at room temperature for 5 minutes (caution: initial reaction is highly exothermic!), was then heated at 85 °C for 24 h, and then allowed to cool to room temperature. The suspension was then concentrated *in vacuo* yielding a crude brownish-white solid. The solid was transferred to a 50 mL conical centrifuge tube and was suspended in diethyl ether (45 mL). The tube was subjected to centrifugation at 5000 rpm for 1 minute and the solvent was decanted. This procedure was repeated four additional times. The precipitate was then dried under reduced pressure to yield a brownish-white solid. (3.45 g, 87 % yield). ¹H NMR (CDCl₃,

400 MHz) δ 1.95 (m, 6H), 2.28 (m, 4H), 3.72 (t, 4H, $J = 5.8$ Hz), 3.86 (t, 4H, $J = 7.3$ Hz). ^{13}C NMR (CDCl_3 , 100 MHz) δ 21.1, 21.4, 21.8, 60.4, 62.7.

Note: this solid contained ~25% of the piperidinium bromide. This could be removed via trituration with 2-propanol, but never to below 20%.

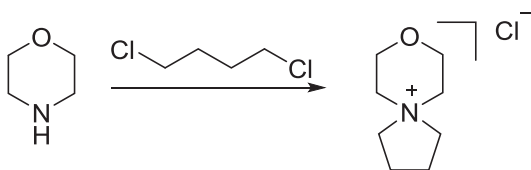
Spirocyclic morpholinium bromide (spMPBr)



To a 20 mL scintillation vial equipped with a stir bar was added morpholine (1.55 mL, 18.0 mmol, 1.00 equiv) and 1,4-dibromobutane (2.15 mL, 18.0 mmol, 1.00 equiv) via syringe. The resulting mixture was stirred at room temperature for 5 minutes (caution: initial reaction is highly exothermic!), was then heated at 85 °C for 24 h, and then allowed to cool to room temperature. The suspension was then then concentrated *in vacuo* yielding a crude brownish-white solid. The solid was transferred to a 50 mL conical centrifuge tube and was suspended in diethyl ether (45 mL). The tube was subjected to centrifugation at 5000 rpm for 1 minute and the solvent was decanted. This procedure was repeated four additional times. The precipitate was then dried under reduced pressure to yield a brown solid (3.46 g, 87 % yield). ^1H NMR (CDCl_3 , 400 MHz) 2.28 (m, 4H), 3.81 (t, 4H, $J = 4.91$ Hz), 4.03 (t, 4H, $J = 7.27$ Hz), 4.08 (t, 4H, $J = 3.92$ Hz) δ ^{13}C NMR (CDCl_3 , 100 MHz) δ 21.54, 59.35, 62.41, 63.30.

Note: this solid contained ~20% of the morpholinium bromide. This could be removed via trituration with 2-propanol, but never to below 15%.

Spirocyclic morpholinium chloride (spMPCl)

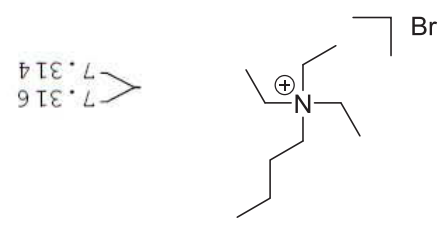
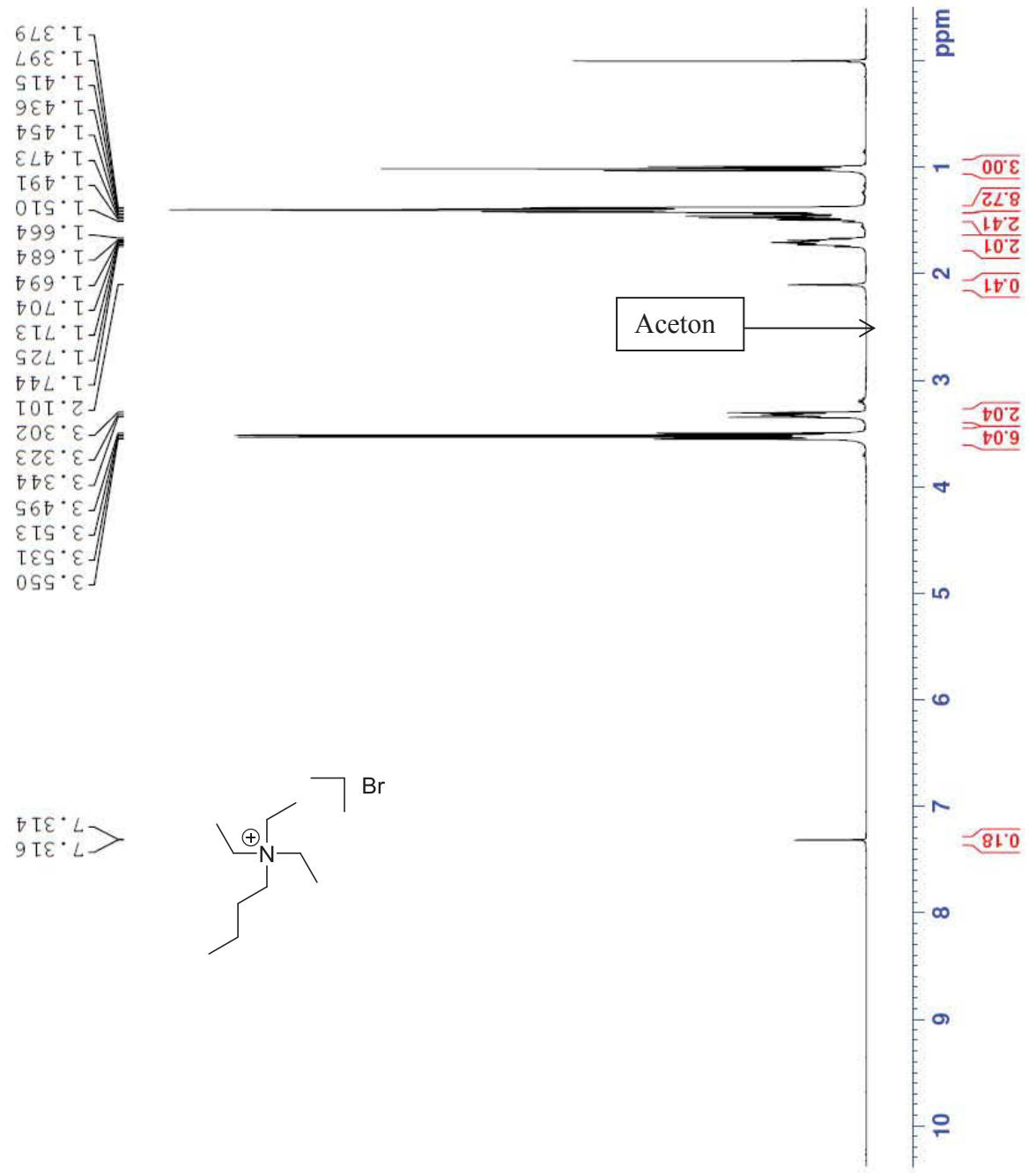


To a 20 mL scintillation vial equipped with a stir bar was added morpholine (2.35 mL, 27.0 mmol, 1.50 equiv) and 1,4-chlorobutane (1.97 mL, 18.0 mmol, 1.00 equiv) via syringe. The resulting mixture was stirred at room temperature for 5 minutes (caution: initial reaction is highly exothermic!), was then heated at 85 °C for 24 h, and then allowed to cool to room temperature. The suspension was then then concentrated *in*

vacuo yielding a crude brownish-white solid. The solid was transferred to a 50 mL conical centrifuge tube and was suspended in diethyl ether (45 mL). The tube was subjected to centrifugation at 5000 rpm for 1 minute and the solvent was decanted. This procedure was repeated four additional times. The precipitate was then dried under reduced pressure to yield a brownish-white solid. (2.80 g, 88 % yield). ¹H NMR (CDCl₃, 400 MHz) 2.27 (m, 4H), 3.75 (t, 4H, *J* = 4.96 Hz), 3.97 (t, 4H, *J* = 4.98 Hz), 4.02 (t, 4H, *J* = 3.92 Hz) δ ¹³C NMR (CDCl₃, 100 MHz) δ 21.5, 43.0, 59.3, 62.4, 63.2, 63.5

Note: this solid contained ~40% of morpholinium chloride.

Current: 6.0k, Voltage: 1.0k
 NAME: AcetBr-2018-10-10-10
 PROCNO: 1
 P2 - Acquisition Parameters
 INSTRUM: spect
 F1: 400.1524711 MHz
 F2: 400.1524711 MHz
 SFO1: 400.1524711 MHz
 SFO2: 400.1524711 MHz
 P2 - Processing parameters
 SI: 32768
 SF: 400.1524711 MHz
 DSF: 131072
 BPF: 0
 GB: 0
 PC: 1.00

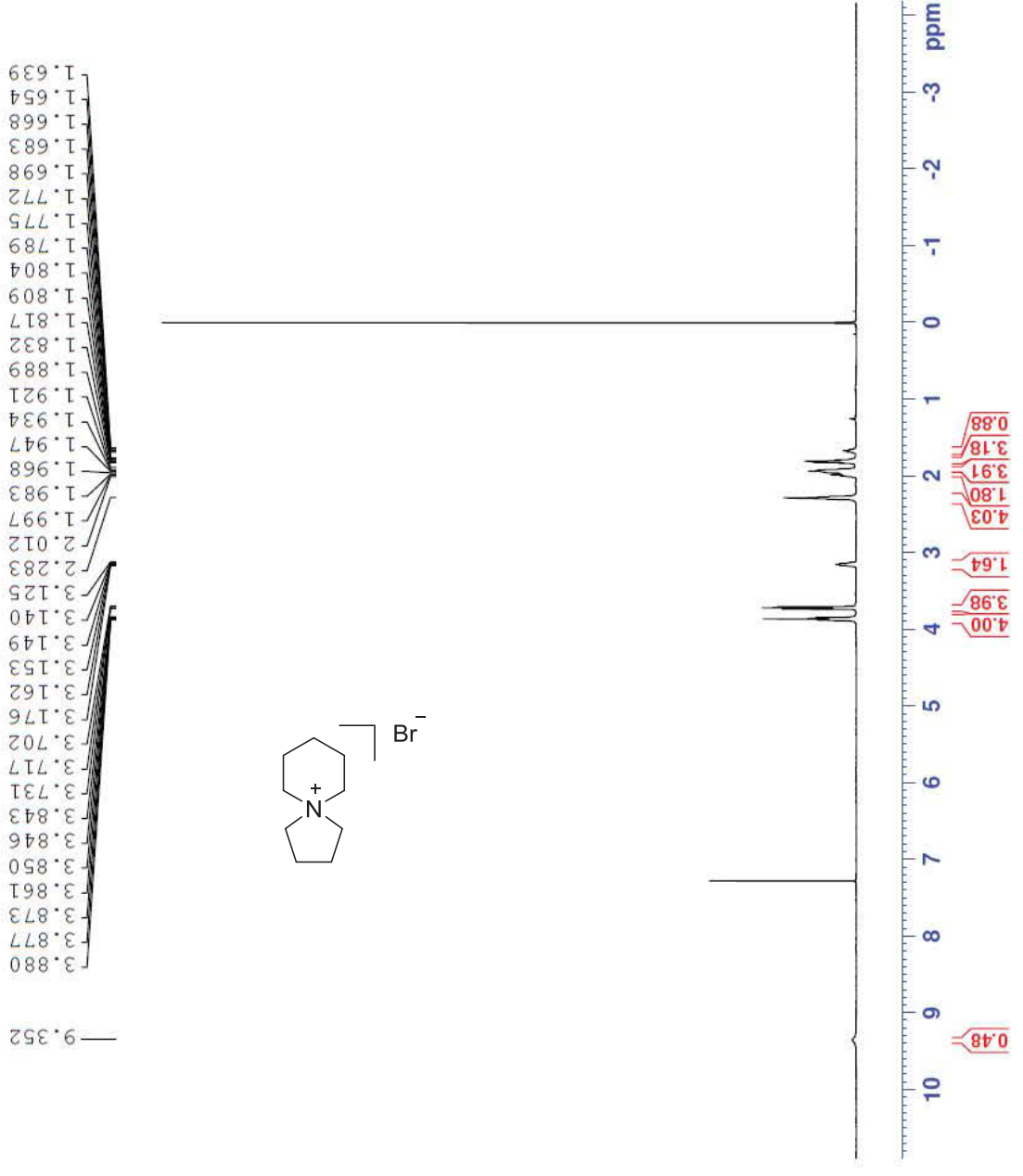


Current Data Parameters
 NAME Oct26-2015-10mihali Pip 3
 EXPNO 10
 PROCNO 1

F2 - Acquisition Parameters
 Date_ 20151028
 Time_ 12.16
 INSTRUM spect
 PROBHD 5 mm PABBI 1H/
 PULPROG zg30
 TD 65536
 SOLVENT CDCl3
 NS 128
 DS 0
 SWH 8276.146 Hz
 FIDRES 0.1126314 Hz
 AQ 3.9583745 sec
 RG 256
 DW 60.400 usec
 DE 6.00 usec
 TE 300.0 K
 FI 2.00000000 sec
 D1 1
 TD0 1

===== CHANNEL f1 =====
 NUC1 1H
 P1 7.83 usec
 PL1 -1.80 dB
 PL1W 9.92294312 W
 SF01 400.1324710 MHz

F2 - Processing parameters
 SI 32768
 SF 400.1300025 MHz
 EM
 WDW 0
 SSB 0
 LB 0.30 Hz
 GB 0
 PC 1.00



Current Data Parameters
 NAME Aug29-2015-11mhall 2nd pip number liqor
 KEYNO 11
 PRNO 11

F2 - Acquisition Parameters
 Date_ 20150829
 Time_ 15:48
 INSTRUM spect
 PULPROG zgpg30
 TD 65536
 SFO2 400.1516006 MHz
 SOLVENT CDCl3
 DS 4
 FWHM 2483.261 Hz
 AQ 1.3621488 sec
 RG 2056
 DR 6.55 umsec
 TE 300.2 K
 D11 0.0300000 sec
 T10 1

CHANNEL F1
 NUC1 13C
 P1 2.00 umsec
 PL1 -2.00 dB
 FLM 50.9356400 MHz
 SFO1 100.6278931 MHz

CHANNEL F2
 NUC2 13C
 P2 0.00 umsec
 PL2 15.00 dB
 PL12 15.00 dB
 F2 400.1516006 MHz
 SFO2 400.1516006 MHz

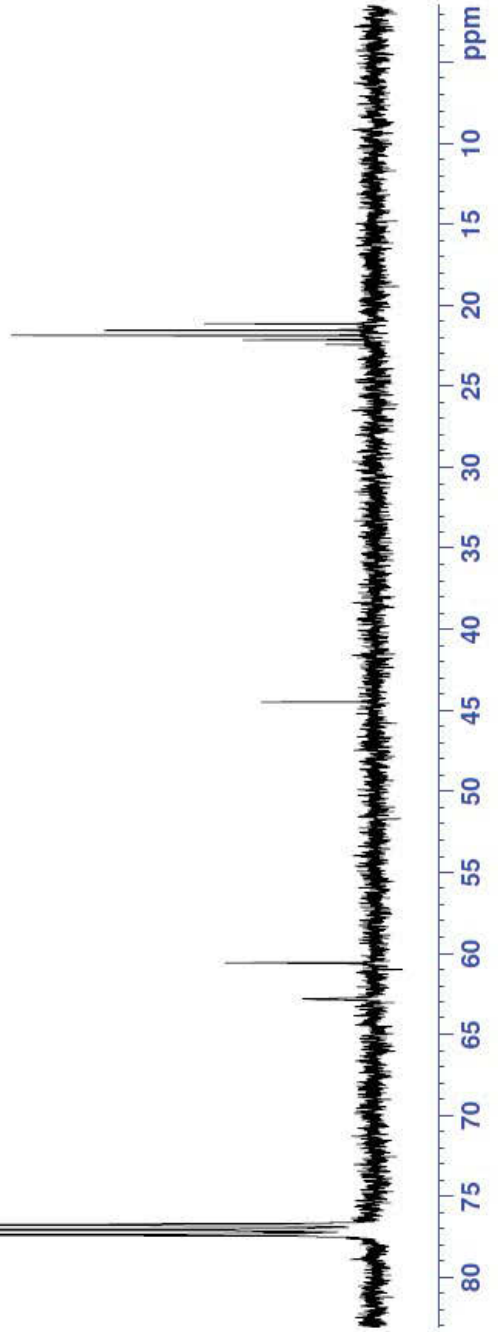
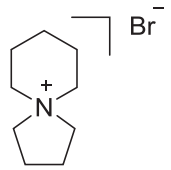
F2 - Processing parameters
 SI 32768
 SF 100.6177699 MHz
 SFR 0
 GB 0
 BR 1.00 Hz
 BPC 1.40

22.376
 22.097
 21.820
 21.496
 21.093

44.452

60.563
 62.781

76.723
 77.041
 77.243
 77.358



Current Data Parameters
 NAME Oct28-2015-jmbhai1 Morph 2
 EXPNO 11
 PROCNO 1

F2 - Acquisition Parameters
 Date_ 20151028
 Time 13.54
 INSTRUM spect
 PROBHD 5 mm PABBI 1H/
 PULPROG zg30
 TD 65536
 SOLVENT CDCl3
 NS 128
 DS 0
 SWH 8278.146 Hz
 FIDRES 0.126314 Hz
 AQ 3.9583745 sec
 RG 181
 DW 60.480 usec
 DE 6.150 usec
 TE 300.0 K
 D1 2.00000000 sec
 TD0 1

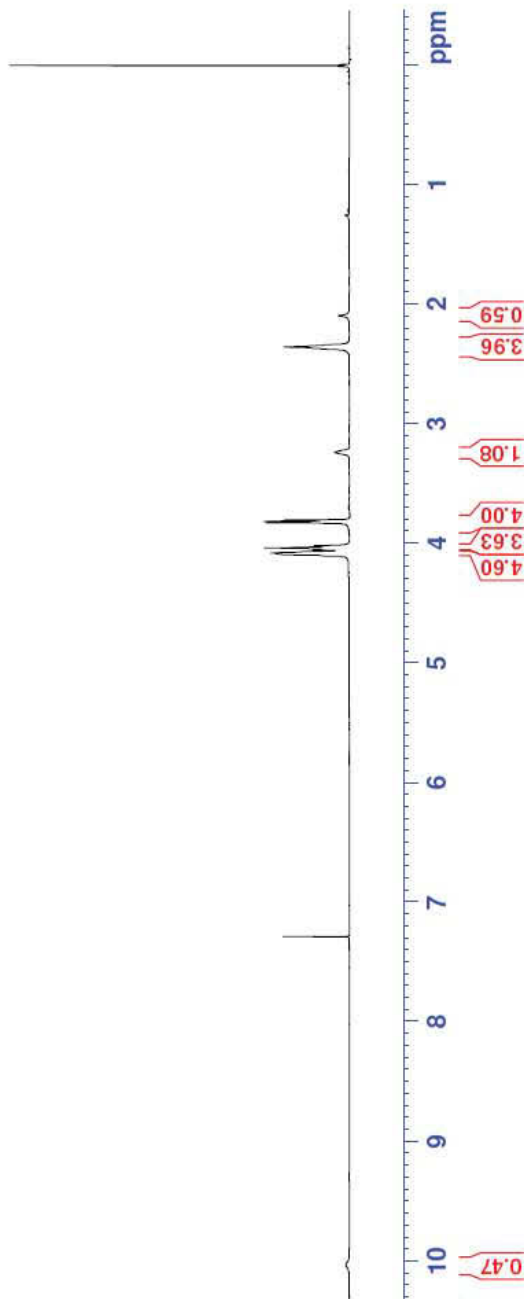
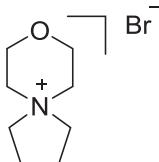
CHANNEL f1
 NUC1 1H
 P1 7.83 usec
 PL1 -1.80 dB
 PL1W 9.92294312 W
 SFO1 400.1324710 MHz

F2 - Processing parameters
 SI 32768
 SF 400.1299993 MHz
 SEW EM
 SSB 0
 LB 0.30 Hz
 GB 0
 PC 1.00

4.101
 4.089
 4.077
 4.069
 4.052
 4.033
 4.015
 3.825
 3.813
 3.801
 3.234
 2.353
 2.092

7.286

10.031



Current Data Parameters
 NAME Oct28-2015-jjmihali Morph 2
 EXPNO 12
 PROCNO 1

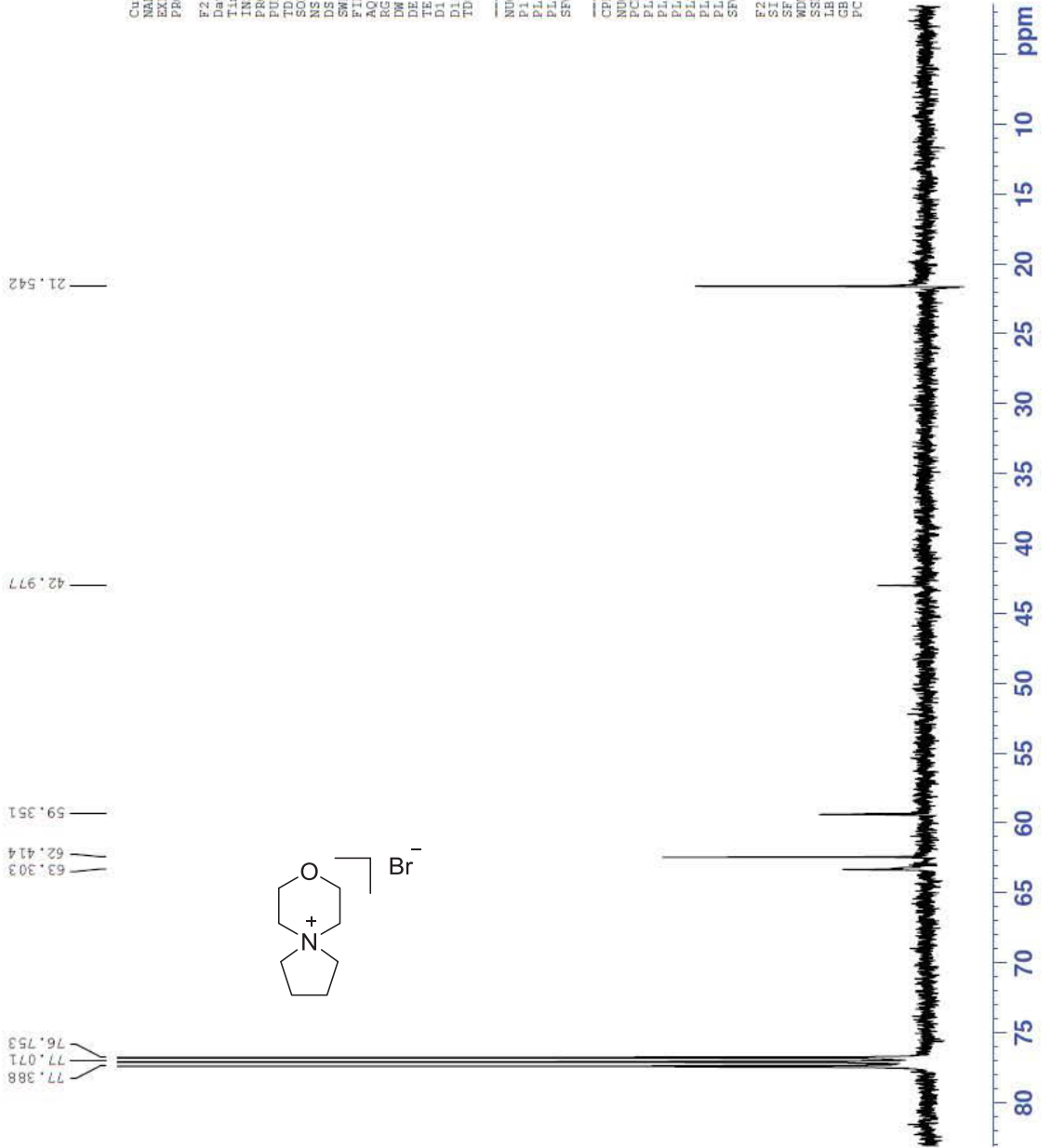
F2 - Acquisition Parameters

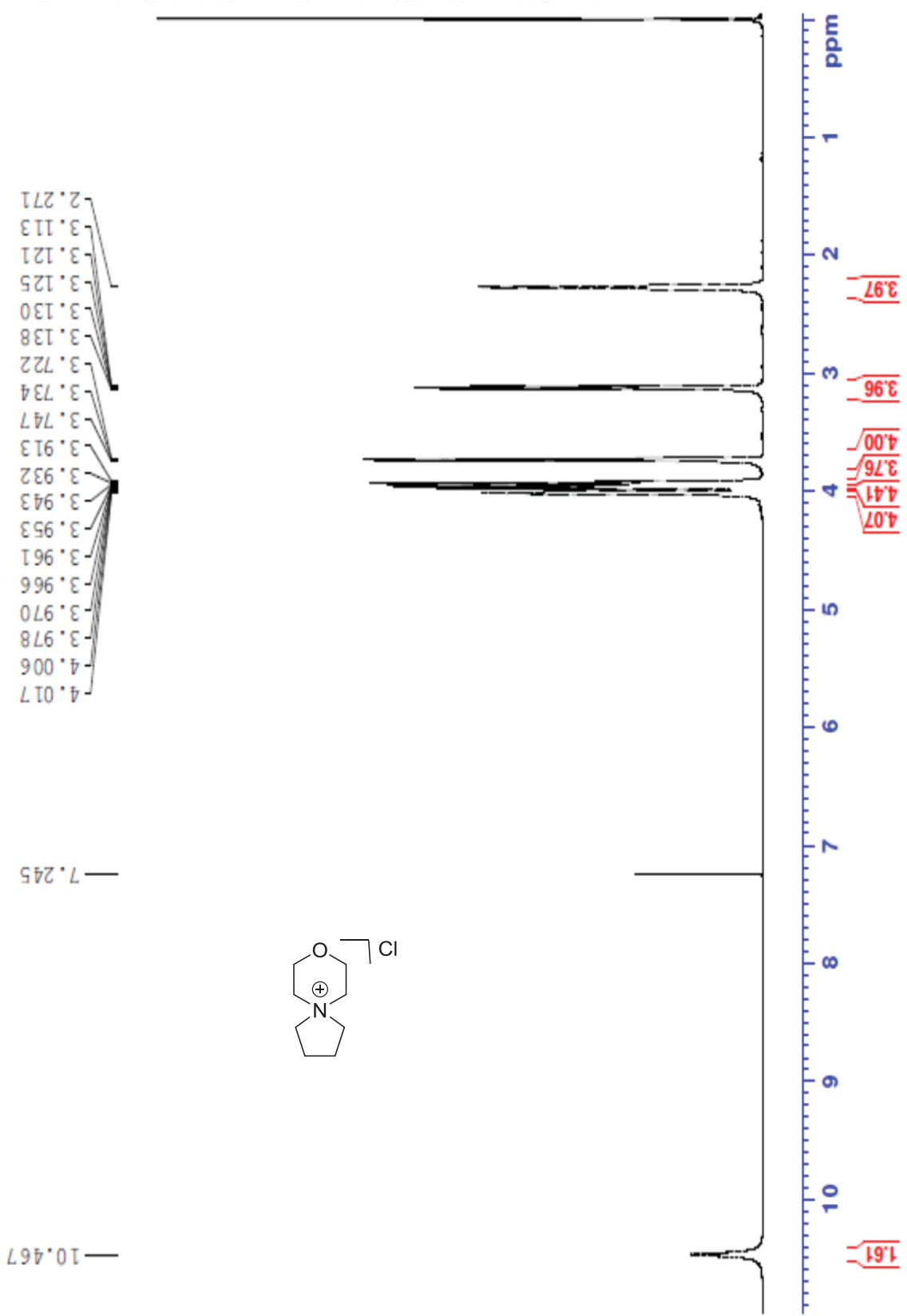
Date_ 20151028
 Time 14.56
 INSTRUM spect
 PROBO 5 mm PABBI 1H/
 PULPROG zgpg30
 TD 65536
 SOLVENT CDCl3
 NS 1024
 DS 4
 SWH 23980.814 Hz
 FIDRES 0.365918 Hz
 AQ 1.3664256 sec
 RG 181
 DW 20.850 usec
 DE 6.50 usec
 TE 300.0 K
 D1 2.00000000 sec
 D11 0.03000000 sec
 TDO 1

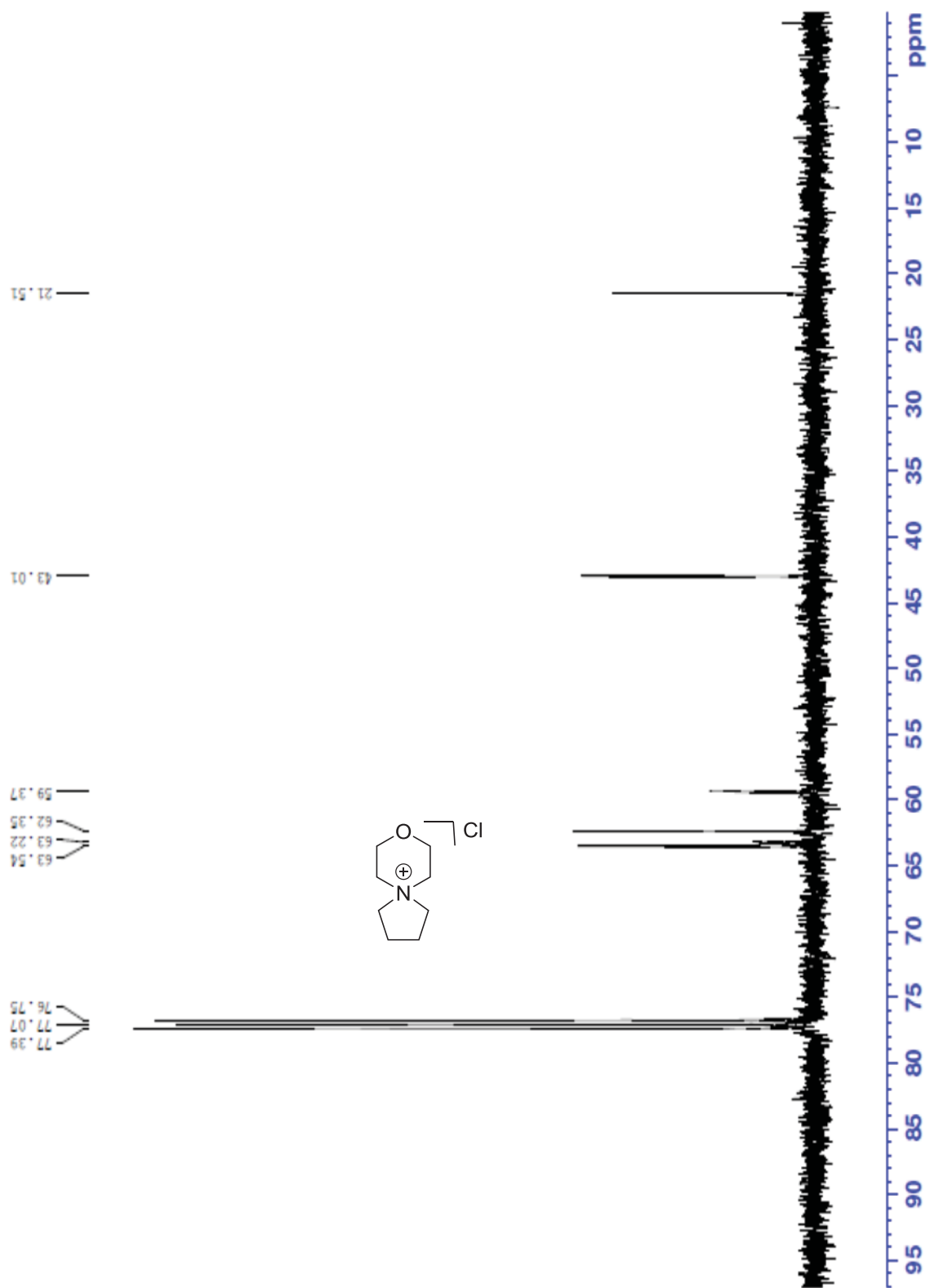
CHANNEL f1
 NUC1 13C
 P1 14.90 usec
 PL1 -3.78 dB
 PL1W 69.57576752 W
 SFO1 100.6228298 MHz

CHANNEL f2
 CPDPRG2 waitz16
 NUC2 1H
 PCPD2 75.00 usec
 PL2 -1.80 dB
 PL12 17.72 dB
 PL13 120.00 dB
 PL14 9.92200000 W
 PL15 0.17282572 W
 PL16 0 W
 PL17 0.11082572 W
 SFO2 400.1316005 MHz

F2 - Processing parameters
 SI 32768
 SF 100.6127690 MHz
 MDW EM
 SSB 0
 LB 1.00 Hz
 GB 0
 PC 1.40







III. NMR Spectra of MOFs After Attempted Ammonium Cation Exchange

```

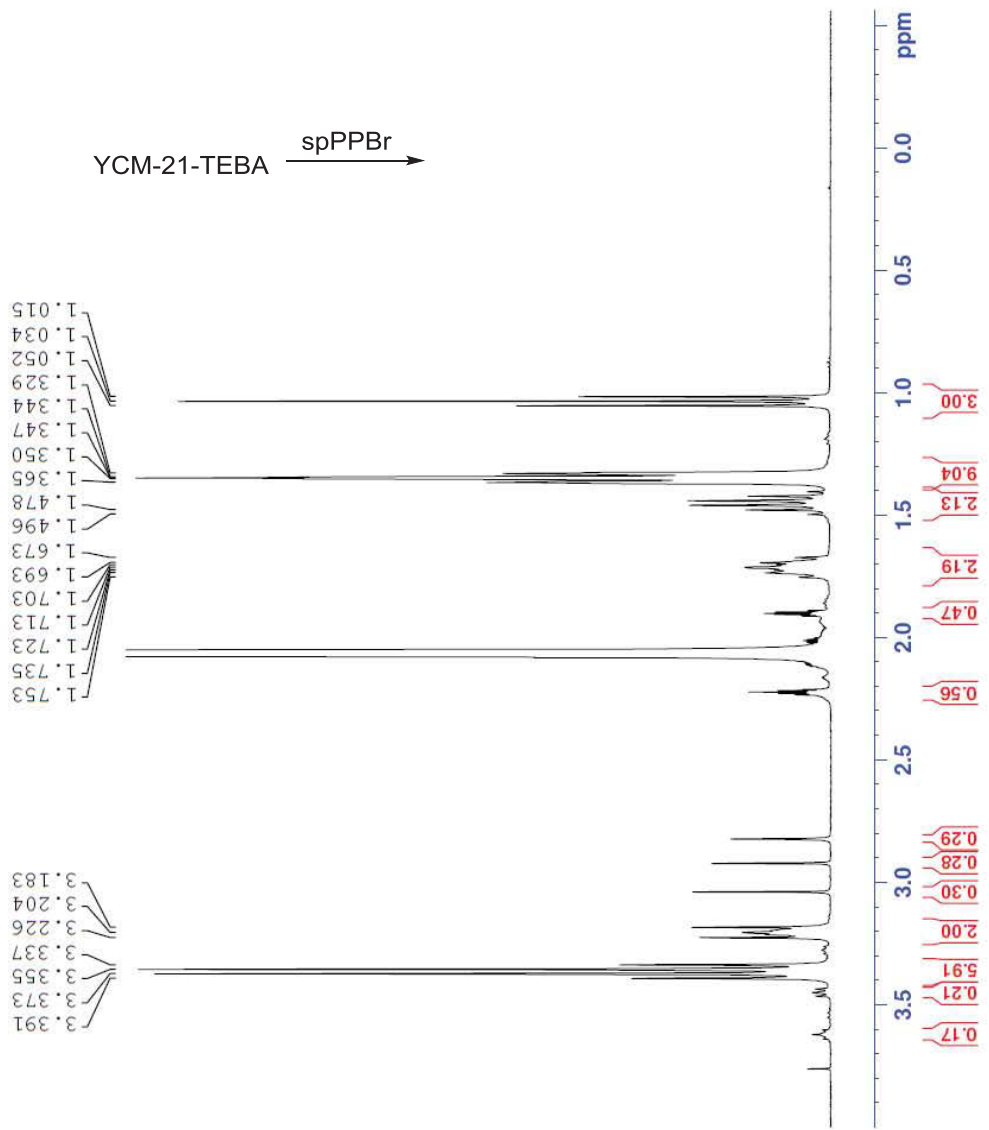
Current Data Parameters
NAME      jjm-3-30A D4
EXPNO    10
PROCNO   1

F2 - Acquisition Parameters
Date_    20151021
Time     15.56
INSTRUM  spect
PROBHD   5 mm PABBI IH/
PULPROG  zg30
ID       65536
SOLVENT  Acetic
NS       300
DS       0
SWH      16025.641 Hz
FIDRES   0.244532 Hz
AQ       2.0447233 sec
RG       456.1
DW       31.200 usec
DE       6.50 usec
TE       300.0 K
D1       2.00000000 sec
TD0      1

===== CHANNEL f1 =====
NUC1     1H
P1       7.83 usec
PL1     -1.80 dB
FLL1     9.92294312 W
SFO1     400.1324710 MHz

F2 - Processing parameters
SI       32768
SF       400.1300000 MHz
WDW      EM
SSB      0
LB       0.30 Hz
GB       0
PC       1.00

```



```

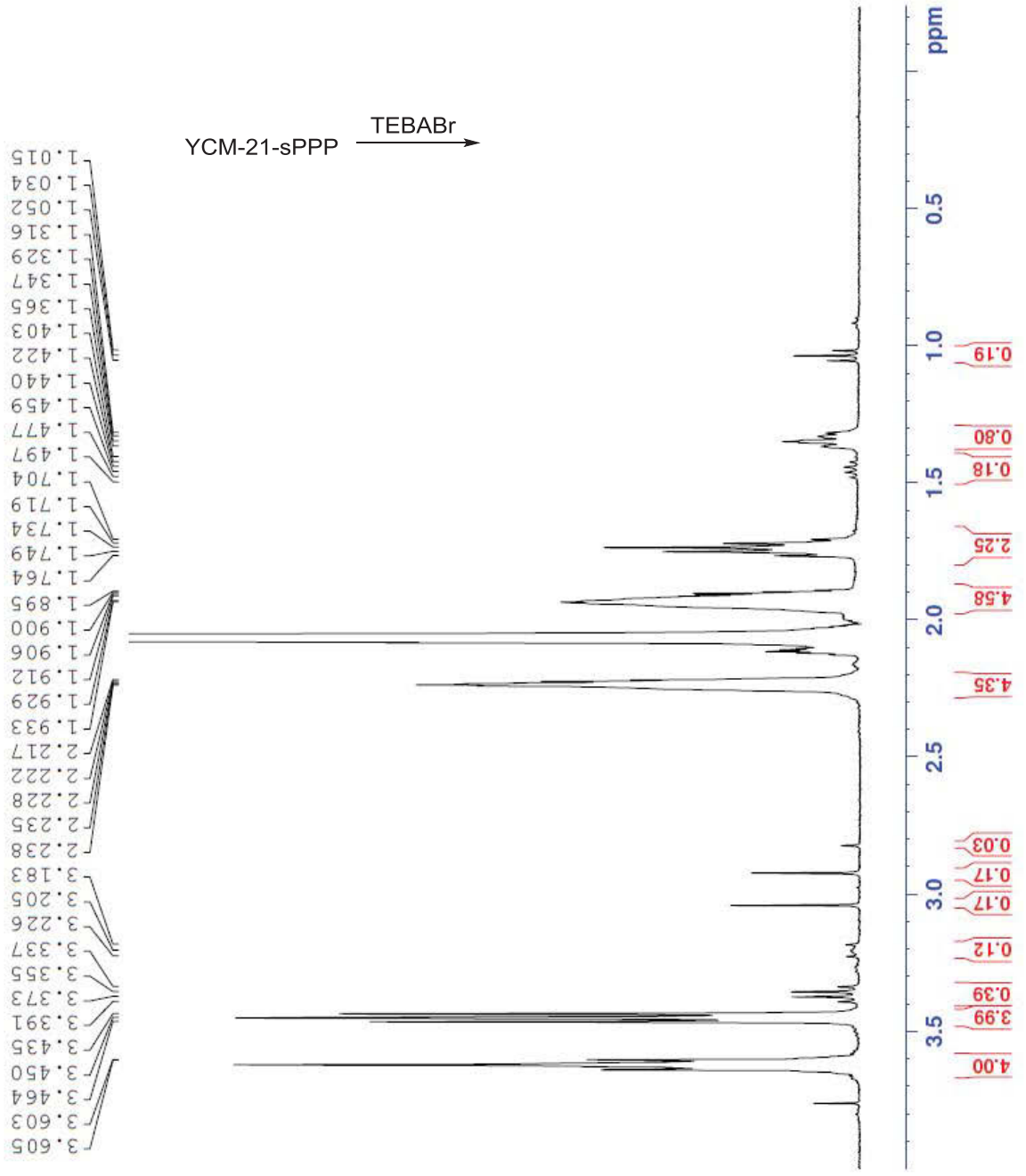
Current Data Parameters
NAME      jjm-3-30B D4
EXPNO    13
PROCNO   1

F2 - Acquisition Parameters
Date_    20151021
Time     17.44
INSTRUM  spect
PROBHD   5 mm PABBI 1H/
PULPROG  zg30
TD        65536
SOLVENT  Acetic
NS        128
DS        0
SWH       8278.146 Hz
FIDRES    0.126314 Hz
AQ         3.9583745 sec
RG         362
DE         60.400 usec
TE         6.50 usec
TD0        300.0 K
DI         2.00000000 sec
TD0        1

===== CHANNEL f1 =====
NUC1      1H
P1         7.83 usec
PL1        -1.80 dB
PL1W       9.92294312 W
SFO1       400.1324710 MHz

F2 - Processing parameters
SI         32768
SF         400.1300000 MHz
WDW        EM
SSB        0
LB         0.30 Hz
GB         0
PC         1.00

```



II. Supplemental Figures

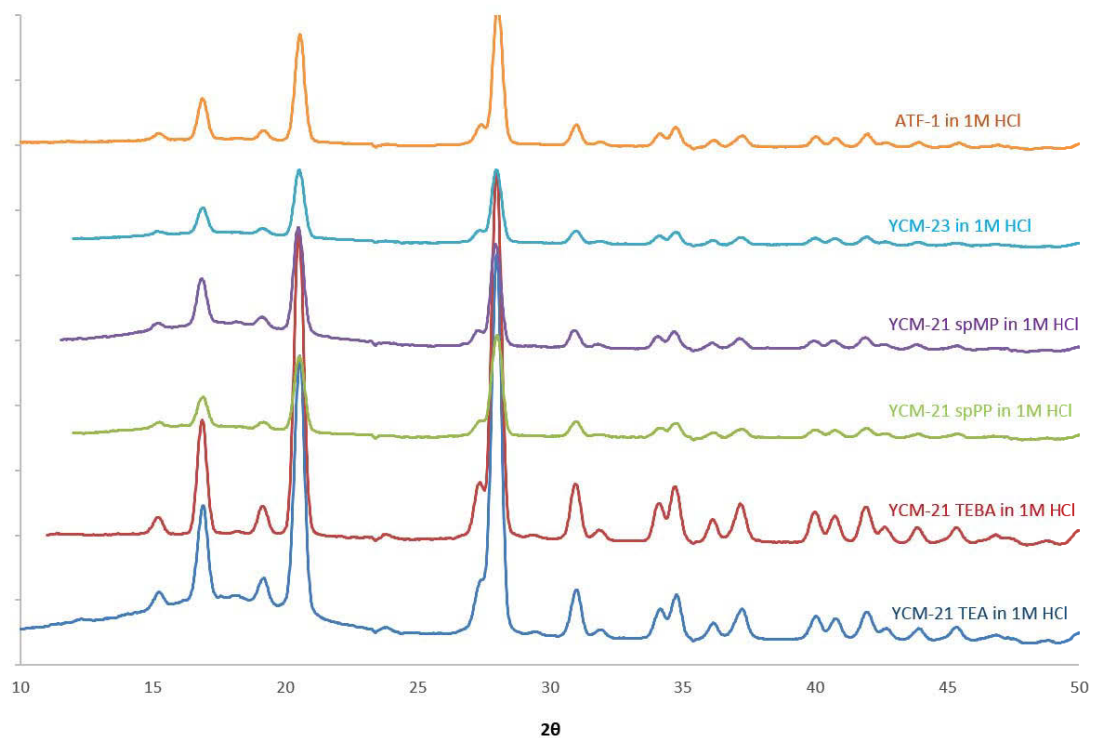


Figure 30: PXR D Patterns of ATF-1, YCM-21 series, and YCM-23 after being soaked in 1M HCl for one week.

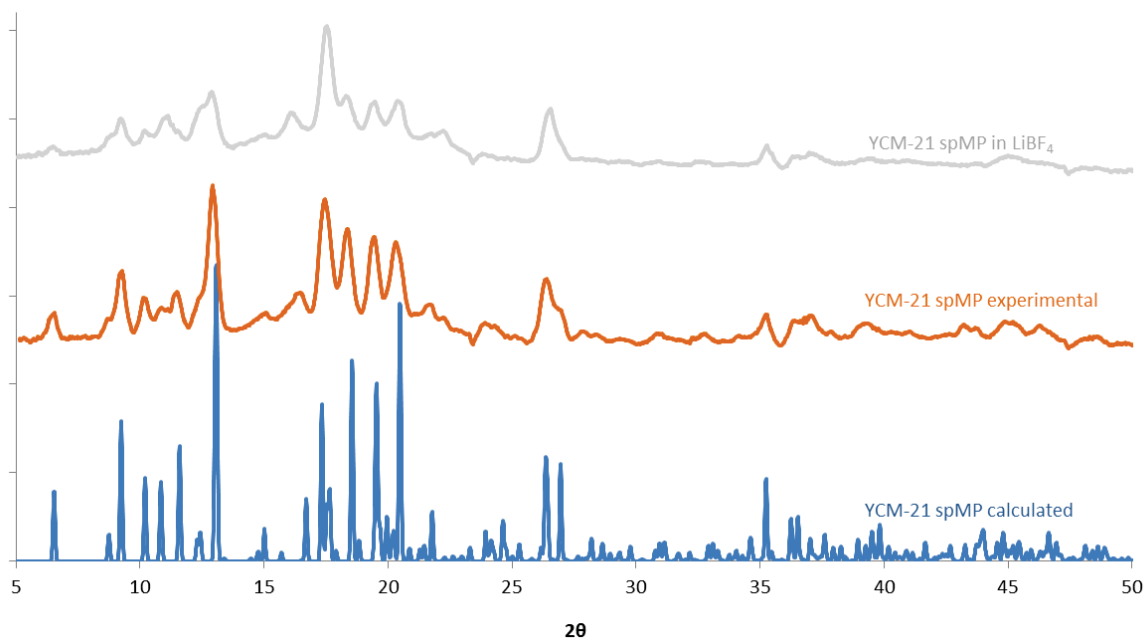


Figure 31: PXR D Patterns of YCM-21-spMP after Li^+ uptake

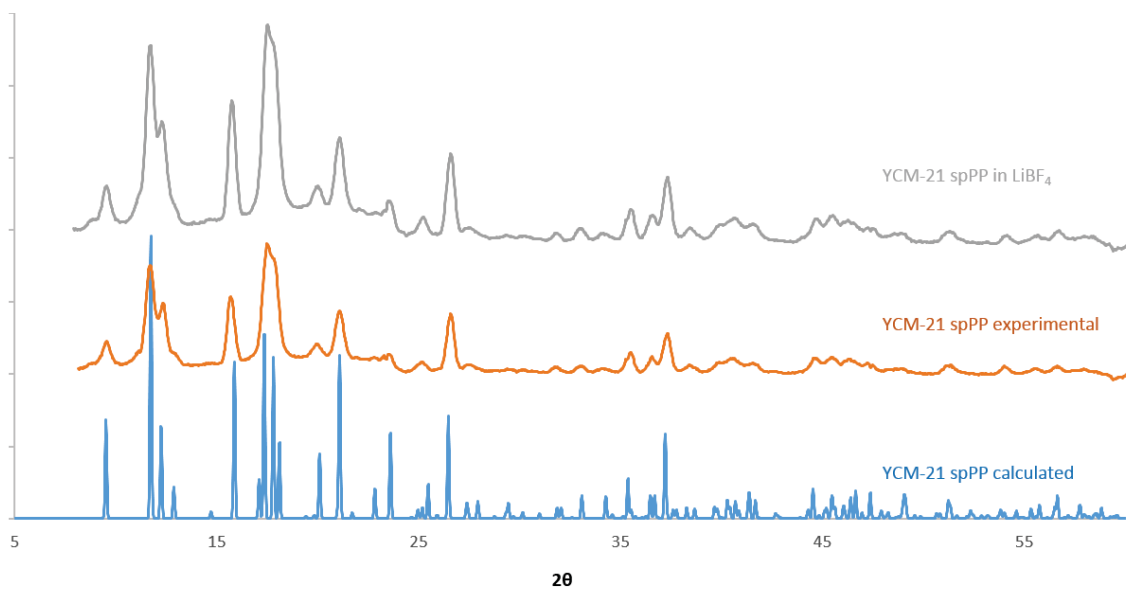


Figure 32: PXR D Patterns of YCM-21-spPP after Li⁺ uptake

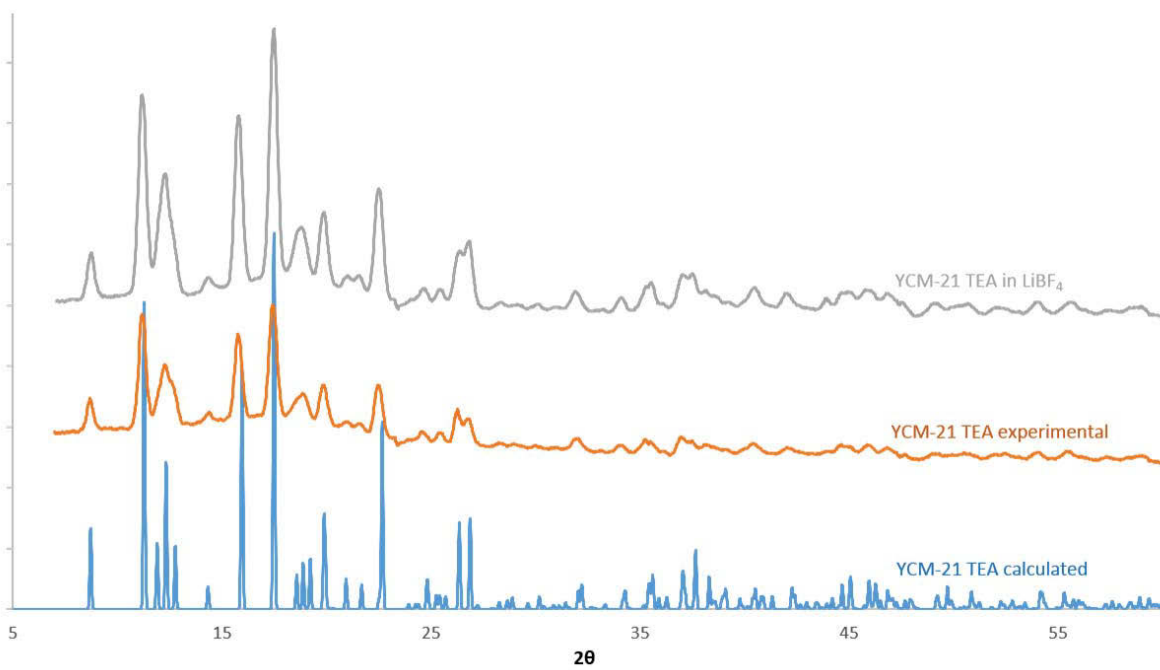


Figure 33: PXR D Patterns of YCM-21-TEA after Li⁺ uptake

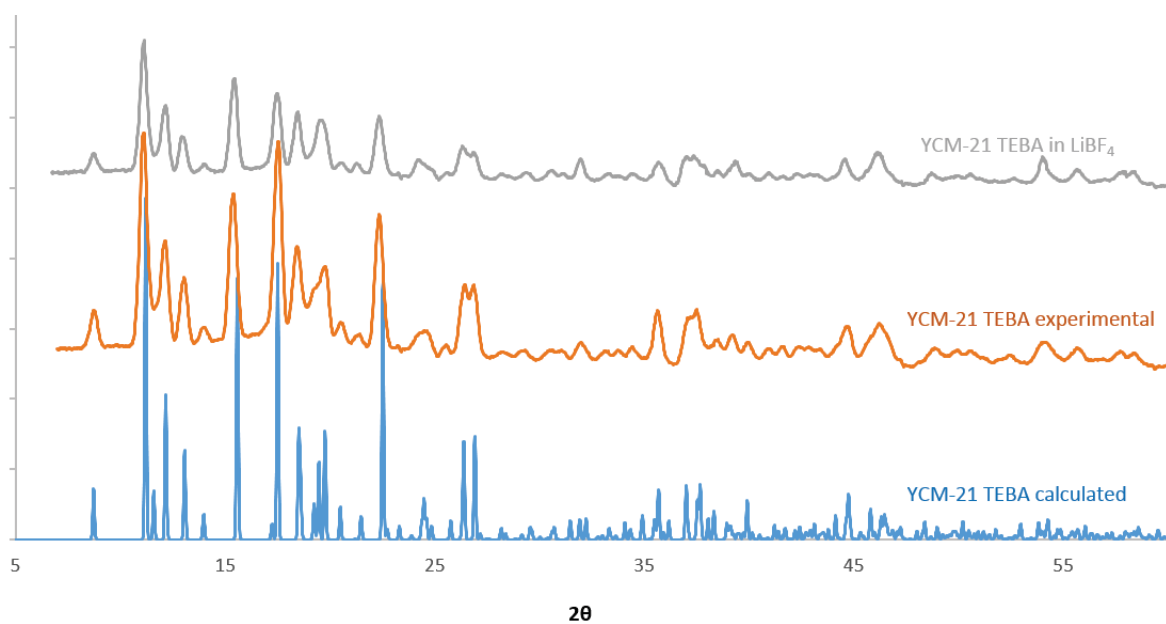


Figure 34: PXR D Patterns of YCM-21-TEBA after Li^+ uptake

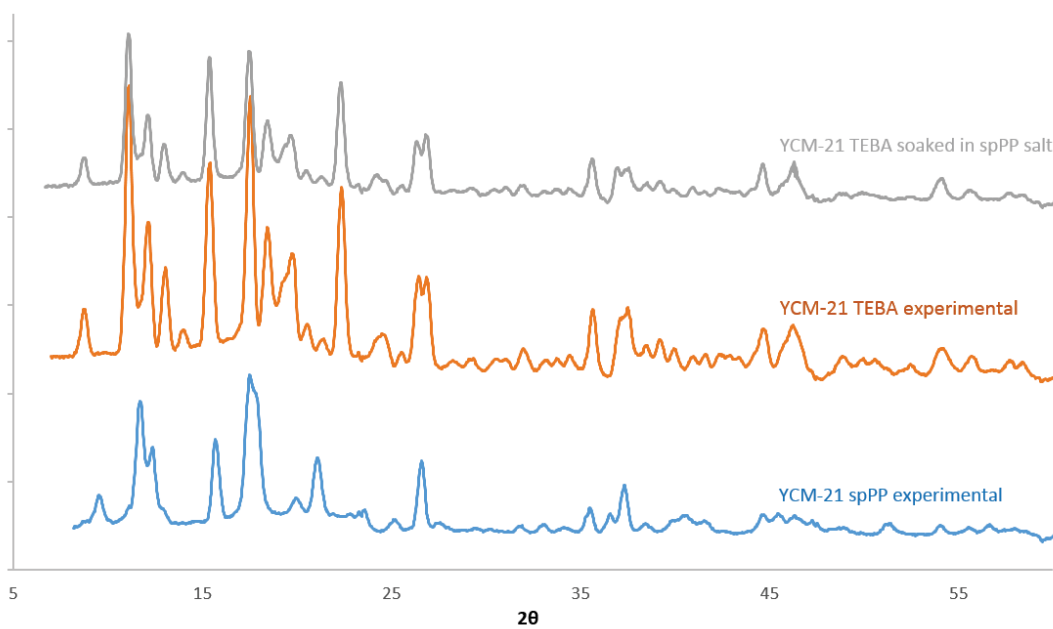


Figure 35: PXR D Patterns of YCM-21-TEBA after being soaked in DMF solution of spPPBr

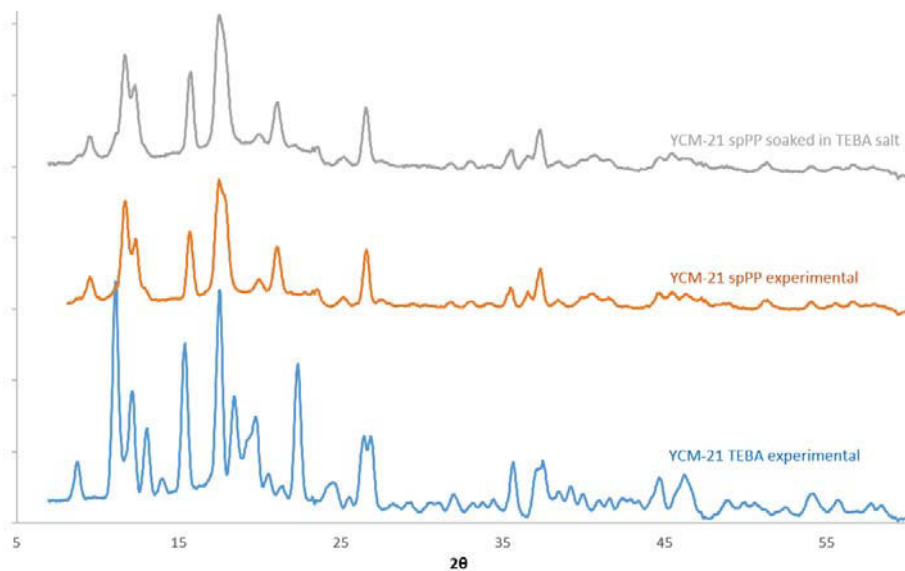


Figure 36: PXRD Patterns of YCM-21-spPP after being soaked in DMF solution of TEBABr

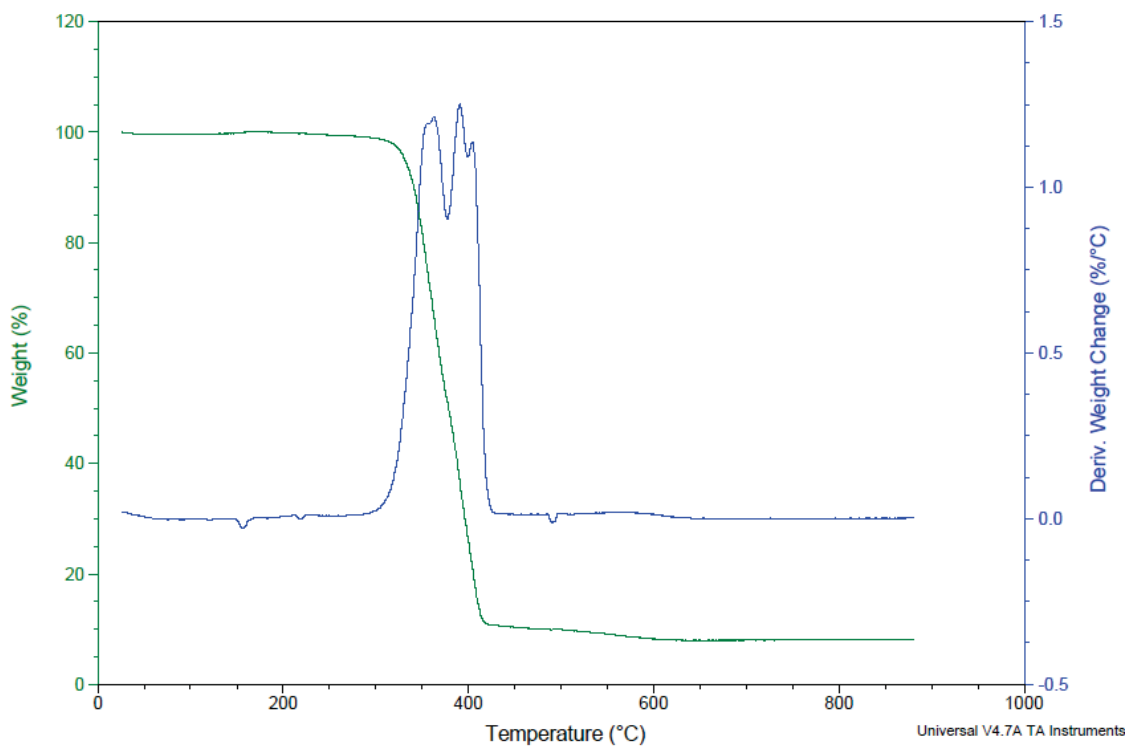


Figure 37: TGA for YCM-21-TEA

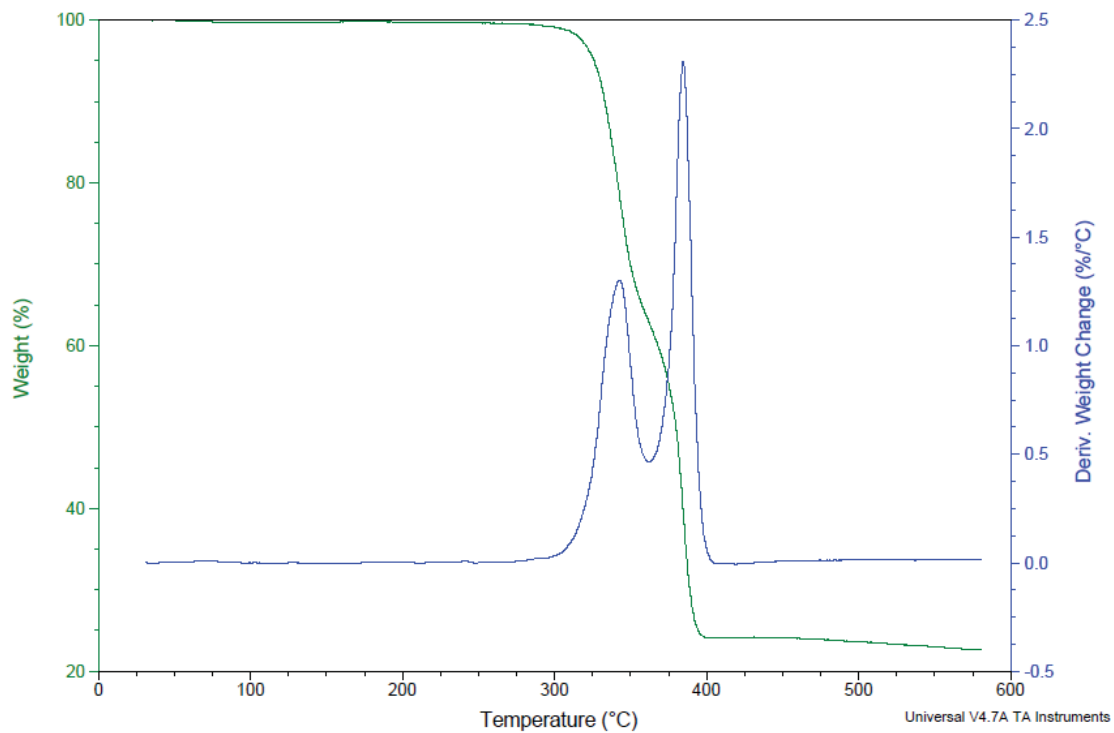


Figure 38: TGA for YCM-21-TEBA

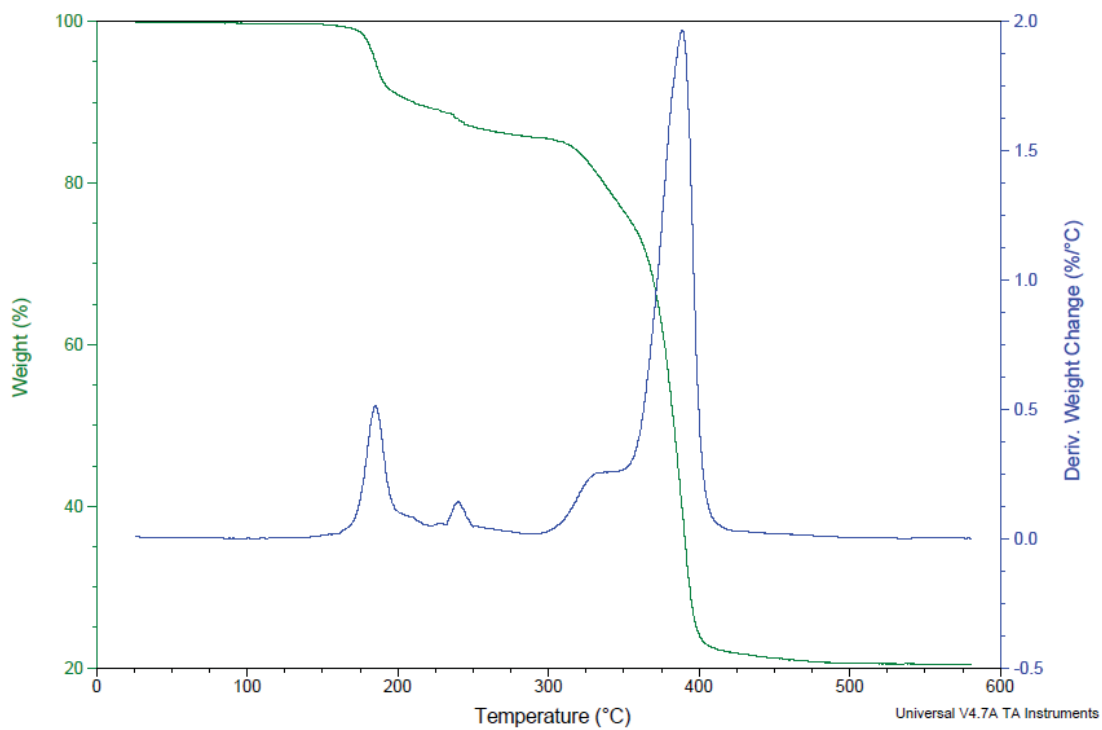


Figure 39: TGA for YCM-21-spMP

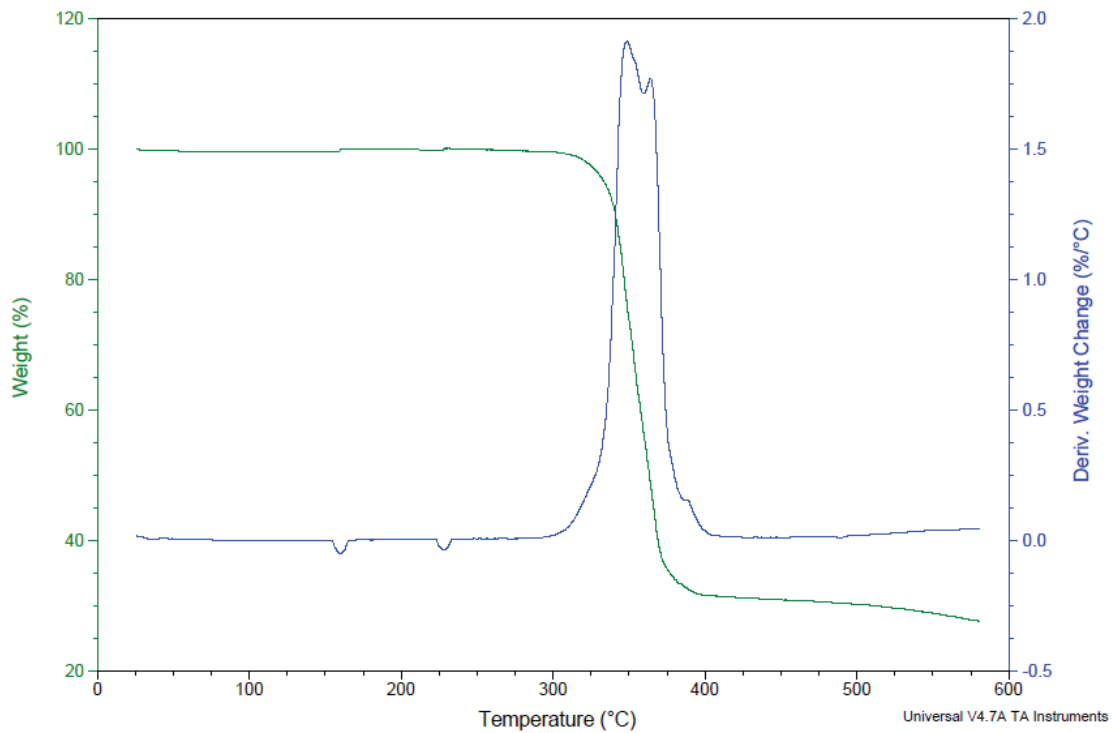


Figure 40: TGA for YCM-21-spPP

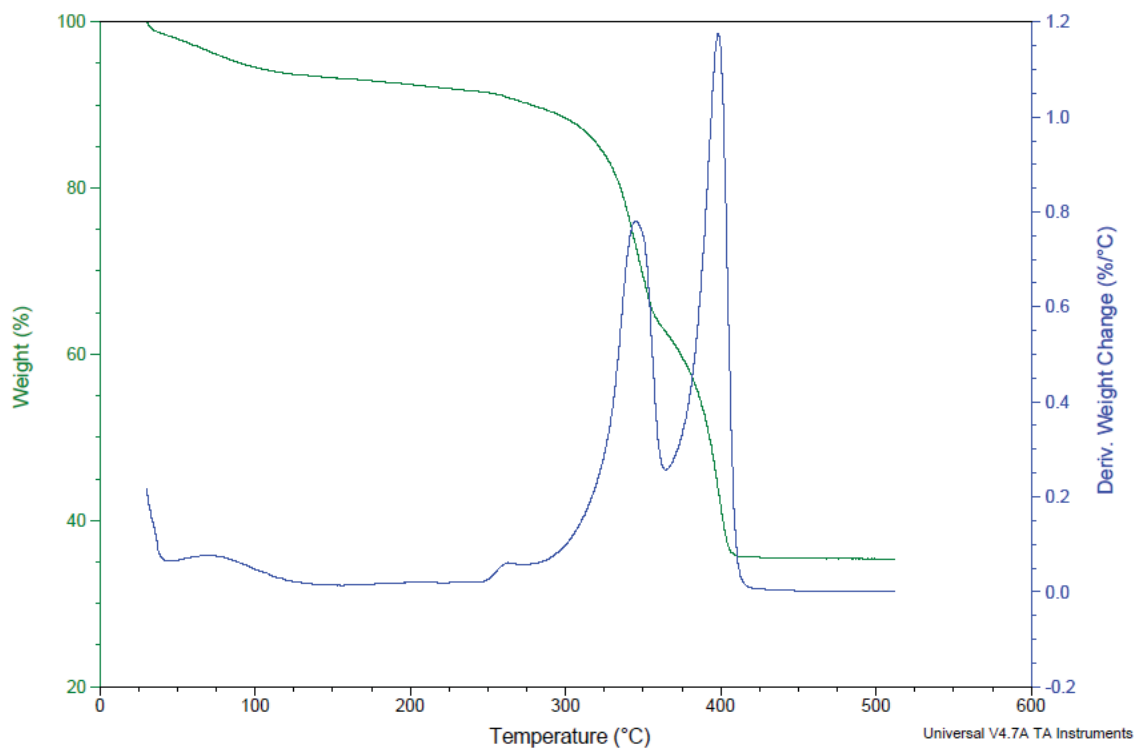


Figure 41: TGA for YCM-22

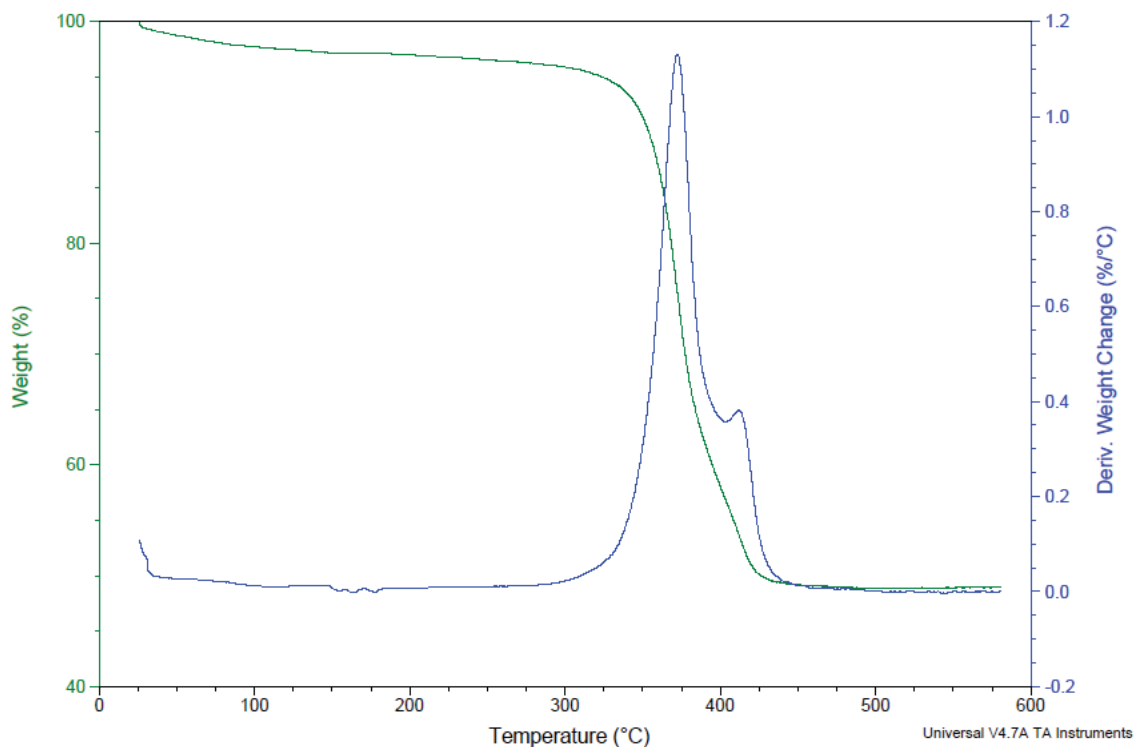


Figure 42: TGA for YCM-23

III. X-ray Crystallography

X-ray Single Crystal Structure Analysis

Data were collected using a Bruker Quest CMOS diffractometer with Mo- $K\alpha$ radiation ($\lambda = 0.71073 \text{ \AA}$), or a Bruker AXS X8 Prospector CCD diffractometer with Cu- $K\alpha$ radiation with $1\mu\text{S}$ microsources and laterally graded multilayer (Goebel) mirrors for monochromatization. Single crystals were mounted on Mitegen micromesh mounts using a trace of mineral oil and cooled in-situ to 100(2) K for data collection. Frames were collected, reflections were indexed and processed, and the files scaled and corrected for absorption using APEX2.ⁱ The space groups were assigned and the structures were solved by direct methods using XPREP within the SHELXTL suite of programsⁱⁱ and refined by full matrix least squares against F^2 with all reflections using Shelxl2013 or 2014ⁱⁱⁱ and the graphical interface Shelxle.^{iv} H atoms attached to carbon and nitrogen atoms were positioned geometrically and constrained to ride on their parent atoms, with carbon hydrogen bond distances of 0.95 \AA for alkene and aromatic C-H, 1.00, 0.99 and 0.98 \AA for aliphatic C-H, CH_2 and CH_3 , and 0.88 \AA for N-H moieties, respectively. Hydroxyl H atoms were refined with an O-H distance restraint of 0.84(2) \AA . Methyl H atoms were allowed to rotate but not to tip to best fit the experimental electron density. $U_{\text{iso}}(\text{H})$ values were set to a multiple of $U_{\text{eq}}(\text{O/C/N})$ with 1.5 for CH_3 and OH, and 1.2 for C-H, CH_2 and N-H units, respectively. Details of disorder and other special considerations for each structure are given

in the Supporting Information and in the Crystallographic Information Files, CIF. Complete crystallographic data, in CIF format, have been deposited with the Cambridge Crystallographic Data Centre. CCDC 1439149 to 1439155 contains the supplementary crystallographic data for this paper. These data can be obtained free of charge from The Cambridge Crystallographic Data Centre via www.ccdc.cam.ac.uk/data_request/cif.

X-ray Powder Diffraction

Powder XRD patterns of small samples were collected on a Bruker AXS X8 Prospector CCD single crystal diffractometer using the “pilot” plugin for collection of multicrystalline XRD patterns. The instrument is equipped with a copper $1\mu\text{S}$ microsource with a laterally graded multilayer (Goebel) mirror for monochromatization ($\lambda = 1.54178 \text{ \AA}$, beam size 0.1-0.2 mm) and an ApexII CCD area detector. Powder samples were thoroughly ground to assure a representative number of crystallites to be present in the X-ray beam. Powder samples were mixed with small amounts of mineral oil and mounted onto a 0.4 mm diameter Mitegen micromesh mount for data collection. Samples were centered in the beam using the instrument’s mounting microscope video camera. Data were collected in an emulated theta-2theta setup using the Apex2 software package of Bruker AXS. The sample mount was aligned horizontally ($\text{Chi} = 0^\circ$) and theta angles were set to eight different angles between 12 and 96° to cover a range equivalent to a 0 to 110° range of a powder X-ray diffractometer operated in Debye Scherrer mode (omega angles of each run were set to half the theta values). Samples were rotated around the mount’s spindle axis during measurement (360 rotation around phi), typical exposure times were 30 seconds per frame collected. The eight individual patterns taken were corrected for unequal sample to detector surface distance (“unwarped”) and were combined into one continuous pattern using the “pilot plugin” software embedded in the Apex2 software package. Data were integrated over 2theta, converted in powder XRD patterns in Bruker “raw” format and were further processed with standard powder XRD software packages.

Table 2. Tabular Data for Crystal Structures of YCM-20 Series

For all structures: $Z = 4$. Experiments were carried out at 100 K. Data collection used ω and ϕ scans.

	YCM-21-TEBA	YCM-21-TEBA'	YCM-22
Crystal data			
Chemical formula	$C_{12}H_4InO_8S_2 \cdot C_{10}H_{24}N$	$C_{12}H_4InO_8S_2 \cdot C_{10}H_{24}N$	$C_6H_2Cl_3InO_4S \cdot 2(C_2H_8N)$
M_r	613.39	613.39	483.49
Crystal system, space group	Monoclinic, $C2/c$	Tetragonal, $P4_1$	Orthorhombic, $Cmcm$
a, b, c (Å)	13.6085 (8), 15.2415 (8), 11.4260 (6)	10.2339(10), 10.2339(10), 23.648(2)	12.2419(7), 13.2271(7), 10.2621(6)
α, β, γ (°)	90, 96.329 (2), 90	90, 90, 90	90, 90, 90
V (Å ³)	2355.5 (2)	2476.7 (5)	1661.69 (16)
$F(000)$	1248	1248	960
D_x (Mg m ⁻³)	1.730	1.645	1.933
Radiation type	Mo $K\alpha$	Mo $K\alpha$	Mo $K\alpha$
No. of reflections for cell measurement	4006	9109	9127
θ range (°) for cell measurement	2.6–30.3	2.6–28.3	2.3–36.3
μ (mm ⁻¹)	1.23	1.17	2.04
Crystal shape	Prism	Block	Plate
Colour	Colourless	Colourless	Colourless
Crystal size (mm)	0.10 × 0.05 × 0.04	0.23 × 0.19 × 0.16	0.27 × 0.26 × 0.12
Data collection			
Diffractometer	Bruker AXS D8 Quest CMOS diffractometer	Bruker AXS D8 Quest CMOS diffractometer	Bruker AXS D8 Quest CMOS diffractometer
Radiation source	I- μ -S microsource X-ray tube	I- μ -S microsource X-ray tube	I- μ -S microsource X-ray tube
Monochromator	Laterally graded multilayer (Goebel) mirror	Laterally graded multilayer (Goebel) mirror	Laterally graded multilayer (Goebel) mirror
Absorption correction	Multi-scan, Apex2 v2014.11 (Bruker, 2014)	Multi-scan, Apex2 v2014.1-1 (Bruker, 2014)	Multi-scan, Apex2 v2014.1-1 (Bruker, 2014)
T_{min}, T_{max}	0.684, 0.746	0.594, 0.746	0.636, 0.747
No. of measured, independent and observed [$I > 2\sigma(I)$] reflections	10836, 3485, 2827	15843, 6074, 5299	46833, 2190, 2096
R_{int}	0.057	0.046	0.034

θ values ($^{\circ}$)	$\theta_{\max} = 30.5, \theta_{\min} = 2.6$	$\theta_{\max} = 28.3, \theta_{\min} = 2.6$	$\theta_{\max} = 36.4, \theta_{\min} = 2.3$
$(\sin \theta/\lambda)_{\max}$ (\AA^{-1})	0.715	0.667	0.834
Range of h, k, l	$h = -17 \rightarrow 19, k = -20 \rightarrow 20, l = -16 \rightarrow 14$	$h = -13 \rightarrow 13, k = -13 \rightarrow 13, l = -31 \rightarrow 30$	$h = -20 \rightarrow 20, k = -22 \rightarrow 22, l = -17 \rightarrow 17$
Refinement			
$R[F^2 > 2\sigma(F^2)], wR(F^2), S$	0.042, 0.071, 1.08	0.053, 0.106, 1.15	0.016, 0.039, 1.20
No. of reflections	3485	6074	2190
No. of parameters	204	409	64
No. of restraints	0	467	0
H-atom treatment	H-atom parameters constrained	H-atom parameters constrained	H-atom parameters constrained
$\Delta\rho_{\max}, \Delta\rho_{\min}$ ($e \text{\AA}^{-3}$)	0.76, -1.19	1.22, -1.11	1.10, -0.45
Absolute structure parameter	–	-0.012 (18)	–

	YCM-21-spMP	YCM-21-spPP	YCM-23
Crystal data			
Chemical formula	$\text{C}_{12}\text{H}_4\text{InO}_8\text{S}_2 \cdot \text{C}_8\text{H}_{16}\text{NO} \cdot 0.5(\text{C}_4\text{H}_8\text{O}_2) \cdot \text{C}_3\text{H}_7\text{NO}$	$\text{C}_{12}\text{H}_4\text{InO}_8\text{S}_2 \cdot \text{C}_9\text{H}_{18}\text{N}$	$\text{C}_{18}\text{H}_{20}\text{In}_2\text{N}_2\text{O}_{12}\text{S}_2$
M_r	714.46	595.33	750.12
Crystal system, space group	Monoclinic, $P2_1/c$	Tetragonal, $P4_12_12$	Monoclinic, $C2/c$
a, b, c (\AA)	10.1955(7), 10.2208(7), 27.279(2)	10.2068(10), 10.2068(10), 22.305(2)	13.2957(6), 17.3545(6), 13.7460(7)
α, β, γ ($^{\circ}$)	90, 97.605 (2), 90	90, 90, 90	90, 116.0241 (18), 90
V (\AA^3)	2817.6 (3)	2323.7 (5)	2850.2 (2)
$F(000)$	1456	1200	1472
D_x (Mg m^{-3})	1.684	1.702	1.748
Radiation type	Mo $K\alpha$	Mo $K\alpha$	Mo $K\alpha$
No. of reflections for cell measurement	9712	9953	7662
θ range ($^{\circ}$) for cell measurement	2.3–36.8	2.2–31.7	2.9–30.5
μ (mm^{-1})	1.05	1.24	1.82
Crystal shape	Plate	Rod	Block
Colour	Colourless	Colourless	Colourless

Crystal size (mm)	0.36 × 0.24 × 0.06	0.20 × 0.09 × 0.08	0.11 × 0.05 × 0.04
Data collection			
Diffractometer	Bruker AXS D8 Quest CMOS diffractometer	Bruker AXS D8 Quest CMOS diffractometer	Bruker AXS D8 Quest CMOS diffractometer
Radiation source	I- μ -S microsource X-ray tube	I- μ -S microsource X-ray tube	I- μ -S microsource X-ray tube
Monochromator	Laterally graded multilayer (Goebel) mirror	Laterally graded multilayer (Goebel) mirror	Laterally graded multilayer (Goebel) mirror
Absorption correction	Multi-scan, Apex2 v2014.1-1 (Bruker, 2014)	Multi-scan, Apex2 v2014.1-1 (Bruker, 2014)	Multi-scan, Apex2 v2014.1-1 (Bruker, 2014)
T_{\min} , T_{\max}	0.657, 0.747	0.660, 0.746	0.516, 0.746
No. of measured, independent and observed [$I > 2\sigma(I)$] reflections	97527, 97527, 87199	18698, 3664, 3414	11121, 3479, 2966
R_{int}	n/a	0.036	0.043
θ values ($^{\circ}$)	$\theta_{\max} = 37.3$, $\theta_{\min} = 2.5$	$\theta_{\max} = 32.2$, $\theta_{\min} = 2.2$	$\theta_{\max} = 28.3$, $\theta_{\min} = 2.4$
$(\sin \theta/\lambda)_{\max}$ (\AA^{-1})	0.852	0.750	0.667
Range of h , k , l	$h = -16 \rightarrow 16$, $k = -17 \rightarrow 17$, $l = -46 \rightarrow 46$	$h = -12 \rightarrow 15$, $k = -13 \rightarrow 11$, $l = -27 \rightarrow 32$	$h = -16 \rightarrow 17$, $k = -22 \rightarrow 22$, $l = -18 \rightarrow 15$
Refinement			
$R[F^2 > 2\sigma(F^2)]$, $wR(F^2)$, S	0.051, 0.132, 1.08	0.049, 0.111, 1.38	0.059, 0.126, 1.13
No. of reflections	97527	3664	3479
No. of parameters	421	196	266
No. of restraints	200	111	190
H-atom treatment	H-atom parameters constrained	H-atom parameters constrained	H atoms treated by a mixture of independent and constrained refinement
$\Delta\rho_{\max}$, $\Delta\rho_{\min}$ (e \AA^{-3})	2.84, -1.83	1.71, -0.91	2.39, -1.40
Absolute structure parameter	–	0.21 (7)	–

YCM-21-TEA	
Crystal data	
Chemical formula	C ₂₀ H ₂₄ InNO ₈ S ₂
<i>M_r</i>	585.34
Crystal system, space group	Monoclinic, <i>C2/c</i>
<i>a</i> , <i>b</i> , <i>c</i> (Å)	13.9564(7), 14.8593(8), 11.1801(6)
α , β , γ (°)	90, 96.977 (3), 90
<i>V</i> (Å ³)	2301.4 (2)
<i>F</i> (000)	1184
<i>D_x</i> (Mg m ⁻³)	1.689
Radiation type	Cu <i>K</i> α
No. of reflections for cell measurement	3408
θ range (°) for cell measurement	4.4–66.3
μ (mm ⁻¹)	10.32
Crystal shape	Block
Colour	Colourless
Crystal size (mm)	0.04 × 0.03 × 0.03
Data collection	
Diffractometer	Bruker AXS X8 Prospector CCD diffractometer
Radiation source	I- μ -S microsource X-ray tube
Monochromator	Laterally graded multilayer (Goebel) mirror
Absorption correction	Multi-scan, Apex2 v2014.11 (Bruker, 2014)
<i>T_{min}</i> , <i>T_{max}</i>	0.631, 0.753
No. of measured, independent and observed [<i>I</i> > 2σ(<i>I</i>)] reflections	8769, 1999, 1776
<i>R_{int}</i>	0.061
θ values (°)	θ_{\max} = 67.1, θ_{\min} = 4.4
(sin θ/λ) _{max} (Å ⁻¹)	0.597
Range of <i>h</i> , <i>k</i> , <i>l</i>	<i>h</i> = -16→16, <i>k</i> = -17→17, <i>l</i> = -13→13
Refinement	
<i>R</i> [<i>F</i> ² > 2σ(<i>F</i> ²)], <i>wR</i> (<i>F</i> ²), <i>S</i>	0.043, 0.098, 1.09
No. of reflections	1999
No. of parameters	186
No. of restraints	54

H-atom treatment	H-atom parameters constrained
$\Delta\rho_{\max}, \Delta\rho_{\min}$ (e Å ⁻³)	1.60, -0.97

Additional Notes for Crystal Structures:

YCM-21-TEA

The tetraethyl ammonium cation is disordered around a twofold axis with the nitrogen atom located on that axis. The carbon atoms were refined as 1:1 disordered by symmetry. The C and N atoms of the disordered cation were subjected to a rigid bond restraint (RIGU). No geometry restraints were applied.

YCM-21-TEBA

The structure is isomorphous to its tetraethyl ammonium counterpart and was solved by isomorphous replacement. The triethylbutyl ammonium cation is disordered around a twofold axis with the nitrogen atom located on that axis. The carbon atoms were refined as 1:1 disordered by symmetry. No restraints for geometry or thermal parameters were applied.

YCM-21-TEBA'

The cation is disordered around the ammonium N atom. The two orientations were restrained to have similar geometries, atoms were subjected to a rigid bond restraint, and U_{ij} components of atoms closer than 1.7 Å were restrained to be similar. The ADPs of the two N atoms were constrained to be identical. Subject to these conditions, the occupancy ratio refined to 0.620(8) to 0.380(8).

YCM-21-spPP

The organic cation is disordered across a twofold rotation axis, superimposing five and six membered rings atop of one another. C-N and C-C bond lengths within the disordered section were restrained to be each similar, the C atoms around the nitrogen were restrained to approximate tetrahedral geometry, and the atoms were subjected to a rigid bond restraint.

YCM-21-spMP

The crystal under investigation was found to be non-merohedrally twinned. The orientation matrices for the two components were identified using the program

Cell_Now [Sheldrick, G. M. (2011). University of Göttingen, Germany.], with the two components being related by a 180° rotation around the real a-axis. Integration using Saint of the Apex2 program suite [Apex2 v2014.1, Bruker AXS Inc.: Madison (WI), USA, 2009.] proved problematic due to excessive multiple overlap of reflections, resulting in large numbers of rejected reflections. Attempts were made to adjust integration parameters to avoid excessive rejections (through adjustments to integration queue size, blending of profiles, integration box slicing and twin overlap parameters), which led to less but still substantial numbers of rejected reflections. With no complete data set obtainable through simultaneous integration of both twin domains, the data were instead handled as if not twinned, with only the major domain integrated, and converted into an hklf 5 type format hkl file after integration using the "Make HKLF5 File" routine as implemented in WinGX [L. J. Farrugia, J. Appl. Cryst. (2012), 45, 849-854.]. The twin law matrix used was $\begin{pmatrix} 1 & 0 & 0 \\ 0 & -1 & 0 \\ -0.714 & 0 & -1 \end{pmatrix}$. The Overlap R1 and R2 values used were 0.35, i.e. reflections with a discriminator function less or equal to overlap radius of 0.35 were counted as overlapped, all others as single. The discriminator function used was the "delta function on index non-integrality". No reflections were omitted.

The structure was solved using direct methods with the hklf 4 type file and was refined using the hklf 5 type file, resulting in a BASF value of 0.1303(8). No Rint value (`_diffn_reflvs_av_R_equivalents`) is obtainable for the hklf 5 type file using the WinGX routine.

A DMF molecule was refined as flip disordered. The two moieties were restrained to have similar geometries and the U_{ij} components of ADPs of atoms were restrained to be similar if closer than 1.7 Å (SIMU restraint in Shelxl2014). The minor moiety atoms were restrained to be approximately isotropic, and subjected to a rigid bond restraint (RIGU). Subject to these conditions, the occupancy ratio refined to 0.823(12) to 0.177(12).

Several low angle reflections were affected by the beam stop and were omitted from the refinement. The reflections were 1 0 4, 1 0 2 and symmetry equivalent permutations, and -1 2 -1 and permutations.

YCM-23

A DMF molecule, H bonded to the framework hydroxyl group, was refined as disordered over three positions. The three moieties were restrained to be flat, and to have similar geometries and the U_{ij} components of the ADPs of atoms closer than 1.7 Å were restrained to be similar. Subject to these conditions, the occupancy rates refined to 0.431(3), 0.329(3) and 0.240(3).

Table 3: YCM-31 Crystal Data

Crystal data	
Chemical formula	$2(\text{C}_{27}\text{H}_{15}\text{Br}_{0.18}\text{Cl}_{0.82}\text{InO}_6) \cdot 2(\text{C}_8\text{H}_{16}\text{NO}) \cdot 5(\text{C}_3\text{H}_7\text{NO})$
M_r	1837.42
Crystal system, space group	Triclinic, $P1$
Temperature (K)	100
a, b, c (Å)	11.4531 (5), 12.7416 (6), 15.0415 (7)
α, β, γ (°)	69.8530 (19), 82.7367 (19), 84.3103 (19)
V (Å ³)	2040.53 (16)
Z	1
Radiation type	Mo $K\alpha$
μ (mm ⁻¹)	0.87
Crystal size (mm)	0.25 × 0.15 × 0.13
Data collection	
Diffractometer	Bruker AXS D8 Quest CMOS diffractometer
Absorption correction	Multi-scan Apex2 v2014.1-1 (Bruker, 2014)
T_{\min}, T_{\max}	0.691, 0.747
No. of measured, independent and observed [$I > 2\sigma(I)$] reflections	117922, 15673, 12929
R_{int}	0.041
$(\sin \theta/\lambda)_{\text{max}}$ (Å ⁻¹)	0.772
Refinement	
$R[F^2 > 2\sigma(F^2)], wR(F^2), S$	0.045, 0.123, 1.07
No. of reflections	15673
No. of parameters	755
No. of restraints	885
H-atom treatment	H-atom parameters constrained
$\Delta\rho_{\text{max}}, \Delta\rho_{\text{min}}$ (e Å ⁻³)	3.02, -0.93

Computer programs: Apex2 v2014.1-1 (Bruker, 2014), *S*AINT V8.34A (Bruker, 2014), *S*HELXS97 (Sheldrick, 2008), *S*HELXL2014/7 (Sheldrick, 2014), SHELXLE Rev656 (Hübschle *et al.*, 2011).

Supporting information

▾ Crystallographic data

(Quest15mz156_0m)

Crystal data

$2(\text{C}_{27}\text{H}_{15}\text{Br}_{0.18}\text{Cl}_{0.82}\text{InO}_6) \cdot 2(\text{C}_8\text{H}_{16}\text{NO}) \cdot 5(\text{C}_3\text{H}_7\text{NO})$	$Z = 1$
$M_r = 1837.42$	$F(000) = 946.6$
Triclinic, $P1$	$D_x = 1.495$ Mg

	m^{-3}
$a = 11.4531 (5) \text{ \AA}$	Mo $K\alpha$ radiation, $\lambda = 0.71073 \text{ \AA}$
$b = 12.7416 (6) \text{ \AA}$	Cell parameters from 9408 reflections
$c = 15.0415 (7) \text{ \AA}$	$\theta = 2.4\text{--}32.9^\circ$
$\alpha = 69.8530 (19)^\circ$	$\mu = 0.87 \text{ mm}^{-1}$
$\beta = 82.7367 (19)^\circ$	$T = 100 \text{ K}$
$\gamma = 84.3103 (19)^\circ$	Block, colourless
$V = 2040.53 (16) \text{ \AA}^3$	$0.25 \times 0.15 \times$ 0.13 mm

Data collection

Bruker AXS D8 Quest CMOS diffractometer	15673 independent reflections
Radiation source: I- μ -S microsource X-ray tube	12929 reflections with $I > 2\sigma(I)$
Laterally graded multilayer (Goebel) mirror monochromator	$R_{\text{int}} = 0.041$
ω and ϕ scans	$\theta_{\text{max}} = 33.3^\circ$, $\theta_{\text{min}} = 2.4^\circ$
Absorption correction: multi-scan Apex2 v2014.1-1 (Bruker, 2014)	$h = -17 \rightarrow 17$
$T_{\text{min}} = 0.691$, $T_{\text{max}} = 0.747$	$k = -19 \rightarrow 19$
117922 measured reflections	$l = -23 \rightarrow 23$

Refinement

Refinement on F^2	Primary atom site location: structure-invariant direct methods
Least-squares matrix: full	Secondary atom site location: difference Fourier map
$R[F^2 > 2\sigma(F^2)] = 0.045$	Hydrogen site location: inferred from neighbouring sites
$wR(F^2) = 0.123$	H-atom parameters constrained
$S = 1.07$	$w = 1/[\sigma^2(F_o^2) + (0.0564P)^2 + 3.3741P]$ where $P = (F_o^2 + 2F_c^2)/3$
15673 reflections	$(\Delta/\sigma)_{\text{max}} = 0.001$
755 parameters	$\Delta\rho_{\text{max}} = 3.02 \text{ e \AA}^{-3}$
885 restraints	$\Delta\rho_{\text{min}} = -0.93 \text{ e \AA}^{-3}$

Special details

Geometry. All e.s.d.'s (except the e.s.d. in the dihedral angle between two l.s. planes) are estimated using the full covariance matrix. The cell e.s.d.'s are taken into account individually in the estimation of e.s.d.'s in distances, angles and torsion angles; correlations between e.s.d.'s in cell parameters are only used when they are defined by crystal symmetry. An approximate (isotropic) treatment of cell e.s.d.'s is used for estimating e.s.d.'s involving l.s. planes.

Refinement. The halide site was refined as disordered between chloride and bromide. The ADPs of the two halogens were set to be identical, and the In—Br distance was restrained to be not shorter than 2.6 Angstroms. Subject to these conditions, the occupancy ratio refined to 0.818 (3) to 0.182 (3).

The spirocyclic ammonium cation is disordered over two orientations. The two moieties were restrained to be similar in geometry, and the U^{ij} components of the ADPs of their atoms closer than 1.7 Angstroms were restrained to be similar. Subject to these conditions, the occupancy ratio refined to 0.772 (4) to 0.228 (4).

Three sites occupied by DMF molecules are present in the crystal structure, two of them disordered. All DMF moieties were restrained to be similar in geometry, and the U^{ij} components of the ADPs of their atoms closer than 1.7 Angstroms were restrained to be similar for the disordered moieties. One site was refined to be disordered over three orientations. The three moieties were restrained to be flat. Subject to these conditions their occupancy rates refined to 0.257 (3), 0.283 (3) and 0.460 (3). The other disordered site is located close to an inversion center with mutually exclusive positions. The molecules at the half occupied sites are in addition in close proximity to the major moiety of the spirocyclic ammonium cation, and were additionally split in two moieties. ADPs of equivalent atoms in the two moieties were constrained to be identical. Subject to these conditions, the occupancy ratio refined to 0.371 (6) to 0.129 (6).

A general anti-bumping restraint was applied to avoid close contacts of minor moiety H atoms.

Fractional atomic coordinates and isotropic or equivalent isotropic displacement parameters (\AA^2)

	<i>x</i>	<i>y</i>	<i>z</i>	$U_{\text{iso}}^*/U_{\text{eq}}$	Occ. (<1)
C1	0.66503 (18)	0.66064 (19)	-0.12751 (15)	0.0191 (4)	
C2	0.58319 (17)	0.71440 (17)	-0.06805 (14)	0.0171 (3)	
C3	0.57485 (18)	0.83041 (18)	-0.09169 (15)	0.0186 (4)	
H3	0.6267	0.8747	-0.1420	0.022*	
C4	0.49132 (18)	0.88175 (17)	-0.04222 (15)	0.0183 (4)	
H4	0.4850	0.9611	-0.0601	0.022*	
C5	0.41620 (17)	0.81761 (17)	0.03383 (14)	0.0157 (3)	
C6	0.42700 (18)	0.70071 (17)	0.05924 (15)	0.0194 (4)	
H6	0.3779	0.6560	0.1115	0.023*	
C7	0.50925 (19)	0.65006 (18)	0.00834 (16)	0.0204 (4)	
H7	0.5153	0.5708	0.0256	0.024*	

C8	0.32366 (17)	0.87352 (17)	0.08322 (14)	0.0159 (3)	
C9	0.26715 (17)	0.97412 (17)	0.03106 (14)	0.0164 (3)	
H9	0.2887	1.0060	-0.0354	0.020*	
C10	0.17932 (17)	1.02844 (16)	0.07547 (14)	0.0157 (3)	
C11	0.14782 (18)	0.98118 (17)	0.17311 (14)	0.0169 (3)	
H11	0.0896	1.0189	0.2039	0.020*	
C12	0.20109 (18)	0.87885 (17)	0.22606 (14)	0.0172 (3)	
C13	0.28973 (18)	0.82597 (17)	0.18064 (14)	0.0175 (3)	
H13	0.3273	0.7571	0.2163	0.021*	
C14	0.11620 (17)	1.13238 (16)	0.01806 (14)	0.0161 (3)	
C15	0.06057 (19)	1.13279 (17)	-0.05938 (15)	0.0186 (4)	
H15	0.0668	1.0676	-0.0771	0.022*	
C16	-0.00394 (19)	1.22802 (17)	-0.11083 (15)	0.0184 (4)	
H16	-0.0447	1.2266	-0.1616	0.022*	
C17	-0.00859 (18)	1.32559 (16)	-0.08778 (14)	0.0168 (3)	
C18	0.05003 (19)	1.32664 (17)	-0.01219 (15)	0.0189 (4)	
H18	0.0489	1.3936	0.0024	0.023*	
C19	0.10998 (19)	1.23002 (17)	0.04177 (15)	0.0190 (4)	
H19	0.1468	1.2302	0.0949	0.023*	
C20	-0.07751 (18)	1.42627 (17)	-0.14477 (14)	0.0171 (3)	
C21	0.15483 (19)	0.82377 (18)	0.32701 (14)	0.0191 (4)	
C22	0.1098 (2)	0.8873 (2)	0.38466 (16)	0.0238 (4)	
H22	0.1184	0.9658	0.3621	0.029*	
C23	0.0527 (2)	0.8364 (2)	0.47479 (16)	0.0242 (4)	
H23	0.0218	0.8802	0.5132	0.029*	
C24	0.0409 (2)	0.72110 (19)	0.50851 (15)	0.0218 (4)	
C25	0.0901 (2)	0.65672 (19)	0.45346 (16)	0.0234 (4)	
H25	0.0850	0.5777	0.4775	0.028*	
C26	0.1466 (2)	0.70743 (18)	0.36350 (15)	0.0219 (4)	
H26	0.1799	0.6628	0.3264	0.026*	
C27	-0.0335 (2)	0.6680 (2)	0.59958 (15)	0.0229 (4)	
N1	0.7246 (2)	0.2961 (3)	0.2056 (2)	0.0268 (5)	0.772 (4)
C28	0.6114 (3)	0.3443 (4)	0.2444 (3)	0.0369 (8)	0.772 (4)
H28A	0.5913	0.3016	0.3125	0.044*	0.772 (4)
H28B	0.5449	0.3441	0.2083	0.044*	0.772 (4)
C29	0.6411 (5)	0.4673 (5)	0.2302 (4)	0.0537 (11)	0.772 (4)
H29A	0.5713	0.5199	0.2132	0.064*	0.772 (4)
H29B	0.6677	0.4717	0.2889	0.064*	0.772 (4)
C30	0.7411 (5)	0.4950 (5)	0.1480 (7)	0.0453 (14)	0.772 (4)
H30A	0.7173	0.5613	0.0942	0.054*	0.772 (4)
H30B	0.8135	0.5105	0.1697	0.054*	0.772 (4)
C31	0.7615 (5)	0.3920 (4)	0.1182 (3)	0.0371 (9)	0.772 (4)
H31A	0.7136	0.3990	0.0659	0.045*	0.772 (4)
H31B	0.8457	0.3811	0.0966	0.045*	0.772 (4)
C32	0.6995 (3)	0.1936 (3)	0.1842 (3)	0.0322 (7)	0.772 (4)

H32A	0.6579	0.1407	0.2413	0.039*	0.772 (4)
H32B	0.6475	0.2156	0.1322	0.039*	0.772 (4)
C33	0.8122 (3)	0.1366 (4)	0.1555 (3)	0.0394 (8)	0.772 (4)
H33A	0.7935	0.0700	0.1415	0.047*	0.772 (4)
H33B	0.8520	0.1885	0.0969	0.047*	0.772 (4)
O7	0.8886 (3)	0.1033 (3)	0.2282 (3)	0.0428 (8)	0.772 (4)
C34	0.9190 (3)	0.1977 (4)	0.2457 (3)	0.0375 (8)	0.772 (4)
H34A	0.9603	0.2481	0.1870	0.045*	0.772 (4)
H34B	0.9743	0.1737	0.2955	0.045*	0.772 (4)
C35	0.8144 (3)	0.2613 (3)	0.2771 (2)	0.0299 (7)	0.772 (4)
H35A	0.8406	0.3288	0.2854	0.036*	0.772 (4)
H35B	0.7775	0.2139	0.3393	0.036*	0.772 (4)
N1B	0.7645 (10)	0.3037 (9)	0.1702 (8)	0.0350 (17)	0.228 (4)
C28B	0.6466 (12)	0.3145 (12)	0.2252 (11)	0.043 (2)	0.228 (4)
H28C	0.6532	0.2795	0.2944	0.051*	0.228 (4)
H28D	0.5871	0.2758	0.2076	0.051*	0.228 (4)
C29B	0.6083 (12)	0.4420 (12)	0.2007 (10)	0.045 (2)	0.228 (4)
H29C	0.5415	0.4634	0.1610	0.054*	0.228 (4)
H29D	0.5859	0.4615	0.2591	0.054*	0.228 (4)
C30B	0.721 (2)	0.4991 (17)	0.145 (2)	0.048 (3)	0.228 (4)
H30C	0.7015	0.5736	0.0985	0.057*	0.228 (4)
H30D	0.7747	0.5073	0.1885	0.057*	0.228 (4)
C31B	0.7737 (17)	0.4172 (13)	0.0957 (12)	0.041 (3)	0.228 (4)
H31C	0.7293	0.4232	0.0416	0.049*	0.228 (4)
H31D	0.8571	0.4319	0.0715	0.049*	0.228 (4)
C32B	0.7678 (12)	0.2120 (10)	0.1274 (9)	0.038 (2)	0.228 (4)
H32C	0.6971	0.2223	0.0928	0.046*	0.228 (4)
H32D	0.8381	0.2184	0.0807	0.046*	0.228 (4)
C33B	0.7713 (13)	0.0978 (11)	0.2005 (11)	0.044 (2)	0.228 (4)
H33C	0.6964	0.0880	0.2425	0.052*	0.228 (4)
H33D	0.7783	0.0412	0.1683	0.052*	0.228 (4)
O7B	0.8669 (13)	0.0793 (12)	0.2565 (10)	0.049 (2)	0.228 (4)
C34B	0.8689 (13)	0.1594 (11)	0.2983 (10)	0.042 (2)	0.228 (4)
H34C	0.9414	0.1452	0.3312	0.051*	0.228 (4)
H34D	0.8008	0.1507	0.3474	0.051*	0.228 (4)
C35B	0.8648 (10)	0.2779 (10)	0.2319 (8)	0.0334 (19)	0.228 (4)
H35C	0.9402	0.2917	0.1907	0.040*	0.228 (4)
H35D	0.8563	0.3290	0.2694	0.040*	0.228 (4)
O1	0.73341 (14)	0.72307 (13)	-0.19473 (11)	0.0201 (3)	
O2	0.66546 (15)	0.55819 (15)	-0.11320 (13)	0.0270 (4)	
O3	-0.15587 (13)	1.41331 (13)	-0.19163 (11)	0.0187 (3)	
O4	-0.05690 (14)	1.52341 (12)	-0.14773 (11)	0.0198 (3)	
O5	-0.08723 (15)	0.73027 (15)	0.64428 (12)	0.0253 (3)	
O6	-0.04558 (17)	0.56503 (15)	0.62992 (13)	0.0307 (4)	
O8	0.3453 (3)	0.1098 (3)	0.7941 (2)	0.0787 (11)	

C36	0.2954 (4)	0.2070 (4)	0.7669 (3)	0.0638 (12)	
H36	0.3031	0.2561	0.8009	0.077*	
N2	0.2341 (3)	0.2424 (3)	0.6941 (2)	0.0595 (9)	
C37	0.2131 (6)	0.1787 (5)	0.6388 (4)	0.099 (2)	
H37A	0.1289	0.1660	0.6467	0.148*	
H37B	0.2585	0.1066	0.6593	0.148*	
H37C	0.2374	0.2191	0.5717	0.148*	
C38	0.1725 (4)	0.3535 (4)	0.6683 (4)	0.0754 (14)	
H38A	0.1903	0.3921	0.7108	0.113*	
H38B	0.0873	0.3457	0.6745	0.113*	
H38C	0.1988	0.3972	0.6024	0.113*	
O9	0.6096 (17)	-0.0495 (10)	0.6616 (8)	0.102 (5)	0.257 (3)
C39	0.6195 (13)	-0.0089 (8)	0.5718 (8)	0.070 (3)	0.257 (3)
H39	0.6473	-0.0569	0.5364	0.084*	0.257 (3)
N3	0.5931 (10)	0.0958 (7)	0.5260 (6)	0.078 (3)	0.257 (3)
C40	0.5516 (15)	0.1766 (9)	0.5678 (9)	0.062 (3)	0.257 (3)
H40A	0.6186	0.2095	0.5808	0.093*	0.257 (3)
H40B	0.5032	0.1416	0.6276	0.093*	0.257 (3)
H40C	0.5038	0.2355	0.5244	0.093*	0.257 (3)
C41	0.6060 (19)	0.1382 (12)	0.4217 (6)	0.064 (5)	0.257 (3)
H41A	0.5338	0.1274	0.3981	0.096*	0.257 (3)
H41B	0.6728	0.0975	0.3981	0.096*	0.257 (3)
H41C	0.6201	0.2182	0.3991	0.096*	0.257 (3)
O9B	0.5833 (11)	-0.0086 (9)	0.6703 (5)	0.059 (3)	0.283 (3)
C39B	0.5807 (10)	0.0529 (8)	0.5842 (6)	0.072 (3)	0.283 (3)
H39B	0.5331	0.1210	0.5697	0.086*	0.283 (3)
N3B	0.6406 (9)	0.0266 (8)	0.5148 (5)	0.072 (2)	0.283 (3)
C40B	0.7150 (14)	-0.0700 (11)	0.5252 (9)	0.077 (4)	0.283 (3)
H40D	0.7875	-0.0507	0.4825	0.115*	0.283 (3)
H40E	0.6749	-0.1247	0.5091	0.115*	0.283 (3)
H40F	0.7344	-0.1023	0.5911	0.115*	0.283 (3)
C41B	0.6346 (19)	0.1009 (14)	0.4162 (6)	0.063 (4)	0.283 (3)
H41D	0.7114	0.0977	0.3798	0.095*	0.283 (3)
H41E	0.6141	0.1778	0.4150	0.095*	0.283 (3)
H41F	0.5744	0.0767	0.3878	0.095*	0.283 (3)
O9C	0.6269 (9)	0.0858 (7)	0.4153 (3)	0.067 (2)	0.460 (3)
C39C	0.5874 (7)	0.0982 (6)	0.4936 (4)	0.067 (2)	0.460 (3)
H39C	0.5350	0.1611	0.4930	0.080*	0.460 (3)
N3C	0.6159 (5)	0.0282 (5)	0.5748 (3)	0.0439 (15)	0.460 (3)
C40C	0.6903 (9)	-0.0687 (7)	0.5868 (6)	0.085 (3)	0.460 (3)
H40G	0.7429	-0.0603	0.5284	0.127*	0.460 (3)
H40H	0.6427	-0.1333	0.6007	0.127*	0.460 (3)
H40I	0.7374	-0.0802	0.6398	0.127*	0.460 (3)
C41C	0.5661 (11)	0.0452 (9)	0.6638 (5)	0.097 (4)	0.460 (3)
H41G	0.6274	0.0282	0.7074	0.146*	0.460 (3)

H41H	0.5014	-0.0044	0.6931	0.146*	0.460 (3)
H41I	0.5360	0.1233	0.6504	0.146*	0.460 (3)
O10	0.7218 (13)	0.4094 (15)	0.3837 (11)	0.138 (6)	0.371 (6)
C42	0.6629 (11)	0.3668 (15)	0.4623 (11)	0.099 (5)	0.371 (6)
H42	0.6798	0.2895	0.4952	0.118*	0.371 (6)
N4	0.582 (2)	0.4175 (14)	0.5023 (10)	0.071 (3)	0.371 (6)
C43	0.545 (2)	0.5297 (12)	0.4515 (14)	0.110 (7)	0.371 (6)
H43A	0.6034	0.5804	0.4520	0.166*	0.371 (6)
H43B	0.4687	0.5492	0.4817	0.166*	0.371 (6)
H43C	0.5361	0.5369	0.3856	0.166*	0.371 (6)
C44	0.5212 (14)	0.3635 (15)	0.5956 (11)	0.083 (4)	0.371 (6)
H44A	0.4362	0.3686	0.5906	0.124*	0.371 (6)
H44B	0.5369	0.4010	0.6395	0.124*	0.371 (6)
H44C	0.5493	0.2846	0.6196	0.124*	0.371 (6)
O10B	0.649 (4)	0.426 (3)	0.308 (3)	0.138 (6)	0.129 (6)
C42B	0.602 (3)	0.504 (3)	0.335 (2)	0.099 (5)	0.129 (6)
H42B	0.5707	0.5667	0.2871	0.118*	0.129 (6)
N4B	0.589 (3)	0.513 (3)	0.421 (2)	0.071 (3)	0.129 (6)
C43B	0.499 (5)	0.593 (4)	0.434 (4)	0.110 (7)	0.129 (6)
H43D	0.4955	0.5947	0.4986	0.166*	0.129 (6)
H43E	0.5179	0.6676	0.3883	0.166*	0.129 (6)
H43F	0.4233	0.5737	0.4225	0.166*	0.129 (6)
C44B	0.588 (8)	0.408 (5)	0.502 (4)	0.083 (4)	0.129 (6)
H44D	0.5782	0.4247	0.5617	0.124*	0.129 (6)
H44E	0.5228	0.3642	0.5010	0.124*	0.129 (6)
H44F	0.6629	0.3637	0.4989	0.124*	0.129 (6)
In1	0.80701 (2)	0.59539 (2)	-0.25517 (2)	0.01838 (5)	
Cl1	0.6598 (3)	0.6060 (4)	-0.3615 (3)	0.0345 (4)	0.818 (3)
Br1	0.6469 (7)	0.5909 (9)	-0.3497 (6)	0.0345 (4)	0.182 (3)

Atomic displacement parameters (\AA^2)

	U^{11}	U^{22}	U^{33}	U^{12}	U^{13}	U^{23}
C1	0.0136 (8)	0.0246 (9)	0.0199 (9)	0.0006 (7)	0.0022 (7)	-0.0104 (8)
C2	0.0137 (8)	0.0203 (9)	0.0178 (8)	-0.0005 (6)	0.0031 (6)	-0.0090 (7)
C3	0.0176 (8)	0.0206 (9)	0.0169 (8)	-0.0031 (7)	0.0055 (7)	-0.0073 (7)
C4	0.0181 (8)	0.0179 (8)	0.0182 (9)	-0.0034 (7)	0.0052 (7)	-0.0070 (7)
C5	0.0147 (8)	0.0173 (8)	0.0148 (8)	-0.0003 (6)	0.0029 (6)	-0.0065 (7)
C6	0.0184 (9)	0.0178 (9)	0.0193 (9)	-0.0009 (7)	0.0062 (7)	-0.0057 (7)
C7	0.0192 (9)	0.0180 (9)	0.0225 (9)	-0.0010 (7)	0.0058 (7)	-0.0078 (7)
C8	0.0150 (8)	0.0172 (8)	0.0147 (8)	-0.0008 (6)	0.0037 (6)	-0.0060 (7)
C9	0.0168 (8)	0.0170 (8)	0.0141 (8)	-0.0011 (6)	0.0036 (6)	-0.0053 (6)
C10	0.0153 (8)	0.0154 (8)	0.0154 (8)	-0.0012 (6)	0.0019 (6)	-0.0050 (6)
C11	0.0164 (8)	0.0181 (8)	0.0156 (8)	0.0000 (6)	0.0024 (6)	-0.0066 (7)
C12	0.0175 (8)	0.0193 (8)	0.0132 (8)	-0.0008 (7)	0.0028 (6)	-0.0052 (7)

C13	0.0168 (8)	0.0192 (9)	0.0145 (8)	0.0008 (7)	0.0021 (6)	-0.0048 (7)
C14	0.0155 (8)	0.0153 (8)	0.0154 (8)	-0.0008 (6)	0.0025 (6)	-0.0038 (6)
C15	0.0210 (9)	0.0154 (8)	0.0194 (9)	0.0010 (7)	-0.0002 (7)	-0.0072 (7)
C16	0.0198 (9)	0.0170 (8)	0.0185 (9)	0.0001 (7)	-0.0007 (7)	-0.0069 (7)
C17	0.0170 (8)	0.0149 (8)	0.0171 (8)	-0.0001 (6)	0.0015 (6)	-0.0051 (7)
C18	0.0223 (9)	0.0148 (8)	0.0204 (9)	-0.0010 (7)	-0.0016 (7)	-0.0071 (7)
C19	0.0215 (9)	0.0171 (8)	0.0180 (9)	-0.0012 (7)	-0.0019 (7)	-0.0056 (7)
C20	0.0167 (8)	0.0191 (8)	0.0138 (8)	-0.0002 (7)	0.0045 (6)	-0.0057 (7)
C21	0.0200 (9)	0.0213 (9)	0.0133 (8)	0.0008 (7)	0.0042 (7)	-0.0048 (7)
C22	0.0303 (11)	0.0221 (10)	0.0168 (9)	-0.0009 (8)	0.0060 (8)	-0.0068 (8)
C23	0.0307 (11)	0.0241 (10)	0.0157 (9)	0.0006 (8)	0.0068 (8)	-0.0078 (8)
C24	0.0240 (10)	0.0237 (10)	0.0136 (8)	0.0007 (8)	0.0059 (7)	-0.0044 (7)
C25	0.0292 (11)	0.0198 (9)	0.0170 (9)	-0.0001 (8)	0.0061 (8)	-0.0042 (7)
C26	0.0277 (10)	0.0191 (9)	0.0155 (8)	0.0014 (8)	0.0058 (7)	-0.0051 (7)
C27	0.0222 (9)	0.0293 (11)	0.0137 (8)	0.0009 (8)	0.0026 (7)	-0.0051 (8)
N1	0.0175 (11)	0.0379 (14)	0.0239 (12)	-0.0014 (10)	0.0024 (9)	-0.0106 (11)
C28	0.0225 (15)	0.046 (2)	0.0418 (19)	-0.0012 (14)	0.0070 (13)	-0.0183 (16)
C29	0.039 (2)	0.058 (2)	0.064 (3)	0.0020 (19)	0.004 (2)	-0.025 (2)
C30	0.032 (2)	0.0360 (19)	0.054 (2)	0.0001 (17)	0.004 (2)	-0.0011 (18)
C31	0.0290 (17)	0.043 (2)	0.031 (2)	-0.0039 (16)	0.0030 (15)	-0.0031 (16)
C32	0.0258 (14)	0.0426 (17)	0.0330 (15)	-0.0057 (12)	-0.0033 (12)	-0.0178 (13)
C33	0.0329 (17)	0.048 (2)	0.045 (2)	-0.0019 (15)	-0.0009 (15)	-0.0265 (17)
O7	0.0355 (16)	0.0461 (19)	0.050 (2)	0.0035 (13)	-0.0046 (14)	-0.0210 (16)
C34	0.0290 (15)	0.050 (2)	0.0355 (17)	0.0027 (14)	-0.0042 (13)	-0.0185 (15)
C35	0.0266 (14)	0.0392 (17)	0.0259 (14)	-0.0012 (12)	-0.0054 (12)	-0.0125 (13)
N1B	0.029 (3)	0.043 (3)	0.032 (3)	-0.008 (3)	0.000 (3)	-0.011 (3)
C28B	0.032 (4)	0.048 (4)	0.042 (4)	-0.002 (3)	0.005 (3)	-0.011 (3)
C29B	0.029 (4)	0.047 (4)	0.048 (4)	-0.003 (4)	0.002 (4)	-0.006 (4)
C30B	0.036 (5)	0.047 (4)	0.050 (4)	0.000 (4)	0.003 (4)	-0.005 (4)
C31B	0.032 (4)	0.041 (4)	0.041 (4)	-0.005 (4)	0.003 (4)	-0.005 (4)

C32B	0.035 (4)	0.044 (4)	0.039 (4)	-0.009 (3)	-0.003 (3)	-0.018 (3)
C33B	0.039 (4)	0.048 (4)	0.046 (4)	-0.009 (4)	-0.004 (4)	-0.017 (4)
O7B	0.044 (4)	0.051 (4)	0.051 (4)	-0.006 (4)	-0.001 (4)	-0.017 (4)
C34B	0.037 (4)	0.051 (4)	0.039 (4)	-0.005 (4)	-0.005 (4)	-0.012 (4)
C35B	0.023 (3)	0.047 (4)	0.030 (4)	-0.003 (3)	0.001 (3)	-0.014 (3)
O1	0.0193 (7)	0.0229 (7)	0.0170 (7)	0.0001 (5)	0.0054 (5)	-0.0079 (6)
O2	0.0251 (8)	0.0231 (8)	0.0328 (9)	-0.0004 (6)	0.0106 (7)	-0.0143 (7)
O3	0.0184 (6)	0.0190 (7)	0.0181 (7)	-0.0001 (5)	0.0005 (5)	-0.0064 (5)
O4	0.0227 (7)	0.0143 (6)	0.0211 (7)	0.0009 (5)	-0.0001 (6)	-0.0054 (5)
O5	0.0270 (8)	0.0288 (8)	0.0179 (7)	-0.0022 (6)	0.0090 (6)	-0.0088 (6)
O6	0.0365 (9)	0.0266 (8)	0.0210 (8)	-0.0004 (7)	0.0125 (7)	-0.0035 (6)
O8	0.0619 (19)	0.104 (3)	0.0425 (15)	0.0067 (18)	-0.0072 (13)	0.0083 (16)
C36	0.050 (2)	0.074 (3)	0.048 (2)	-0.011 (2)	-0.0021 (17)	0.0044 (19)
N2	0.0518 (18)	0.064 (2)	0.0528 (19)	-0.0149 (16)	-0.0052 (15)	-0.0031 (16)
C37	0.112 (5)	0.100 (5)	0.092 (4)	0.019 (4)	-0.055 (4)	-0.033 (4)
C38	0.068 (3)	0.069 (3)	0.072 (3)	-0.015 (2)	-0.024 (2)	0.006 (2)
O9	0.103 (7)	0.087 (8)	0.078 (7)	-0.023 (7)	0.000 (6)	0.022 (7)
C39	0.068 (4)	0.071 (5)	0.056 (4)	-0.006 (4)	-0.011 (4)	-0.002 (4)
N3	0.072 (4)	0.075 (4)	0.066 (4)	-0.010 (4)	-0.001 (4)	0.002 (4)
C40	0.063 (7)	0.061 (7)	0.054 (6)	-0.010 (6)	-0.006 (6)	-0.007 (6)
C41	0.058 (7)	0.059 (8)	0.046 (6)	-0.013 (7)	-0.002 (6)	0.022 (6)
O9B	0.084 (6)	0.057 (6)	0.036 (4)	-0.045 (5)	-0.007 (4)	-0.007 (4)
C39B	0.073 (5)	0.072 (4)	0.055 (4)	-0.015 (4)	-0.012 (4)	0.002 (4)
N3B	0.069 (4)	0.059 (4)	0.071 (4)	-0.012 (4)	-0.006 (4)	0.003 (4)
C40B	0.069 (8)	0.074 (8)	0.083 (8)	0.002 (7)	0.003 (7)	-0.026 (7)
C41B	0.093 (8)	0.061 (8)	0.040 (7)	-0.033 (7)	-0.006 (7)	-0.015 (6)
O9C	0.097 (5)	0.061 (4)	0.031 (3)	-0.047 (4)	0.012 (3)	0.003 (3)
C39C	0.069 (4)	0.070 (4)	0.045 (3)	-0.014 (3)	-0.017 (3)	0.007 (3)
N3C	0.047 (3)	0.054 (3)	0.025 (2)	-0.031 (3)	-0.008 (2)	0.004 (2)
C40C	0.089 (6)	0.068 (5)	0.093 (6)	0.001 (5)	-0.031 (5)	-0.017 (5)
C41C	0.115 (7)	0.086 (7)	0.083 (6)	-0.023 (6)	-0.003 (6)	-0.017 (6)
O10	0.101 (9)	0.157 (12)	0.119 (11)	-0.028 (9)	0.002 (8)	-0.001 (10)
C42	0.080 (9)	0.099 (10)	0.114 (11)	-0.017 (8)	-0.011 (8)	-0.028 (9)
N4	0.067 (7)	0.080 (7)	0.081 (7)	0.002 (6)	-0.017 (6)	-0.044 (6)
C43	0.154 (18)	0.074 (11)	0.141 (15)	0.016 (10)	-0.085 (13)	-0.065 (11)
C44	0.066 (8)	0.101 (12)	0.091 (11)	-0.024 (8)	0.010 (8)	-0.046 (9)
O10B	0.101 (9)	0.157 (12)	0.119 (11)	-0.028 (9)	0.002 (8)	-0.001 (10)
C42B	0.080 (9)	0.099 (10)	0.114 (11)	-0.017 (8)	-0.011 (8)	-0.028 (9)
N4B	0.067 (7)	0.080 (7)	0.081 (7)	0.002 (6)	-0.017 (6)	-0.044 (6)
C43B	0.154 (18)	0.074 (11)	0.141 (15)	0.016 (10)	-0.085 (13)	-0.065 (11)
C44B	0.066 (8)	0.101 (12)	0.091 (11)	-0.024 (8)	0.010 (8)	-0.046 (9)
In1	0.01900	0.01854	0.01562	0.00203 (5)	0.00367 (5)	-0.00593

	(7)	(7)	(7)			(5)
C11	0.0215 (9)	0.0505 (14)	0.0334 (11)	-0.0057 (6)	-0.0018 (6)	-0.0158 (9)
Br1	0.0215 (9)	0.0505 (14)	0.0334 (11)	-0.0057 (6)	-0.0018 (6)	-0.0158 (9)

Geometric parameters (Å, °)

C1—O2	1.247 (3)	C31B—H31C	0.9900
C1—O1	1.280 (3)	C31B—H31D	0.9900
C1—C2	1.493 (3)	C32B—C33B	1.492 (14)
C1—In1	2.658 (2)	C32B—H32C	0.9900
C2—C3	1.392 (3)	C32B—H32D	0.9900
C2—C7	1.397 (3)	C33B—O7B	1.418 (15)
C3—C4	1.388 (3)	C33B—H33C	0.9900
C3—H3	0.9500	C33B—H33D	0.9900
C4—C5	1.401 (3)	O7B—C34B	1.373 (15)
C4—H4	0.9500	C34B—C35B	1.497 (14)
C5—C6	1.401 (3)	C34B—H34C	0.9900
C5—C8	1.483 (3)	C34B—H34D	0.9900
C6—C7	1.388 (3)	C35B—H35C	0.9900
C6—H6	0.9500	C35B—H35D	0.9900
C7—H7	0.9500	O1—In1	2.1763 (15)
C8—C9	1.396 (3)	O2—In1	2.4480 (17)
C8—C13	1.399 (3)	O3—In1 ^I	2.2037 (15)
C9—C10	1.396 (3)	O4—In1 ^I	2.2836 (16)
C9—H9	0.9500	O5—In1 ^{II}	2.2061 (17)
C10—C11	1.396 (3)	O6—In1 ^{II}	2.3623 (17)
C10—C14	1.484 (3)	O8—C36	1.264 (5)
C11—C12	1.399 (3)	C36—N2	1.299 (4)
C11—H11	0.9500	C36—H36	0.9500
C12—C13	1.399 (3)	N2—C37	1.400 (5)
C12—C21	1.488 (3)	N2—C38	1.465 (5)
C13—H13	0.9500	C37—H37A	0.9800
C14—C15	1.395 (3)	C37—H37B	0.9800
C14—C19	1.401 (3)	C37—H37C	0.9800
C15—C16	1.392 (3)	C38—H38A	0.9800
C15—H15	0.9500	C38—H38B	0.9800
C16—C17	1.396 (3)	C38—H38C	0.9800
C16—H16	0.9500	O9—C39	1.264 (5)
C17—C18	1.396 (3)	C39—N3	1.298 (4)
C17—C20	1.489 (3)	C39—H39	0.9500
C18—C19	1.390 (3)	N3—C40	1.400 (6)
C18—H18	0.9500	N3—C41	1.465 (5)
C19—H19	0.9500	C40—H40A	0.9800

C20—O3	1.264 (3)	C40—H40B	0.9800
C20—O4	1.268 (3)	C40—H40C	0.9800
C20—In1 ^I	2.584 (2)	C41—H41A	0.9800
C21—C22	1.400 (3)	C41—H41B	0.9800
C21—C26	1.401 (3)	C41—H41C	0.9800
C22—C23	1.393 (3)	O9B—C39B	1.264 (5)
C22—H22	0.9500	C39B—N3B	1.298 (4)
C23—C24	1.393 (3)	C39B—H39B	0.9500
C23—H23	0.9500	N3B—C40B	1.400 (6)
C24—C25	1.391 (3)	N3B—C41B	1.465 (5)
C24—C27	1.497 (3)	C40B—H40D	0.9800
C25—C26	1.388 (3)	C40B—H40E	0.9800
C25—H25	0.9500	C40B—H40F	0.9800
C26—H26	0.9500	C41B—H41D	0.9800
C27—O6	1.248 (3)	C41B—H41E	0.9800
C27—O5	1.275 (3)	C41B—H41F	0.9800
C27—In1 ^{II}	2.627 (2)	O9C—C39C	1.264 (5)
N1—C31	1.502 (5)	C39C—N3C	1.298 (4)
N1—C35	1.507 (4)	C39C—H39C	0.9500
N1—C32	1.509 (5)	N3C—C40C	1.400 (6)
N1—C28	1.515 (5)	N3C—C41C	1.465 (5)
C28—C29	1.574 (7)	C40C—H40G	0.9800
C28—H28A	0.9900	C40C—H40H	0.9800
C28—H28B	0.9900	C40C—H40I	0.9800
C29—C30	1.544 (7)	C41C—H41G	0.9800
C29—H29A	0.9900	C41C—H41H	0.9800
C29—H29B	0.9900	C41C—H41I	0.9800
C30—C31	1.515 (7)	O10—C42	1.256 (15)
C30—H30A	0.9900	C42—N4	1.283 (15)
C30—H30B	0.9900	C42—H42	0.9500
C31—H31A	0.9900	N4—C43	1.422 (14)
C31—H31B	0.9900	N4—C44	1.454 (16)
C32—C33	1.506 (5)	C43—H43A	0.9800
C32—H32A	0.9900	C43—H43B	0.9800
C32—H32B	0.9900	C43—H43C	0.9800
C33—O7	1.411 (5)	C44—H44A	0.9800
C33—H33A	0.9900	C44—H44B	0.9800
C33—H33B	0.9900	C44—H44C	0.9800
O7—C34	1.401 (5)	O10B—C42B	1.253 (18)
C34—C35	1.497 (5)	C42B—N4B	1.313 (18)
C34—H34A	0.9900	C42B—H42B	0.9500
C34—H34B	0.9900	N4B—C43B	1.425 (18)
C35—H35A	0.9900	N4B—C44B	1.472 (19)
C35—H35B	0.9900	C43B—H43D	0.9800
N1B—C31B	1.497 (14)	C43B—H43E	0.9800

N1B—C35B	1.507 (12)	C43B—H43F	0.9800
N1B—C32B	1.511 (13)	C44B—H44D	0.9800
N1B—C28B	1.512 (14)	C44B—H44E	0.9800
C28B—C29B	1.568 (15)	C44B—H44F	0.9800
C28B—H28C	0.9900	In1—O3 ^{III}	2.2037 (15)
C28B—H28D	0.9900	In1—O5 ^{IV}	2.2061 (17)
C29B—C30B	1.543 (16)	In1—O4 ^{III}	2.2835 (16)
C29B—O10B	1.68 (5)	In1—O6 ^{IV}	2.3623 (17)
C29B—H29C	0.9900	In1—Cl1	2.431 (5)
C29B—H29D	0.9900	In1—Br1	2.475 (9)
C30B—C31B	1.518 (16)	In1—C20 ^{III}	2.584 (2)
C30B—H30C	0.9900	In1—C27 ^{IV}	2.627 (2)
C30B—H30D	0.9900		
O2—C1—O1	120.86 (19)	C32B—C33B—H33C	109.2
O2—C1—C2	121.06 (19)	O7B—C33B—H33D	109.2
O1—C1—C2	118.07 (19)	C32B—C33B—H33D	109.2
O2—C1—In1	66.65 (11)	H33C—C33B—H33D	107.9
O1—C1—In1	54.34 (10)	C34B—O7B—C33B	113.0 (13)
C2—C1—In1	171.04 (16)	O7B—C34B—C35B	115.3 (11)
C3—C2—C7	119.10 (18)	O7B—C34B—H34C	108.5
C3—C2—C1	120.10 (18)	C35B—C34B—H34C	108.5
C7—C2—C1	120.69 (19)	O7B—C34B—H34D	108.5
C4—C3—C2	120.46 (18)	C35B—C34B—H34D	108.5
C4—C3—H3	119.8	H34C—C34B—H34D	107.5
C2—C3—H3	119.8	C34B—C35B—N1B	112.4 (10)
C3—C4—C5	120.60 (19)	C34B—C35B—H35C	109.1
C3—C4—H4	119.7	N1B—C35B—H35C	109.1
C5—C4—H4	119.7	C34B—C35B—H35D	109.1
C4—C5—C6	118.83 (17)	N1B—C35B—H35D	109.1
C4—C5—C8	120.11 (18)	H35C—C35B—H35D	107.9
C6—C5—C8	121.00 (17)	C1—O1—In1	97.12 (13)
C7—C6—C5	120.24 (18)	C1—O2—In1	85.46 (13)
C7—C6—H6	119.9	C20—O3—In1 ^I	92.26 (12)
C5—C6—H6	119.9	C20—O4—In1 ^I	88.55 (13)
C6—C7—C2	120.72 (19)	C27—O5—In1 ^{II}	94.15 (14)
C6—C7—H7	119.6	C27—O6—In1 ^{II}	87.70 (13)
C2—C7—H7	119.6	O8—C36—N2	122.4 (4)
C9—C8—C13	119.31 (17)	O8—C36—H36	118.8
C9—C8—C5	119.39 (17)	N2—C36—H36	118.8
C13—C8—C5	121.28 (18)	C36—N2—C37	125.0 (4)
C10—C9—C8	120.71 (18)	C36—N2—C38	120.5 (4)
C10—C9—H9	119.6	C37—N2—C38	114.4 (3)
C8—C9—H9	119.6	N2—C37—H37A	109.5
C9—C10—C11	119.41 (18)	N2—C37—H37B	109.5
C9—C10—C14	119.92 (17)	H37A—C37—H37B	109.5

C11—C10—C14	120.60 (17)	N2—C37—H37C	109.5
C10—C11—C12	120.71 (18)	H37A—C37—H37C	109.5
C10—C11—H11	119.6	H37B—C37—H37C	109.5
C12—C11—H11	119.6	N2—C38—H38A	109.5
C11—C12—C13	119.15 (18)	N2—C38—H38B	109.5
C11—C12—C21	119.23 (17)	H38A—C38—H38B	109.5
C13—C12—C21	121.38 (18)	N2—C38—H38C	109.5
C8—C13—C12	120.67 (18)	H38A—C38—H38C	109.5
C8—C13—H13	119.7	H38B—C38—H38C	109.5
C12—C13—H13	119.7	O9—C39—N3	122.7 (5)
C15—C14—C19	119.40 (18)	O9—C39—H39	118.7
C15—C14—C10	119.91 (18)	N3—C39—H39	118.7
C19—C14—C10	120.68 (19)	C39—N3—C40	125.4 (4)
C16—C15—C14	120.47 (19)	C39—N3—C41	120.3 (4)
C16—C15—H15	119.8	C40—N3—C41	114.3 (4)
C14—C15—H15	119.8	N3—C40—H40A	109.5
C15—C16—C17	119.9 (2)	N3—C40—H40B	109.5
C15—C16—H16	120.0	H40A—C40—H40B	109.5
C17—C16—H16	120.0	N3—C40—H40C	109.5
C16—C17—C18	119.79 (19)	H40A—C40—H40C	109.5
C16—C17—C20	118.54 (19)	H40B—C40—H40C	109.5
C18—C17—C20	121.67 (18)	N3—C41—H41A	109.5
C19—C18—C17	120.19 (19)	N3—C41—H41B	109.5
C19—C18—H18	119.9	H41A—C41—H41B	109.5
C17—C18—H18	119.9	N3—C41—H41C	109.5
C18—C19—C14	120.1 (2)	H41A—C41—H41C	109.5
C18—C19—H19	119.9	H41B—C41—H41C	109.5
C14—C19—H19	119.9	O9B—C39B—N3B	122.5 (5)
O3—C20—O4	120.47 (19)	O9B—C39B—H39B	118.8
O3—C20—C17	118.71 (18)	N3B—C39B—H39B	118.8
O4—C20—C17	120.80 (19)	C39B—N3B—C40B	125.2 (4)
O3—C20—In1 ¹	58.46 (11)	C39B—N3B—C41B	120.4 (4)
O4—C20—In1 ¹	62.08 (11)	C40B—N3B—C41B	114.4 (4)
C17—C20—In1 ¹	175.40 (14)	N3B—C40B—H40D	109.5
C22—C21—C26	118.73 (19)	N3B—C40B—H40E	109.5
C22—C21—C12	120.96 (19)	H40D—C40B—H40E	109.5
C26—C21—C12	120.10 (18)	N3B—C40B—H40F	109.5
C23—C22—C21	120.6 (2)	H40D—C40B—H40F	109.5
C23—C22—H22	119.7	H40E—C40B—H40F	109.5
C21—C22—H22	119.7	N3B—C41B—H41D	109.5
C22—C23—C24	119.9 (2)	N3B—C41B—H41E	109.5
C22—C23—H23	120.0	H41D—C41B—H41E	109.5
C24—C23—H23	120.0	N3B—C41B—H41F	109.5
C25—C24—C23	119.82 (19)	H41D—C41B—H41F	109.5
C25—C24—C27	119.8 (2)	H41E—C41B—H41F	109.5

C23—C24—C27	120.14 (19)	O9C—C39C—N3C	122.3 (5)
C26—C25—C24	120.2 (2)	O9C—C39C—H39C	118.8
C26—C25—H25	119.9	N3C—C39C—H39C	118.8
C24—C25—H25	119.9	C39C—N3C—C40C	125.3 (4)
C25—C26—C21	120.57 (19)	C39C—N3C—C41C	120.3 (4)
C25—C26—H26	119.7	C40C—N3C—C41C	114.4 (4)
C21—C26—H26	119.7	N3C—C40C—H40G	109.5
O6—C27—O5	120.4 (2)	N3C—C40C—H40H	109.5
O6—C27—C24	120.7 (2)	H40G—C40C—H40H	109.5
O5—C27—C24	118.9 (2)	N3C—C40C—H40I	109.5
O6—C27—In1 ^{II}	63.97 (12)	H40G—C40C—H40I	109.5
O5—C27—In1 ^{II}	56.89 (11)	H40H—C40C—H40I	109.5
C24—C27—In1 ^{II}	170.52 (16)	N3C—C41C—H41G	109.5
C31—N1—C35	112.7 (3)	N3C—C41C—H41H	109.5
C31—N1—C32	113.4 (3)	H41G—C41C—H41H	109.5
C35—N1—C32	107.9 (3)	N3C—C41C—H41I	109.5
C31—N1—C28	102.2 (3)	H41G—C41C—H41I	109.5
C35—N1—C28	111.0 (3)	H41H—C41C—H41I	109.5
C32—N1—C28	109.6 (3)	O10—C42—N4	126.2 (17)
N1—C28—C29	103.3 (3)	O10—C42—H42	116.9
N1—C28—H28A	111.1	N4—C42—H42	116.9
C29—C28—H28A	111.1	C42—N4—C43	119.0 (15)
N1—C28—H28B	111.1	C42—N4—C44	123.1 (14)
C29—C28—H28B	111.1	C43—N4—C44	117.8 (16)
H28A—C28—H28B	109.1	N4—C43—H43A	109.5
C30—C29—C28	104.7 (4)	N4—C43—H43B	109.5
C30—C29—H29A	110.8	H43A—C43—H43B	109.5
C28—C29—H29A	110.8	N4—C43—H43C	109.5
C30—C29—H29B	110.8	H43A—C43—H43C	109.5
C28—C29—H29B	110.8	H43B—C43—H43C	109.5
H29A—C29—H29B	108.9	N4—C44—H44A	109.5
C31—C30—C29	105.4 (4)	N4—C44—H44B	109.5
C31—C30—H30A	110.7	H44A—C44—H44B	109.5
C29—C30—H30A	110.7	N4—C44—H44C	109.5
C31—C30—H30B	110.7	H44A—C44—H44C	109.5
C29—C30—H30B	110.7	H44B—C44—H44C	109.5
H30A—C30—H30B	108.8	C42B—O10B—C29B	109 (3)
N1—C31—C30	105.3 (4)	O10B—C42B—N4B	130 (3)
N1—C31—H31A	110.7	O10B—C42B—H42B	115.2
C30—C31—H31A	110.7	N4B—C42B—H42B	115.2
N1—C31—H31B	110.7	C42B—N4B—C43B	114 (2)
C30—C31—H31B	110.7	C42B—N4B—C44B	117 (3)
H31A—C31—H31B	108.8	C43B—N4B—C44B	113 (3)
C33—C32—N1	110.8 (3)	N4B—C43B—H43D	109.5
C33—C32—H32A	109.5	N4B—C43B—H43E	109.5

N1—C32—H32A	109.5	H43D—C43B—H43E	109.5
C33—C32—H32B	109.5	N4B—C43B—H43F	109.5
N1—C32—H32B	109.5	H43D—C43B—H43F	109.5
H32A—C32—H32B	108.1	H43E—C43B—H43F	109.5
O7—C33—C32	111.2 (3)	N4B—C44B—H44D	109.5
O7—C33—H33A	109.4	N4B—C44B—H44E	109.5
C32—C33—H33A	109.4	H44D—C44B—H44E	109.5
O7—C33—H33B	109.4	N4B—C44B—H44F	109.5
C32—C33—H33B	109.4	H44D—C44B—H44F	109.5
H33A—C33—H33B	108.0	H44E—C44B—H44F	109.5
C34—O7—C33	109.6 (4)	O1—In1—O3 ^{III}	132.58 (6)
O7—C34—C35	112.9 (3)	O1—In1—O5 ^{IV}	84.71 (6)
O7—C34—H34A	109.0	O3 ^{III} —In1—O5 ^{IV}	132.50 (6)
C35—C34—H34A	109.0	O1—In1—O4 ^{III}	94.43 (6)
O7—C34—H34B	109.0	O3 ^{III} —In1—O4 ^{III}	58.63 (6)
C35—C34—H34B	109.0	O5 ^{IV} —In1—O4 ^{III}	96.76 (6)
H34A—C34—H34B	107.8	O1—In1—O6 ^{IV}	141.62 (6)
C34—C35—N1	111.4 (3)	O3 ^{III} —In1—O6 ^{IV}	79.78 (6)
C34—C35—H35A	109.4	O5 ^{IV} —In1—O6 ^{IV}	57.16 (6)
N1—C35—H35A	109.4	O4 ^{III} —In1—O6 ^{IV}	86.65 (6)
C34—C35—H35B	109.4	O1—In1—Cl1	100.60 (14)
N1—C35—H35B	109.4	O3 ^{III} —In1—Cl1	102.22 (13)
H35A—C35—H35B	108.0	O5 ^{IV} —In1—Cl1	96.44 (9)
C31B—N1B—C35B	110.6 (11)	O4 ^{III} —In1—Cl1	160.82 (13)
C31B—N1B—C32B	112.2 (11)	O6 ^{IV} —In1—Cl1	88.87 (12)
C35B—N1B—C32B	107.7 (9)	O1—In1—O2	56.39 (6)
C31B—N1B—C28B	102.8 (10)	O3 ^{III} —In1—O2	80.82 (6)
C35B—N1B—C28B	112.1 (10)	O5 ^{IV} —In1—O2	140.93 (6)
C32B—N1B—C28B	111.5 (10)	O4 ^{III} —In1—O2	84.00 (6)
N1B—C28B—C29B	108.4 (9)	O6 ^{IV} —In1—O2	160.58 (6)
N1B—C28B—H28C	110.0	Cl1—In1—O2	94.39 (10)
C29B—C28B—H28C	110.0	O1—In1—Br1	100.8 (3)
N1B—C28B—H28D	110.0	O3 ^{III} —In1—Br1	98.1 (2)
C29B—C28B—H28D	110.0	O5 ^{IV} —In1—Br1	102.33 (17)
H28C—C28B—H28D	108.4	O4 ^{III} —In1—Br1	156.5 (2)
C30B—C29B—C28B	102.6 (11)	O6 ^{IV} —In1—Br1	92.3 (2)
C30B—C29B—O10B	95 (2)	O2—In1—Br1	89.59 (19)
C28B—C29B—O10B	85.0 (16)	O1—In1—C20 ^{III}	116.25 (6)
C30B—C29B—H29C	111.3	O3 ^{III} —In1—C20 ^{III}	29.28 (6)
C28B—C29B—H29C	111.3	O5 ^{IV} —In1—C20 ^{III}	116.45 (7)
O10B—C29B—H29C	144.2	O4 ^{III} —In1—C20 ^{III}	29.37 (6)
C30B—C29B—H29D	111.3	O6 ^{IV} —In1—C20 ^{III}	81.41 (6)
C28B—C29B—H29D	111.3	Cl1—In1—C20 ^{III}	131.45 (13)
O10B—C29B—H29D	36.1	O2—In1—C20 ^{III}	82.11 (6)
H29C—C29B—H29D	109.2	Br1—In1—C20 ^{III}	127.4 (2)

C31B—C30B—C29B	101.9 (14)	O1—In1—C27 ^{iv}	113.67 (7)
C31B—C30B—H30C	111.4	O3 ⁱⁱⁱ —In1—C27 ^{iv}	106.93 (6)
C29B—C30B—H30C	111.4	O5 ^{iv} —In1—C27 ^{iv}	28.96 (7)
C31B—C30B—H30D	111.4	O4 ⁱⁱⁱ —In1—C27 ^{iv}	93.89 (6)
C29B—C30B—H30D	111.4	O6 ^{iv} —In1—C27 ^{iv}	28.33 (7)
H30C—C30B—H30D	109.2	Cl1—In1—C27 ^{iv}	90.95 (9)
N1B—C31B—C30B	105.3 (13)	O2—In1—C27 ^{iv}	169.46 (7)
N1B—C31B—H31C	110.7	Br1—In1—C27 ^{iv}	96.23 (17)
C30B—C31B—H31C	110.7	C20 ⁱⁱⁱ —In1—C27 ^{iv}	101.09 (7)
N1B—C31B—H31D	110.7	O1—In1—C1	28.54 (6)
C30B—C31B—H31D	110.7	O3 ⁱⁱⁱ —In1—C1	107.18 (6)
H31C—C31B—H31D	108.8	O5 ^{iv} —In1—C1	113.24 (6)
C33B—C32B—N1B	112.6 (10)	O4 ⁱⁱⁱ —In1—C1	90.15 (6)
C33B—C32B—H32C	109.1	O6 ^{iv} —In1—C1	169.31 (7)
N1B—C32B—H32C	109.1	Cl1—In1—C1	97.36 (12)
C33B—C32B—H32D	109.1	O2—In1—C1	27.89 (6)
N1B—C32B—H32D	109.1	Br1—In1—C1	94.7 (2)
H32C—C32B—H32D	107.8	C20 ⁱⁱⁱ —In1—C1	100.64 (6)
O7B—C33B—C32B	112.2 (11)	C27 ^{iv} —In1—C1	142.19 (7)
O7B—C33B—H33C	109.2		
O2—C1—C2—C3	-172.9 (2)	C35—N1—C28—C29	79.4 (4)
O1—C1—C2—C3	5.9 (3)	C32—N1—C28—C29	-161.6 (4)
O2—C1—C2—C7	3.3 (3)	N1—C28—C29—C30	24.5 (6)
O1—C1—C2—C7	-177.9 (2)	C28—C29—C30—C31	1.2 (7)
C7—C2—C3—C4	-2.3 (3)	C35—N1—C31—C30	-76.4 (5)
C1—C2—C3—C4	174.0 (2)	C32—N1—C31—C30	160.8 (4)
C2—C3—C4—C5	1.7 (3)	C28—N1—C31—C30	42.9 (5)
C3—C4—C5—C6	0.1 (3)	C29—C30—C31—N1	-27.1 (7)
C3—C4—C5—C8	-177.1 (2)	C31—N1—C32—C33	72.6 (4)
C4—C5—C6—C7	-1.3 (3)	C35—N1—C32—C33	-52.9 (4)
C8—C5—C6—C7	175.9 (2)	C28—N1—C32—C33	-173.9 (3)
C5—C6—C7—C2	0.7 (3)	N1—C32—C33—O7	59.4 (5)
C3—C2—C7—C6	1.1 (3)	C32—C33—O7—C34	-61.4 (5)
C1—C2—C7—C6	-175.2 (2)	C33—O7—C34—C35	60.2 (4)
C4—C5—C8—C9	34.9 (3)	O7—C34—C35—N1	-56.4 (4)
C6—C5—C8—C9	-142.3 (2)	C31—N1—C35—C34	-74.8 (4)
C4—C5—C8—C13	-146.7 (2)	C32—N1—C35—C34	51.1 (4)
C6—C5—C8—C13	36.0 (3)	C28—N1—C35—C34	171.2 (3)
C13—C8—C9—C10	1.3 (3)	C31B—N1B—C28B— C29B	-16.5 (16)
C5—C8—C9—C10	179.70 (19)	C35B—N1B—C28B— C29B	102.4 (13)
C8—C9—C10—C11	-0.1 (3)	C32B—N1B—C28B— C29B	-136.8 (12)
C8—C9—C10—C14	-177.02 (19)	N1B—C28B—C29B—	-10 (2)

		C30B	
C9—C10—C11—C12	-1.7 (3)	N1B—C28B—C29B—O10B	-104.0 (18)
C14—C10—C11—C12	175.18 (19)	C28B—C29B—C30B—C31B	32 (2)
C10—C11—C12—C13	2.3 (3)	O10B—C29B—C30B—C31B	118 (2)
C10—C11—C12—C21	-172.2 (2)	C35B—N1B—C31B—C30B	-82.0 (19)
C9—C8—C13—C12	-0.7 (3)	C32B—N1B—C31B—C30B	157.7 (16)
C5—C8—C13—C12	-179.08 (19)	C28B—N1B—C31B—C30B	37.8 (19)
C11—C12—C13—C8	-1.0 (3)	C29B—C30B—C31B—N1B	-45 (2)
C21—C12—C13—C8	173.3 (2)	C31B—N1B—C32B—C33B	174.0 (12)
C9—C10—C14—C15	54.7 (3)	C35B—N1B—C32B—C33B	52.0 (14)
C11—C10—C14—C15	-122.1 (2)	C28B—N1B—C32B—C33B	-71.3 (14)
C9—C10—C14—C19	-126.4 (2)	N1B—C32B—C33B—O7B	-55.4 (17)
C11—C10—C14—C19	56.7 (3)	C32B—C33B—O7B—C34B	54.4 (18)
C19—C14—C15—C16	-2.1 (3)	C33B—O7B—C34B—C35B	-53.0 (17)
C10—C14—C15—C16	176.73 (18)	O7B—C34B—C35B—N1B	51.6 (16)
C14—C15—C16—C17	3.0 (3)	C31B—N1B—C35B—C34B	-172.0 (12)
C15—C16—C17—C18	-1.0 (3)	C32B—N1B—C35B—C34B	-49.0 (13)
C15—C16—C17—C20	179.47 (18)	C28B—N1B—C35B—C34B	74.0 (13)
C16—C17—C18—C19	-1.9 (3)	O2—C1—O1—In1	4.5 (2)
C20—C17—C18—C19	177.63 (19)	C2—C1—O1—In1	-174.37 (16)
C17—C18—C19—C14	2.8 (3)	O1—C1—O2—In1	-3.9 (2)
C15—C14—C19—C18	-0.8 (3)	C2—C1—O2—In1	174.85 (19)
C10—C14—C19—C18	-179.62 (19)	O4—C20—O3—In1 ^I	3.01 (19)
C16—C17—C20—O3	20.6 (3)	C17—C20—O3—In1 ^I	-175.81 (15)
C18—C17—C20—O3	-158.95 (19)	O3—C20—O4—In1 ^I	-2.90 (18)
C16—C17—C20—O4	-158.24 (19)	C17—C20—O4—In1 ^I	175.89 (16)
C18—C17—C20—O4	22.2 (3)	O6—C27—O5—In1 ^{II}	-7.8 (3)
C11—C12—C21—C22	-34.5 (3)	C24—C27—O5—In1 ^{II}	170.10 (19)

C13—C12—C21—C22	151.2 (2)	O5—C27—O6—In1 ⁱⁱ	7.3 (2)
C11—C12—C21—C26	140.1 (2)	C24—C27—O6—In1 ⁱⁱ	-170.6 (2)
C13—C12—C21—C26	-34.2 (3)	O8—C36—N2—C37	1.5 (7)
C26—C21—C22—C23	-3.2 (4)	O8—C36—N2—C38	176.6 (4)
C12—C21—C22—C23	171.5 (2)	O9—C39—N3—C40	0.2 (4)
C21—C22—C23—C24	0.6 (4)	O9—C39—N3—C41	-179.9 (3)
C22—C23—C24—C25	2.4 (4)	O9B—C39B—N3B— C40B	-0.5 (4)
C22—C23—C24—C27	-172.1 (2)	O9B—C39B—N3B— C41B	180.0 (3)
C23—C24—C25—C26	-2.7 (4)	O9C—C39C—N3C— C40C	-1.1 (4)
C27—C24—C25—C26	171.9 (2)	O9C—C39C—N3C— C41C	-178.9 (3)
C24—C25—C26—C21	0.0 (4)	O10—C42—N4—C43	7 (3)
C22—C21—C26—C25	2.9 (4)	O10—C42—N4—C44	-177 (2)
C12—C21—C26—C25	-171.8 (2)	C30B—C29B—O10B— C42B	97 (3)
C25—C24—C27—O6	4.7 (4)	C28B—C29B—O10B— C42B	-161 (3)
C23—C24—C27—O6	179.3 (2)	C29B—O10B—C42B— N4B	164 (3)
C25—C24—C27—O5	-173.2 (2)	O10B—C42B—N4B— C43B	-160 (4)
C23—C24—C27—O5	1.4 (3)	O10B—C42B—N4B— C44B	-25 (6)
C31—N1—C28—C29	-41.0 (4)		

Symmetry codes: (i) $x-1, y+1, z$; (ii) $x-1, y, z+1$; (iii) $x+1, y-1, z$; (iv) $x+1, y, z-1$.

Table 4: YCM-32 Crystal Data

Crystal data	
Chemical formula	C ₆₂ H ₅₀ Cl ₂ In ₂ NO ₁₂
M_r	1301.57
Crystal system, space group	Monoclinic, $C2/c$
Temperature (K)	100
a, b, c (Å)	32.6605 (18), 11.9586 (5), 18.655 (1)
β (°)	102.002 (3)

$V(\text{\AA}^3)$	7126.9 (6)
Z	4
Radiation type	Mo $K\alpha$
μ (mm ⁻¹)	0.77
Crystal size (mm)	0.06 × 0.04 × 0.03
Data collection	
Diffractometer	Bruker AXS D8 Quest CMOS diffractometer
Absorption correction	Multi-scan Apex2 v2014.11 (Bruker, 2014)
T_{\min}, T_{\max}	0.700, 0.746
No. of measured, independent and observed [$I > 2\sigma(I)$] reflections	114839, 8854, 6399
R_{int}	0.133
$(\sin \theta/\lambda)_{\text{max}}$ (Å ⁻¹)	0.668
Refinement	
$R[F^2 > 2\sigma(F^2)], wR(F^2), S$	0.050, 0.125, 1.05
No. of reflections	8854
No. of parameters	398
No. of restraints	106
H-atom treatment	H-atom parameters constrained
	$w = 1/[\sigma^2(F_o^2) + (0.0501P)^2 + 33.8785P]$ where $P = (F_o^2 + 2F_c^2)/3$
$\Delta\rho_{\text{max}}, \Delta\rho_{\text{min}}$ (e Å ⁻³)	1.93, -0.65

Computer programs: Apex2 v2014.11 (Bruker, 2014), *SAINT* V8.34A (Bruker, 2014), *SHELXS97* (Sheldrick, 2008), *SHELXL2014/7* (Sheldrick, 2014), *SHELXLE* Rev714 (Hübschle *et al.*, 2011).

Supporting information

▸ Crystallographic data

(jjm_3_76b_dtg_0m_sq)

Crystal data

$C_{62}H_{50}Cl_2In_2NO_{12}$	$F(000) = 2628$
$M_r = 1301.57$	$D_x = 1.213 \text{ Mg m}^{-3}$
Monoclinic, $C2/c$	Mo $K\alpha$ radiation, $\lambda = 0.71073 \text{ \AA}$
$a = 32.6605 (18) \text{ \AA}$	Cell parameters from 9944 reflections
$b = 11.9586 (5) \text{ \AA}$	$\theta = 2.2\text{--}28.1^\circ$
$c = 18.655 (1) \text{ \AA}$	$\mu = 0.77 \text{ mm}^{-1}$
$\beta = 102.002 (3)^\circ$	$T = 100 \text{ K}$
$V = 7126.9 (6) \text{ \AA}^3$	Fragment, colourless
$Z = 4$	$0.06 \times 0.04 \times 0.03 \text{ mm}$

Data collection

Bruker AXS D8 Quest CMOS diffractometer	8854 independent reflections
Radiation source: I-mu-S microsource X-ray tube	6399 reflections with $I > 2\sigma(I)$
Laterally graded multilayer (Goebel) mirror monochromator	$R_{\text{int}} = 0.133$
ω and ϕ scans	$\theta_{\text{max}} = 28.3^\circ$, $\theta_{\text{min}} = 2.2^\circ$
Absorption correction: multi-scan Apex2 v2014.11 (Bruker, 2014)	$h = -43 \rightarrow 43$
$T_{\text{min}} = 0.700$, $T_{\text{max}} = 0.746$	$k = -15 \rightarrow 15$

114839 measured reflections	$l = -24 \rightarrow 24$
-----------------------------	--------------------------

Refinement

Refinement on F^2	Primary atom site location: structure-invariant direct methods
Least-squares matrix: full	Secondary atom site location: difference Fourier map
$R[F^2 > 2\sigma(F^2)] = 0.050$	Hydrogen site location: inferred from neighbouring sites
$wR(F^2) = 0.125$	H-atom parameters constrained
$S = 1.05$	$w = 1/[\sigma^2(F_o^2) + (0.0501P)^2 + 33.8785P]$ where $P = (F_o^2 + 2F_c^2)/3$
8854 reflections	$(\Delta/\sigma)_{\max} = 0.003$
398 parameters	$\Delta\rho_{\max} = 1.93 \text{ e } \text{\AA}^{-3}$
106 restraints	$\Delta\rho_{\min} = -0.65 \text{ e } \text{\AA}^{-3}$

Special details

<p><i>Geometry.</i> All e.s.d.'s (except the e.s.d. in the dihedral angle between two l.s. planes) are estimated using the full covariance matrix. The cell e.s.d.'s are taken into account individually in the estimation of e.s.d.'s in distances, angles and torsion angles; correlations between e.s.d.'s in cell parameters are only used when they are defined by crystal symmetry. An approximate (isotropic) treatment of cell e.s.d.'s is used for estimating e.s.d.'s involving l.s. planes.</p>
<p><i>Refinement.</i> The tetra butyl ammonium cation is located on a two fold axis, creating half of the cation through application of the symmetry element. The cation is in addition disordered over two moieties, with the exception of the nitrogen atom, which is shared between the moieties. Equivalent C—C bond lengths and 1,3 C···N distances were each restrained to be similar, and U^{ij} components of ADPs were restrained to be similar if closer than 1.7 Angstroms. Subject to these conditions, the occupancy ratio refined to 0.544 (8) to 0.456 (8). The structure contains 4 independent solvent accessible voids of 489 Å³ each, and 1998.8 combined. The residual electron density peaks are not</p>

arranged in an interpretable pattern. The cif and fcf files were thus corrected for using reverse Fourier transform methods using the SQUEEZE routine (P. van der Sluis & A.L. Spek (1990). Acta Cryst. A46, 194–201) as implemented in the program *PLATON*. The resultant files were used in the further refinement. (The FAB file with details of the Squeeze results is appended to this cif file). The Squeeze procedure corrected for 547.7 electrons within the solvent accessible voids.

Fractional atomic coordinates and isotropic or equivalent isotropic displacement parameters (\AA^2)

	<i>x</i>	<i>y</i>	<i>z</i>	$U_{\text{iso}}^*/U_{\text{eq}}$	Occ. (<1)
In1	0.63993 (2)	1.01176 (2)	0.53702 (2)	0.02230 (8)	
Cl1	0.63878 (4)	1.05952 (10)	0.66146 (6)	0.0437 (3)	
O1	0.56884 (8)	0.9747 (2)	0.51321 (16)	0.0322 (6)	
C1	0.57761 (12)	0.8718 (3)	0.5101 (2)	0.0230 (7)	
O2	0.61413 (9)	0.8391 (2)	0.52438 (15)	0.0301 (6)	
C2	0.54234 (11)	0.7911 (3)	0.4855 (2)	0.0225 (7)	
O3	0.20015 (8)	0.4245 (2)	0.53843 (16)	0.0331 (6)	
C3	0.50090 (12)	0.8269 (3)	0.4783 (2)	0.0265 (8)	
H3	0.4952	0.9019	0.4899	0.032*	
O4	0.20282 (9)	0.6064 (2)	0.53694 (17)	0.0348 (7)	
C4	0.46795 (12)	0.7532 (3)	0.4542 (2)	0.0269 (8)	
H4	0.4399	0.7778	0.4498	0.032*	
O5	0.38472 (8)	0.1711 (2)	0.02162 (14)	0.0254 (6)	
C5	0.47611 (11)	0.6429 (3)	0.43657 (19)	0.0226 (7)	
O6	0.36993 (9)	0.0292 (2)	0.08554 (14)	0.0285 (6)	
C6	0.51781 (11)	0.6089 (3)	0.4424 (2)	0.0245 (8)	
H6	0.5237	0.5348	0.4293	0.029*	

C7	0.55034 (12)	0.6825 (3)	0.4670 (2)	0.0263 (8)	
H7	0.5784	0.6583	0.4712	0.032*	
C8	0.44087 (11)	0.5642 (3)	0.4124 (2)	0.0233 (7)	
C9	0.40609 (12)	0.5691 (3)	0.4451 (2)	0.0247 (8)	
H9	0.4046	0.6259	0.4801	0.030*	
C10	0.37345 (12)	0.4920 (3)	0.4273 (2)	0.0246 (7)	
C11	0.37548 (12)	0.4122 (3)	0.3739 (2)	0.0259 (8)	
H11	0.3535	0.3591	0.3614	0.031*	
C12	0.40896 (12)	0.4081 (3)	0.3383 (2)	0.0260 (8)	
C13	0.44186 (12)	0.4845 (3)	0.3585 (2)	0.0273 (8)	
H13	0.4651	0.4817	0.3351	0.033*	
C14	0.21950 (11)	0.5122 (3)	0.5324 (2)	0.0265 (8)	
C15	0.26210 (12)	0.5071 (3)	0.5142 (2)	0.0275 (8)	
C16	0.28448 (12)	0.6045 (3)	0.5064 (2)	0.0291 (9)	
H16	0.2742	0.6748	0.5186	0.035*	
C17	0.32120 (12)	0.5997 (3)	0.4811 (2)	0.0286 (9)	
H17	0.3363	0.6663	0.4769	0.034*	
C18	0.33630 (12)	0.4971 (3)	0.4617 (2)	0.0265 (8)	
C19	0.31556 (13)	0.3989 (3)	0.4740 (2)	0.0322 (9)	
H19	0.3267	0.3282	0.4650	0.039*	
C20	0.27876 (13)	0.4048 (3)	0.4993 (2)	0.0333 (9)	
H20	0.2646	0.3378	0.5067	0.040*	
C21	0.38214 (11)	0.1283 (3)	0.0810 (2)	0.0234 (8)	
C22	0.39284 (12)	0.1966 (3)	0.15012 (19)	0.0238 (8)	

C23	0.38380 (13)	0.1563 (3)	0.2149 (2)	0.0283 (8)	
H23	0.3728	0.0830	0.2166	0.034*	
C24	0.39083 (13)	0.2232 (3)	0.2773 (2)	0.0287 (8)	
H24	0.3847	0.1952	0.3215	0.034*	
C25	0.40682 (12)	0.3311 (3)	0.2753 (2)	0.0269 (8)	
C26	0.41749 (15)	0.3690 (3)	0.2107 (2)	0.0379 (10)	
H26	0.4297	0.4408	0.2093	0.046*	
C27	0.41023 (15)	0.3019 (3)	0.1489 (2)	0.0363 (10)	
H27	0.4173	0.3286	0.1050	0.044*	
N1	0.5000	0.9179 (5)	0.2500	0.0681 (17)	
C28	0.4764 (3)	0.9873 (8)	0.2949 (5)	0.072 (3)	0.544 (8)
H28A	0.4660	0.9379	0.3299	0.086*	0.544 (8)
H28B	0.4517	1.0208	0.2620	0.086*	0.544 (8)
C29	0.5028 (7)	1.0812 (16)	0.3380 (12)	0.087 (7)	0.544 (8)
H29A	0.5229	1.0489	0.3792	0.131*	0.544 (8)
H29B	0.4844	1.1336	0.3566	0.131*	0.544 (8)
H29C	0.5179	1.1210	0.3056	0.131*	0.544 (8)
C30	0.5308 (3)	0.8436 (9)	0.3019 (5)	0.089 (3)	0.544 (8)
H30A	0.5410	0.8878	0.3469	0.107*	0.544 (8)
H30B	0.5143	0.7808	0.3161	0.107*	0.544 (8)
C31	0.5686 (5)	0.7933 (18)	0.2803 (11)	0.129 (6)	0.544 (8)
H31A	0.5674	0.8074	0.2281	0.193*	0.544 (8)
H31B	0.5690	0.7125	0.2891	0.193*	0.544 (8)
H31C	0.5940	0.8272	0.3094	0.193*	0.544 (8)

C28B	0.4770 (3)	0.9934 (9)	0.1880 (4)	0.060 (3)	0.456 (8)
H28C	0.4615	0.9454	0.1483	0.072*	0.456 (8)
H28D	0.4561	1.0385	0.2069	0.072*	0.456 (8)
C29B	0.5044 (8)	1.0714 (13)	0.1559 (10)	0.058 (5)	0.456 (8)
H29D	0.5163	1.1278	0.1925	0.088*	0.456 (8)
H29E	0.4877	1.1086	0.1128	0.088*	0.456 (8)
H29F	0.5270	1.0289	0.1415	0.088*	0.456 (8)
C30B	0.4693 (3)	0.8474 (10)	0.2798 (7)	0.091 (3)	0.456 (8)
H30C	0.4431	0.8904	0.2768	0.109*	0.456 (8)
H30D	0.4809	0.8316	0.3322	0.109*	0.456 (8)
C31B	0.4588 (8)	0.7351 (13)	0.2388 (10)	0.120 (7)	0.456 (8)
H31D	0.4439	0.6864	0.2670	0.180*	0.456 (8)
H31E	0.4848	0.6986	0.2330	0.180*	0.456 (8)
H31F	0.4411	0.7492	0.1904	0.180*	0.456 (8)

Atomic displacement parameters (\AA^2)

	U^{11}	U^{22}	U^{33}	U^{12}	U^{13}	U^{23}
In1	0.02046 (13)	0.02221 (13)	0.02395 (14)	-0.00565 (10)	0.00399 (9)	0.00300 (10)
Cl1	0.0594 (8)	0.0485 (6)	0.0233 (5)	-0.0155 (5)	0.0089 (5)	0.0002 (4)
O1	0.0239 (14)	0.0258 (13)	0.0477 (18)	-0.0057 (11)	0.0094 (12)	-0.0028 (12)
C1	0.027 (2)	0.0214 (16)	0.0226 (19)	-0.0046 (14)	0.0105 (15)	0.0033 (13)
O2	0.0270 (15)	0.0218 (12)	0.0389 (16)	-0.0076 (11)	0.0008 (12)	0.0060 (11)

C2	0.0217 (19)	0.0224 (16)	0.0243 (19)	-0.0065 (14)	0.0068 (15)	-0.0012 (14)
O3	0.0226 (15)	0.0325 (14)	0.0449 (18)	-0.0043 (11)	0.0084 (13)	0.0077 (12)
C3	0.027 (2)	0.0240 (17)	0.031 (2)	-0.0057 (15)	0.0136 (17)	-0.0045 (15)
O4	0.0257 (15)	0.0321 (14)	0.0470 (18)	-0.0067 (12)	0.0085 (13)	-0.0023 (13)
C4	0.0222 (19)	0.0294 (18)	0.031 (2)	-0.0057 (15)	0.0095 (16)	-0.0067 (15)
O5	0.0291 (15)	0.0253 (12)	0.0225 (14)	0.0028 (11)	0.0069 (11)	-0.0032 (10)
C5	0.0218 (19)	0.0258 (17)	0.0210 (18)	-0.0060 (14)	0.0059 (15)	-0.0033 (14)
O6	0.0332 (15)	0.0266 (13)	0.0249 (14)	-0.0045 (11)	0.0040 (11)	-0.0028 (10)
C6	0.0215 (19)	0.0226 (16)	0.029 (2)	-0.0020 (14)	0.0046 (15)	-0.0030 (14)
C7	0.0203 (19)	0.0284 (18)	0.030 (2)	-0.0016 (15)	0.0034 (15)	0.0000 (15)
C8	0.0204 (19)	0.0253 (17)	0.0242 (19)	-0.0037 (14)	0.0045 (15)	-0.0013 (14)
C9	0.0241 (19)	0.0223 (17)	0.026 (2)	-0.0036 (14)	0.0003 (15)	-0.0033 (14)
C10	0.0253 (18)	0.0213 (16)	0.0277 (19)	-0.0041 (14)	0.0066 (15)	-0.0015 (14)
C11	0.028 (2)	0.0247 (17)	0.024 (2)	-0.0085 (15)	0.0035 (16)	-0.0037 (14)
C12	0.034 (2)	0.0232 (17)	0.0211 (19)	-0.0057 (15)	0.0056 (16)	-0.0037 (14)

C13	0.0256 (19)	0.0293 (18)	0.0272 (19)	-0.0074 (15)	0.0058 (15)	-0.0044 (15)
C14	0.0208 (18)	0.0278 (18)	0.0275 (19)	-0.0028 (15)	-0.0030 (14)	-0.0028 (15)
C15	0.0237 (18)	0.0271 (18)	0.032 (2)	-0.0089 (15)	0.0067 (15)	-0.0003 (15)
C16	0.024 (2)	0.0250 (18)	0.038 (2)	-0.0071 (15)	0.0064 (17)	-0.0027 (16)
C17	0.025 (2)	0.0226 (17)	0.038 (2)	-0.0104 (15)	0.0064 (17)	-0.0033 (15)
C18	0.0245 (18)	0.0248 (18)	0.0298 (19)	-0.0074 (15)	0.0048 (15)	-0.0033 (15)
C19	0.035 (2)	0.0215 (17)	0.043 (2)	-0.0019 (16)	0.0141 (19)	-0.0011 (16)
C20	0.035 (2)	0.0222 (18)	0.046 (3)	-0.0102 (16)	0.015 (2)	-0.0007 (16)
C21	0.0167 (18)	0.0215 (16)	0.032 (2)	0.0021 (13)	0.0056 (15)	0.0004 (14)
C22	0.0251 (19)	0.0258 (17)	0.0205 (18)	-0.0014 (14)	0.0046 (15)	-0.0041 (14)
C23	0.033 (2)	0.0230 (17)	0.029 (2)	-0.0042 (15)	0.0079 (17)	-0.0028 (15)
C24	0.038 (2)	0.0239 (17)	0.025 (2)	-0.0007 (16)	0.0094 (17)	-0.0016 (14)
C25	0.029 (2)	0.0277 (18)	0.0238 (19)	-0.0042 (15)	0.0042 (16)	-0.0061 (14)
C26	0.053 (3)	0.030 (2)	0.033 (2)	-0.0183 (19)	0.013 (2)	-0.0090 (17)
C27	0.052 (3)	0.032 (2)	0.026 (2)	-0.0128 (19)	0.0124 (19)	-0.0036 (16)

N1	0.102 (5)	0.074 (4)	0.032 (3)	0.000	0.024 (3)	0.000
C28	0.095 (6)	0.085 (6)	0.041 (4)	-0.007 (5)	0.027 (4)	-0.003 (4)
C29	0.065 (9)	0.129 (14)	0.069 (11)	0.000 (10)	0.019 (8)	-0.046 (11)
C30	0.128 (7)	0.095 (6)	0.048 (5)	0.028 (6)	0.025 (5)	0.008 (5)
C31	0.150 (14)	0.155 (14)	0.090 (11)	0.049 (12)	0.044 (10)	0.039 (11)
C28B	0.070 (7)	0.081 (7)	0.027 (5)	0.012 (6)	0.007 (5)	0.001 (5)
C29B	0.098 (14)	0.055 (8)	0.021 (7)	0.013 (8)	0.011 (8)	-0.003 (6)
C30B	0.129 (6)	0.096 (6)	0.052 (5)	-0.019 (5)	0.030 (5)	-0.002 (5)
C31B	0.206 (16)	0.095 (11)	0.058 (9)	-0.084 (11)	0.024 (12)	-0.006 (8)

Geometric parameters (Å, °)

In1—O3 ¹	2.222 (3)	C17—H17	0.9500
In1—O2	2.224 (2)	C18—C19	1.398 (5)
In1—O6 ⁱⁱ	2.251 (3)	C19—C20	1.382 (6)
In1—O5 ⁱⁱ	2.260 (2)	C19—H19	0.9500
In1—O1	2.314 (3)	C20—H20	0.9500
In1—O4 ¹	2.346 (3)	C21—C22	1.504 (5)
In1—C11	2.3986 (11)	C21—In1 ^{iv}	2.579 (4)
In1—C21 ⁱⁱ	2.579 (4)	C22—C27	1.385 (5)
In1—C1	2.603 (4)	C22—C23	1.388 (5)
In1—C14 ¹	2.618 (4)	C23—C24	1.391 (5)
O1—C1	1.268 (4)	C23—H23	0.9500
C1—O2	1.230 (5)	C24—C25	1.395 (5)
C1—C2	1.499 (5)	C24—H24	0.9500

C2—C7	1.383 (5)	C25—C26	1.397 (6)
C2—C3	1.399 (5)	C26—C27	1.385 (5)
O3—C14	1.242 (4)	C26—H26	0.9500
O3—In1 ^{III}	2.222 (3)	C27—H27	0.9500
C3—C4	1.392 (5)	N1—C28 ^V	1.502 (8)
C3—H3	0.9500	N1—C28	1.502 (8)
O4—C14	1.262 (5)	N1—C30B	1.504 (9)
O4—In1 ^{III}	2.346 (3)	N1—C30B ^V	1.504 (9)
C4—C5	1.398 (5)	N1—C30 ^V	1.528 (9)
C4—H4	0.9500	N1—C30	1.528 (9)
O5—C21	1.239 (4)	N1—C28B ^V	1.534 (8)
O5—In1 ^{IV}	2.260 (2)	N1—C28B	1.534 (8)
C5—C6	1.404 (5)	C28—C29	1.537 (16)
C5—C8	1.482 (5)	C28—H28A	0.9900
O6—C21	1.259 (4)	C28—H28B	0.9900
O6—In1 ^{IV}	2.251 (3)	C29—H29A	0.9800
C6—C7	1.382 (5)	C29—H29B	0.9800
C6—H6	0.9500	C29—H29C	0.9800
C7—H7	0.9500	C30—C31	1.503 (14)
C8—C13	1.392 (5)	C30—H30A	0.9900
C8—C9	1.398 (5)	C30—H30B	0.9900
C9—C10	1.397 (5)	C31—H31A	0.9800
C9—H9	0.9500	C31—H31B	0.9800
C10—C11	1.391 (5)	C31—H31C	0.9800

C10—C18	1.487 (5)	C28B—C29B	1.499 (16)
C11—C12	1.394 (5)	C28B—H28C	0.9900
C11—H11	0.9500	C28B—H28D	0.9900
C12—C13	1.401 (5)	C29B—H29D	0.9800
C12—C25	1.483 (5)	C29B—H29E	0.9800
C13—H13	0.9500	C29B—H29F	0.9800
C14—C15	1.500 (5)	C30B—C31B	1.548 (15)
C14—In1 ^{III}	2.618 (4)	C30B—H30C	0.9900
C15—C20	1.390 (5)	C30B—H30D	0.9900
C15—C16	1.399 (5)	C31B—H31D	0.9800
C16—C17	1.378 (5)	C31B—H31E	0.9800
C16—H16	0.9500	C31B—H31F	0.9800
C17—C18	1.398 (5)		
O3 ^I —In1—O2	83.12 (10)	C16—C15—C14	121.3 (3)
O3 ^I —In1—O6 ^{II}	89.71 (10)	C17—C16—C15	120.8 (4)
O2—In1—O6 ^{II}	90.41 (10)	C17—C16—H16	119.6
O3 ^I —In1—O5 ^{II}	128.84 (10)	C15—C16—H16	119.6
O2—In1—O5 ^{II}	129.95 (10)	C16—C17—C18	120.3 (3)
O6 ^{II} —In1—O5 ^{II}	57.93 (9)	C16—C17—H17	119.8
O3 ^I —In1—O1	139.69 (10)	C18—C17—H17	119.8
O2—In1—O1	57.24 (10)	C17—C18—C19	119.0 (4)
O6 ^{II} —In1—O1	84.07 (10)	C17—C18—C10	120.8 (3)
O5 ^{II} —In1—O1	79.99 (9)	C19—C18—C10	120.2 (3)
O3 ^I —In1—O4 ^I	56.89 (10)	C20—C19—C18	119.9 (4)

O2—In1—O4 ⁱ	139.53 (10)	C20—C19—H19	120.0
O6 ⁱⁱ —In1—O4 ⁱ	83.98 (10)	C18—C19—H19	120.0
O5 ⁱⁱ —In1—O4 ⁱ	79.44 (10)	C19—C20—C15	121.2 (3)
O1—In1—O4 ⁱ	159.39 (10)	C19—C20—H20	119.4
O3 ⁱ —In1—C11	107.00 (8)	C15—C20—H20	119.4
O2—In1—C11	103.99 (8)	O5—C21—O6	122.0 (3)
O6 ⁱⁱ —In1—C11	158.93 (7)	O5—C21—C22	119.7 (3)
O5 ⁱⁱ —In1—C11	101.07 (7)	O6—C21—C22	118.3 (3)
O1—In1—C11	90.82 (8)	O5—C21—In1 ^{iv}	61.22 (19)
O4 ⁱ —In1—C11	94.34 (8)	O6—C21—In1 ^{iv}	60.81 (19)
O3 ⁱ —In1—C21 ⁱⁱ	110.70 (11)	C22—C21—In1 ^{iv}	177.3 (3)
O2—In1—C21 ⁱⁱ	112.25 (11)	C27—C22—C23	119.5 (3)
O6 ⁱⁱ —In1—C21 ⁱⁱ	29.22 (10)	C27—C22—C21	120.2 (3)
O5 ⁱⁱ —In1—C21 ⁱⁱ	28.72 (10)	C23—C22—C21	120.3 (3)
O1—In1—C21 ⁱⁱ	81.29 (11)	C22—C23—C24	120.0 (3)
O4 ⁱ —In1—C21 ⁱⁱ	80.09 (11)	C22—C23—H23	120.0
C11—In1—C21 ⁱⁱ	129.78 (9)	C24—C23—H23	120.0
O3 ⁱ —In1—C1	110.79 (11)	C23—C24—C25	120.5 (4)
O2—In1—C1	28.16 (10)	C23—C24—H24	119.8
O6 ⁱⁱ —In1—C1	85.55 (11)	C25—C24—H24	119.8
O5 ⁱⁱ —In1—C1	105.26 (10)	C24—C25—C26	119.0 (3)
O1—In1—C1	29.14 (10)	C24—C25—C12	120.7 (3)
O4 ⁱ —In1—C1	163.79 (11)	C26—C25—C12	120.2 (3)
C11—In1—C1	99.84 (8)	C27—C26—C25	120.1 (4)

O21 ⁱⁱ —In1—C1	96.56 (11)	C27—C26—H26	120.0
O3 ⁱ —In1—C14 ⁱ	28.24 (10)	C25—C26—H26	120.0
O2—In1—C14 ⁱ	110.81 (11)	C22—C27—C26	120.8 (4)
O6 ⁱⁱ —In1—C14 ⁱ	84.27 (11)	C22—C27—H27	119.6
O5 ⁱⁱ —In1—C14 ⁱ	103.81 (11)	C26—C27—H27	119.6
O1—In1—C14 ⁱ	163.19 (11)	C28 ^v —N1—C28	113.0 (8)
O4 ⁱ —In1—C14 ⁱ	28.80 (10)	C30B—N1—C30B ^v	111.7 (9)
C11—In1—C14 ⁱ	104.28 (9)	C28 ^v —N1—C30 ^v	108.3 (5)
C21 ⁱⁱ —In1—C14 ⁱ	94.25 (12)	C28—N1—C30 ^v	109.2 (5)
C1—In1—C14 ⁱ	137.46 (11)	C28 ^v —N1—C30	109.2 (5)
C1—O1—In1	88.1 (2)	C28—N1—C30	108.3 (5)
O2—C1—O1	121.1 (3)	C30 ^v —N1—C30	108.8 (8)
O2—C1—C2	120.7 (3)	C30B—N1—C28B ^v	108.1 (5)
O1—C1—C2	118.1 (3)	C30B ^v —N1—C28B ^v	110.5 (6)
O2—C1—In1	58.55 (18)	C30B—N1—C28B	110.5 (6)
O1—C1—In1	62.73 (19)	C30B ^v —N1—C28B	108.1 (5)
C2—C1—In1	173.3 (3)	C28B ^v —N1—C28B	107.9 (8)
C1—O2—In1	93.3 (2)	N1—C28—C29	113.4 (9)
C7—C2—C3	119.5 (3)	N1—C28—H28A	108.9
C7—C2—C1	120.5 (3)	C29—C28—H28A	108.9
C3—C2—C1	119.9 (3)	N1—C28—H28B	108.9
C14—O3—In1 ⁱⁱⁱ	93.9 (2)	C29—C28—H28B	108.9
C4—C3—C2	120.3 (3)	H28A—C28—H28B	107.7
C4—C3—H3	119.8	C28—C29—H29A	109.5

C2—C3—H3	119.8	C28—C29—H29B	109.5
C14—O4—In1 ^{III}	87.7 (2)	H29A—C29—H29B	109.5
C3—C4—C5	120.1 (4)	C28—C29—H29C	109.5
C3—C4—H4	120.0	H29A—C29—H29C	109.5
C5—C4—H4	120.0	H29B—C29—H29C	109.5
C21—O5—In1 ^{IV}	90.1 (2)	C31—C30—N1	122.1 (9)
C4—C5—C6	119.0 (3)	C31—C30—H30A	106.8
C4—C5—C8	119.7 (3)	N1—C30—H30A	106.8
C6—C5—C8	121.3 (3)	C31—C30—H30B	106.8
C21—O6—In1 ^{IV}	90.0 (2)	N1—C30—H30B	106.8
C7—C6—C5	120.5 (3)	H30A—C30—H30B	106.7
C7—C6—H6	119.7	C30—C31—H31A	109.5
C5—C6—H6	119.7	C30—C31—H31B	109.5
C6—C7—C2	120.6 (4)	H31A—C31—H31B	109.5
C6—C7—H7	119.7	C30—C31—H31C	109.5
C2—C7—H7	119.7	H31A—C31—H31C	109.5
C13—C8—C9	119.2 (3)	H31B—C31—H31C	109.5
C13—C8—C5	121.4 (3)	C29B—C28B—N1	115.4 (10)
C9—C8—C5	119.4 (3)	C29B—C28B—H28C	108.4
C10—C9—C8	121.2 (3)	N1—C28B—H28C	108.4
C10—C9—H9	119.4	C29B—C28B—H28D	108.4
C8—C9—H9	119.4	N1—C28B—H28D	108.4
C11—C10—C9	118.4 (3)	H28C—C28B—H28D	107.5
C11—C10—C18	120.1 (3)	C28B—C29B—H29D	109.5

C9—C10—C18	121.4 (3)	C28B—C29B—H29E	109.5
C10—C11—C12	121.6 (3)	H29D—C29B—H29E	109.5
C10—C11—H11	119.2	C28B—C29B—H29F	109.5
C12—C11—H11	119.2	H29D—C29B—H29F	109.5
C11—C12—C13	118.9 (3)	H29E—C29B—H29F	109.5
C11—C12—C25	119.2 (3)	N1—C30B—C31B	113.6 (9)
C13—C12—C25	121.7 (4)	N1—C30B—H30C	108.8
C8—C13—C12	120.6 (4)	C31B—C30B—H30C	108.8
C8—C13—H13	119.7	N1—C30B—H30D	108.8
C12—C13—H13	119.7	C31B—C30B—H30D	108.8
O3—C14—O4	120.9 (4)	H30C—C30B—H30D	107.7
O3—C14—C15	120.0 (3)	C30B—C31B—H31D	109.5
O4—C14—C15	119.0 (3)	C30B—C31B—H31E	109.5
O3—C14—In1 ^{III}	57.9 (2)	H31D—C31B—H31E	109.5
O4—C14—In1 ^{III}	63.5 (2)	C30B—C31B—H31F	109.5
C15—C14—In1 ^{III}	168.8 (3)	H31D—C31B—H31F	109.5
C20—C15—C16	118.5 (4)	H31E—C31B—H31F	109.5
C20—C15—C14	120.0 (3)		
In1—O1—C1—O2	5.0 (4)	C15—C16—C17—C18	1.1 (6)
In1—O1—C1—C2	-172.5 (3)	C16—C17—C18—C19	-5.3 (6)
O1—C1—O2—In1	-5.2 (4)	C16—C17—C18—C10	173.7 (4)
C2—C1—O2—In1	172.2 (3)	C11—C10—C18—C17	-144.2 (4)
O2—C1—C2—C7	-10.6 (5)	C9—C10—C18—C17	33.0 (6)
O1—C1—C2—C7	166.9 (4)	C11—C10—C18—C19	34.8 (6)

O2—C1—C2—C3	172.0 (4)	C9—C10—C18—C19	-148.0 (4)
O1—C1—C2—C3	-10.4 (5)	C17—C18—C19—C20	5.3 (6)
C7—C2—C3—C4	1.4 (6)	C10—C18—C19—C20	-173.7 (4)
C1—C2—C3—C4	178.8 (3)	C18—C19—C20—C15	-1.1 (7)
C2—C3—C4—C5	-0.5 (6)	C16—C15—C20—C19	-3.0 (6)
C3—C4—C5—C6	-1.0 (6)	C14—C15—C20—C19	172.2 (4)
C3—C4—C5—C8	178.8 (3)	In1 ^{iv} —O5—C21—O6	1.5 (4)
C4—C5—C6—C7	1.6 (6)	In1 ^{iv} —O5—C21—C22	-177.0 (3)
C8—C5—C6—C7	-178.2 (3)	In1 ^{iv} —O6—C21—O5	-1.5 (4)
C5—C6—C7—C2	-0.7 (6)	In1 ^{iv} —O6—C21—C22	177.0 (3)
C3—C2—C7—C6	-0.8 (6)	O5—C21—C22—C27	-7.7 (6)
C1—C2—C7—C6	-178.2 (3)	O6—C21—C22—C27	173.7 (4)
C4—C5—C8—C13	143.1 (4)	O5—C21—C22—C23	169.7 (4)
C6—C5—C8—C13	-37.1 (5)	O6—C21—C22—C23	-8.9 (5)
C4—C5—C8—C9	-37.8 (5)	C27—C22—C23—C24	2.3 (6)
C6—C5—C8—C9	142.0 (4)	C21—C22—C23—C24	-175.1 (4)
C13—C8—C9—C10	3.3 (6)	C22—C23—C24—C25	0.2 (6)
C5—C8—C9—C10	-175.8 (3)	C23—C24—C25—C26	-3.0 (6)
C8—C9—C10—C11	-2.5 (5)	C23—C24—C25—C12	171.6 (4)
C8—C9—C10—C18	-179.7 (3)	C11—C12—C25—C24	-41.4 (6)
C9—C10—C11—C12	-0.2 (6)	C13—C12—C25—C24	144.8 (4)
C18—C10—C11—C12	177.1 (3)	C11—C12—C25—C26	133.1 (4)
C10—C11—C12—C13	1.9 (6)	C13—C12—C25—C26	-40.7 (6)
C10—C11—C12—C25	-172.1 (4)	C24—C25—C26—C27	3.2 (7)

C9—C8—C13—C12	-1.5 (6)	C12—C25—C26—C27	-171.4 (4)
C5—C8—C13—C12	177.6 (3)	C23—C22—C27—C26	-2.0 (7)
C11—C12—C13—C8	-1.0 (6)	C21—C22—C27—C26	175.4 (4)
C25—C12—C13—C8	172.8 (4)	C25—C26—C27—C22	-0.7 (7)
In1 ^{III} —O3—C14—O4	8.4 (4)	C28 ^v —N1—C28—C29	-48.1 (12)
In1 ^{III} —O3—C14—C15	-167.1 (3)	C30 ^v —N1—C28—C29	-168.6 (12)
In1 ^{III} —O4—C14—O3	-8.0 (4)	C30—N1—C28—C29	73.0 (14)
In1 ^{III} —O4—C14—C15	167.6 (3)	C28 ^v —N1—C30—C31	-35.6 (15)
O3—C14—C15—C20	4.2 (6)	C28—N1—C30—C31	-159.0 (13)
O4—C14—C15—C20	-171.4 (4)	C30 ^v —N1—C30—C31	82.4 (14)
In1 ^{III} —C14—C15—C20	-71.4 (14)	C30B—N1—C28B— C29B	177.6 (10)
O3—C14—C15—C16	179.3 (4)	C30B ^v —N1—C28B— C29B	-59.9 (12)
O4—C14—C15—C16	3.7 (6)	C28B ^v —N1—C28B— C29B	59.6 (10)
In1 ^{III} —C14—C15—C16	103.7 (13)	C30B ^v —N1—C30B— C31B	-32.1 (11)
C20—C15—C16—C17	3.1 (6)	C28B ^v —N1—C30B— C31B	-153.8 (13)
C14—C15—C16—C17	-172.1 (4)	C28B—N1—C30B— C31B	88.3 (14)

Symmetry codes: (i) $x+1/2, y+1/2, z$; (ii) $-x+1, y+1, -z+1/2$; (iii) $x-1/2, y-1/2, z$; (iv) $-x+1, y-1, -z+1/2$; (v) $-x+1, y, -z+1/2$.

Table 5: YCM-41 Crystal Data

Crystal data

Chemical formula	$C_{70}H_{40}Br_2In_3O_{20} \cdot 2(C_8H_{20}N)$
M_r	1965.80
Crystal system, space group	Orthorhombic, $P222_1$
Temperature (K)	150
a, b, c (Å)	9.3894 (19), 15.536 (4), 34.201 (7)
V (Å ³)	4988.9 (18)
Z	2
Radiation type	Mo $K\alpha$
μ (mm ⁻¹)	1.55
Crystal size (mm)	0.40 × 0.20 × 0.20
Data collection	
Diffractometer	Bruker AXS D8 Quest CMOS diffractometer
Absorption correction	Multi-scan Apex2 v2014.11 (Bruker, 2014)
T_{\min}, T_{\max}	0.485, 0.746
No. of measured, independent and observed [$I > 2\sigma(I)$] reflections	80376, 13363, 7492
R_{int}	0.194
$(\sin \theta/\lambda)_{\text{max}}$ (Å ⁻¹)	0.715
Refinement	
$R[F^2 > 2\sigma(F^2)], wR(F^2), S$	0.100, 0.283, 0.99
No. of reflections	13363
No. of parameters	545
No. of restraints	605

H-atom treatment	H-atom parameters constrained	
$\Delta\rho_{\max}, \Delta\rho_{\min}$ (e Å ⁻³)	2.88, -1.98	
Absolute structure	Refined as an inversion twin.	
Absolute structure parameter	0.12 (3)	
Computer programs: Apex2 v2014.11 (Bruker, 2014), <i>SAINTE</i> V8.34A (Bruker, 2014), <i>SHELXS97</i> (Sheldrick, 2008), <i>SHELXL2014/7</i> (Sheldrick, 2014), SHELXLE Rev714 (Hübschle <i>et al.</i> , 2011).		
Supporting information		
▾ Crystallographic data		
YCM-41		
Crystal data		
C ₇₀ H ₄₀ Br ₂ In ₃ O ₂₀ ·2(C ₈ H ₂₀ N)	$D_x = 1.309 \text{ Mg m}^{-3}$	
$M_r = 1965.80$	Mo $K\alpha$ radiation, $\lambda = 0.71073 \text{ \AA}$	
Orthorhombic, $P222_1$	Cell parameters from 9926 reflections	
$a = 9.3894 (19) \text{ \AA}$	$\theta = 2.3\text{--}25.9^\circ$	
$b = 15.536 (4) \text{ \AA}$	$\mu = 1.55 \text{ mm}^{-1}$	
$c = 34.201 (7) \text{ \AA}$	$T = 150 \text{ K}$	
$V = 4988.9 (18) \text{ \AA}^3$	Needle, colourless	
$Z = 2$	$0.40 \times 0.20 \times 0.20 \text{ mm}$	
$F(000) = 1974$		
Data collection		
Bruker AXS D8 Quest CMOS diffractometer	13363 independent reflections	
Radiation source: I-mu-S microsource X-ray tube	7492 reflections with $I > 2\sigma(I)$	
Laterally graded multilayer	$R_{\text{int}} = 0.194$	

(Goebel) mirror monochromator		
ω and ϕ scans	$\theta_{\max} = 30.5^\circ$, $\theta_{\min} = 2.2^\circ$	
Absorption correction: multi-scan Apex2 v2014.11 (Bruker, 2014)	$h = -13 \rightarrow 12$	
$T_{\min} = 0.485$, $T_{\max} = 0.746$	$k = -22 \rightarrow 21$	
80376 measured reflections	$l = -47 \rightarrow 48$	
Refinement		
Refinement on F^2	Hydrogen site location: inferred from neighbouring sites	
Least-squares matrix: full	H-atom parameters constrained	
$R[F^2 > 2\sigma(F^2)] = 0.100$	$w = 1/[\sigma^2(F_o^2) + (0.1748P)^2]$ where $P = (F_o^2 + 2F_c^2)/3$	
$wR(F^2) = 0.283$	$(\Delta/\sigma)_{\max} = 0.001$	
$S = 0.99$	$\Delta\rho_{\max} = 2.88 \text{ e } \text{\AA}^{-3}$	
13363 reflections	$\Delta\rho_{\min} = -1.98 \text{ e } \text{\AA}^{-3}$	
545 parameters	Absolute structure: Refined as an inversion twin.	
605 restraints	Absolute structure parameter: 0.12 (3)	

Special details

Geometry. All e.s.d.'s (except the e.s.d. in the dihedral angle between two l.s. planes) are estimated using the full covariance matrix. The cell e.s.d.'s are taken into account individually in the estimation of e.s.d.'s in distances, angles and torsion angles; correlations between e.s.d.'s in cell parameters are only used when they are defined by crystal symmetry. An approximate (isotropic) treatment of cell e.s.d.'s is used for estimating e.s.d.'s involving l.s. planes.

Refinement. Refined as a 2-component inversion twin.

The structure consists of a relatively well defined metal-ligand framework, and interstitial areas filled with tetraethyl ammonium cations and solvate molecules. One ammonium cation is relatively well resolved, another is disordered and ill defined, and the third cation as well as solvate molecules are not resolved.

Due to the low data quality a global rigid body restraint was applied for all C, N and O atoms (RIGU in *SHELXL*). For the disordered tetraethyl ammonium cation an additional similarity restraint was applied. U^{ij} components of ADPs were restrained to be similar if closer than 1.7 Angstrom. The C—C distances between carboxylate and *ipso* carbon atoms of phenyl rings were restrained to be 1.45 Angstrom. The distances of the carboxylate C atoms to the next indium atom were refined to be all similar. Neighboring C atoms C22 and C23 were constrained to have identical ADPs. The two moieties of the disordered tetra ethyl ammonium ion was restrained to be similar to the not disordered ammonium cation, and to have approximate local tetrahedral geometry around the nitrogen atom. A weak anti-bumping restraint was applied to keep atoms of the disordered moieties from approaching too closely to the main framework. Subject to these conditions the occupancy ratio of the disordered cation refined to 0.56 (3) to 0.44 (3).

The structure contains two additional solvent and cation accessible voids of 649 Å³ each. No substantial electron density peaks were found in the solvent accessible voids (less than two electron per cubic Angstrom) and the residual electron density peaks were not arranged in an interpretable pattern. The *hkl* file was thus corrected for using reverse Fourier transform methods using the SQUEEZE routine (P. van der Sluis & A.L. Spek (1990). *Acta Cryst.* A46, 194–201) as implemented in the program *PLATON*. The resultant files were used in the further refinement. (The FAB file with details of the Squeeze results is appended to this cif file). The Squeeze procedure corrected for 342 electrons within each of the two solvent accessible voids.

Fractional atomic coordinates and isotropic or equivalent isotropic displacement parameters (Å²)

	<i>x</i>	<i>y</i>	<i>z</i>	$U_{\text{iso}}^*/U_{\text{eq}}$	Occ. (<1)
C1	−0.9060 (17)	−0.1246 (10)	0.3170 (3)	0.039 (3)	
C2	−0.853 (2)	−0.1626 (10)	0.3528 (3)	0.047 (4)	
C3	−0.865 (2)	−0.2506 (11)	0.3600 (5)	0.057 (5)	
H3	−0.9221	−0.2859	0.3437	0.069*	
C4	−0.787 (3)	−0.2880 (13)	0.3934 (5)	0.072 (7)	

H4	-0.7780	-0.3485	0.3963	0.087*	
C5	-0.727 (2)	-0.2315 (12)	0.4207 (5)	0.056 (4)	
C6	-0.717 (3)	-0.1469 (13)	0.4139 (5)	0.065 (5)	
H6	-0.6647	-0.1120	0.4315	0.078*	
C7	-0.783 (2)	-0.1080 (12)	0.3811 (5)	0.061 (5)	
H7	-0.7822	-0.0473	0.3779	0.073*	
C8	-0.4441 (17)	-0.3688 (11)	0.5568 (3)	0.038 (3)	
C9	-0.515 (2)	-0.3364 (11)	0.5221 (4)	0.050 (4)	
C10	-0.507 (2)	-0.3765 (11)	0.4854 (4)	0.048 (4)	
H10	-0.4539	-0.4282	0.4834	0.058*	
C11	-0.570 (2)	-0.3472 (12)	0.4533 (4)	0.047 (4)	
H11	-0.5623	-0.3785	0.4295	0.057*	
C12	-0.648 (3)	-0.2706 (13)	0.4544 (5)	0.059 (5)	
C13	-0.660 (2)	-0.2273 (15)	0.4914 (5)	0.064 (5)	
H13	-0.7143	-0.1761	0.4938	0.077*	
C14	-0.590 (2)	-0.2613 (11)	0.5236 (4)	0.049 (4)	
H14	-0.5942	-0.2310	0.5476	0.058*	
C15	-0.7586 (12)	0.0063 (11)	0.2235 (4)	0.034 (3)	
C16	-0.6378 (14)	0.0539 (11)	0.2083 (5)	0.048 (4)	
C17	-0.644 (2)	0.1446 (14)	0.2024 (7)	0.067 (5)	
H17	-0.7335	0.1714	0.2074	0.080*	
C18	-0.528 (2)	0.2014 (15)	0.1893 (8)	0.075 (7)	
H18	-0.5355	0.2618	0.1855	0.090*	
C19	-0.3954 (19)	0.1494 (13)	0.1828 (5)	0.049 (4)	

C20	-0.3848 (19)	0.0648 (13)	0.1893 (5)	0.055 (4)	
H20	-0.2960	0.0365	0.1857	0.066*	
C21	-0.510 (2)	0.0149 (13)	0.2021 (5)	0.057 (5)	
H21	-0.5017	-0.0454	0.2061	0.068*	
C22	0.1161 (12)	0.3383 (7)	0.1316 (4)	0.0306 (19)	
C23	-0.0141 (12)	0.2967 (8)	0.1444 (4)	0.0306 (19)	
C24	-0.1529 (18)	0.3026 (12)	0.1259 (5)	0.048 (4)	
H24	-0.1654	0.3433	0.1055	0.058*	
C25	-0.269 (2)	0.2513 (14)	0.1366 (6)	0.064 (6)	
H25	-0.3520	0.2524	0.1206	0.077*	
C26	-0.2686 (18)	0.1986 (12)	0.1696 (5)	0.046 (4)	
C27	-0.1379 (17)	0.1929 (11)	0.1903 (6)	0.049 (4)	
H27	-0.1287	0.1563	0.2124	0.058*	
C28	-0.0288 (19)	0.2400 (14)	0.1779 (6)	0.062 (6)	
H28	0.0539	0.2360	0.1938	0.074*	
C29	0.5743 (12)	0.4669 (11)	0.1596 (4)	0.036 (3)	
C30	0.6965 (12)	0.4641 (12)	0.1855 (4)	0.042 (4)	
C31	0.8336 (17)	0.4988 (11)	0.1742 (5)	0.040 (3)	
H31	0.8449	0.5218	0.1486	0.048*	
C32	0.9469 (15)	0.4993 (12)	0.1990 (4)	0.039 (3)	
H32	1.0340	0.5243	0.1907	0.047*	
C33	0.9385 (14)	0.4643 (9)	0.2365 (4)	0.029 (3)	
C34	0.8081 (13)	0.4366 (11)	0.2497 (4)	0.040 (3)	
H34	0.7959	0.4213	0.2764	0.048*	

C35	0.6927 (14)	0.4311 (12)	0.2236 (4)	0.038 (3)	
H35	0.6080	0.4036	0.2323	0.045*	
C36	0.370 (2)	0.6475 (14)	0.2436 (7)	0.075 (6)	
H36A	0.3910	0.6084	0.2215	0.091*	
H36B	0.3576	0.6113	0.2672	0.091*	
C37	0.2321 (19)	0.6904 (14)	0.2355 (8)	0.076 (6)	
H37A	0.2437	0.7304	0.2135	0.114*	
H37B	0.2013	0.7223	0.2587	0.114*	
H37C	0.1604	0.6471	0.2288	0.114*	
C38	0.521 (3)	0.7598 (15)	0.2144 (5)	0.080 (6)	
H38A	0.4365	0.7981	0.2125	0.096*	
H38B	0.6036	0.7974	0.2195	0.096*	
C39	0.542 (3)	0.7224 (19)	0.1754 (6)	0.116 (12)	
H39A	0.4926	0.7577	0.1559	0.173*	
H39B	0.5033	0.6638	0.1749	0.173*	
H39C	0.6438	0.7208	0.1694	0.173*	
In1	-1.0000	-0.06144 (11)	0.2500	0.0344 (4)	
In2	0.33435 (10)	0.43698 (7)	0.12050 (3)	0.0330 (3)	
N1	0.5000	0.7059 (14)	0.2500	0.068 (5)	
O1	-0.9151 (13)	-0.0435 (8)	0.3129 (3)	0.048 (3)	
O2	-0.9536 (15)	-0.1741 (8)	0.2906 (3)	0.053 (3)	
O3	-0.3800 (11)	-0.4416 (8)	0.5555 (2)	0.039 (2)	
O4	-0.4451 (13)	-0.3304 (7)	0.5886 (3)	0.039 (2)	
O5	-0.7661 (9)	-0.0583 (8)	0.2257 (2)	0.032 (2)	

O6	-0.8684 (14)	0.0499 (10)	0.2326 (4)	0.064 (3)	
O7	0.1032 (13)	0.3783 (10)	0.0998 (4)	0.061 (3)	
O8	0.2014 (13)	0.3515 (10)	0.1565 (4)	0.060 (3)	
O9	0.5772 (10)	0.4926 (8)	0.1273 (3)	0.044 (3)	
O10	0.4644 (10)	0.4252 (8)	0.1726 (3)	0.040 (2)	
Br1	0.22444 (19)	0.58507 (11)	0.12604 (5)	0.0497 (5)	
N2	-0.031 (2)	0.5000	0.0000	0.108 (9)	
C40	0.063 (3)	0.4490 (19)	-0.0271 (8)	0.136 (15)	0.56 (3)
H40A	0.0141	0.4461	-0.0527	0.164*	0.56 (3)
H40B	0.1511	0.4833	-0.0312	0.164*	0.56 (3)
C41	0.109 (6)	0.361 (3)	-0.0175 (18)	0.138 (19)	0.56 (3)
H41A	0.1689	0.3387	-0.0385	0.207*	0.56 (3)
H41B	0.1624	0.3618	0.0071	0.207*	0.56 (3)
H41C	0.0244	0.3244	-0.0145	0.207*	0.56 (3)
C42	-0.121 (3)	0.4403 (18)	0.0233 (9)	0.159 (16)	0.56 (3)
H42A	-0.1800	0.4078	0.0043	0.190*	0.56 (3)
H42B	-0.0561	0.3981	0.0355	0.190*	0.56 (3)
C43	-0.217 (5)	0.469 (4)	0.0538 (13)	0.14 (2)	0.56 (3)
H43A	-0.2660	0.4196	0.0652	0.217*	0.56 (3)
H43B	-0.1626	0.4991	0.0741	0.217*	0.56 (3)
H43C	-0.2876	0.5088	0.0426	0.217*	0.56 (3)
C40B	0.062 (4)	0.4290 (15)	0.0153 (11)	0.152 (15)	0.44 (3)
H40C	0.1619	0.4456	0.0100	0.182*	0.44 (3)
H40D	0.0506	0.4282	0.0441	0.182*	0.44 (3)

C41B	0.045 (10)	0.340 (2)	0.002 (2)	0.17 (2)	0.44 (3)
H41D	0.1140	0.3030	0.0149	0.249*	0.44 (3)
H41E	-0.0520	0.3202	0.0077	0.249*	0.44 (3)
H41F	0.0601	0.3377	-0.0266	0.249*	0.44 (3)
C42B	-0.123 (4)	0.534 (2)	0.0321 (6)	0.147 (18)	0.44 (3)
H42C	-0.0879	0.5930	0.0379	0.176*	0.44 (3)
H42D	-0.2194	0.5409	0.0209	0.176*	0.44 (3)
C43B	-0.140 (7)	0.492 (3)	0.0692 (10)	0.11 (2)	0.44 (3)
H43D	-0.2049	0.5255	0.0857	0.165*	0.44 (3)
H43E	-0.1801	0.4343	0.0651	0.165*	0.44 (3)
H43F	-0.0474	0.4869	0.0822	0.165*	0.44 (3)

Atomic displacement parameters (\AA^2)

	U^{11}	U^{22}	U^{33}	U^{12}	U^{13}	U^{23}
C1	0.034 (8)	0.046 (6)	0.038 (6)	0.007 (5)	-0.006 (5)	0.001 (4)
C2	0.061 (10)	0.040 (6)	0.038 (6)	0.004 (6)	-0.013 (6)	0.004 (5)
C3	0.087 (14)	0.038 (6)	0.047 (7)	-0.001 (7)	-0.029 (9)	0.002 (5)
C4	0.117 (17)	0.046 (8)	0.054 (8)	0.008 (8)	-0.040 (10)	0.002 (6)
C5	0.071 (11)	0.053 (7)	0.045 (6)	0.017 (7)	-0.019 (7)	-0.005 (5)
C6	0.089 (14)	0.055 (7)	0.050 (8)	0.010 (7)	-0.034 (9)	-0.007 (6)
C7	0.078 (13)	0.052 (8)	0.054 (7)	0.005 (7)	-0.035 (9)	-0.002 (6)
C8	0.041 (8)	0.051 (7)	0.022 (5)	0.007 (6)	-0.007 (5)	0.001 (4)
C9	0.066 (10)	0.052 (7)	0.032 (5)	0.013 (7)	-0.011 (5)	-0.003 (5)
C10	0.070 (11)	0.044 (8)	0.030 (5)	0.015 (8)	-0.015 (6)	-0.003 (5)

C11	0.056 (10)	0.051 (8)	0.035 (6)	0.006 (7)	-0.012 (6)	-0.003 (5)
C12	0.077 (12)	0.057 (8)	0.042 (6)	0.017 (8)	-0.016 (6)	-0.001 (5)
C13	0.068 (12)	0.085 (10)	0.040 (6)	0.018 (10)	-0.018 (7)	-0.007 (6)
C14	0.067 (11)	0.045 (7)	0.034 (6)	0.016 (8)	-0.011 (6)	-0.011 (5)
C15	0.020 (5)	0.052 (6)	0.030 (6)	-0.007 (5)	-0.007 (5)	-0.006 (5)
C16	0.027 (6)	0.054 (7)	0.064 (9)	-0.006 (5)	0.006 (5)	-0.002 (6)
C17	0.030 (8)	0.058 (7)	0.113 (15)	-0.004 (6)	0.013 (8)	0.008 (7)
C18	0.026 (7)	0.065 (9)	0.135 (18)	-0.002 (6)	0.012 (8)	0.029 (9)
C19	0.028 (6)	0.060 (7)	0.059 (9)	-0.005 (5)	-0.007 (5)	0.004 (6)
C20	0.033 (7)	0.056 (7)	0.077 (10)	-0.006 (6)	0.003 (7)	-0.001 (7)
C21	0.036 (6)	0.048 (8)	0.087 (13)	-0.001 (6)	0.007 (7)	-0.004 (7)
C22	0.034 (4)	0.009 (4)	0.049 (4)	-0.001 (3)	-0.009 (3)	-0.006 (3)
C23	0.034 (4)	0.009 (4)	0.049 (4)	-0.001 (3)	-0.009 (3)	-0.006 (3)
C24	0.029 (6)	0.060 (9)	0.056 (8)	-0.010 (6)	-0.013 (6)	0.011 (7)
C25	0.030 (7)	0.082 (12)	0.080 (9)	-0.025 (8)	-0.024 (7)	0.031 (9)
C26	0.022 (6)	0.049 (8)	0.068 (8)	-0.003 (5)	-0.009 (5)	0.009 (6)
C27	0.019 (6)	0.041 (9)	0.086 (10)	-0.011 (5)	-0.017 (6)	0.025 (8)
C28	0.027 (7)	0.078 (12)	0.081 (9)	-0.028 (7)	-0.026 (6)	0.037 (9)
C29	0.019 (5)	0.058 (9)	0.029 (5)	-0.016 (5)	-0.002 (4)	-0.008 (5)
C30	0.018 (5)	0.067 (10)	0.039 (5)	-0.008 (5)	-0.001 (4)	-0.005 (5)
C31	0.017 (5)	0.057 (9)	0.045 (6)	-0.008 (6)	0.001 (5)	-0.003 (6)
C32	0.016 (5)	0.059 (9)	0.042 (6)	-0.009 (6)	0.002 (5)	-0.001 (6)
C33	0.010 (5)	0.034 (7)	0.042 (6)	0.000 (5)	0.005 (4)	-0.009 (5)
C34	0.011 (5)	0.068 (10)	0.040 (6)	-0.002 (5)	0.003 (4)	0.004 (7)

C35	0.016 (6)	0.056 (9)	0.042 (5)	-0.007 (6)	0.000 (4)	0.000 (6)
C36	0.055 (9)	0.073 (11)	0.099 (14)	-0.014 (8)	0.015 (9)	0.010 (10)
C37	0.048 (10)	0.054 (12)	0.125 (18)	-0.013 (8)	-0.001 (10)	-0.005 (11)
C38	0.069 (15)	0.091 (13)	0.081 (10)	-0.031 (12)	-0.012 (9)	0.002 (8)
C39	0.14 (3)	0.105 (19)	0.100 (12)	-0.09 (2)	0.019 (13)	-0.022 (11)
In1	0.0243 (7)	0.0443 (9)	0.0345 (7)	0.000	-0.0055 (5)	0.000
In2	0.0230 (5)	0.0454 (6)	0.0307 (4)	0.0004 (5)	0.0008 (4)	-0.0008 (5)
N1	0.041 (10)	0.076 (13)	0.088 (11)	0.000	0.016 (8)	0.000
O1	0.042 (7)	0.049 (5)	0.053 (6)	0.002 (5)	-0.014 (5)	0.003 (4)
O2	0.060 (8)	0.056 (7)	0.045 (5)	0.004 (6)	-0.017 (5)	0.000 (5)
O3	0.039 (6)	0.050 (5)	0.029 (4)	0.002 (5)	-0.007 (4)	0.001 (4)
O4	0.049 (7)	0.044 (6)	0.026 (4)	0.006 (5)	-0.005 (4)	0.002 (4)
O5	0.012 (4)	0.050 (5)	0.035 (4)	-0.013 (4)	0.009 (3)	-0.014 (4)
O6	0.043 (6)	0.070 (8)	0.078 (8)	0.009 (6)	0.011 (5)	0.007 (6)
O7	0.029 (6)	0.080 (9)	0.074 (6)	-0.006 (6)	-0.005 (5)	0.017 (6)
O8	0.029 (6)	0.080 (9)	0.072 (6)	-0.015 (6)	-0.002 (5)	0.004 (6)
O9	0.023 (5)	0.068 (7)	0.040 (5)	-0.003 (5)	-0.006 (4)	0.000 (5)
O10	0.014 (4)	0.052 (7)	0.052 (5)	-0.003 (4)	0.000 (4)	-0.001 (5)
Br1	0.0393 (9)	0.0400 (9)	0.0699 (10)	0.0053 (7)	0.0112 (8)	-0.0027 (8)
N2	0.040 (13)	0.21 (3)	0.076 (14)	0.000	0.000	0.000 (15)
C40	0.09 (2)	0.21 (3)	0.11 (2)	0.020 (18)	0.029 (18)	0.01 (2)
C41	0.07 (3)	0.21 (3)	0.13 (4)	0.01 (2)	0.05 (3)	0.02 (2)
C42	0.11 (2)	0.21 (3)	0.15 (2)	0.010 (17)	0.07 (2)	0.01 (2)
C43	0.10 (3)	0.22 (5)	0.11 (3)	0.05 (3)	0.05 (3)	0.05 (3)

C40B	0.10 (2)	0.23 (3)	0.12 (3)	0.039 (18)	0.00 (2)	0.00 (2)
C41B	0.16 (5)	0.23 (3)	0.11 (5)	0.03 (2)	0.01 (4)	0.00 (2)
C42B	0.12 (3)	0.20 (3)	0.11 (2)	0.03 (2)	0.050 (18)	0.03 (2)
C43B	0.07 (4)	0.16 (5)	0.10 (2)	0.02 (4)	0.04 (2)	0.01 (2)

Geometric parameters (Å, °)

C1—O2	1.268 (19)	C34—H34	0.9500
C1—O1	1.270 (19)	C35—H35	0.9500
C1—C2	1.4503 (14)	C36—C37	1.48 (2)
C1—In1	2.644 (9)	C36—N1	1.540 (18)
C2—C3	1.39 (2)	C36—H36A	0.9900
C2—C7	1.44 (2)	C36—H36B	0.9900
C3—C4	1.47 (2)	C37—H37A	0.9800
C3—H3	0.9500	C37—H37B	0.9800
C4—C5	1.40 (3)	C37—H37C	0.9800
C4—H4	0.9500	C38—C39	1.47 (2)
C5—C6	1.34 (3)	C38—N1	1.492 (18)
C5—C12	1.50 (2)	C38—H38A	0.9900
C6—C7	1.42 (2)	C38—H38B	0.9900
C6—H6	0.9500	C39—H39A	0.9800
C7—H7	0.9500	C39—H39B	0.9800
C8—O4	1.238 (17)	C39—H39C	0.9800
C8—O3	1.282 (19)	In1—O6 ⁱⁱⁱ	2.207 (15)
C8—C9	1.4502 (14)	In1—O6	2.207 (15)

C8—In2 ¹	2.631 (10)	In1—O2	2.276 (12)
C9—C14	1.36 (2)	In1—O2 ⁱⁱⁱ	2.276 (12)
C9—C10	1.40 (2)	In1—O1	2.310 (11)
C10—C11	1.33 (2)	In1—O1 ⁱⁱⁱ	2.310 (11)
C10—H10	0.9500	In1—O5 ⁱⁱⁱ	2.349 (8)
C11—C12	1.40 (3)	In1—O5	2.349 (8)
C11—H11	0.9500	In1—C1 ⁱⁱⁱ	2.644 (9)
C12—C13	1.44 (2)	In1—C15 ⁱⁱⁱ	2.658 (10)
C13—C14	1.39 (2)	In2—O10	2.169 (10)
C13—H13	0.9500	In2—O8	2.201 (13)
C14—H14	0.9500	In2—O4 ^{iv}	2.239 (11)
C15—O5	1.008 (17)	In2—O3 ^{iv}	2.265 (9)
C15—O6	1.27 (2)	In2—O9	2.450 (10)
C15—C16	1.4503 (14)	In2—O7	2.458 (13)
C15—In1	2.658 (10)	In2—Br1	2.529 (2)
C16—C21	1.36 (3)	In2—C8 ^{iv}	2.631 (10)
C16—C17	1.43 (3)	N1—C38 ^v	1.492 (18)
C17—C18	1.48 (3)	N1—C36 ^v	1.540 (18)
C17—H17	0.9500	O3—In2 ¹	2.265 (9)
C18—C19	1.50 (3)	O4—In2 ¹	2.239 (11)
C18—H18	0.9500	N2—C42	1.49 (2)
C19—C20	1.34 (3)	N2—C42 ^{vi}	1.49 (2)
C19—C26	1.49 (2)	N2—C42B ^{vi}	1.49 (2)
C20—C21	1.48 (3)	N2—C42B	1.49 (2)

C20—H20	0.9500	N2—C40B ^{vi}	1.50 (2)
C21—H21	0.9500	N2—C40B	1.50 (2)
C22—O8	1.189 (17)	N2—C40 ^{vi}	1.51 (2)
C22—O7	1.257 (18)	N2—C40	1.51 (2)
C22—C23	1.4506 (14)	C40—C41	1.47 (3)
C22—In2	2.587 (10)	C40—H40A	0.9900
C23—C24	1.45 (2)	C40—H40B	0.9900
C23—C28	1.45 (2)	C41—H41A	0.9800
C24—C25	1.40 (2)	C41—H41B	0.9800
C24—H24	0.9500	C41—H41C	0.9800
C25—C26	1.39 (2)	C42—C43	1.45 (3)
C25—H25	0.9500	C42—H42A	0.9900
C26—C27	1.42 (2)	C42—H42B	0.9900
C27—C28	1.33 (2)	C43—H43A	0.9800
C27—H27	0.9500	C43—H43B	0.9800
C28—H28	0.9500	C43—H43C	0.9800
C29—O9	1.175 (17)	C40B—C41B	1.47 (3)
C29—O10	1.298 (17)	C40B—H40C	0.9900
C29—C30	1.4502 (14)	C40B—H40D	0.9900
C29—In2	2.661 (9)	C41B—H41D	0.9800
C30—C35	1.40 (2)	C41B—H41E	0.9800
C30—C31	1.45 (2)	C41B—H41F	0.9800
C31—C32	1.36 (2)	C42B—C43B	1.44 (3)
C31—H31	0.9500	C42B—H42C	0.9900

C32—C33	1.39 (2)	C42B—H42D	0.9900
C32—H32	0.9500	C43B—H43D	0.9800
C33—C34	1.374 (18)	C43B—H43E	0.9800
C33—C33 ⁱⁱ	1.48 (3)	C43B—H43F	0.9800
C34—C35	1.406 (18)		
O2—C1—O1	119.9 (10)	O6—In1—O5	50.6 (4)
O2—C1—C2	118.4 (14)	O2—In1—O5	93.1 (5)
O1—C1—C2	121.4 (14)	O2 ⁱⁱⁱ —In1—O5	88.8 (4)
O2—C1—In1	59.4 (6)	O1—In1—O5	90.3 (4)
O1—C1—In1	60.9 (6)	O1 ⁱⁱⁱ —In1—O5	89.4 (4)
C2—C1—In1	177.4 (12)	O5 ⁱⁱⁱ —In1—O5	177.6 (6)
C3—C2—C7	119.7 (12)	O6 ⁱⁱⁱ —In1—C1 ⁱⁱⁱ	109.7 (5)
C3—C2—C1	121.4 (15)	O6—In1—C1 ⁱⁱⁱ	104.1 (5)
C7—C2—C1	118.9 (15)	O2—In1—C1 ⁱⁱⁱ	107.9 (5)
C2—C3—C4	118.9 (16)	O2 ⁱⁱⁱ —In1—C1 ⁱⁱⁱ	28.6 (5)
C2—C3—H3	120.6	O1—In1—C1 ⁱⁱⁱ	165.1 (5)
C4—C3—H3	120.6	O1 ⁱⁱⁱ —In1—C1 ⁱⁱⁱ	28.7 (5)
C5—C4—C3	118.0 (17)	O5 ⁱⁱⁱ —In1—C1 ⁱⁱⁱ	90.2 (4)
C5—C4—H4	121.0	O5—In1—C1 ⁱⁱⁱ	90.7 (4)
C3—C4—H4	121.0	O6 ⁱⁱⁱ —In1—C1	104.1 (5)
C6—C5—C4	121.8 (16)	O6—In1—C1	109.7 (5)
C6—C5—C12	119.9 (18)	O2—In1—C1	28.6 (5)
C4—C5—C12	117.2 (17)	O2 ⁱⁱⁱ —In1—C1	107.9 (5)
C5—C6—C7	121.8 (18)	O1—In1—C1	28.7 (5)

C5—C6—H6	119.1	O1 ⁱⁱⁱ —In1—C1	165.1 (5)
C7—C6—H6	119.1	O5 ⁱⁱⁱ —In1—C1	90.7 (4)
C6—C7—C2	118.5 (16)	O5—In1—C1	90.2 (4)
C6—C7—H7	120.7	C1 ⁱⁱⁱ —In1—C1	136.5 (7)
C2—C7—H7	120.7	O6 ⁱⁱⁱ —In1—C15	105.0 (5)
O4—C8—O3	117.4 (10)	O6—In1—C15	28.4 (5)
O4—C8—C9	123.2 (14)	O2—In1—C15	110.4 (5)
O3—C8—C9	119.4 (13)	O2 ⁱⁱⁱ —In1—C15	105.1 (5)
O4—C8—In2 ¹	58.1 (6)	O1—In1—C15	88.6 (4)
O3—C8—In2 ¹	59.4 (6)	O1 ⁱⁱⁱ —In1—C15	85.9 (4)
C9—C8—In2 ¹	175.0 (14)	O5 ⁱⁱⁱ —In1—C15	155.5 (5)
C14—C9—C10	115.9 (12)	O5—In1—C15	22.1 (4)
C14—C9—C8	120.3 (14)	C1 ⁱⁱⁱ —In1—C15	97.8 (5)
C10—C9—C8	123.8 (15)	C1—In1—C15	99.0 (5)
C11—C10—C9	124.6 (16)	O6 ⁱⁱⁱ —In1—C15 ⁱⁱⁱ	28.4 (5)
C11—C10—H10	117.7	O6—In1—C15 ⁱⁱⁱ	105.0 (5)
C9—C10—H10	117.7	O2—In1—C15 ⁱⁱⁱ	105.1 (5)
C10—C11—C12	120.1 (16)	O2 ⁱⁱⁱ —In1—C15 ⁱⁱⁱ	110.4 (5)
C10—C11—H11	119.9	O1—In1—C15 ⁱⁱⁱ	85.9 (4)
C12—C11—H11	119.9	O1 ⁱⁱⁱ —In1—C15 ⁱⁱⁱ	88.6 (4)
C11—C12—C13	117.5 (16)	O5 ⁱⁱⁱ —In1—C15 ⁱⁱⁱ	22.1 (4)
C11—C12—C5	125.8 (15)	O5—In1—C15 ⁱⁱⁱ	155.5 (5)
C13—C12—C5	116.6 (17)	C1 ⁱⁱⁱ —In1—C15 ⁱⁱⁱ	99.0 (5)
C14—C13—C12	118.9 (19)	C1—In1—C15 ⁱⁱⁱ	97.8 (5)

C14—C13—H13	120.5	C15—In1—C15 ^{III}	133.4 (7)
C12—C13—H13	120.5	O10—In2—O8	78.9 (4)
C9—C14—C13	122.9 (15)	O10—In2—O4 ^{IV}	94.4 (4)
C9—C14—H14	118.6	O8—In2—O4 ^{IV}	95.2 (5)
C13—C14—H14	118.6	O10—In2—O3 ^{IV}	134.7 (4)
O5—C15—O6	117.1 (12)	O8—In2—O3 ^{IV}	132.5 (5)
O5—C15—C16	126.1 (16)	O4 ^{IV} —In2—O3 ^{IV}	57.1 (4)
O6—C15—C16	116.7 (15)	O10—In2—O9	55.1 (4)
O5—C15—In1	61.4 (7)	O8—In2—O9	133.5 (4)
O6—C15—In1	55.7 (8)	O4 ^{IV} —In2—O9	82.8 (4)
C16—C15—In1	172.2 (12)	O3 ^{IV} —In2—O9	84.6 (4)
C21—C16—C17	117.2 (14)	O10—In2—O7	134.6 (4)
C21—C16—C15	121.2 (16)	O8—In2—O7	55.7 (4)
C17—C16—C15	121.5 (16)	O4 ^{IV} —In2—O7	89.7 (5)
C16—C17—C18	127.1 (18)	O3 ^{IV} —In2—O7	84.1 (4)
C16—C17—H17	116.5	O9—In2—O7	168.6 (4)
C18—C17—H17	116.5	O10—In2—Br1	104.2 (3)
C17—C18—C19	109.7 (18)	O8—In2—Br1	106.0 (4)
C17—C18—H18	125.1	O4 ^{IV} —In2—Br1	154.0 (3)
C19—C18—H18	125.1	O3 ^{IV} —In2—Br1	97.0 (3)
C20—C19—C26	119.8 (17)	O9—In2—Br1	93.0 (3)
C20—C19—C18	124.6 (17)	O7—In2—Br1	89.9 (4)
C26—C19—C18	115.6 (16)	O10—In2—C22	106.0 (4)
C19—C20—C21	120.4 (18)	O8—In2—C22	27.2 (4)

C19—C20—H20	119.8	O4 ^{IV} —In2—C22	90.1 (4)
C21—C20—H20	119.8	O3 ^{IV} —In2—C22	108.2 (4)
C16—C21—C20	121.1 (17)	O9—In2—C22	158.8 (4)
C16—C21—H21	119.5	O7—In2—C22	28.7 (4)
C20—C21—H21	119.5	Br1—In2—C22	101.8 (3)
O8—C22—O7	126.9 (12)	O10—In2—C8 ^{IV}	115.2 (4)
O8—C22—C23	115.3 (12)	O8—In2—C8 ^{IV}	116.2 (5)
O7—C22—C23	113.6 (12)	O4 ^{IV} —In2—C8 ^{IV}	28.0 (4)
O8—C22—In2	58.0 (7)	O3 ^{IV} —In2—C8 ^{IV}	29.2 (4)
O7—C22—In2	70.0 (7)	O9—In2—C8 ^{IV}	81.7 (5)
C23—C22—In2	167.4 (10)	O7—In2—C8 ^{IV}	87.6 (5)
C22—C23—C24	126.6 (12)	Br1—In2—C8 ^{IV}	126.0 (3)
C22—C23—C28	126.1 (13)	C22—In2—C8 ^{IV}	101.1 (5)
C24—C23—C28	107.3 (11)	O10—In2—C29	28.9 (4)
C25—C24—C23	123.4 (14)	O8—In2—C29	107.7 (4)
C25—C24—H24	118.3	O4 ^{IV} —In2—C29	88.9 (5)
C23—C24—H24	118.3	O3 ^{IV} —In2—C29	109.1 (4)
C26—C25—C24	122.8 (16)	O9—In2—C29	26.2 (4)
C26—C25—H25	118.6	O7—In2—C29	163.1 (4)
C24—C25—H25	118.6	Br1—In2—C29	98.6 (4)
C25—C26—C27	116.3 (15)	C22—In2—C29	134.5 (5)
C25—C26—C19	123.1 (15)	C8 ^{IV} —In2—C29	98.9 (5)
C27—C26—C19	120.6 (15)	C38 ^V —N1—C38	112 (2)
C28—C27—C26	118.3 (16)	C38 ^V —N1—C36 ^V	108.5 (13)

C28—C27—H27	120.9	C38—N1—C36 ^v	110.2 (15)
C26—C27—H27	120.9	C38 ^v —N1—C36	110.2 (15)
C27—C28—C23	131.2 (15)	C38—N1—C36	108.5 (13)
C27—C28—H28	114.4	C36 ^v —N1—C36	108 (2)
C23—C28—H28	114.4	C1—O1—In1	90.4 (8)
O9—C29—O10	120.8 (10)	C1—O2—In1	92.0 (9)
O9—C29—C30	124.5 (12)	C8—O3—In2 ¹	91.5 (7)
O10—C29—C30	113.8 (12)	C8—O4—In2 ¹	93.9 (9)
O9—C29—In2	66.8 (6)	C15—O5—In1	96.5 (9)
O10—C29—In2	54.0 (5)	C15—O6—In1	95.9 (10)
C30—C29—In2	166.3 (12)	C22—O7—In2	81.3 (8)
C35—C30—C31	114.1 (11)	C22—O8—In2	94.8 (9)
C35—C30—C29	124.0 (13)	C29—O9—In2	87.0 (8)
C31—C30—C29	121.9 (13)	C29—O10—In2	97.1 (7)
C32—C31—C30	121.9 (14)	C42—N2—C42 ^{vi}	110.4 (16)
C32—C31—H31	119.0	C42B ^{vi} —N2—C42B	109.4 (18)
C30—C31—H31	119.0	C42B ^{vi} —N2—C40B ^{vi}	109.9 (9)
C31—C32—C33	121.8 (14)	C42B—N2—C40B ^{vi}	109.3 (8)
C31—C32—H32	119.1	C42B ^{vi} —N2—C40B	109.3 (8)
C33—C32—H32	119.1	C42B—N2—C40B	109.9 (9)
C34—C33—C32	118.4 (13)	C40B ^{vi} —N2—C40B	109.1 (18)
C34—C33—C33 ⁱⁱ	119.3 (14)	C42—N2—C40 ^{vi}	109.5 (8)
C32—C33—C33 ⁱⁱ	122.0 (14)	C42 ^{vi} —N2—C40 ^{vi}	109.7 (9)
C33—C34—C35	119.8 (13)	C42—N2—C40	109.7 (9)

C33—C34—H34	120.1	C42 ^{vi} —N2—C40	109.5 (8)
C35—C34—H34	120.1	C40 ^{vi} —N2—C40	108.1 (16)
C30—C35—C34	123.2 (12)	C41—C40—N2	121 (2)
C30—C35—H35	118.4	C41—C40—H40A	107.0
C34—C35—H35	118.4	N2—C40—H40A	107.0
C37—C36—N1	117.0 (15)	C41—C40—H40B	107.0
C37—C36—H36A	108.0	N2—C40—H40B	107.0
N1—C36—H36A	108.0	H40A—C40—H40B	106.7
C37—C36—H36B	108.0	C40—C41—H41A	109.5
N1—C36—H36B	108.0	C40—C41—H41B	109.5
H36A—C36—H36B	107.3	H41A—C41—H41B	109.5
C36—C37—H37A	109.5	C40—C41—H41C	109.5
C36—C37—H37B	109.5	H41A—C41—H41C	109.5
H37A—C37—H37B	109.5	H41B—C41—H41C	109.5
C36—C37—H37C	109.5	C43—C42—N2	123 (2)
H37A—C37—H37C	109.5	C43—C42—H42A	106.6
H37B—C37—H37C	109.5	N2—C42—H42A	106.6
C39—C38—N1	122.5 (19)	C43—C42—H42B	106.6
C39—C38—H38A	106.7	N2—C42—H42B	106.6
N1—C38—H38A	106.7	H42A—C42—H42B	106.5
C39—C38—H38B	106.7	C42—C43—H43A	109.5
N1—C38—H38B	106.7	C42—C43—H43B	109.5
H38A—C38—H38B	106.6	H43A—C43—H43B	109.5
C38—C39—H39A	109.5	C42—C43—H43C	109.5

C38—C39—H39B	109.5	H43A—C43—H43C	109.5
H39A—C39—H39B	109.5	H43B—C43—H43C	109.5
C38—C39—H39C	109.5	C41B—C40B—N2	121 (3)
H39A—C39—H39C	109.5	C41B—C40B—H40C	107.1
H39B—C39—H39C	109.5	N2—C40B—H40C	107.1
O6 ⁱⁱⁱ —In1—O6	76.8 (7)	C41B—C40B—H40D	107.1
O6 ⁱⁱⁱ —In1—O2	123.0 (5)	N2—C40B—H40D	107.1
O6—In1—O2	131.3 (5)	H40C—C40B—H40D	106.8
O6 ⁱⁱⁱ —In1—O2 ⁱⁱⁱ	131.3 (5)	C40B—C41B—H41D	109.5
O6—In1—O2 ⁱⁱⁱ	123.0 (5)	C40B—C41B—H41E	109.5
O2—In1—O2 ⁱⁱⁱ	79.5 (6)	H41D—C41B—H41E	109.5
O6 ⁱⁱⁱ —In1—O1	81.2 (5)	C40B—C41B—H41F	109.5
O6—In1—O1	87.9 (5)	H41D—C41B—H41F	109.5
O2—In1—O1	57.3 (4)	H41E—C41B—H41F	109.5
O2 ⁱⁱⁱ —In1—O1	136.6 (4)	C43B—C42B—N2	123 (3)
O6 ⁱⁱⁱ —In1—O1 ⁱⁱⁱ	87.9 (5)	C43B—C42B—H42C	106.5
O6—In1—O1 ⁱⁱⁱ	81.2 (5)	N2—C42B—H42C	106.5
O2—In1—O1 ⁱⁱⁱ	136.6 (4)	C43B—C42B—H42D	106.5
O2 ⁱⁱⁱ —In1—O1 ⁱⁱⁱ	57.3 (4)	N2—C42B—H42D	106.5
O1—In1—O1 ⁱⁱⁱ	166.1 (6)	H42C—C42B—H42D	106.5
O6 ⁱⁱⁱ —In1—O5 ⁱⁱⁱ	50.6 (4)	C42B—C43B—H43D	109.5
O6—In1—O5 ⁱⁱⁱ	127.1 (5)	C42B—C43B—H43E	109.5
O2—In1—O5 ⁱⁱⁱ	88.8 (4)	H43D—C43B—H43E	109.5
O2 ⁱⁱⁱ —In1—O5 ⁱⁱⁱ	93.1 (5)	C42B—C43B—H43F	109.5

O1—In1—O5 ^{III}	89.4 (4)	H43D—C43B—H43F	109.5
O1 ^{III} —In1—O5 ^{III}	90.3 (4)	H43E—C43B—H43F	109.5
O6 ^{III} —In1—O5	127.1 (5)		
O2—C1—C2—C3	-6 (3)	C18—C19—C26—C27	126 (2)
O1—C1—C2—C3	169.0 (19)	C25—C26—C27—C28	3 (3)
O2—C1—C2—C7	173.0 (17)	C19—C26—C27—C28	-178 (2)
O1—C1—C2—C7	-12 (3)	C26—C27—C28—C23	-3 (4)
C7—C2—C3—C4	-10 (3)	C22—C23—C28—C27	-173 (2)
C1—C2—C3—C4	169.4 (19)	C24—C23—C28—C27	6 (3)
C2—C3—C4—C5	12 (3)	O9—C29—C30—C35	-178.1 (17)
C3—C4—C5—C6	-12 (4)	O10—C29—C30—C35	-9 (2)
C3—C4—C5—C12	-180 (2)	In2—C29—C30—C35	-35 (6)
C4—C5—C6—C7	8 (4)	O9—C29—C30—C31	4 (3)
C12—C5—C6—C7	176 (2)	O10—C29—C30—C31	173.2 (16)
C5—C6—C7—C2	-5 (4)	In2—C29—C30—C31	148 (4)
C3—C2—C7—C6	6 (3)	C35—C30—C31—C32	-1 (3)
C1—C2—C7—C6	-173 (2)	C29—C30—C31—C32	177.3 (16)
O4—C8—C9—C14	-1 (3)	C30—C31—C32—C33	2 (3)
O3—C8—C9—C14	176.6 (18)	C31—C32—C33—C34	-7 (2)
O4—C8—C9—C10	176.0 (19)	C31—C32—C33—C33 ^{II}	179.6 (14)
O3—C8—C9—C10	-6 (3)	C32—C33—C34—C35	10 (2)
C14—C9—C10—C11	-2 (3)	C33 ^{II} —C33—C34—C35	-175.9 (12)
C8—C9—C10—C11	-179 (2)	C31—C30—C35—C34	4 (3)
C9—C10—C11—C12	1 (3)	C29—C30—C35—C34	-173.4 (17)

C10—C11—C12—C13	-2 (3)	C33—C34—C35—C30	-10 (3)
C10—C11—C12—C5	-178 (2)	C39—C38—N1—C38 ^v	-180 (3)
C6—C5—C12—C11	-136 (2)	C39—C38—N1—C36 ^v	60 (3)
C4—C5—C12—C11	32 (4)	C39—C38—N1—C36	-58 (3)
C6—C5—C12—C13	48 (3)	C37—C36—N1—C38 ^v	64 (2)
C4—C5—C12—C13	-144 (2)	C37—C36—N1—C38	-59 (2)
C11—C12—C13—C14	2 (3)	C37—C36—N1—C36 ^v	-178 (3)
C5—C12—C13—C14	179 (2)	O2—C1—O1—In1	-6.3 (17)
C10—C9—C14—C13	2 (3)	C2—C1—O1—In1	178.8 (16)
C8—C9—C14—C13	-180 (2)	O1—C1—O2—In1	6.4 (17)
C12—C13—C14—C9	-3 (4)	C2—C1—O2—In1	-178.5 (15)
O5—C15—C16—C21	-13 (3)	O4—C8—O3—In2 ¹	3.8 (16)
O6—C15—C16—C21	172.3 (15)	C9—C8—O3—In2 ¹	-174.4 (15)
O5—C15—C16—C17	172.6 (19)	O3—C8—O4—In2 ¹	-3.8 (16)
O6—C15—C16—C17	-3 (3)	C9—C8—O4—In2 ¹	174.2 (16)
C21—C16—C17—C18	1 (3)	O6—C15—O5—In1	-2.3 (15)
C15—C16—C17—C18	176 (2)	C16—C15—O5—In1	-177.4 (14)
C16—C17—C18—C19	0 (4)	O5—C15—O6—In1	2.5 (16)
C17—C18—C19—C20	-2 (3)	C16—C15—O6—In1	178.0 (11)
C17—C18—C19—C26	-179.9 (18)	O8—C22—O7—In2	11.3 (16)
C26—C19—C20—C21	-179.4 (16)	C23—C22—O7—In2	166.9 (10)
C18—C19—C20—C21	3 (3)	O7—C22—O8—In2	-12.5 (18)
C17—C16—C21—C20	-1 (3)	C23—C22—O8—In2	-167.8 (10)
C15—C16—C21—C20	-175.6 (15)	O10—C29—O9—In2	2.8 (15)

C19—C20—C21—C16	-1 (3)	C30—C29—O9—In2	171.2 (16)
O8—C22—C23—C24	154.1 (16)	O9—C29—O10—In2	-3.2 (17)
O7—C22—C23—C24	-5 (2)	C30—C29—O10—In2	-172.8 (12)
In2—C22—C23—C24	99 (5)	C42—N2—C40—C41	-28 (4)
O8—C22—C23—C28	-27 (2)	C42 ^{vi} —N2—C40—C41	-149 (4)
O7—C22—C23—C28	174.3 (17)	C40 ^{vi} —N2—C40—C41	91 (4)
In2—C22—C23—C28	-82 (5)	C42 ^{vi} —N2—C42—C43	-63 (3)
C22—C23—C24—C25	170.7 (18)	C40 ^{vi} —N2—C42—C43	58 (3)
C28—C23—C24—C25	-8 (3)	C40—N2—C42—C43	176 (3)
C23—C24—C25—C26	10 (4)	C42B ^{vi} —N2—C40B— C41B	-6 (6)
C24—C25—C26—C27	-6 (3)	C42B—N2—C40B— C41B	114 (6)
C24—C25—C26—C19	175 (2)	C40B ^{vi} —N2—C40B— C41B	-126 (6)
C20—C19—C26—C25	127 (2)	C42B ^{vi} —N2—C42B— C43B	107 (5)
C18—C19—C26—C25	-55 (3)	C40B ^{vi} —N2—C42B— C43B	-132 (4)
C20—C19—C26—C27	-52 (3)	C40B—N2—C42B— C43B	-13 (5)

Symmetry codes: (i) $-x, -y, z+1/2$; (ii) $-x+2, y, -z+1/2$; (iii) $-x-2, y, -z+1/2$; (iv) $-x, -y, z-1/2$; (v) $-x+1, y, -z+1/2$; (vi) $x, -y+1, -z$.

Computer programs: Apex2 v2014.1-1 (Bruker, 2014), Apex2 v2014.11 (Bruker, 2014), SAINT V8.34A (Bruker, 2014), SHELXS97 (Sheldrick, 2008), SHELXL2014/7 (Sheldrick, 2014), SHELXLE Rev656 (Hübschle *et al.*, 2011), SHELXLE Rev714 (Hübschle *et al.*, 2011).

VI. References:

⁽ⁱ⁾ Apex2 v2014.1, Bruker AXS Inc.: Madison (WI), USA, 2009.

⁽ⁱⁱ⁾ (a) SHELXTL (Version 6.14) (2000-2003) Bruker Advanced X-ray Solutions, Bruker AXS Inc., Madison, Wisconsin: USA. (b) Sheldrick, G. M. *Acta Cryst. A* **2008**, *64*, 112-122.

⁽ⁱⁱⁱ⁾ (a) Sheldrick, G. M. *Acta Cryst. C*, **2015**, *71*, 3-8. (b) Sheldrick, G. M. **2013**. University of Göttingen, Germany.

^(iv) Hübschle, C. B., Sheldrick, G. M. and Dittrich, B. *J. Appl. Cryst.*, **2011**, *44*, 1281-1284.